



TECHNISCHE UNIVERSITÄT MÜNCHEN

Ingenieur fakultät Bau Geo Umwelt
Lehrstuhl für Wasserbau und Wasserwirtschaft

Application of the Ecohydraulic Model on Hydraulic and Water Resources Engineering

Weiwei Yao

Vollständiger Abdruck der von der Ingenieur fakultät Bau Geo Umwelt
der Technischen Universität München zur Erlangung des akademischen Grades
eines

Doktors – Ingenieurs
genehmigten Dissertation.

Vorsitzende: Prof. Dr. Liqiu Meng
Prüfer der Dissertation:

1. Prof. Dr. Peter Rutschmann
2. Prof. Dr. Kinzelbach Wolfgang

Die Dissertation wurde am 11.07.2016 bei der Technischen Universität München eingereicht und durch die Fakultät für Ingenieur fakultät Bau Geo Umwelt am 19.10.2016 angenommen.



TECHNISCHE UNIVERSITÄT MÜNCHEN

Ingenieurfacultät Bau Geo Umwelt

Lehrstuhl und Versuchsanstalt für Wasserbau und Wasserwirtschaft

Application of the Ecohydraulic Model on Hydraulic and Water Resources Engineering

Weiwei Yao

Complete copy of the dissertation approved by degree-awarding institution of Ingenieurfacultät Bau Geo Umwelt of the Technische Universität München in partial fulfillment of the requirements for the degree of

Doktor-Ingenieurs (Dr.-Ing.)

Chairman: Univ.-Prof. Liqiu Meng

Dissertation examiners:

1. Univ.-Prof. Peter Rutschmann
2. Univ.-Prof. Kinzelbach Wolfgang

The dissertation was submitted to the Technische Universität München on 11.07.2016 and accepted by the degree-awarding institution of Ingenieurfacultät Bau Geo Umwelt on 19.10.2016

Abstract: Ecohydraulics includes the role of physical processes such as hydraulics, sediment transport, and geomorphology in ecological systems. In recent decades, a number of numerical models were developed for simulating hydraulic, hydromorphological, and ecological processes. There are very few model systems existing which could simultaneously simulate hydromorphodynamic processes, habitat quality distributions, and population status. Therefore, this research work aims to develop an ecohydraulic model system which combines advanced numerical methods and ecological theories to explore the dynamics and interplay between fluvial processes in rivers and the quality of physical habitat for fish and their density distribution.

The main objective of this study is to develop fish habitat suitability and fish population models as well as to incorporate these models into a hydromorphodynamic software. The fish habitat suitability models assess habitat quality based on abiotic parameters, namely flow velocity, depth, substrate, and temperature (if relevant), all of which are derived from the 2D hydromorphodynamic numerical model system TELEMAC. The relationships between these parameters and habitat features are represented as habitat suitability curves. Four different methods are used to combine these curves into global indices of habitat quality. The quality of habitat can therefore be predicted for a given stretch of river under certain flow conditions. Two different simulation models of population dynamics of fish are developed. The first model is converted from a logistic population concept, where model parameters are related to the time-dependent fish habitat conditions (e.g. weighted usable areas and overall suitability index). The second model is based on an age structured model concept with numbers as the only state vector. Age-specific fecundities and survival rates depend on the habitat qualities defined. The hydromorphodynamic, habitat, and population models are linked together in one model system.

The practical applicability of the developed system to ecohydraulics modelling was explored through three case studies and compared with as well as validated using available observed data. On the basis of the calculated results, the model system is proven to be efficient in describing population dynamics of the European grayling (*Thymallus thymallus*. L.) in the Aare River in Switzerland. Satisfactory predictions of the long-term population evolution of the rainbow trout (*Oncorhynchus mykiss*), brown trout (*Salmo trutta*) and flannelmouth sucker (*Catostomus latipinnis*) in the Colorado River in the United States were obtained. Furthermore, the effects of the Da-Wei Power Plant in the Jiao-Mu River in China on the schizothorax (*Schizothorax*) and schizothorax (*Racoma*) fish species were investigated. The efficiency of fish stocking strategies was evaluated and optimal fish stocking numbers were also proposed. The developed ecohydraulic model system provided very promising results, which highlighted the fundamental role of the temporal variability of hydromorphological parameters in structuring populations

of fish species. Simulating population trends in anticipation of any changes in water management mode, using the software developed in this study can provide decision-makers with useful information to optimise their management measures.

Zusammenfassung: Ökohydraulik als transdisziplinäre Forschungsdisziplin beschäftigt sich mit den Interaktionen zwischen Hydraulik und Ökosystem, indem hydraulische und ökologische Systembeschreibungen miteinander verknüpft werden. In den vergangenen Jahrzehnten wurde eine Vielzahl von numerischen Modellen zur Beschreibung von hydraulischen, hydromorphologischen und ökologischen Prozessen entwickelt. Jedoch existieren kaum Systeme, die die hydromorphologischen Prozesse mit Habitateignungsverteilung oder einem Populationsbestand koppeln. Daher ist es notwendig die ökohydraulischen Modellierungsansätze zu verbessern, um aus der Verknüpfung von hydraulischen Modellen und ökologischen Modellierungsansätzen auf die Dynamik und das Zusammenspiel zwischen fluvialen Prozessen und der Fischhabitatqualität zu schließen.

Der Schwerpunkt dieser Arbeit lag auf der Entwicklung zweier Modelle. Eines zur Erfassung der Fischhabitateignung und ein weiteres zur Beschreibung der Fischpopulation. Zudem wurden beide Modelle in ein bestehendes hydrodynamisches Simulationsmodell integriert. Das Modell zur Erfassung der Fischhabitateignung gibt Auskunft über die Habitatqualität, dies erfolgt auf Basis abiotischer Parameter wie der Fließgeschwindigkeit, Fließtiefe und Sohlsubstratbeschaffenheit. Die hydromorphologischen Ergebnisse wurden mittels TELEMAC-2D gewonnen. Der funktionale Zusammenhang der hydromorphologischen Parameter und der Habitateigenschaften lässt sich durch Habitateignungskurven beschreiben. Im Rahmen der Untersuchungen wurden vier unterschiedliche Kombinationsmethodiken für die Gewinnung eines globalen Habitatqualitätsindex getestet. So lässt sich für einen gegebenen Flussabschnitt mit klar definierten Strömungsbedingungen die Habitatqualität bestimmen. Des Weiteren wurden zwei Simulationsmodelle zur Beschreibung Populationsentwicklung entwickelt. Das erste Modell leitet sich von einem logistischen Populationsmodell ab. Bei diesem Modell werden zeitabhängige Fischhabitatbedingungen (z. B. gewichtete nutzbare Fläche und Geamteignungsindex) an die Modellparameter gekoppelt. Das zweite Modell basiert auf einem Altersstrukturmodellkonzept mit Nummern als einzigem Zustandsvektor. Die altersspezifischen Fruchtbarkeits- und Überleberaten hängen von der jeweiligen Habitatqualität ab. Das hydromorphologische Model, Fischhabitats-, und Fischpopulationsmodel sind in ein Gesamtmodellsystem eingebettet worden.

Die praktische Anwendung erfolgte anhand dreier Fallstudien. Dies ermöglichte die entwickelten ökohydraulischen Modellierungsansätze untereinander zu vergleichen und anhand der erhobenen Messdaten zu validieren. Die erste Fallstudie beschäftigt sich mit der Beschreibung der Äschenpopulation im Fluss Aare in der Schweiz. Die Simulationsergebnisse zeigen, dass die entwickelten Modelle in der Lage sind eine Beschreibung der Populationsdynamik der europäischen Äsche (*Thymallus thymallus*).

L) zu liefern. Im zweiten Anwendungsfall, der die Langzeitauswirkungen auf Populationsentwicklung infolge flussbaulichen Maßnahmen am Colorado (US) untersucht, konnten für die Regenbogenforelle (*Oncorhynchus mykiss*), die Bachforelle (*Salmo trutta*) und den Lappenmaul-Saugkarpfen (*Catostomus latipinnis*) zufriedenstellende Prognosen erstellt werden. Der dritte Anwendungsfall gelegen am Jiao-Mu in Da-Wei (China) beschäftigt sich mit dem Einfluss des Kraftwerks auf die Spezies der schizothorax (*Schizothorax*) und der schizothorax (*Racoma*). Die geplanten Fischbesatzmaßnahmen wurden auf ihre Wirksamkeit hin untersucht und optimiert, um die optimale Anzahl an Besatzfischen zu bestimmen. Das entwickelte ökohydraulische Modellierungssystem liefert vielversprechende Ergebnisse, allen voran wird der Einfluss der zeitlich variablen hydromorphologischen Parameter auf die Fischpopulationsstruktur deutlich. Die simulierten Populationsentwicklungstendenzen reagieren auf jegliche Veränderungen in der Wasserbewirtschaftung. Entscheidungsträger können auf diese Weise mit hilfreichen Informationen versorgt werden, um eine optimale Lösung erarbeiten zu können.

Contents

Part A: Background and basics	1
1 Introduction.....	1
1.1 Background	1
1.2 Motivation of the research	3
1.3 Contribution of this research.....	3
1.4 Outline of thesis content	3
2 Literature review.....	5
2.1 General	5
2.2 River hydrodynamic and hydromorphology	5
2.3 Ecological habitat model.....	7
2.4 Ecological population model	9
Part B: Ecohydraulic modeling	13
3 Ecohydraulic modeling system concept	13
3.1 Model concept of hydrodynamic processes	14
3.2 Model concept on hydromorphology processes	17
3.2.1 Bed-load calculation formula	17
3.2.2 Suspended load calculation formula.....	21
3.2.3 Numerical scheme	23
3.3 Habitat model description	24
3.3.1 Fish SI curves habitat model	25
3.3.2 Fuzzy logic habitat model.....	26
3.3.3 Habitat indices	29
3.3.4 The recommend habitat model in this study.....	30
3.4 Population model description.....	30
3.4.1 Logistic population model	31
3.4.2 Age structure population model	32
Part C: Ecohydraulic model applications	35
4 Model application in the Aare River	37
4.1 Introduction	37
4.2 Study area and collected data.....	37
4.3 Model setup.....	40
4.4 Model validation	44
4.5 Model results.....	46
4.5.1 Hydrodynamic and hydromorphology simulations	46
4.5.2 Habitat quality simulation	49
4.5.3 Population number analysis based on the logistic population model	53
4.5.4 Population density analysis based on the logistic population model	56

4.5.5	Population number analysis based on the matrix population model	57
4.5.6	Population density analysis based on the matrix population model	64
4.6	Discussion	65
4.7	Conclusion	67
5	Model application in the Colorado River	68
5.1	Introduction	68
5.2	Model setup	72
5.2.1	Habitat model	72
5.2.2	Population model	76
5.2.3	Initial and boundary conditions for hydraulic and hydromorphology models	78
5.3	Result and discussion	79
5.3.1	Hydrodynamic and hydromorphology simulations	79
5.3.2	Habitat quality simulation	85
5.3.3	Habitat sensitivity analysis	90
5.3.4	Population number analysis based on the logistic population model	96
5.3.5	Population density analysis based on the logistic population model	105
5.3.6	Fish population analysis based on the fish length distribution model	110
5.4	Conclusions	114
6	Model application in the Jiao-Mu River	116
6.1	Introduction	116
6.2	Study area and ecosystem situation in the Jiao-Mu River	118
6.3	Model setup	123
6.3.1	Hydrodynamic and hydromorphology models	123
6.3.2	Habitat model	124
6.3.3	Population model	124
6.3.4	Fish stocking strategy	125
6.4	Result and discussion	126
6.4.1	Without considering Da-Wei Dam construction effects	127
6.4.2	With Considering Da-Wei Dam construction effects	129
6.4.3	The logistic population model analysis for the five different scenarios	132
6.4.4	The matrix population model analysis for the five different scenarios	139
6.5	Conclusion	148

Part D: Conclusions and suggestions for further research	150
7 Conclusions.....	150
7.1 Summary of the work.....	150
7.2 Final remark and future research	152
Acknowledgements	153
List of figures	154
List of tables.....	159
Reference	160
Notations	178
Abbreviations	181
Appendix I:	182
Appendix II:	184
Appendix III:.....	189
Appendix IV:	197
Appendix V:.....	207

Part A: Background and Basics

1 Introduction

1.1 Background

Ecohydraulics often requires the use or development of advanced numerical models as well as ecological theories that can provide accurate results for river and aquatic organisms management (Lancaster & Downes, 2010; Rice et al., 2010). Many researchers and experts are working in this area which is at the current stage, able to provide better knowledge to fulfill both hydraulic engineering and ecological requirements, and of course this generates additional meaningful research topics, such as developing river and fish physical habitat models and population models (Wang et al., 2013). It is recognized that hydraulic engineers, geomorphologists, river managers, ecologists, biologists, and other experts and researchers, who are working at increasingly more complicated levels, reach deeper understanding of those subjects, and achieve more truly interdisciplinary knowhow. They can develop more effective approaches to handle freshwater hydraulic and river infrastructure such as dam effects on river deformation, to predict aquatic species number and fish density fluctuation trends (Lancaster & Downes, 2010). Balancing ecological systems and citizen requirements call for innovative and effective solutions which will ensure that the needs of both aquatic species and humans are met.

Ecohydraulic topics include passage facilities for aquatic species, such as fish passages and fish lifts, hydrodynamic modeling such as the ecological flow requirements downstream from the dam and in stream flow needs, hydromorphology modeling such as reservoir sediment management and river restoration, habitat modeling (physical habitat quality determination, habitat replacement, habitat restoration or creation, dam effects on habitat, low temperature on reservoir effects on habitat), and population modeling (fish species number and density prediction) (Kemp, 2012; Reid et al., 2010). At the current stage, besides further research on hydrodynamic and morphology, habitat and population models have become indispensable tools for river management, stream habitat restoration and fish population prediction (Fausch et al., 2002; Jones et al., 2003; Katopodis & Aadland, 2006).

In ecohydraulic model system, river and stream physical conditions such as flow velocity, river depth, and substratum information form unique habitats, which facilitate the growth and survival of fish species (Panfil et al. 1999; Armstrong et al. 2003; Yi et al. 2010). Many river ecologists and ecohydraulic researchers confirmed that physical habitat features are the key factors for determining the river aquatic community potential (Lammert & Allan, 1999; Fu et al. 2007; Mouton et al. 2007; Nagaya et al. 2008; Wang et al. 2009). Habitat models are an ecologically friendly way to predict river ecosystem evolution for

fish species. Habitat models are very useful tools for predicting suitability of fish habitats in river systems, and this can help river managers to make an effective management decision (Tomsic et al., 2007). Habitat models are also a powerful tool for suggesting conservation strategies for endangered fish species (Knapp, 2005, Knapp et al., 2007). Besides habitat models, population models are widely used for determining species abundance and diversity (Bartholow et al., 1993; Bartholow., 1996). Population models have a wide range of application, and have been recommended as an effective tool in predicting and protecting fish populations (Harvey et al., 2009).

Ecohydraulic approaches have been accepted by many relevant organizations and institutions; frameworks have been developed and their applications distributed worldwide. For example, China, the biggest developing country in the world, has proposed very strict rules for water resources management and ecological flow definitions due to habitat fragmentation during the past (Judd, 2010; Zhang et al., 2010). Currently, there are many rivers and lakes ecological restoration projects in progress, such as the Mian River ecological restoration project, the Qianling Lake habitat restoration strategy for China Spini-barbus (*Spinibarbus sinensis Bleeker*), and many others (Miller, 2012). In Europe, The EU Water Framework Directive (WFD) also provides an integrated method of managing freshwater ecosystems (Commission, 2000; Acreman & Ferguson, 2010; Hering et al., 2010). Many academic conferences have been organized for open discussion of the concepts of ecohydraulics such as 1st IAHR, 2nd IAHR, 3rd IAHR Europe, and IAHR international congress. Additionally, a Fish Habitat Symposium was organized in Barcelona, Spain, which was the largest symposium at the International Congress on the Biology of Fish, 5th – 9th July 2010 (Katopodis, 2012; Rutschmann et al., 2014; Yao et al., 2014). In USA and Canada, ecohydraulics issues about fish habitat connectivity and suitability are attracting great attention and are particularly popular with the U.S. Geological Survey (USGS), the Institute of Ecology, the Institute of Ecosystem, and Fish Management authorities (Conway et al., 2010; Palmer et al., 2010; Silva et al., 2011).

In this present study, following the ecohydraulic modeling concepts, an ecohydraulic model system is proposed and applied to hydraulic and water resources engineering. The model system contains four models: (1) The hydrodynamic model, (2) the hydromorphology model, (3) the selected target fish species habitat evaluation model based on suitability index curves (SI curves) and variables calculated from hydrodynamic and hydro deformation models, (4) the population model which is used to simulate and predict the fish species number fluctuation as well as fish species population density. This approach enables hydraulic process study, habitat quality assessment, and population status evaluation.

1.2 Motivation of the research

The development of the ecohydraulic modeling concept is a result of the need for quantitative methods to assess and analyze environmental impacts of water resources infrastructure, develop mitigation measures, and restore aquatic ecosystems. Following from this motivation, the overall goal of this dissertation intends to develop an ecohydraulic model system for the assessment of hydraulic processes, fish habitat qualities, and fish population status. The proposed ecohydraulic modeling framework aims to dynamically assess habitat quality, population numbers, and density fluctuations. In this framework, all relevant hydrodynamic and hydromorphological dynamics are considered and quantified.

1.3 Contribution of this research

The main achievements of the dissertation are as follows:

- Development of an ecohydraulic model system, which includes four models: the hydrodynamic model, the hydromorphology model, the habitat model, and the population model.
- Apply the model to the Aare River (Switzerland) and the Colorado River (USA) with one and three target fish species respectively.
- Use this model to predict the dam construction effects and fish stocking effects on the Jiao-Mu River (China).

1.4 Outline of dissertation content

This dissertation is structured into four parts with seven chapters dealing with different topics. Part A includes Chapters 1 and 2, which introduce the background and basics; Part B includes Chapter 3 which introduces the ecohydraulic model; Part C includes Chapters 4, 5 and 6 which introduce three ecohydraulic model applications; Part D includes Chapter 7 which introduces the conclusions and suggestions for further research. More specifically:

Chapter 1: Including the introduction, motivation of the research, contribution of the dissertation and the content of the dissertation.

Chapter 2: Follows the literature review connected with topics of the present research.

Chapter 3: Follows and introduces the ecohydraulic model systems concepts.

Chapter 4: Treats the application of the model to the European grayling (*Thymallus thymallus*) in the Swiss Aare River by means of a case study. It also compares the habitat and population model predictive performance with surveyed data.

Chapter 5: Presents the application of the model to three fish species in the American Colorado River. In this case study, five subareas in the Colorado River have been chosen to simulate the hydrodynamic, hydromorphology, and habitat and population status for the rainbow trout (*Oncorhynchus mykiss*), brown trout (*Salmo trutta*) and flannelmouth sucker (*Catostomus latipinnis*) from 2000 to 2009.

Chapter 6: Treats another important factor in ecohydraulics and predicts the effects of dam construction and fish stocking on the river ecosystem. Two fish species, schizothorax (*Schizothorax*) and schizothorax (*Racoma*), were selected as target fish species for the stretch of the Jiao-Mu River which was investigated.

Chapter 7: Summarizes the work and gives suggestions for further research.

2 Literature review

2.1 General

The aim of this chapter is to give an overview of the literature relevant to the ecohydraulics research topics discussed in this dissertation. The present research belongs to the interdisciplinary field of hydraulics and ecology according to the scientific nomenclature (Katopodis, 2012). A multitudinous amount of literature is produced in ecohydraulic disciplines, especially in the sub-disciplines hydrodynamics, hydromorphology, and habitat modeling. It is self-evident that the ecohydraulic discipline is booming with many special issues since the 1990s (Mitsch, 2012). There are applications in many areas such as river restoration projects, dam building evaluations, aquatic ecosystem issues, fish habitat evaluations, and fish population simulations and regulations.

Traditional ecological knowledge represents experience acquired directly from human contact with the environment (Berkers, 1993). It is difficult to apply the traditional ecological knowledge to ecological resource assessments, evaluations, restorations, and sustainability efforts. This is due to a lack of guidance on implementing the traditional ecological assessment and evaluation in public areas. Therefore, the practice of traditional ecological knowledge predictions should be based on some standardized rules or policy requirements.

Combining traditional ecological knowledge with numerical modeling technology is a more comprehensible and testable way to assess and manage ecological issues (Usher, 2000). Ecohydraulic models have been developed and widely applied since the 1980s via ecological knowledge accumulation and advanced methodologies for assessing the environmental quality of river systems (Milhous et al., 1984, 1989; Parasiewicz, P. 2001, 2003, 2007; Almeida et al., 2009; Wang et al., 2009, 2013; Yi et al., 2010).

2.2 River hydrodynamic and hydromorphology

Physical modeling and computational simulations are widely used in river engineering analysis for describing the river hydrodynamics and hydromorphology. A physical model can provide directly visible results, but it is time- and resource-consuming. For physical models, similarity between model and prototype has to be checked due to possible scale effects in models with reduced length scale. Computational simulations produce full-scale predictions that are cost- as well as time-efficient. The results of numerical models mainly depend on how well the physical processes are mathematically described through governing equations, boundary conditions, and empirical relations (Vaughan et al., 2009; Bratrich et al., 2004). Therefore, the computational simulations are essential for solving real engineering problems.

The calculation of flow and sediment transport is one of the most important tasks in river engineering and river ecosystem assessment (Wu, 2007). However, river flow and sediment transport are some of the most complex and least understood processes in nature. It is extremely difficult to find analytical solutions for most problems in river engineering, and it is utterly tedious to achieve numerical solutions without the help of high-speed computers. To overcome these problems, numerical simulation models have been significantly improved and progressively applied in river engineering with the advances in numerical simulation technology.

For the hydrodynamic and hydromorphology modeling, there are many existing models and they can be classified as one-dimensional (1D), vertical two-dimensional (2D-V), horizontal two-dimensional (2D-H), and three-dimensional (3D) according to the model dimensionality. For example, the 1D models are mainly used in both short-term and long-term simulations of flow and sediment transport processes in long and complicated river systems including reservoirs, estuaries, and/or over long time periods. The 2D and 3D models are mainly used to predict the morpho-dynamic processes under complex flows and complex geometrical conditions in more detail. Such computations demand much higher CPU times than 1D models and are therefore restricted in river length or time length prediction.

The flow states are categorized as steady, quasi-steady or unsteady status. The steady flow is not included the time derivative term. Quasi-steady models divide an unsteady hydrograph into many time intervals and every time interval is represented as a steady flow. Quasi-steady models are mostly applied in the simulation of long-term fluvial processes in rivers and streams. An unsteady model is more general and is often used to simulate unsteady hydrodynamic and hydromorphology processes.

Many parameters including numbers of sediment size classes, sediment transport models, and sediment transport status are considered in the hydromorphology model. Briefly, the sediment size classes can be classified as one single size class or by multiple classes according to different sizes. The sediment transport modes are divided into bed-load and suspended load transport. The sediment transport states are often classified as equilibrium and non-equilibrium (Wu et al., 2000; Wilcock et al., 2003). Regarding the numerical methods, finite difference, finite volume, finite element, the spectral method, finite analytic, efficient element models can be used to solve the hydrodynamic and hydromorphology model. The choice of a specific model depends on the nature of the problem, the experience of the modeler, and the capacity of the computer being used (Wu, 2008).

2.3 Ecological habitat model

Over the past decade, a major trend in river habitat assessment has been shifted from narrow studies that concentrate on a single approach to diversity methods. Models that link fish species SI curves to physical conditions in rivers are becoming a very effective tool to assess the river habitat qualities (Raleigh & Zuckerman, 1986; Brooks, 1997; Wang et al., 2013). The habitat approach is particularly useful for analyzing the ecological impacts caused by dam constructions, determining the suitable environmental discharge, and evaluating the influence on surrounding environments, such as analyzing the effects of dam construction on fish abundance (Huang et al., 2010; Ligon et al., 1995). The first habitat model was developed in the 1970s by the United States Fish and Wildlife Service (Bryant, 1973; USFWS, 1980; Tomsic et al., 2007). In the 1980s, Bovee (1982) developed a habitat model and applied it in river management based on physical variables including depth, velocity and substrates. Later on, the physical habitat simulation model (PHABSIM), instream flow requirements (CASiMiR), MesoHABSIM, River2D, EVHA, and HABSCORE were developed and applied to assess stream habitat features (Bovee, 1982, 1986; Ginot, 1995; Jorde & Bratrich, 2000; Alfredsen & Killingtveit, 1996; Parasiewicz, 2001). More recently, habitat model has become a very useful tool for river management. For example, Software for Assisted Habitat Modeling (SAHM), a software developed by U.S. Geological Survey, has been used in analyzing the endangered species and invasive species in many case studies (Steffler, & Blackburn, 2002; Armstrong et al., 2003; Mouton et al., 2007; Bovee et al., 2008; Nagaya et al., 2008; Stohlgren et al., 2010; Talbert, 2012; Zhou et al., 2014). Moreover, habitat suitability curves (SI curves) have been developed and combined with habitat models based on fish species for fish species habitat suitability analyzing (Edwards et al., 1983; McMahon et al., 1984; Raleigh, 1984; Valdez, et al., 1990). Therefore, habitat modeling is a meaningful tool in river management and is an important component of ecohydraulic model system. An exhaustive overview of current habitat simulation models is given in the following:

PHABSIM

PHABSIM was originally developed by the US Fish and Wildlife Service, and has been used since the 1970s. PHABSIM has experienced a series of modification and updates in later times (Dunbar et al., 1996; Jowett, 1997). Currently, PHABSIM is one of the most popular modeling tools and the model concept has been accepted by ongoing research (Waddle, 2001).

PHABSIM is a numerical model tool which offers the prediction of flow changes such as microhabitat, physical habitat and life stage changes based on field measurements,

hydraulic calibration, and species physical habitat preference (depth, velocity, and substrate preferences). PHABSIM is used to obtain a representation of the physical stream and thus make the stream links to habitat through biological considerations.

PHABSIM fits within the instream flow incremental methodology (IFIM) framework and PHABSIM is a computer model including a suite of software that allows analyses of changes in physical habitat via changes in flow or channel morphology. This model uses streamflow and species SI curves to obtain an assessment of the habitat quantity. PHABSIM is useful in providing a qualitative comparison for different management options.

It should be noted that almost all applications of PHABSIM only address physical habitats. Factors such as water quality, temperature, and sediment transport that are important for habitat and population evaluation do not include in the PHABSIM model. Moreover, the PHABSIM model is inappropriate when both ecological habitat and population status needs to be consider (Spence & Hickley 2000). On balance, PHABSIM is a useful tool, but should not be considered to be the panacea. It has been shown that this numerical tool is particularly useful for comparing the impacts of natural, existing, and potential flow management scenarios to assist in making defensible water resource decision. Obviously, the accuracy of the hydrodynamic model inside PHABSIM should be improved. The other module such as sediment transport can be included in the model to promote a more comprehensive modeling system.

River2D

River2D is a 2D depth averaged finite element hydrodynamic model and has been customized for fish habitat evaluation studies. The hydrodynamic River2D tool for fish habitat modeling was developed by the University of Alberta, Canada (Blackburn & Steffler, 2002). River2D model consists of four programs: R2D_Bed, R2D_Ice, R2D_Mesh, and River2D. R2D_Bed was designed for editing bed topography data on an individual point and channel index files used in habitat analysis. The relevant physical characteristics of the channel bed necessary for flow modeling, the bed elevation and the bed roughness, can be edited in R2D_Bed. R2D_Ice provides the user with an effective graphical environment for the development of ice topography files. Various commands allow the user to modify ice properties globally, regionally, or individually. Break lines can be inserted into ice topography to define the edge of the ice in partially ice-covered domains. R2D_Mesh provides a relatively easy way to effectively compute the mesh generating environment for 2D depth average finite element hydrodynamic modeling. The hydrodynamic River2D tool is also used to analyze and visualize the fish habitat results (Milhous et al., 1989).

River2D has a wide range of applications (Wheaton et al., 2004; Wu & Mao, 2007). River2D is specifically useful in terms of accuracy and time efficiency. Compared to PHABSIM, River2D is able to evaluate complex flow conditions, which cannot be simulated by PHABSIM. Similar to the same limitation as PHABSIM, River2D does not include the hydromorphology model, and the turbulence model needs further enhanced (Loranger & Kenner, 2005; Gard, 2009; 2010).

CASiMiR

CASiMiR model is a habitat model relied on a fuzzy logic based rule system, and is used for physical and biological parameterization. The CASiMiR software is a joint development by University of Stuttgart and SJE Consultants for ecohydraulics research (Schneider et al., 2010). The structure of CASiMiR is based on a fuzzy logic system (see Chapter 3).

MesoHabsim

MesoHabsim is a habitat simulation model that changes the scale of physical parameters and biological response assessments from micro to mesoscale (Gostner, 2012). Micro-habitat surveys are replaced by macrohabitat mapping of whole river sections to match the scale of restoration measures. In MesoHabsim model, logistic regression is applied to describe the fish habitat in response to the environmental attributes, whereby aquatic biota is represented by community rather than by single species.

2.4 Ecological population model

The population models were used in ecohydraulic systems and fish species management. The population modeling studies population dynamics in order to obtain a better understanding of complex interactions and processes work of population ecology. The first population model was developed by Pierre Francois Verhulst in 1838, which was a logistic population growth model (Verhulst, 1938). In the 20th century, population model became a particular interesting model to biologists since the increased pressure on the limited sustenance caused by increased human population and human activities. Recently, ecological population modeling, especially aquatic population modeling raises great attention. Researchers found that the population models are highly connected with the habitat model and the population models can also be evolved from habitat modeling.

Many studies recommended population models as an effective tool for evaluating the fish populations protection, particularly for endangered fish species protection which influenced by dam construction and river restoration (Hess., 1996; Morris & Doak., 2002; Coggins & Walters., 2009; Korman et al., 2009; Ibrahim et al., 2014). One example is the individual-based model (IBM), which can be used to describe the population traits

with distribution, and it can explicit representation of individual performance and local interactions (Deangelis & Gross, 1992; Grimm., 1999; Hall et al., 2006). Other population models have been developed as well, such as InSTREAM model (Harvey et al., 2009) and Salmon model (Bartholow et al., 1993; Bartholow., 1996). In addition, another population model was developed by Burnhill to simulate the cumulative barrier and passage effects of mainstream hydropower dams on migratory fish population in the Lower Mekong Basin (Burnhill, 2009). Some other fish population models were developed by Naghibi & Lence (2012), Korman et al., (2012), and Ibrahim et al., (2014). Among these models, the most popular model is the IBM. The IBM model is particularly useful for modeling small species populations with complicated life histories when extensive data is available (Dunning et al., 1995; Murdoch et al., 1992; Peck & Hufnagl, 2012). The MARK program provides population parameter estimated from marked animals when they are re-encountered at a later time phase (White & Burnham, 1999). An exhaustive overview of current population simulation models is given in the following:

SALMOD: It is a computer model that simulates the dynamics of freshwater salmonid populations and was developed by U. S. Geological Survey Midcontinent Ecological Science Center. The conceptual model was developed to evaluate the Trinity River chinook restoration. In this model, fish eggs and fish mortality are directly related to variable micro and macrohabitat limitations, and also related to the timing and amount of streamflow and other meteorological variables. Habitat quality and capacity are characterized by the hydraulic and thermal properties of individual meso-habitats. SALMOD model processes include spawning (with redd superimposition and incubation losses), growth (including egg maturation), mortality, and movement (freshet-induced, habitat-induced, and seasonal) (Bartholow, et al., 2001). The structure of this model is shown in Figure 2.1.

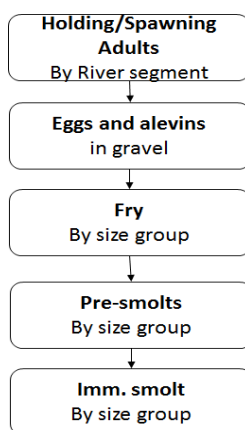


Figure 2.1: Model structure of the SALMOD.

CVI: The CVI watershed tool is a population model response to stream fish habitat and hydrologic alteration. The CVI watershed tool is composed of Hydro Tool, Clustering Tool, Habitat Suitability Tool, and Bioaccumulation and Aquatic System Simulator

(BASS). Hydro Tool is mainly used for predicting mean depth, width, and streamflow for small streams and these parameters are important for the growth and survival of fish species at different life stages. Clustering Tool is used to predict fish community response to various proposed environmental restorations in the region using an empirical approach. The Habitat Suitability Tool is the same as previously described (Chapter 2.3). The BASS is a simulation model for fish management. BASS is a general and extremely flexible FORTRAN 95 model that simulates fish chemical bioaccumulation, fish individual, and population growth dynamics of age structured fish communities (Rashleigh et al, 2004).

InSTREAM: This is the individual-based stream trout research and environmental assessment model. The InSTREAM model can evaluate the effects of habitat changes on different animal population alterations. The InSTREAM model can predict how trout populations respond to changes in any of the inputs that drive the model. These input factors include the flow, temperature, turbidity, and channel morphology. InSTREAM can also predict how fish populations respond to changes in ecological conditions such as food availability or mortality risk. The InSTREAM model is a useful tool for addressing many basic ecological research questions (Harvey et al., 2009). The typical application structure of InSTREAM is shown in Figure 2.2.

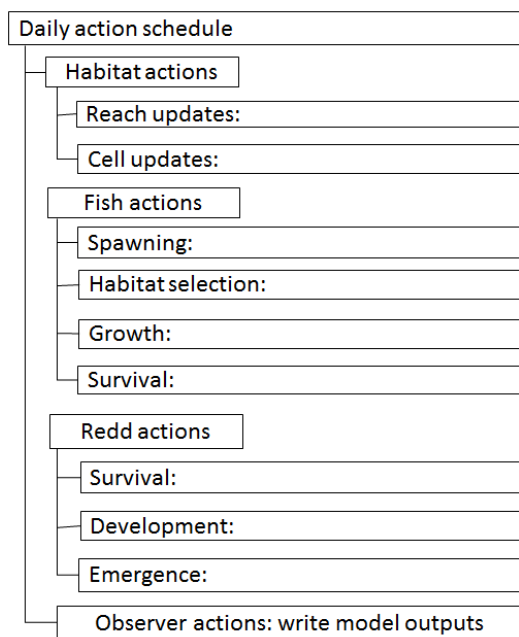


Figure 2.2: The daily action of the InSTREAM.

MARK: The program computes the estimation of model parameters and provides estimations of population size via numerical maximum likelihood techniques. The parameters can be constrained by age or group, using the parameter index matrix. A set of common models for screening data are initially provided with group effects and time effects. The logistic and matrix functions to the parameters of the model are included (White &

Burnham, 1999). This program is a free windows program and needs a large amount of data from marked animals when they are re-encountered at the later time.

Logistic population modeling: This considers a differential equation which is well established for modeling the evolution of total population numbers. The logistic population model is based on a logistic function or the logistic curve which is composed of the initial value, maximum value, and a growth rate function (Brauer et al., 2001). This technique has been proved to yield useful results in many case studies (Schaefer, 1954; Piegorsch et al., 1994). Although such an apparently gross simplification may be criticized, such models are still applied in studies of disparate phenomena, such as the dynamic fluctuations of fish population numbers (Shepherd & Stojkov, 2007).

Matrix population modeling: This is a specific type of population model that uses matrix algebra. It is a form of algebraic shorthand for summarizing a larger number of frequent repetitious and tedious algebraic computations. The basic matrix population model is composed of the population vector on all individual's life stages and an age-classes matrix. The matrix contains the parameters of birth and survival rates (Caswell, 2001). Matrix population modeling is mainly used in age structure population dynamics predictions in time-varying environments. It is very useful for population viability analyzes in field studies and in aquatic ecosystems (Retout et al, 2002; Baxter et al, 2006).

Overall, ecohydraulic studies have paved the way for paradigm shifts in engineering designs, habitat quality assessments, habitat restorations, dam construction effects, fish population management, maintenance of water resource, and aquatic resources infrastructure projects. Ecohydraulic studies also provide the opportunities to recast, innovate, and minimize negative aspects at the project and increase the possibility to achieve a high level of ecological integrity.

Part B: Ecohydraulic modeling

3 Ecohydraulic modeling system concept

This chapter presents a 2D ecohydraulic model system which includes hydrodynamic modeling, hydromorphology modeling, habitat modeling, and population modeling. The objective is to focus on the dynamic behavior of river and stream ecosystems as they play a significant role in this dissertation. From the physical understanding, river ecosystem can be composed by a hydrodynamic part, hydromorphology part, habitat part, and population part. The hydrodynamic and hydromorphology parts respond to external forces such as hydrological variations, riverbed deformation over time and other hydrodynamic effects. The habitat models can mainly be divided into two types, namely SI curves habitat models and fuzzy habitat models. For habitat models based on SI curves, the parameters affecting the fish habitat quality need to be define and the SI curves of those parameters need to be determined. The fuzzy rules, also called expert knowledge, are the core of fuzzy habitat models. Besides habitat models, population models are also described in this chapter. The flowchart of the ecohydraulic model system is shown in Figure 3.1.

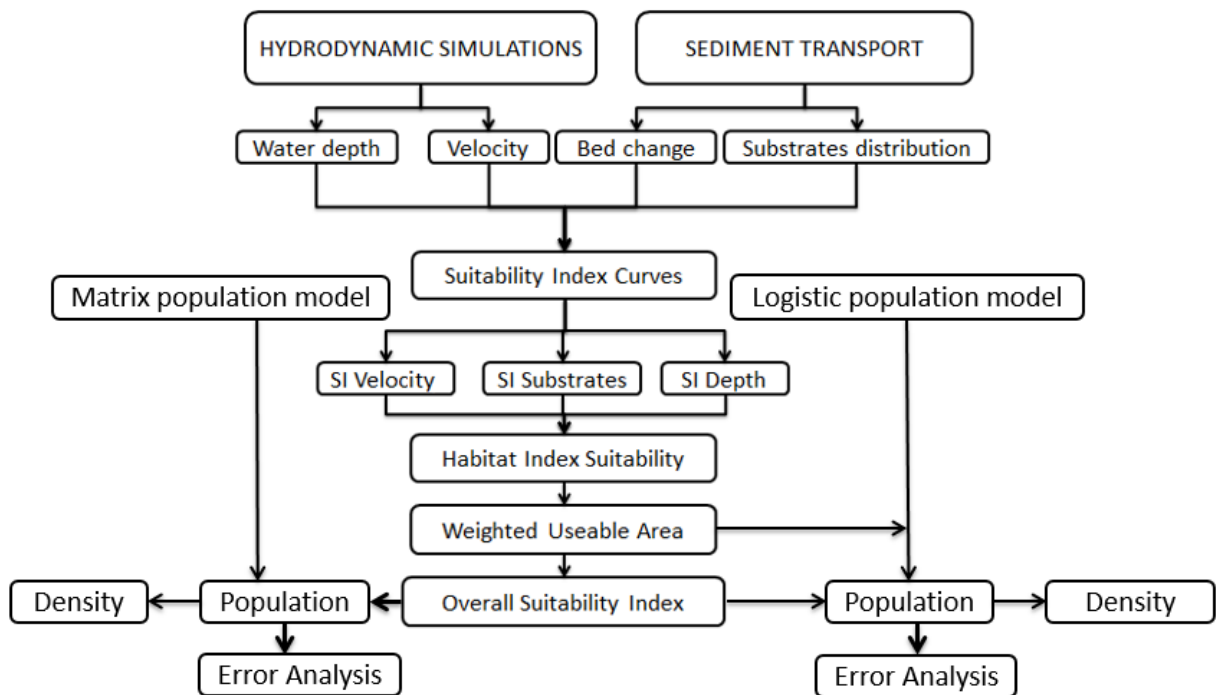


Figure 3.1: The flowchart of the ecohydraulic modeling.

3.1 Model concept of hydrodynamic processes

The Navier-Stokes conservation equations for momentum and energy expressed in partial differential form. They are used to model complex water flows in many applications. However, when considering a problem in which the horizontal scale is much larger than the vertical then the shallow water equations will suffice and can replace the more complex Navier-Stokes equations. From the Reynolds-averaged Navier-Stokes equation to the shallow water equation, several assumptions have to be applied.

Assumption 1 (Boussinesq approximation): The Boussinesq approximation states that if density variations are small, the density may be assumed constant in all terms except the gravitational term. This is due to turbulence eddies small variations occur in the flow velocities and pressure. Usually, these variations are too small to be represented in a numerical scheme unless the grid is chosen very fine.

Assumption 2 (Eddy viscosity concept or Boussinesq hypothesis): Reynolds stresses like viscous stresses depend on the deformation of the mean flow.

Assumption 3 (for shallow water): (1) The characteristics of the horizontal length scale is much larger than the characteristic of the vertical length scale. (2) The variation of the vertical velocity is small in comparison with the variation of the horizontal velocity.

2D shallow water equations are based on the solution of the 2D incompressible Reynolds averaged Navier-Stokes equations, subject to the assumptions of neglecting acceleration on vertical direction and constant density.

The continuity equation is written as:

$$\frac{\partial h}{\partial t} + u \frac{\partial h}{\partial x} + v \frac{\partial h}{\partial y} = 0 \quad (3-1)$$

And the two horizontal momentum equations for the x- and y- component, respectively

$$\frac{\partial u}{\partial t} + u \frac{\partial u}{\partial x} + v \frac{\partial u}{\partial y} = -g \frac{\partial \eta}{\partial x} + \frac{1}{h} \left(\frac{\partial h \tau_{xx}}{\partial x} + \frac{\partial h \tau_{xy}}{\partial y} \right) - \frac{\tau_{bx}}{\rho h} + f_{cor} v \quad (3-2)$$

$$\frac{\partial v}{\partial t} + u \frac{\partial v}{\partial x} + v \frac{\partial v}{\partial y} = -g \frac{\partial \eta}{\partial y} + \frac{1}{h} \left(\frac{\partial h \tau_{yx}}{\partial x} + \frac{\partial h \tau_{yy}}{\partial y} \right) - \frac{\tau_{by}}{\rho h} - f_{cor} u \quad (3-3)$$

Where u and v are depth integrated velocity components in x and y directions respectively (m/s); t is time (s); g is gravitational acceleration (m/s^2); η is the water surface elevation (m); ρ is the density of water (kg/m^3); h is the water depth (m); f_{cor} is the Coriolis parameter (this number is related to the earth's rotation, for most cases, $f_{cor} = 0$); τ_{xx} , τ_{xy} , τ_{yx} , and τ_{yy} are depth integrated Reynolds stresses (kg/ms^2); and τ_{bx} and τ_{by} are shear stresses on the bed and flow interface (kg/ms^2).

The bed shear stresses τ_{bx} and τ_{by} can be calculated based on the following equations:

$$\tau_{bx} = \rho_w c_f u (u^2 + v^2)^{1/2} \quad (3-4)$$

$$\tau_{by} = \rho_w c_f v (u^2 + v^2)^{1/2} \quad (3-5)$$

Where ρ_w is the water density (kg/m³); C_f is the bottom friction which is calculated based on an empirical formula (-). The bottom friction is used to calculate the total bed shears stress, can be calculated based on different friction law, such as Chezy (3-6), Strickler (3-7), Manning (3-8) and Nikuradse friction laws (3-9).

For the Chezy friction law which is calculated based on:

$$C_f = \frac{2g}{C_h^2} \text{ with } C_h = \frac{1}{n} (r_h)^{1/6} \quad (3-6)$$

Where C_h is Chezy coefficient (m^{1/2}/s); r_h is hydraulic radius (m);

For the Strickler friction law which is calculated based on:

$$C_f = \frac{2g}{K_s^2} \frac{1}{h^{1/3}} \text{ with } K_s = \frac{1}{n} \quad (3-7)$$

Where K_s is Strickler coefficient (m^{1/3}/s); n is Manning coefficient (s/m^{1/3});

For the Manning friction law which is calculated based on:

$$C_f = \frac{2g}{h^{1/3}} n^2 \quad (3-8)$$

Where n is Manning coefficient (s/m^{1/3});

For the Nikuradse friction law which is calculated based on:

$$C_f = 2 \left[\frac{\kappa}{\text{Log}\left(\frac{12h}{S_t}\right)} \right]^2 \text{ with } S_t = 2.5D_{s0} \text{ or } S_t = \left(\frac{25.4}{n}\right)^6 \quad (3-9)$$

Where S_t is the Nikuradse bed roughness (m^{2/3}/s²); κ is the Von Karman constant, in most cases it is equal to 0.4.

From these friction equations, we can notice that they all can be converted in a very similar form which only differs through the friction coefficient. The Table 3.1 lists the Manning coefficient ranges used for the majority of canal and material types.

Table 3.1: Manning coefficient usable ranges for channel types and materials (Chow, 1959).

Type of Channel and materials	Minimum Manning's n	Normal Manning's n	Maximum Manning's n
Concrete	0.007	0.012	0.018
Earth, smooth	0.013	0.018	0.023
Earth channel - clean	0.017	0.022	0.027
Earth channel - gravelly	0.02	0.025	0.03
Earth channel - weedy	0.025	0.03	0.035
Earth channel - stony, cobbles	0.03	0.035	0.04
Glass	0.005	0.01	0.015
Natural streams - clean and straight	0.025	0.03	0.035
Natural streams - major rivers	0.03	0.035	0.04
Natural streams - sluggish with deep pools	0.035	0.04	0.045
Natural channels, very poor condition	0.055	0.06	0.065
Plastic	0.004	0.009	0.014

For the 2D hydrodynamic model, τ_{xx} , τ_{xy} , τ_{yx} , and τ_{yy} are depth integrated Reynolds stresses. They are also called depth averaged turbulence shear stresses which are calculated with the following equations:

$$\tau_{xx} = 2v_t \frac{\partial u}{\partial x}; \quad \tau_{xy} = \tau_{yx} = v_t \left(\frac{\partial u}{\partial y} + \frac{\partial v}{\partial x} \right); \quad \tau_{yy} = 2v_t \frac{\partial v}{\partial y} \quad (3-10)$$

Where v_t is the eddy viscosity (m^2/s); v_t is composed of two parts: turbulence viscosity v_{tt} and water viscosity v_w . In some cases when the turbulence viscosity can be ignored, it can be simply set to v_t is 1×10^{-6} . In most cases, v_t is calculated by a turbulence model, such as Elder's model, k- ε model or k- ω model. Among those models, the most common used and stable model is the k- ε turbulence model. For 2D hydrodynamic models, depth averaged k - ε turbulence models have been developed (Rodi, 1993):

$$v_t = c_\mu \frac{k^2}{\varepsilon} \quad (3-11)$$

$$\frac{\partial k}{\partial t} + u \frac{\partial k}{\partial x} + v \frac{\partial k}{\partial y} = \frac{\partial}{\partial x} \left(\frac{v_t}{\sigma_k} \frac{\partial k}{\partial x} \right) + \frac{\partial}{\partial y} \left(\frac{v_t}{\sigma_k} \frac{\partial k}{\partial y} \right) + P_h + P_{kv} - \varepsilon \quad (3-12)$$

$$\frac{\partial \varepsilon}{\partial t} + u \frac{\partial \varepsilon}{\partial x} + v \frac{\partial \varepsilon}{\partial y} = \frac{\partial}{\partial x} \left(\frac{v_t}{\sigma_\varepsilon} \frac{\partial \varepsilon}{\partial x} \right) + \frac{\partial}{\partial y} \left(\frac{v_t}{\sigma_\varepsilon} \frac{\partial \varepsilon}{\partial y} \right) + C_1 \frac{\varepsilon}{k} P_h + P_{\varepsilon v} - C_2 \frac{\varepsilon}{k} \quad (3-13)$$

With

$$P_h = v_t \left[2 \left(\frac{\partial u}{\partial x} \right)^2 + 2 \left(\frac{\partial v}{\partial y} \right)^2 + \left(\frac{\partial u}{\partial x} + \frac{\partial v}{\partial y} \right)^2 \right], \quad P_{kv} = \frac{1}{c_f^{1/2}} \frac{u_*^3}{h} \quad (3-14)$$

$$P_{ev} = \frac{c_2 c_\mu^{1/2} u_*^4}{(e_* \sigma_t) c_f^{4/3} h^2}, \quad u_* = \left[c_f (u^2 + v^2) \right]^{1/2}, \quad e^* = \frac{\varepsilon_t}{u_* h} \quad (3-15)$$

Where P_h represents the production of turbulent kinetic energy due to shear stresses with horizontal mean velocity gradients; P_{kv} and P_{ev} are productions of k and ε respectively due to vertical velocity gradients particularly near the bottom; u_* is bed shear velocity; σ_t is Prandtl/Schmidt number relating eddy viscosity and diffusivity for scalar transport (equal to 0.7 was chosen). The dimensionless diffusivity e^* is an adjustable empirical parameter which may be measured from dye-spreading experiments. Measurements in wide laboratory flumes have yielded an e^* with value of approximately 0.15 while measurements in natural rivers have given much higher values. e^* is 0.6 has been observed as a typical value for many river situations where the stream is slowly meandering and the side-wall irregularities are moderate. However, in sharply curved channels even much higher values of e^* have been observed. From measurements in the Missouri River, a meandering river with bends up to 180° , values of e^* up to 10 have been found. In previous studies, it was stated that the value of e^* is project dependent and must in general be adjusted to the flow calculated (Rodi, 1993; Bui, 2004). $c_1=1.44$, $c_2=1.92$, $\sigma_k = 1.0$, $\sigma_\varepsilon = 1.3$, $\sigma_k=0.7$, $c_\mu=0.09$.

3.2 Model concept on hydromorphology processes

River hydromorphology processes are based on sediment transport which is the transport of sediment particles by flowing water be it in form of bed-load, and be it in form of suspended load. This transport depends on the size of the bed material particles and the flow conditions (Van Rijn, 1984). The sediment transport model is mainly focused on calculating bed-load, suspended load, riverbed deformation, and riverbed grain size distribution such as main grain size diameters and grain size fractions.

3.2.1 Bed-load calculation formula

Bed-load is defined as the sediment in almost continuous contact with the bed, carried forward by rolling, sliding or hopping (Van Rijn, 1993). Before the bed-load is calculated, the shear stress calculated by the hydrodynamic model should be corrected by a factor μ . The correction factor is required due to the shear stresses obtained from the hydrodynamic model are calculated from the depth average velocity, while the shear stresses used to calculate bed-load transport rate are based on the velocity near river bed:

$$\tau = \mu \tau_0 \quad \text{With } \tau_0 = \frac{1}{2} \rho C_f |U(x, y, z)|^2 \quad (3-16)$$

Where μ is the bed form correction factor which can be calculated by several methods (-). For example, if the grain size in the riverbed is very coarse, it can simply be set $\mu = 1$. In other cases, it can be calculated from the following equations:

$$\mu = \frac{C_f'}{C_f} \quad \text{with } C_f' = 2 \left[\frac{\kappa}{\log\left(\frac{12h}{K_s'}\right)} \right]^2 \quad (3-17)$$

or

$$\mu = \frac{C_f'^{0.75} C_r^{0.25}}{C_f} \quad \text{with } C_r = f(K_r) \quad (3-18)$$

Where K_s' is grain roughness (-); K_r is the wave-induced ripple bed roughness (-); C_f' is the bottom friction used in the hydromorphology model (-); C_r is the quadratic friction (-)

After the skin friction has been defined. The bed-load can be calculated based on numerous, semi-empirical formulae such as Meyer-Peter Müller, Einstein-Brown, England Hansen, Van Rijn, Hunziker equations, and many other researchers (Meyer-Peter Müller, 1948; Einstein, 1942; Brown, 1950; Engelund and Hansen, 1967; Van Rijn 1984; 1993; Hunziker, 1995; Acker and White, 1973; Brunner, 2005; Nielsen et al., 1992). Each of these has different ranges of application. The following paragraphs will describe these bed-load formulae and also their validity ranges for sediment gradation in rivers. The non-dimensional sediment transport rate Q_b is expressed as:

$$Q_b = \frac{Q_s}{\sqrt{\left(\frac{\rho_s}{\rho_w} - 1\right) g D^3}} \quad (3-19)$$

Where Q_b is non-dimensional bed-load (-); Q_s is dimensional sediment bed-load transport rate per unit width ($\text{m}^3/(\text{ms})$); D is particle size parameter (m); g is gravity (m/s^2); ρ_s is the sediment density (kg/m^3); ρ_w is the water density (kg/m^3).

Meyer-Peter-Müller formula (MPM): The MPM equation was one of the earliest equations developed and still one of the most widely used. It is a simple excess shear relationship. It is strictly a bed-load equation developed from flume experiments of sand and gravel under plane bed conditions. Most of the data were developed for relatively uniform gravel substrates. MPM is most successfully applied over the gravel range. It tends to under-predict the transport of finer materials.

The MPM bed-load transport function is based primarily on experimental data and has been extensively tested and used for rivers with relatively coarse sediment. The transport rate is proportional to the difference between the mean shear stress acting on the grain and the critical shear stress. This formula can be used for well-graded sediments and flow conditions that produce other-than-plane bed forms. The general transport equation for the MPM function is represented by:

$$Q_b = \begin{cases} 0 & \theta' \leq 0.47 \\ \alpha(\theta' - \theta_c)^{3/2} & \theta' > 0.47 \end{cases} \quad (3-20a)$$

with

$$\theta' = \frac{\mu\tau_0}{(\rho_s - \rho_w)gD_{50}}; \quad \theta_c = 0.047 \quad (3-20b)$$

Where θ' is the shields number (-); α is MPM parameter (-); ρ_s is sediment density (kg/m^3).

Einstein-Brown formula: This bed-load formula is recommended for gravels and large bed shear stresses. The solid transport rate is expressed as:

$$Q_b = \left(\left(\frac{2}{3} + \frac{36}{D_*} \right)^{0.5} - \left(\frac{36}{D_*} \right)^{0.5} \right) f(\theta') \quad (3-21)$$

$$D_* = D_{50} \left[\frac{\left(\frac{\rho_s - 1}{\rho_w} \right) g}{\nu^2} \right]^{1/3} \quad (3-22)$$

$$f(\theta') = \begin{cases} 2.15e^{\left(\frac{-0.391}{\theta'} \right)} & \text{if } \theta' \leq 0.2 \\ 40\theta'^3 & \end{cases} \quad (3-23)$$

Where D_* is particle size parameter (-); ν is viscosity of water (m^2/s).

Engelund-Hansen formula (for bed-load and suspended load): The Engelund-Hansen formula is a total load predictor which gives adequate results for sandy rivers with substantial suspended load. It is based on flume data with sediment sizes between 0.19 mm and 0.93 mm. It has been extensively tested and was found to be fairly consistent with field data. This formula predicts the total load. It is recommended for fine sediments, in the range 0.2 mm to 1 mm under equilibrium conditions. It can be represented as:

$$Q_b = \frac{0.1}{C_f} \hat{\theta}^{5/2} \quad (3-24)$$

$$\hat{\theta} = \begin{cases} 0 & \text{if } \theta' < 0.06 \\ \sqrt{2.5(\theta' - 0.06)} & \text{if } 0.06 < \theta' < 0.384 \\ 1.065\theta'^{0.176} & \text{if } 0.384 < \theta' < 1.08 \\ \theta' & \text{if } 1.08 < \theta' \end{cases} \quad (3-25)$$

Van Rijn formula: The Van Rijn bed-load transport formula was proposed in 1984 based on experiments performed under uniform flow conditions and fine sediment. The bed-load transport are linked to dimensionless particle parameter D_* and shields number θ' . The reliability of Van Rijn formula is based on a verification study using 580 flume and field data. It can be represented as:

$$Q_b = \frac{0.053}{D_*^{0.3}} \left(\frac{\theta' - \theta_{cr}}{\theta_{cr}} \right)^{2.1} \quad (3-26)$$

$$\theta_{cr} = \begin{cases} 0.24D_*^{-1} & D_* \leq 4 \\ 0.14D_*^{-0.64} & 4 < D_* \leq 10 \\ 0.04D_*^{-0.10} & 10 < D_* \leq 20 \\ 0.013D_*^{0.29} & 20 < D_* \leq 150 \\ 0.045 & 150 \leq D_* \end{cases} \quad (3-27)$$

Besides the bed-load formulae mentioned above, there are many other empirical bed-load calculation formulae such as Bijker, Hunziker, Bailard, Dibajnia and Watanabe (Bailard & Inman, 1981; Bijker, 1971; Dibajnia and Watanabe, 1996; Hunziker & Jaeggi, 2002; Wu et al., 2008). All of the transport rate formulae were verified by intensive experiments. The validity range of the sediment transport formulae was listed in Table 3.2.

Table 3.2: Validity range of the sediment transport formulae.

Validity range of the sediment transport formulae	D_{50} validity range (mm)
Meyer-Peter Müller	0.4-29
Einstein-Brown	0.25-32
Engelund-Hansen	0.19-0.93
Van Rijn	0.2-2.0

For rivers with complex geometries, the following effects may also need to be taken into consideration: effects of the river slope, effects of hiding and exposure, sediment slide (large friction angle), secondary currents (curved channels), tidal flats (large areas with nearly zero water depth), bed roughness prediction, active layer thickness, and mean grain size calculation.

3.2.2 Suspended load calculation formula

Suspended load is the total sediment transport which is maintained in suspension by turbulence in the flowing water for considerable periods of time without contact with the streambed. It moves with practically the same velocity as that of flowing water (Van Rijn, 1993). However, before the suspended load is calculated, we need to determine whether the suspended load should be included in the hydromorphology process. It is quite common to use the Rouse number to determine the suspended load (Van Rijn, 1993). Its definition is as follows:

$$R = \frac{W_s}{\kappa u_*} \quad \begin{array}{ll} 2.0 < R & \text{No suspension} \\ 0.8 < R < 2.0 & \text{Incipient suspension} \\ R < 0.8 & \text{Full suspension} \end{array} \quad (3-28)$$

With $u_* = [c_f (u^2 + v^2)]^{1/2}$, and

$$w_s = \begin{cases} \frac{(s-1)gD_{50}^2}{18\nu} & D_{50} \leq 10^{-4} \\ \frac{10\nu}{D_{50}} \left(\sqrt{1 + 0.01 \frac{(s-1)gD_{50}^2}{18\nu}} - 1 \right) & 10^{-4} \leq D_{50} \leq 10^{-3} \\ 1.1\sqrt{(s-1)gD_{50}} & \text{Otherwise} \end{cases} \quad (3-29)$$

Where R is the Rouse number (-), W_s is settling velocity (m/s), D_{50} is mean diameter of the sediment (m), u_* is bed shear velocity (m/s), c_f is bottom friction (-), s is ρ_s/ρ_0 which is the relative density (-), ν is the fluid viscosity (m^2/s), and g is gravity (m/s^2).

The 2D sediment transport equation for the depth-average suspended load concentration is obtained by integrating the 3D sediment transport equation over the suspended zone. The suspended load transport is calculated by the following equation:

$$\frac{\partial(Ch)}{\partial t} + \frac{\partial(Chu)}{\partial x} + \frac{\partial(Chv)}{\partial y} = \frac{\partial}{\partial x} \left(\varepsilon_t h \frac{\partial C}{\partial x} \right) + \frac{\partial}{\partial y} \left(\varepsilon_t h \frac{\partial C}{\partial y} \right) + E - D \quad (3-30)$$

$$\text{With } \varepsilon_t = \frac{v_t}{\sigma_t} \quad \text{and} \quad E - D = w_s (C_{eq} - C_{ref}) \quad (3-31)$$

Where C is the suspended sediment concentration (kg/m^3); h is water depth (m); D is the deposition rate ($\text{kg}/\text{m}^2\text{s}$), and E is the suspension rate ($\text{kg}/\text{m}^2\text{s}$); $E - D$ is the net exchange of sediment between suspended load and bed-load layer; σ_t is Schmidt number also called Prantl number (0.6); ε_t is turbulence diffusivity scalar (m^2/s); v_t is the turbulence

viscosity (m²/s); C_{eq} is suspended load concentration at reference lever under equilibrium conditions (kg/m³); C_{ref} is suspended load concentration at reference lever (kg/m³).

There are several empirical formulae for calculating volume concentration C_{veq} such as Zyserman and Fredsoe (1994), Van Rijn (1984b). The mass concentration can also converted from the volume concentration based on $C_{eq} = \rho_s C_{veq}$

Zyserman and Fredsoe formula: The Zyserman and Fredsoe formula sets the reference level at two grain size diameters above the bed and determines the near-bed volumetric concentration of suspended load as:

$$C_{veq} = \frac{0.331(\theta' - \theta_{cr})^{1.75}}{1 + 0.72(\theta' - \theta_{cr})^{1.75}} \quad (3-32)$$

$$\text{With } \theta' = \frac{\mu\tau_0}{(\rho_s - \rho_w)gD_{50}} \quad (3-33)$$

Van Rijn formula: Van Rijn (1984b) set the reference level Z_{ref} at the equivalent roughness height k_s or half the bed-form height and established:

$$C_{veq} = 0.015D_{50} \frac{T^{3/2}}{Z_{ref} D_*^{0.3}} \quad (3-34)$$

Where T is the non-dimensional excess bed shear stress or called transport stage number (-), defined as $T = (U*/U_{*cr})^2 - 1$; U_* is the effective bed shear velocity related to grain roughness (m/s), determined by $U_{*cr} = Ug^{0.5}/C_f$; with $C_f = 18 \log(4h/d_{90})$ is the critical bed shear velocity for sediment incipient motion, given by the Shields diagram (-); and d_{50} and d_{90} are the characteristic diameters of bed material (m).

The parameter C_{ref} is calculated based on:

$$C_{ref} = FC \quad (3-35)$$

With

$$F^{-1} = \begin{cases} \frac{1}{(1-Z)} B^R (1 - B^{(1-R)}), \text{ for } R \neq 1 \\ -B \log B, \text{ for } R = 1 \end{cases} \quad (3-36)$$

$$\text{And } B = \frac{Z_{ref}}{h} \quad Z_{ref} = K_r \quad (3-37)$$

Where F is the ratio between the reference and depth-average concentration (-); C is suspended concentration (kg/m³); B is the ratio between the ripple roughness and water depth (-); K_r is the ripple roughness (-); C_{eq} is suspended load concentration at reference level

under equilibrium conditions (kg/m^3); C_{ref} is suspended load concentration at reference level (kg/m^3); R is Rouse number (-).

To calculate the bed evolution affected by bed-load and suspended load, the Exner equation need to be solved (Coleman & Nikora, 2009).

$$(1-p) \frac{\partial Z_f}{\partial t} + \frac{\partial Q_s}{\partial x} + \frac{\partial Q_s}{\partial y} + (E-D) = 0 \quad (3-38)$$

Where p is the non-cohesive bed porosity (-); Z_f is the bottom elevation (m); Q_s is the solid volume transport (bed-load) per unit width ($\text{m}^3/(\text{ms})$); $E-D$ is the net volumetric exchange of sediment between suspended load and bed-load layer at reference level ($\text{m}^3/(\text{ms})$).

3.2.3 Numerical scheme

For the numerical discretization, the most common discrete methods are the finite difference method, finite volume method, finite element method, and the spectral method. For the numerical grids, there are various classification methods for numerical grids such as structured grids, block-structured grids and unstructured grids. The numerical approximation serves for computing variables appearing in the differential equations. For all the schemes, the numerical error should satisfy the convergence criterion of the numerical method.

Initial and boundary conditions

For rigid wall boundary conditions, a wall-function approach is often used and the water level near a rigid wall is usually assumed to have zero gradients in the normal direction to the boundary. For subcritical flow, boundary conditions are needed at inlet and outlet in order to derive a well-posed solution for hydrodynamic and hydromorphology equations. The inlet boundary condition is usually a time series of flow discharge and the velocity at each computational point of the inlet located in a nearly straight reach can be assumed to be proportional to the local flow depth. The boundary condition at the outlet usually is a time series of the measured water stage derived from a stage-discharge rating curve.

For unsteady problems, an appropriate initial condition has to be given. The velocity is set to zero at initial time, water depth is set as a constant value according the flow discharge. The bed roughness is also set according the surveyed river bed substratum. In order to achieve a stable flow and eliminate initially severe waves propagating in the computational domain, a flow stabilization period has to be set. For obtaining a reason-

ble initial riverbed, e.g. a thirty day's simulation time can be performed in order to develop an appropriate river bed. The final solution at the end of this bed development phase can be then set as initial condition.

Numerical solution

After the partial differential equation is discretized and the boundary conditions have been set, the next step is to solve the resulting algebraic equations. If an explicit scheme is used for an unsteady problem, the unknown solution on the new time level only depends on the solution of the old time level, and thus the calculation can be relative easily performed step by step without using an algebraic solver. If an implicit scheme is used for an unsteady problem or a numerical scheme involving more than two grid points for a steady problem, multiple unknowns appear in the algebraic equations that must be solved together. Therefore, an equation solver is required. The implicit scheme is usually more stable and allows for larger time steps than the explicit scheme, yet its overall efficiency depends on the method used to solve the algebraic equations. The algebraic equations can be solved directly or iteratively. Direct methods, such as the Gaussian elimination, are often used to solve linear algebraic equations; iteration methods are usually used for nonlinear equations, because the coefficients have to be updated and the equations have to be solved repeatedly. There are several methods often used for solving algebraic equations in computational river dynamics, for instance Thomas algorithm, Jacobi and Gauss-Seidel iteration methods, Alternating Direction Implicit (ADI) iteration method, TDMA method, SIP iteration method, over-relaxation, and under-relaxation method.

3.3 Habitat model description

Habitat models are the models which include the parameters affecting the conditions for development of biologic or zoologic species. The habitat model described in this dissertation is mainly physically base and includes following parts: morphologic, hydraulic and hydrologic processes. The parameters such as substrate size, type and shape of substrate, roughness, sediment porosity, bathymetry, armourig layer etc. are belonging to the morphologic part. In the hydraulic part, flow velocity, flow depth, shear stress, turbulence, near bed boundary layer, and water transient storage zone etc. are contained. In the hydrologic part, parameters such as base flow, peak flow, and minimum flow or in general flood hydrographs are considered. The Figure 3.2 is an illustration of factors affecting fish habitats (Wu, 2014).

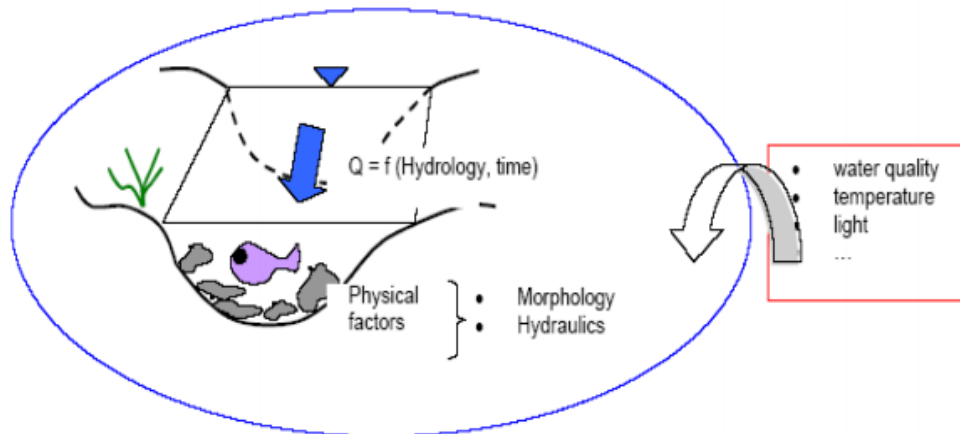


Figure 3.2: Factors affecting the habitat suitability (Wu, 2014).

3.3.1 Fish SI curves habitat model

The SI curves are the true preference of fish with the actual habitat available. Since the 1980s, researchers and engineers started to use SI curves which are needed for theoretically remove environmental bias with regard to a fish species and life stage selection of microhabitat conditions (Nelson, 1984). The most significant parameters used for SI curves are velocity, water depth, and riverbed substrates. Besides that, flow temperature, oxygen concentration, and other parameters may also be included. In order to represent the fish suitability conditions in rivers and channels, a relative preference function needs to be derived for each habitat parameter. Suitable fish SI curves are the decisive components of habitat models as described in many case studies (Wampler, 1985; Waddle, 2001; Yi et al, 2010; Bui et al., 2013).

The two basic components of the habitat model based on SI curves are the SI values and the habitat suitability index (HSI) values. The SI values are derived from hydrodynamic and corresponding habitat suitability criteria. Habitat suitability simulation is based on criteria linked to physical parameters such as velocity and water depth reflecting suitability considerations. SI curves are mainly based on literature, professional judgment, lab studies, or field observations of the frequency distribution for the habitat variables. The HSI values are mainly depended on the SI values and the combination function of SI values. HSI values are derived by quantifying field and laboratory information of each suitability index variable on the effect of the population. The functions of HSI are described as follows:

$$\text{Option 1} \quad HSI_{i,t} = (SI_1 \times SI_2 \times SI_3 \dots SI_n)^{1/n} \quad (3-39)$$

$$\text{Option 2} \quad HSI_{i,t} = \frac{(SI_1 + SI_2 + SI_3 + \dots + SI_n)}{n} \quad (3-40)$$

$$\text{Option 3} \quad HSI_{i,t} = (SI_1 \times SI_2 \times SI_3 \dots SI_n) \quad (3-41)$$

$$\text{Option 4} \quad HSI_{i,t} = \text{Min}(SI_1, SI_2, SI_3, \dots, SI_n) \quad (3-42)$$

Where SI_1 , SI_2 and SI_n are the related suitability indices obtained from the fish SI curves. The graphs of the HSI range from 0 to 1 for the species (0 is indicating the most unsuitable conditions, and 1 is representing the optimal condition).

The example of the habitat suitability criteria and the structure of habitat suitability based on SI curves are shown in Figure 3.3.

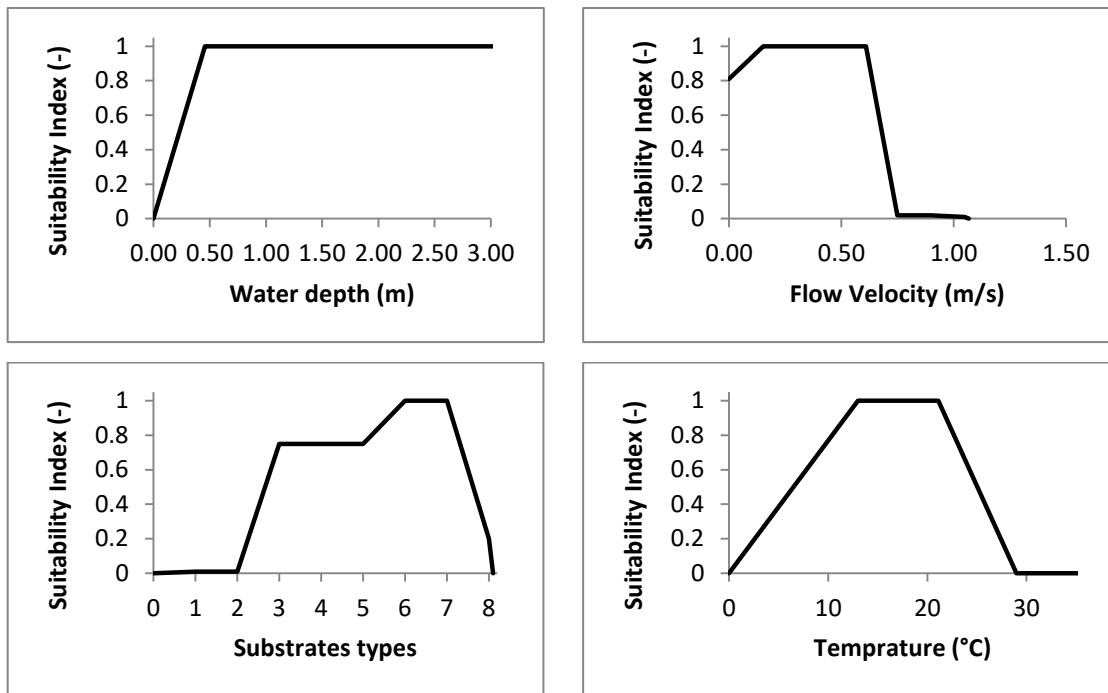


Figure 3.3: An example of SI curves for a selected fish.

3.3.2 Fuzzy logic habitat model

Besides the habitat model based on fish SI curves, there are many applications with fuzzy logic based habitat models. Fuzzy logic habitat models use physical and biological parameters through the application of expert knowledge using a fuzzy logic based rule system.

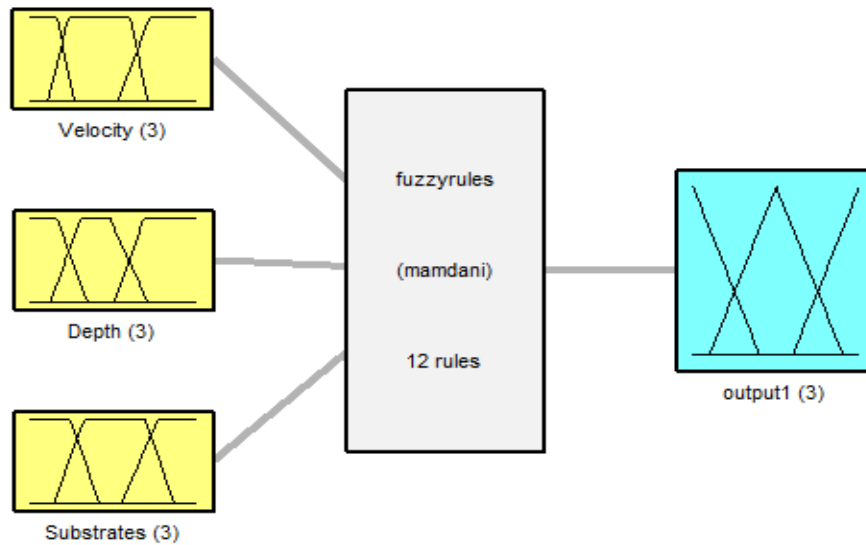


Figure 3.4: The flowchart of a fuzzy logic based habitat model.

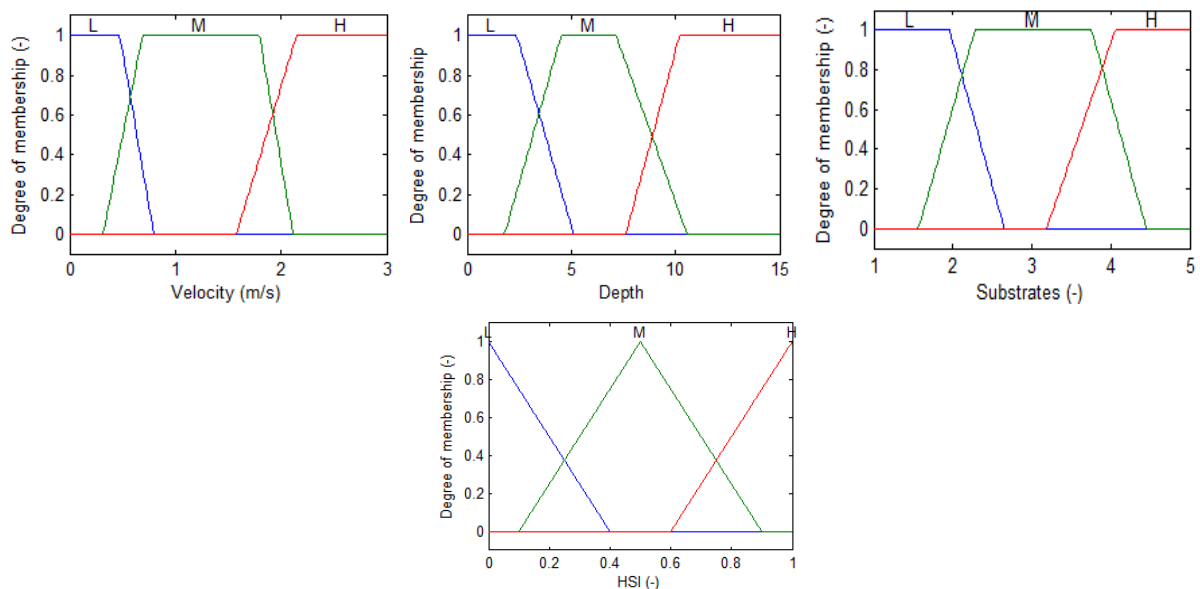


Figure 3.5: Membership functions for the input variables (velocity, water depth, and substrate) and the output variable habitat suitability index.

The structure of fuzzy logic habitat models is based on the fuzzy logic system. A fuzzy logic system (FLS) can be defined as the nonlinear mapping of an input data set to a scalar output data set (Mendel, 1995; Steeb, 2011). The original fuzzy model concept was developed by Zadeh (1965). In fuzzy logic habitat models, the linguistic values such as 'low', 'moderate', and 'high' were assigned to the input variables (velocity, water depth and riverbed substrates) and the output variable (habitat suitability index). These linguistic values were defined by fuzzy rules, a membership function of particular fuzzy rules and indicate the degree to which an element belongs to this fuzzy set. The membership values are ranging from zero to one (Mouton et al, 2009, 2011). For the fuzzy logic based

habitat modeling, there are several steps that need to be done: input selection, output selection, membership definition for input and output, fuzzy rule definition based on the input and output, and the defuzzification. The defuzzification is the process of producing a quantifiable result in standard logic, giving fuzzy sets and corresponding membership degrees. The Figures 3.4 to 3.7 are illustrated the fuzzy logic based habitat model.

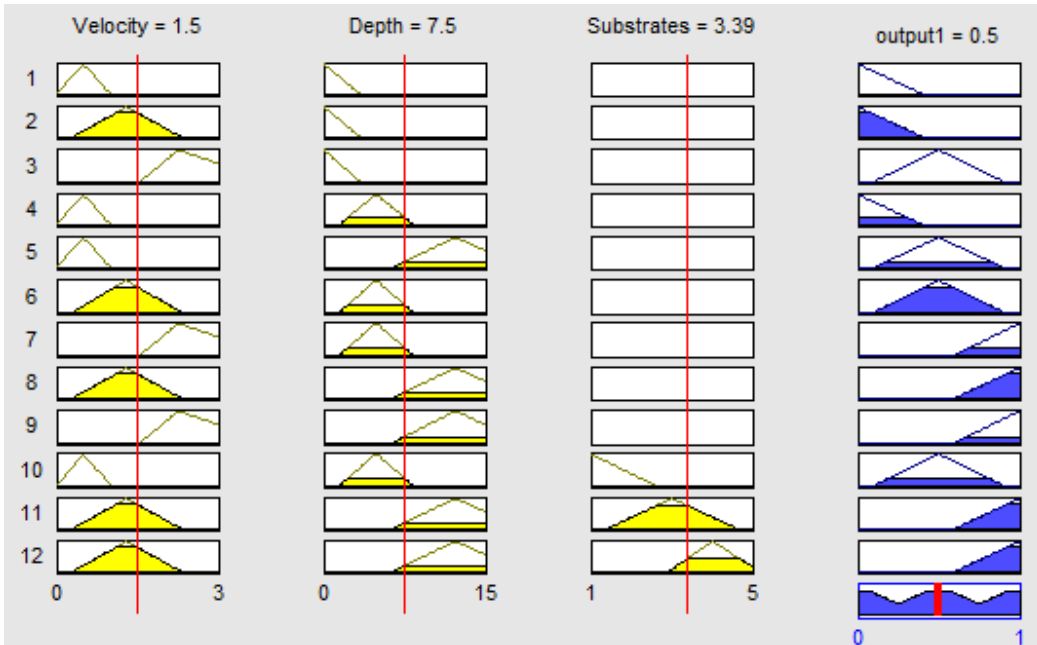


Figure 3.6: Illustration of the fuzzy rule settings.

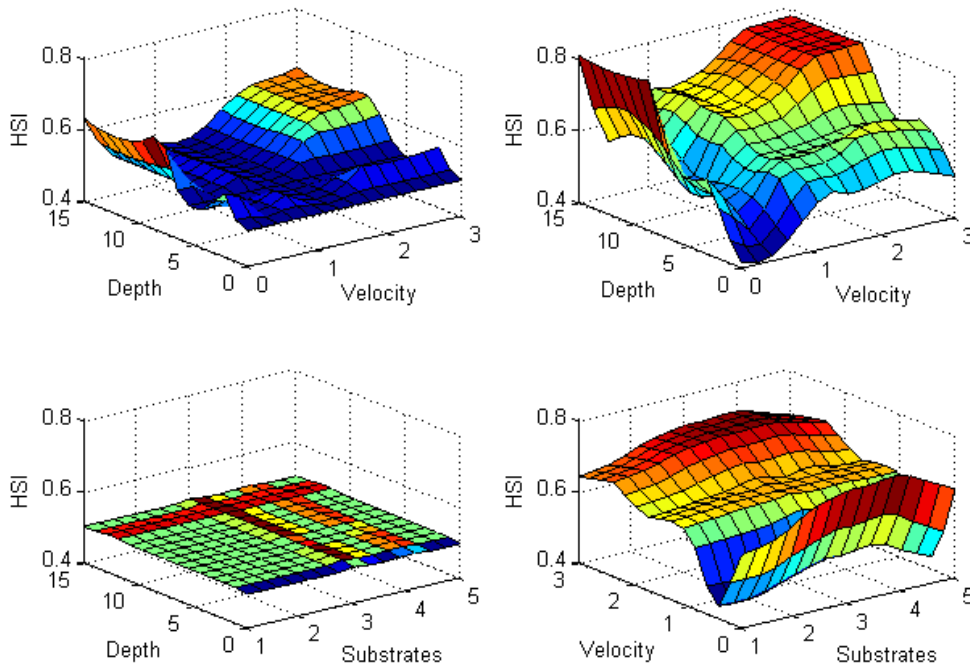


Figure 3.7: Output for habitat suitability index (HSI) after defuzzification.

3.3.3 Habitat indices

Besides the HSI, there are two more parameters of importance that should also be calculated during the habitat modeling process. These are the weighted usable areas (WUA) and the overall suitability index (OSI). The WUA is based on a two-dimensional distribution of the habitat features mapped to the riverbed and illustrated in a projection on a horizontal plane. Based on the HSI values attributed to each mesh cell, the WUA is then obtained by integrating the habitat quality over the computational mesh cell of the entire river stretch using a geometric weighting function:

$$WUA = \sum_{i=1}^M A_i HSI_i \quad (3-43)$$

Where A_i is the horizontal surface of mesh cell i (m^2), HSI_i is the habitat suitability index of mesh cell i and M the number of meshes in the studied river stretch. The OSI is defined as the ratio of the weighted usable area and the total computational domain area in the horizontal plane:

$$OSI = \frac{\sum_{i=1}^M A_i HSI_i}{\sum_{i=1}^M A_i} \quad (3-44)$$

In order to further understand the habitat quality distribution in the river, the habitat quality can be divided into three classes according to the HSI values: ideal habitat proportion (ISP), middle habitat proportion (MSP), and unsuitable habitat proportion (LSP). The ISP, MSP and LSP describe the percentage of ideal, middle and unsuitable habitats in a study site.

$$ISP = \frac{\sum_{i=1}^M A_{i(HSI_{A_i} \geq 0.7)}}{\sum_{i=1}^M A_i} \times 100\% \quad (3-45)$$

$$MSP = \frac{\sum_{i=1}^M A_{i(0.3 \leq HSI_{A_i} < 0.7)}}{\sum_{i=1}^M A_i} \times 100\% \quad (3-46)$$

$$LSP = \frac{\sum_{i=1}^M A_{i(HSI_{A_i} < 0.3)}}{\sum_{i=1}^M A_i} \times 100\% \quad (3-47)$$

3.3.4 The recommend habitat model in this study

Both fish SI curves and fuzzy logic habitat models have been used in many case studies such as fish habitat studies, combined morphodynamic, habitat modeling studies, minimum flow or hydropeaking studies, and river restoration projects. The fuzzy logic habitat model is particularly useful when the SI curves for target fish are uncertain. However, expert knowledge for fish biology information and the fuzzy rules establishment are uncertain and complicated. So that the habitat model recommended in this dissertation is based on the model concepts mentioned on fish SI curves considering turbulent flows and sediment transport. The structure of the habitat model is shown in Figure 3.8.

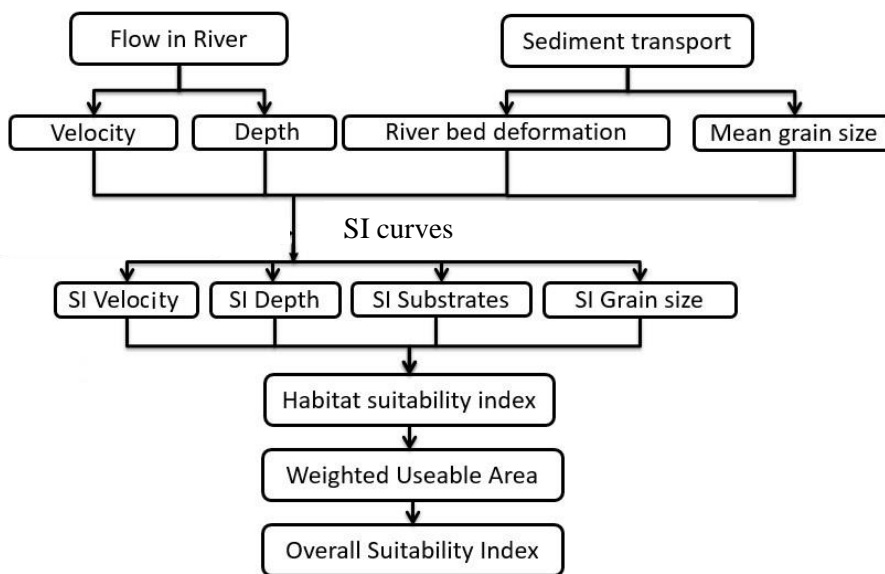


Figure 3.8: Flowchart of the habitat model applied in this dissertation.

3.4 Population model description

A population model is a type of mathematical model that is used to study the dynamic development of populations. These models allow a better understanding of how complex processes responsible for growth or decay of populations interact. Modeling dynamic interactions in nature can provide a manageable way for understanding how population number changes over time. Ecological population modeling is concerned with the in population size, age distribution, and density variations. The ecological population modeling would be affected by the physical environment, the individuals of their species, and the other species.

There are many different population models. Some of the models are only worked on specific cases, and the general robustness is not satisfactory. The purpose of this research

work is the development of a robust population model to simulate or to predict fish population numbers and density changes with time. Among those existing population models, the logistic population model and the matrix population model are described and performed in this dissertation. The logistic population model is converted from a logistic function, which is used for describing the species population number changes. The matrix population model is a model derived from an age structure based concept. The concepts of these two types of population models were applied in the dissertation. The scope of these two models are different, the logistic population model can be only used to predict the fluctuation of total population number. In the matrix population model, the population number changes on each life stage can also be predicted. The input data for the logistic population model and the matrix population model are also different (Renshaw, 1993).

3.4.1 Logistic population model

The first model used in this work, the logistic population model, is originally based on a logistic function. The logistic population model is composed by the growth rate and the fish numbers that the river habitat can support. In this model, the WUA and OSI are used to represent the maximum number and the growth rate respectively. The logistic function is used to represent the changes of fish population number. A detailed description of this logistic population model used in this dissertation can be found in Appendix 1 (Fox, 1970; Russ, 2004; Shepherd, 2007).

In the logistic model, the population number can be calculated as follows:

$$P_{t+\Delta t}^F = \frac{\beta \times WUA_{t+\Delta t}^F \times P_t^F \times e^{\alpha \times (OSI_{t+\Delta t}^F - OSI_t^F)}}{\beta \times WUA_{t+\Delta t}^F + P_t^F \times \left(e^{\alpha \times (OSI_{t+\Delta t}^F - OSI_t^F)} - 1 \right)} \quad (3-48)$$

Where P_t^F and $P_{t+\Delta t}^F$ are population numbers at time t and $t+\Delta t$ for fish species F (-); α and β are model parameters related to the study domain and the present fish species (-); WUA (m^2) and OSI (-) are weighted usable areas and overall suitability index respectively;

In this dissertation, population density $P_{i,t}^F$ in mesh cell i at time t are defined as:

$$P_{i,t}^F = \frac{A_{i,t} \times HSI_{i,t}^F \times P_t^F}{WUA_t^F} \quad (3-49)$$

Where A_i is the horizontal surface of mesh cell i (m^2), HSI_i is the habitat suitability index of mesh cell i (-). $P_{i,t}^F$ is the population density (fish number/per mesh cell).

3.4.2 Age structure population model

The second population model, the matrix population model also named age structure population model, is developed from the classic matrix population model (Caswell, 2001; Aziy-Alaoui, 2002). The classic matrix is one of the most well known ways to describe the changes of population and is very popular in population ecology. In classic matrix population model, the population is divided into groups based on age classes. At each time step, the population is represented by a vector with an element for each age class. The classic matrix model is a square matrix with the same number of rows and columns as the population vector. The birth rate and the survival rate are included in the square matrix. The OSI is also insert into the birth rate and survival rate.

$$\begin{bmatrix} N_{1,t+\Delta t} \\ N_{2,t+\Delta t} \\ \dots \\ N_{i,t+\Delta t} \\ \dots \\ N_{j,t+\Delta t} \\ \dots \\ N_{n-1,t+\Delta t} \\ N_{n,t+\Delta t} \end{bmatrix} = \begin{bmatrix} F_{1,t} & F_{2,t} & \dots & F_{i,t} & \dots & F_{j,t} & \dots & F_{n-1,t} & F_{n,t} \\ S_{1,t} & 0 & \dots & 0 & \dots & 0 & \dots & 0 & 0 \\ \dots & \dots \\ 0 & 0 & \dots & 0 & \dots & 0 & \dots & 0 & 0 \\ \dots & \dots \\ 0 & 0 & \dots & 0 & \dots & 0 & \dots & 0 & 0 \\ \dots & \dots \\ 0 & 0 & \dots & 0 & \dots & 0 & \dots & 0 & 0 \\ 0 & 0 & \dots & 0 & \dots & 0 & \dots & S_{n-1,t} & S_{n,t} \end{bmatrix} \times \begin{bmatrix} N_{1,t} \\ N_{2,t} \\ \dots \\ N_{i,t} \\ \dots \\ N_{j,t} \\ \dots \\ N_{n-1,t} \\ N_{n,t} \end{bmatrix} \quad (3-50)$$

With

$$F_{i,t} = f_{i,t} \times \left(1 + \frac{e^{(OSI_{i,t}-a)} - e^{-(OSI_{i,t}-a)}}{e^{(OSI_{i,t}-a)} + e^{-(OSI_{i,t}-a)}} \right); \quad S_{i,t} = s_{i,t} \times \left(1 + \frac{e^{(OSI_{i,t}-b)} - e^{-(OSI_{i,t}-b)}}{e^{(OSI_{i,t}-b)} + e^{-(OSI_{i,t}-b)}} \right) \quad (3-51)$$

Where $N_{i,t}$ is fish number at time t for fish stage i (-); $s_{i,t}$ is model survival rate at time t (-); $F_{i,t}$ is birth rate of for spawning fish at time t (-); $f_{i,t}$ is the basic birth rate at time t for the stage i (-); $s_{i,t}$ is the basic survival rate at time t for the stage of i (-); a and b are the empirical parameters for spawning fish and other life stages of fish. The a and b were ranged from -1 to 1 (Equation 3-51). The Equation 3-51 shows that when the OSI values are bigger than a and b , the fish population number will show an increasing trend. When the OSI values are smaller than a and b , then the fish population number will show a decreasing trend.

The initial fish numbers at each life stage could be defined based on the surveyed fish number when the intensive fish population assessment are conducted. However, in most case studies, the surveyed fish numbers are not enough to correctly represent the fish age structure. Therefore, the initial fish numbers at each life stage in the matrix population

model need to adjust as the fish population is at steady-state. The definition is as follows: in a surveyed fish sample, a catch curve from fish population is determined based on the method of Robson & Chapman (1961). Based on the catch curve, each life stage' proportions are obtained. The fish numbers of each life stage are equal to the proportions of each life stage multiplied by the total fish number.

We can define four life stages of fish, namely fry fish, juvenile fish, adult fish, and spawning fish. Thus the OSI in birth rate term is calculated by spawning fish SI curves, while the OSI in growth up rate term is converted from fry fish SI curves, juvenile fish SI curves, and adult fish SI curves. In this dissertation, we defined s_1 to s_i belonging to fry fish, s_i to s_j belonging to juvenile fish, and s_j to s_n belonging to adult fish. The fry, juvenile, adult, and spawning OSI values are used to calculate the matrix model adjust factor. More specifically, the OSI values in birth rate terms are calculated by fish SI curves for the spawning period, whereas the OSI values in growth up rate term are derived from fish SI curves averaged over all other life stages.

It is almost impossible to measure the age of surveyed fish. However, it is possible to relate the length of a fish to its age. As surveyed fish data mainly focus on fish length measurement a length-age relation is more meaningful. Therefore, in order to compare modeling results with observations, the matrix population model also can be converted into a fish length distribution model (Figure 3.9).

$$\begin{bmatrix} NL_{1,t+\Delta t} \\ NL_{2,t+\Delta t} \\ \dots \\ NL_{i,t+\Delta t} \\ \dots \\ NL_{j,t+\Delta t} \\ \dots \\ NL_{n-1,t+\Delta t} \\ NL_{n,t+\Delta t} \end{bmatrix} = \begin{bmatrix} F_{1,t} & F_{2,t} & \dots & F_{i,t} & \dots & F_{j,t} & \dots & F_{n-1,t} & F_{n,t} \\ S_{1,t} & 0 & \dots & 0 & \dots & 0 & \dots & 0 & 0 \\ \dots & \dots \\ 0 & 0 & \dots & 0 & \dots & 0 & \dots & 0 & 0 \\ \dots & \dots \\ 0 & 0 & \dots & 0 & \dots & 0 & \dots & 0 & 0 \\ \dots & \dots \\ 0 & 0 & \dots & 0 & \dots & 0 & \dots & 0 & 0 \\ 0 & 0 & \dots & 0 & \dots & 0 & \dots & S_{n-1,t} & S_{n,t} \end{bmatrix} \times \begin{bmatrix} NL_{1,t} \\ NL_{2,t} \\ \dots \\ NL_{i,t} \\ \dots \\ NL_{j,t} \\ \dots \\ NL_{n-1,t} \\ NL_{n,t} \end{bmatrix} \quad (3-52)$$

Where $NL_{i,t}$ and $NL_{i,t+\Delta t}$ are fish number at time t and $t+\Delta t$ for fish length i stage; the other parameters are the same as mentioned before. Of course, the fish length can also be converted to the life stage based on the fish length to age relationship.

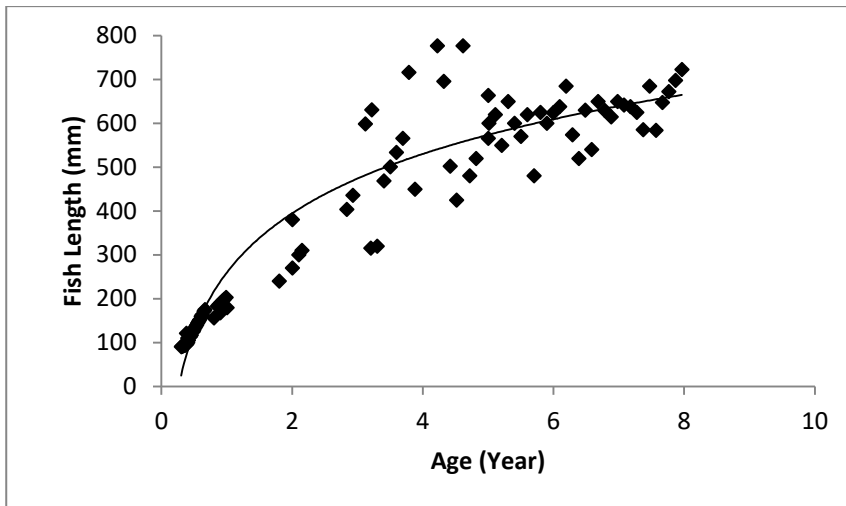


Figure 3.9: Length-at-age relation for a fish species.

In this dissertation, it should be noted that the purpose of this habitat model mainly focuses on prediction rather than to validate of the habitat quality. Further, due to limited data to validate the population model by comparing its predictions against observations, the quantitative accuracy of the model predictions cannot be determined except that the model does appear to effectively simulate inter-annual changes in the size structure of fish population monitored under field data surveys. The main function of habitat and population models should be seen as qualitative tools to evaluate possible habitat quality and corresponding fish density changes as a response to hydrodynamic and hydromorphologic changes. Habitat and population models could also help identifying strategies for habitat restoration and suitable river management.

Part C: Ecohydraulic model applications

In Chapter 4 to Chapter 6, three ecohydraulic model system case studies are presented which cover three rivers and six selected fish species. The use of the modeling system for case study in Switzerland, in USA, and in China involving six different fish species and a comparison of all computational options used ensures a significant test of the ecohydraulic model system.

In Chapter 4, the Aare River in Switzerland was chosen as study river and European grayling (*Thymallus thymallus*. L.) was selected as target fish species. Two scenarios named E1 (without considering hydromorphology model) and E2 (with considering hydromorphology model) were used and four habitat computational options were applied in each scenario for the habitat quality simulation. In each scenario, both the logistic and matrix population models were used to predict the fish number and fish density distribution. The four habitat computational options (O1, O2, O3, and O4) and two population models (the logistic population model and the matrix population model) were applied. The differences between scenario E1 and scenario E2 were also analyzed in this case study.

In Chapter 5, the Colorado River in USA was chosen as a case study and three fish species were chosen as targets fish species, namely the rainbow trout (*Oncorhynchus mykiss*), brown trout (*Salmo trutta*), and flannelmouth sucker (*Catostomus latipinnis*). Five subareas in the Colorado River were chosen to simulate the hydrodynamic, hydromorphology, habitat, and population status for the three fish species from 2000 to 2009. In this case study, two population models: the logistic population model and the matrix population model have been applied to simulate the fish population numbers and density distributions. The fish monitoring data in those five subareas were also used to verify the fish number fluctuation and fish density variation.

In Chapter 6, schizothorax (*Schizothorax*) and schizothorax (*Racoma*) in Jiao-Mu River (China) were selected as target fish species. The ecohydraulic model system was applied to evaluate the effects of the Da-Wei dam construction and possible management strategies. The ecohydraulic model system applied here was composed by a hydrodynamic model, a hydromorphology model, a habitat model, and both the logistic and matrix population models. The schizothorax (*Schizothorax*) and schizothorax (*Racoma*) population number, fish age structure, and fish density distribution were predicted. Based on the fish number prediction, the fish stocking strategies were also evaluated and an optimal fish stocking proposition was worked out.

The outline of the three applications is as follows: An introduction is followed by a study area description and a presentation of the collected data. The used modeling system and the model setup are described, and the results presented and discussion. A conclusion was also provided for each case study.

4 Model application in the Aare River

4.1 Introduction

In this case study, the ecohydraulic model system has been proposed to examine the effects of flow rate alterations on fish habitats, population numbers, and fish population density. The Aare River in Switzerland and the European grayling (*Thymallus thymallus*) were selected as the target case study and the target fish species respectively. The European grayling is a typical species in the Aare River and very sensitive to physical parameter and environmental changes. A pronounced response of the population to changes was expected, and the case study analyzed accordingly. The objective of this chapter is to propose an ecohydraulic model system application for this target fish, and apply the model system for a quantitative analysis of fish habitat and population status from 1970 to 2000.

4.2 Study area and collected data

The study area is located where the Aare River flows out of Lake Thun, 30 km south of Bern. The Aare River is a tributary of the High Rhine and the longest river which rises and ends entirely within Switzerland. The River drains an area of 2,490 km². The river rises in the Aare Glacier of the Bernese Alps in canton Bern, below the Finsteraarhorn and west of the Grimsel Pass, in the south-central part of Switzerland (Mouton et al., 2007). The study area chosen in this case study is a 1.35 km long river stretch which is located downstream of Lake Thun. The width of the river ranges from 70 to 200 m with a 45 m width tributary downstream of the computational domain (Figure 4.1). The average annual flow rate is 111 m³/s with a maximum and minimum discharge of 570 m³/s and 23 m³/s respectively (Figure 4.2). In the computational domain, 50 cross-sections were defined and water depths were measured along each cross-section at equal distances of about 1 m. The substratum compositions were assessed by underwater photography and visual assessment (Mouton et al., 2008). The riverbed is mixed with sand-sized substratum, gravel, and organic clay. Gravel and cobble were deposited extensively on the river bank. In the Aare River, the vegetation density is very high and enriched with eroded tree boles and root wads in the riverbed, which can provide plenty of food for fish species. Geology and substratum information on the Aare River are also available from field surveys (EAWAG, 2002). According to the survey of EAWAG (Swiss Federal Institute for Environmental Science and Technology), there are 16 types of riverbed substrates used to represent the substrate types.

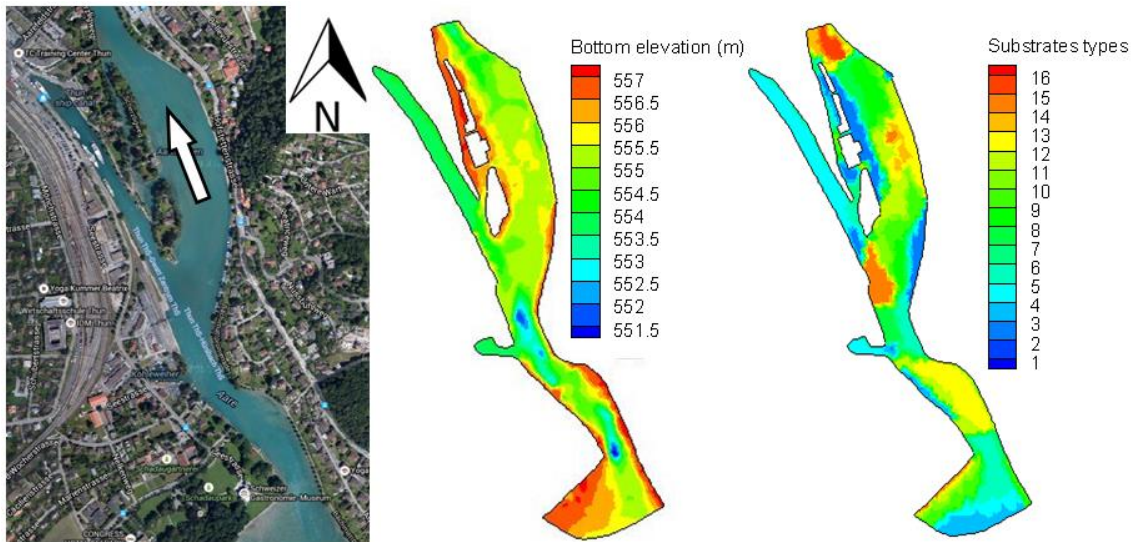


Figure 4.1: Computation domain and substrate types.

The Aare River provides very suitable habitats for the largest populations of fish species with the European grayling (*Thymallus thymallus*) among these. Spawning European grayling were visually identified, localized, and counted by GPS. The living conditions of European grayling depend strongly on the habitat quality in the Aare River. This fish species has a narrow range of suitability for velocity, depth, and substrate. The micro-level changes in the fish habitats may disturb the behavior of spawning European grayling. It may also result in a decrease of the fish population number and density, or even pose an extinction risk to this fish species (Gönczi, 1989). The spawning European grayling prefers velocities between 0.25 m/s and 0.65 m/s, and prefers shallow water to deeper water. The most suitable depth for spawning European grayling ranges from 0.25 to 1.8 m. Regarding substrate preference, this fish species prefers the bottom substratum composed of 10 to 40 percent gravel (2.83 to 45.3 mm), 50 to 60 percent cobbles (90 to 128 mm), and 10 to 30 percent boulders (128 to 256 mm) which are mixed with a few bigger stones (EAWAG, 2002).

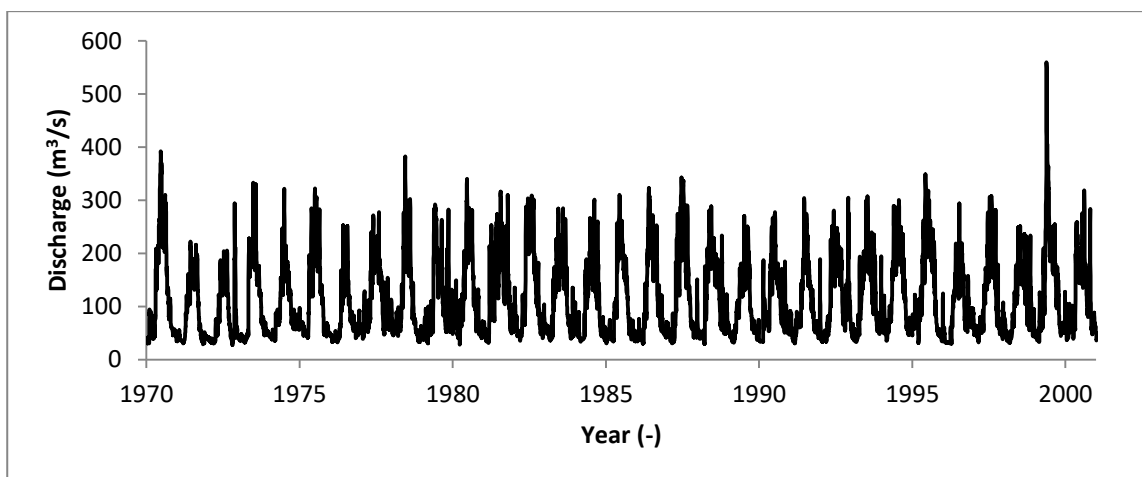


Figure 4.2: Flow hydrograph of the Aare River from 1970 to 2000.

In this case study, the Aare River data included riverbed elevations, riverbed substrates, and flow discharges. A stage-discharge relationship at the outlet was used to simulate hydrodynamic and hydromorphology processes. The whole computational domain was subdivided into 5,403 mesh cells and 9,619 nodes using Blue Kenue software (CHC, 2011). Water depth and flow velocity were calculated at each mesh cell by a two-dimensional hydraulic model, which was generated using TELEMAC-2D software (Dobler et al., 2014). The dynamic sediment transports, including dynamic changes in riverbed and riverbed substratum composition, were simulated by SISYPHE software (Robins & Davies, 2011). The physical parameters flow velocity, water depth, and composition of riverbed substrates were used for establishing the habitat suitability index (HSI). A habitat model was used to define the weighted usable area (WUA), and the overall suitability index (OSI). In addition, the fish population models, which were based on the simulation results of the habitat model, were used to simulate the fish population number changes and the fish density distributions. A flowchart is shown in Figure 4.3. From the flowchart, it can be noticed that this case study includes two scenarios, namely a scenario without considering the hydromorphology model (E1), and a scenario considering the hydromorphology model (E2). In addition, four habitat computational options (O1, O2, O3, and O4) were considered. Based on the four habitat computational options, the corresponding weighted usable area (WUA), overall suitability index (OSI), population number (P. N.), and population density (P. D.) were also simulated. The computational option O1 is presented in this chapter to illustrate the simulation results. The simulation results of the other computational options O2, O3, and O4 are presented in Appendix III.

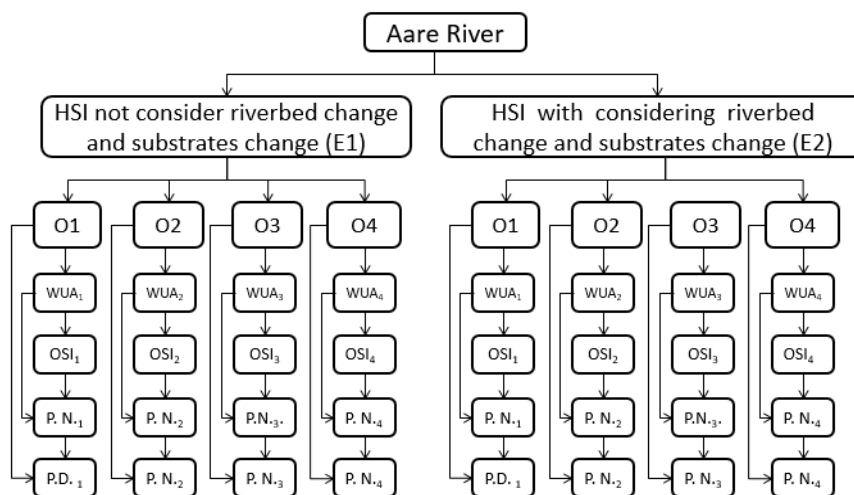


Figure 4.3: Flowchart of the ecohydraulic model system for European grayling in the Aare River.

4.3 Model setup

The Aare River computational domain was adapted as shown in Figure 4.4. The Aare River ecohydraulic model system was developed by integrating a hydrodynamic model, a hydromorphology model, a habitat model, a logistic population model, and a matrix population model. The hydrodynamic model was based on the 2D shallow water equations, which consisted of conservation equations, namely conservation of mass and momentum. The bottom friction and turbulent components were calculated by empirical equation and $k-\varepsilon$ turbulence model respectively (Equations 3-1 to 3-15).

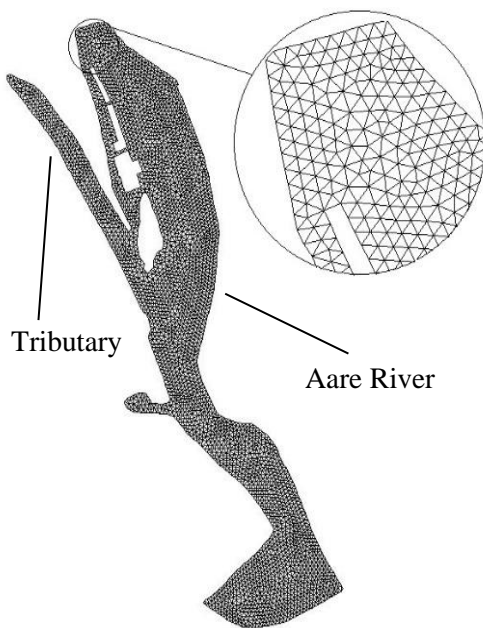


Figure 4.4: Extent of the computational river stretch and the generated mesh.

The sediment transport model was calculated based on semi-empirical formulae, which included bed-load computation, bed evolution, and grain sorting effects. Non-cohesive sediments and their size-fractions have been used for the sediment transport model. The suspended load is not considered here due to the high Rouse number.

The shear stress obtained from hydrodynamic computations needed modification to calculate bed-load transport rate. This was due to the shear stresses obtained from hydrodynamic model were calculated from the depth average velocity, while the shear stresses used to calculate bed-load transport rate were based on the velocity near river bed. The Equation 3.16 was used to modify the shear stress. After the modification of shear stresses, the bed-load transport rate was then calculated as a function of modified shear stresses. The bed slope, hiding/exposure effects, and active layer thickness definitions were used in the sediment transport model. The MPM bed-load formula was used in this case study (Equations 3-20a, 3-20b).

For representation of the riverbed substrate distribution, the sediment has been divided into two layers and ten sediment fractions. In each layer, the sum of all sediment fractions is equal to one. The riverbed substrate distribution was calculated by the following equation:

$$D_m = \sum_{k=1, NSICLA} AVAI(k)D(k) \quad (4-1)$$

Where $AVI(k)$ is the volume fraction k of sediment; $D(k)$ is the mean diameter of sediment fraction k (m); D_m is the mean diameter of the active layer (m).

In this case study, only the three essential variables, which affect growth, survival, abundance, and other measures of fish species' well-being, were selected, namely the flow velocity, the water depth, and the dynamic status of bed substrates. The parameters used for the habitat model were generated by hydrodynamic and hydromorphology models. The data for suitability index curves (SI curves) was mainly obtained from EAWAG's results and other literature (Figure 4.5) (Sempeskei and Gaudin, 1995; Nykänen et al., 2001; Nykänen and Huusko, 2004). The SI is represented by a value ranging from 0 to 1, with 0 for an unsuitable and 1 for the best suitability. The HSI was defined based on four different computational options (Equations 3-39 to 3-42). The physical habitat model used in this study also calculated the WUA and the OSI values (Equations 3-43, 3-44). The WUA and OSI values are used to do the habitat sensitivity analysis and also as inputs for population model. The WUA and OSI values based on spawning SI curves were used in the logistic population model. The OSI values based on fry, juvenile, adult, and spawning SI curves were used in the matrix population model.

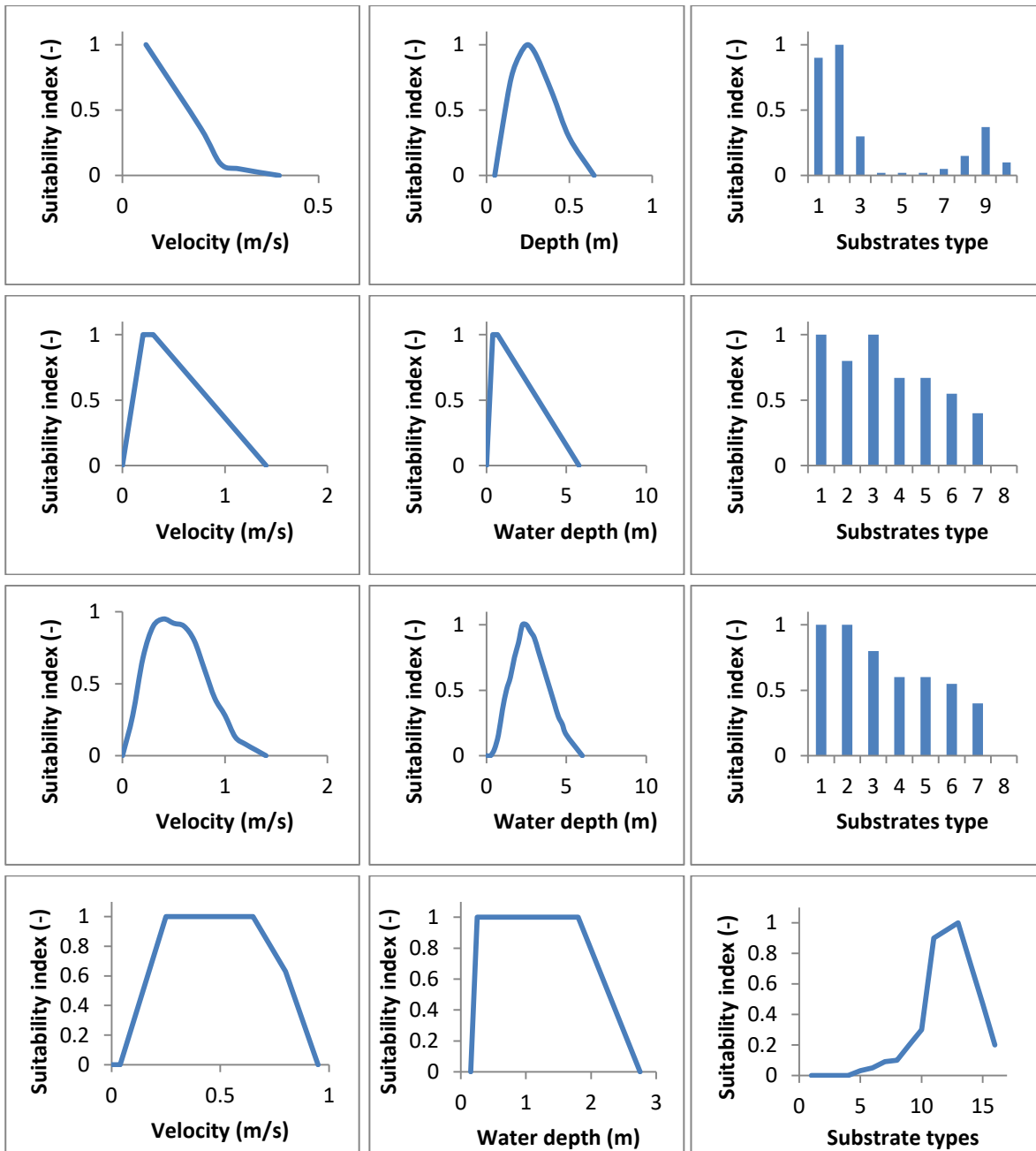


Figure 4.5: Fry, juvenile, adult, and spawning (from upper to down) European grayling SI curves for velocity, water depth and substrate types.

In the logistic population model, the population dynamics results from the habitat model were based on Equation 3-48, and fish density calculations in mesh cell i were based on the Equation 3-49. In order to simulate fish species numbers and densities for all life stages, the second type of the population model, the matrix population model, was applied (Equations 3-51, 3-52). The performance of both the logistic and the matrix population models were examined with the correlation coefficient (Equation 4-2).

$$Correl(P^{sim}, P^{obs}) = \frac{\sum (P^{sim} - \overline{P^{sim}})(P^{obs} - \overline{P^{obs}})}{\sqrt{\sum (P^{sim} - \overline{P^{sim}})^2 (P^{obs} - \overline{P^{obs}})^2}} \quad (4-2)$$

Where P^{sim} is the simulated fish number, P^{obs} is the fish data observed, $\overline{P^{sim}}$ and $\overline{P^{obs}}$ is the average value of P^{sim} and P^{obs} .

The OSI values in birth rate terms are calculated by fish SI curves for the spawning period, whereas the OSI values in growth up rate term are derived from fish SI curves averaged over all other life stages. In this case study, due to unavailability of survival rate and birth rate data in the selected fish species, the f_i and s_i are defined based on the method of Robson & Chapman (1961) and corresponding results are shown in Table 4.1. For the European grayling, the 1st year was defined as fry life stage; the 2nd year was defined as juvenile life stage, and the 3rd to 9th was defined as adult life stage; the spawning life stage was defined as the 3rd to 9th year at spawning season (April & May) (Ingram et al., 2000).

Table 4.1: The survival rate and birth rate of the European grayling for the matrix population model.

Life stage (Year)		1	2	3	4	5	6	7	8	9
European grayling	f_i	0	0	29	37	46	47	48	48	48
	s_i	0.127	0.146	0.171	0.206	0.259	0.35	0.537	0.838	0.0001

In the ecohydraulic model system, the TELEMAC-2D software has been used to solve for the hydrodynamic parameters. The SISYPHE software with a FORTRAN file (new subroutine) was used to solve the sediment transport. In this case study, the habitat computational options and the population models were developed by the author of the dissertation. The Aare River bathymetry was used for the river bed elevations and the boundaries of the computational domain, together with complete settings for initial and boundary conditions. A detailed description of the boundary conditions can be found in Chapter 3, and in the TELEMAC-2D and SISYPHE software user manual (Riadh et al., 2014; Tassi & Villaret, 2014).

Initially four flow discharges were used to validate the ecohydraulic model system. The ecohydraulic model system was used to simulate the European grayling habitat quality, population number, and density distribution based on the four different habitat computational options and two different population models. The simulated fish numbers and fish number surveyed from 1970 to 2000 were compared.

4.4 Model validation

The model validation mainly focuses on the hydrodynamics and a comparison of the habitat quality for spawning grayling. Computed velocities and water depths are compared with those simulation results from the EAWAG report (2002). Water levels with four different discharges (40 m³/s, 70 m³/s, 100 m³/s, and 180 m³/s) were used to validate the hydrodynamic model and habitat model in scenario E1. The differences in velocities and water depths between the presented model system and the results from EAWAG report (2002) are shown in Appendix II (Figure II. 1). The habitat composition, which was simulated based on the EAWAG report, and the ecohydraulic model system are also shown in Appendix II (Figure II. 2 to II. 4). The computed habitat differences between the developed model system and EAWAG report are shown in Figure 4.6. The computed WUA values of four different discharges are shown in Figure 4.7. It can be seen that the presented model simulations agreed well with the EAWAG report calculations, which are based on HYDRO-AS software model for flow calculation, except in a few very small regions (Appendix II). Higher differences were noted near the inlet areas for velocity and water depths at some points in the river. These differences are mainly due to the interpolation error, the models with different implemented boundary condition, and the different velocity distributions at the inlet. Thus, despite some negligible differences, the presented model simulation results are in line with the EAWAG simulation results. When comparing the HSI classes, the simulation results of all four different computational options displayed a reasonable agreement with the EAWAG simulation results. The habitat quality differences in the four computational options and the EAWAG report could be ignored. Therefore, the overall model results have satisfactorily followed the simulated habitat data and the simulated hydrodynamic results in the EAWAG report.

Table 4.2: The parameter descriptions for suitability index class.

SI-class	1	2	3	4	5
Values	0-0.1	0.1-0.2	0.2-0.3	0.3-0.4	0.4-0.5
SI-class	6	7	8	9	10
Values	0.5-0.6	0.6-0.7	0.7-0.8	0.8-0.9	0.9-1

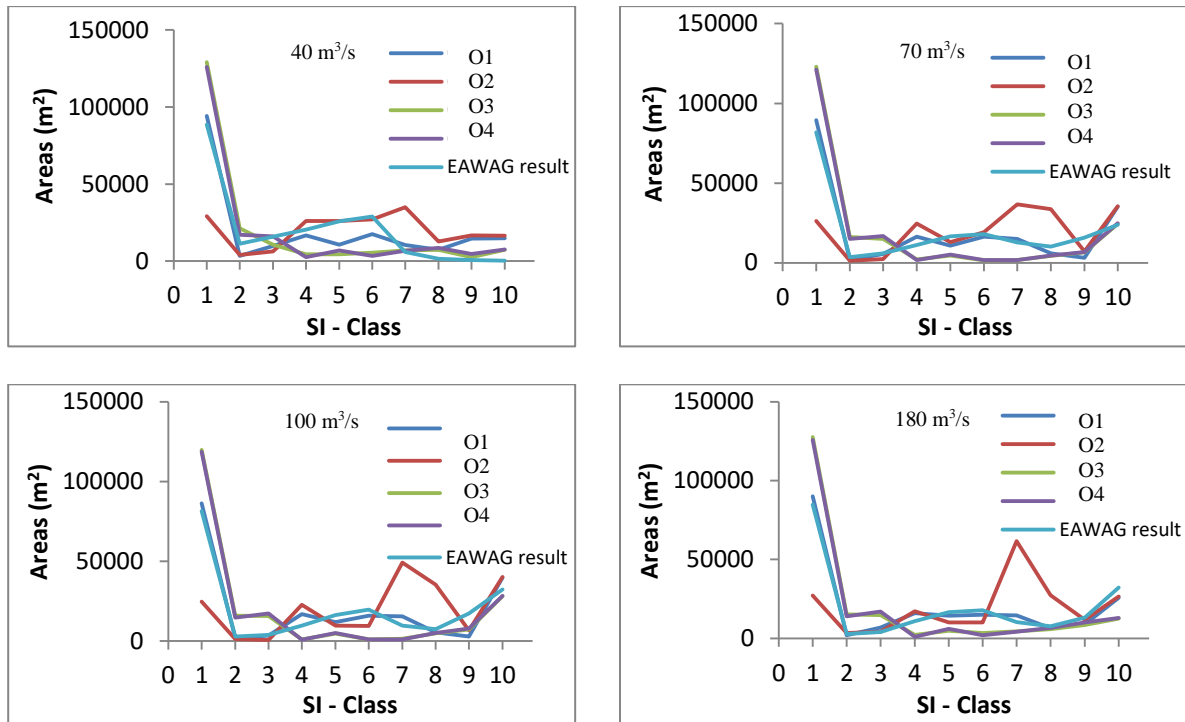


Figure 4.6: The WUA values comparison for four habitat computational options and the EAWAG report.

The SI-class described in Figure 4.6 is shown in following table (Table 4.2):

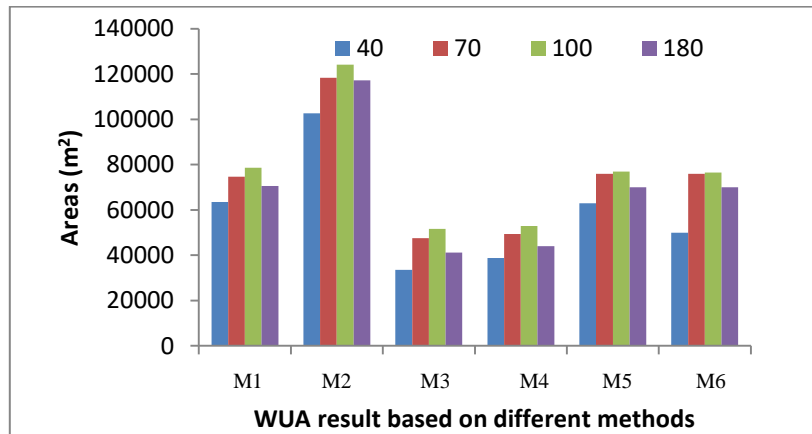


Figure 4.7: The WUA comparison based on six different methods.

The methods described in Figure 4.7 are shown in Table 4.3.

Table 4.3: The parameters for WUA comparison.

Method	Meaning
M1	Simulation based on computational option O1
M2	Simulation based on computational option O2
M3	Simulation based on computational option O3
M4	Simulation based on computational option O4
M5	Simulation based on EAWAG SI curves
M6	Simulation based on EAWAG fuzzy logic method

4.5 Model results

The historical natural flow discharges from 1970 to 2000 were used to predict the habitat quality, population number fluctuations, and population density distributions. In this case study, two hypothetical simulation scenarios (E1 and E2) were made to investigate the physical parameters effects on the European grayling's habitat and population situation. The scenario E1 is the model system composed of a hydrodynamic model, a habitat model, and a population model. The scenario E2 is the model system composed of a hydrodynamic model, a hydromorphology model, a habitat model, and a population model.

4.5.1 Hydrodynamic and hydromorphology simulations

Figures 4.8a, b, and c show the dynamic change of velocities, water depths, and riverbed substrates from 1970 to 2000 in scenario E1 and E2. It can be seen that in the whole computational domain of the Aare River, the two scenarios E1 and E2 have very similar results in terms of velocities, water depths, and substrates distribution in 1970. However, there are noticeable differences between the scenarios E1 and E2 since 1980. More specifically, in 1980, the velocity near the outlet of the Aare River was 1.2 m/s in scenario E2, while the velocity in scenario E1 remained at the level of 1.8 m/s. Likewise, from 1970 to 2000, the substrate diameter showed an increasing trend in scenario E2, especially in areas near the outlet and the other two small regions in the computational domain. However, the water depth difference between scenario E1 and scenario E2 can be ignored from 1970 to 2000.

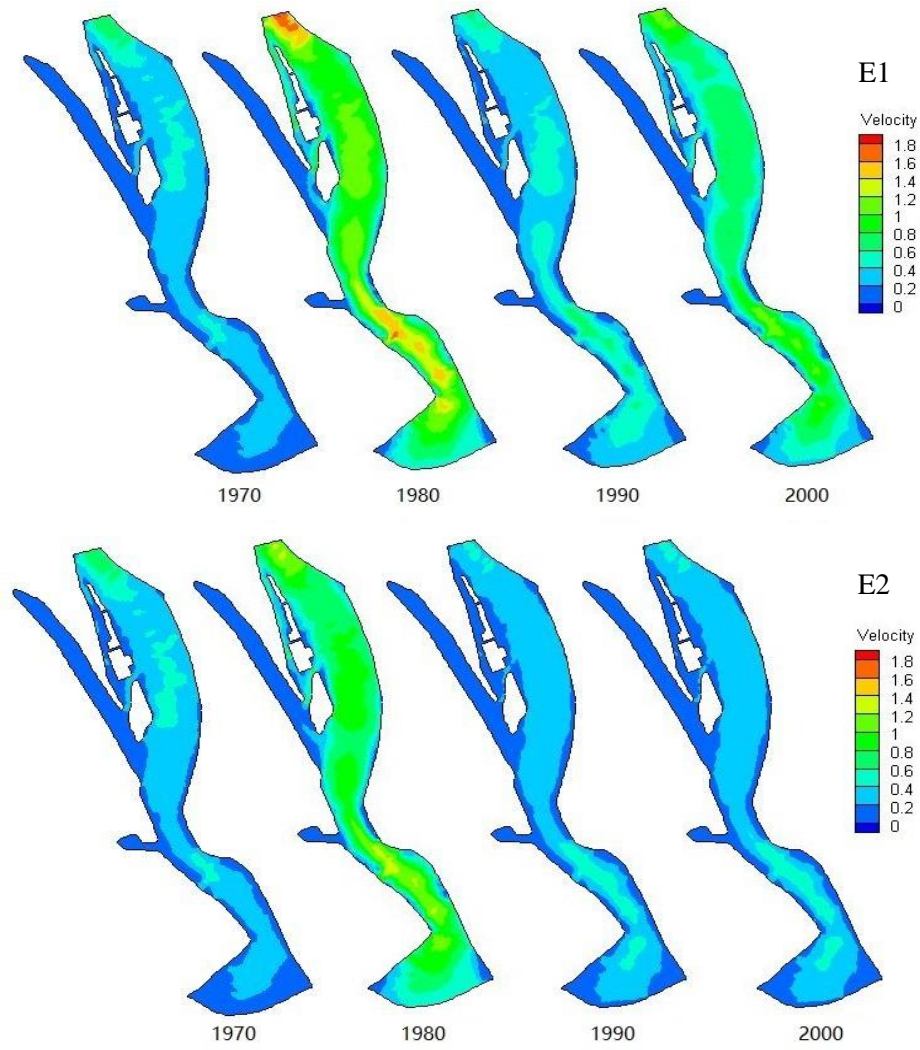


Figure 4.8a: The velocity distributions in 1970, 1980, 1990, and 2000 in scenarios E1 and E2.

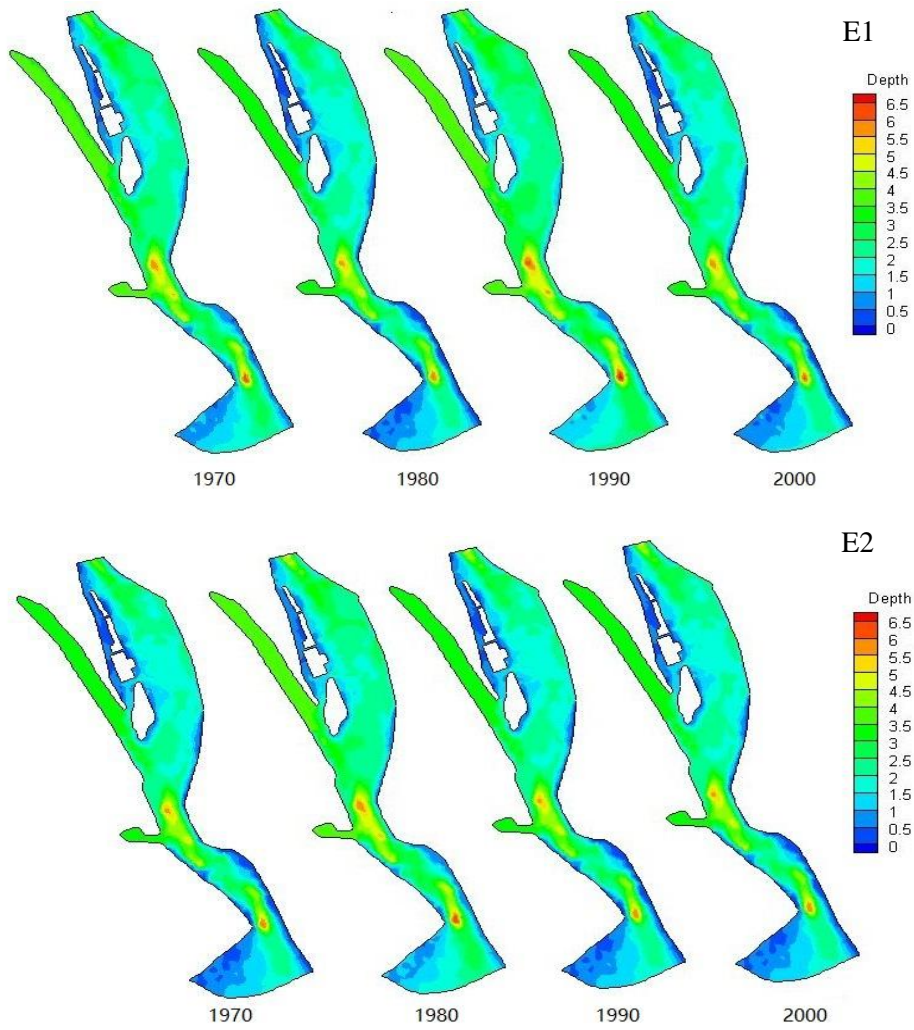


Figure 4.8b: The water depth distributions at 1970, 1980, 1990, and 2000 in scenarios E1 and E2.

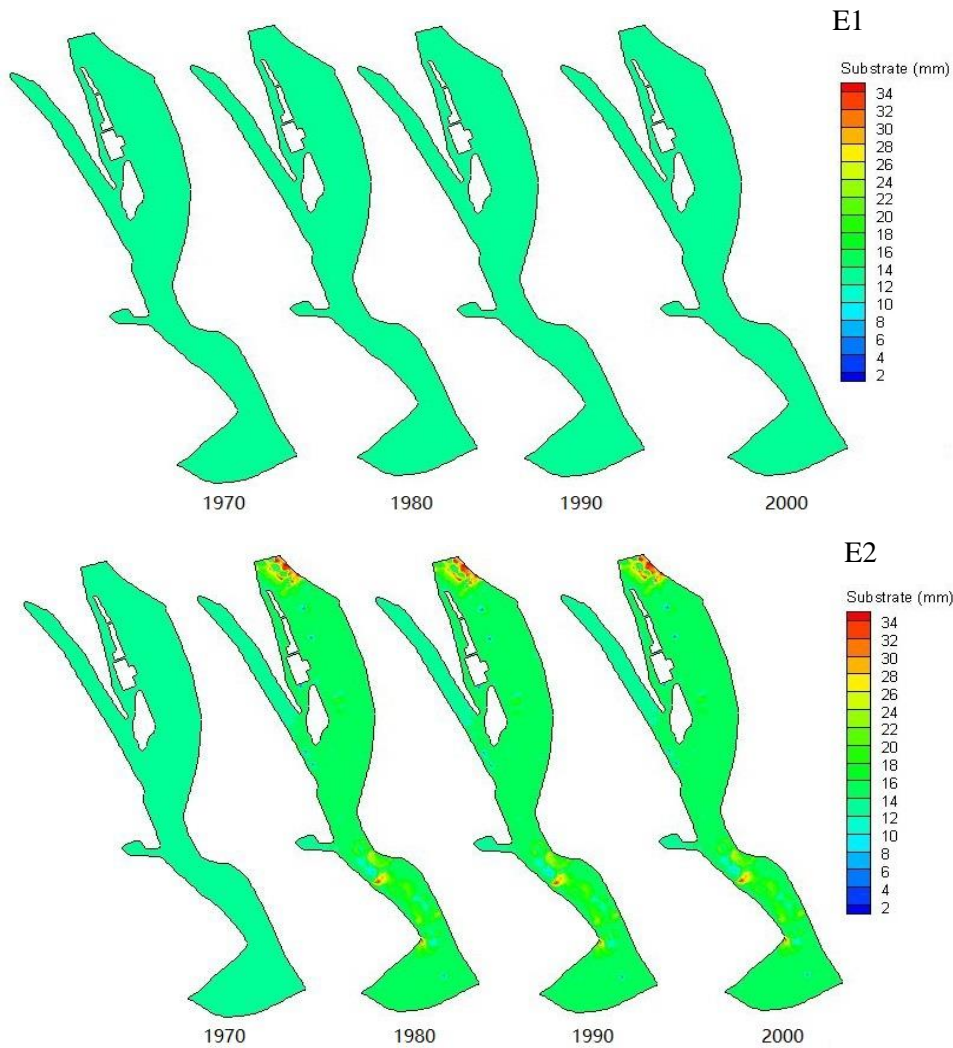


Figure 4.8c: The substrate distributions at 1970, 1980, 1990 and 2000 in scenarios E1 and E2.

4.5.2 Habitat quality simulation

In this case study, the spawning European grayling HSI distributions in scenarios E1 and scenario E2 were determined by combining the SI values for velocity, water depth, and substrate using Equations 3-39, 3-40, 3-41, and 3-42. In scenario E1, the simulation results indicate a high HSI values for the European grayling in the Aare River. However, the HSI distribution calculated by the four different computational options (Equations 3-39 to 3-42) show noticeable differences (Figure 4.9, Figures III.1a, III.1b). The simulation results showed that the best habitat computational option is O2 (Figures III.1a, 1.b). For all four computational options, in 1970, the high HSI values were mainly concentrated in mid-length of the computational domain which is 200 to 500 m away from the inlet and 200 to 600 m away from the outlet. The main difference of HSI distribution from O1 to O4 is the fact that the HSI values in a large areas of the computational domain

is equal to or large than 0.3 for O2, but the HSI values for O1, O3 and O4 are approximately 0 in the areas of near inlet, outlet, tributary, and mid-length along the river stretch. In 1980, 1990, and 2000, the HSI distributions had the same trend as in 1970. The O2 has best habitat quality, while O3 and O4 have the worst habitat quality. The O1 habitat quality is in the middle of O2 and O3/O4.

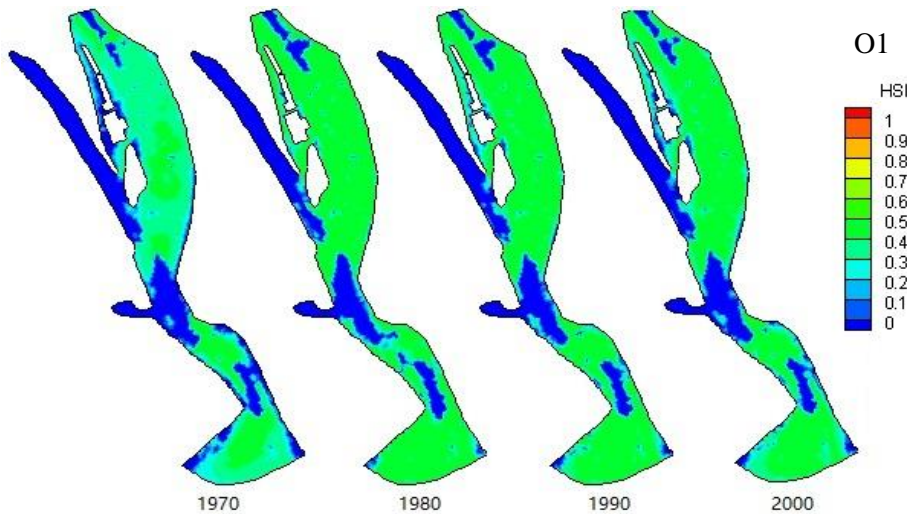


Figure 4.9: The HSI distribution at 1970, 1980, 1990 and 2000 for O1 and in scenario E1 based on spawning SI curves.

Appendix Figures III.2a, 2b and Figure 4.10 show the spawning European grayling HSI distributions in scenario E2, which indicate different trends from that obtained by scenario E1. Comparing the HSI distributions in scenario E2 with E1, the habitat quality in scenario E2 is slightly better than that of E1. More specifically, in 1970, the HSI distribution based on O1 showed the same trends as that of E1, with most of the unsuitable HSI values fallen in the tributary of the Aare River, outlet, and mid-length of the river stretch. The regions with high water depths had low SI values for water depth. For O1, the HSI values for the rest of the domain resulted in a value of approximately 0.5. In 1980, the HSI distributions for O1 was similar to that in 1970 for the majority of areas except some small regions with very high HSI values scattered along the river stretch. In 1990, the HSI distribution had the same trend as the HSI distribution in 1980 for O1, O2, O3 and O4, except that the HSI values improved near the regions with the highest water depths. At the end of the simulation time, i.e. in 2000, regions with high HSI values were very small for all four computational options. High HSI value regions were located in the regions near the outlet and scattered along the axis of the river. For O2, the HSI quality was better than for O1; HSI values for the main river ranged from 0.3 to 0.7, and the HSI values in the river tributary were nearly 0.1. Habitat quality for O3 and O4 were worse than habitat quality for O1 and O2 with low HSI values distributed along the whole river stretch. The Figures III.2a, and 2b also indicate that the HSI distribution based on the O2

produced better habitat quality results than the habitat quality at O1, O3, and O4. The worst HSI distribution was displayed by O3 and O4.

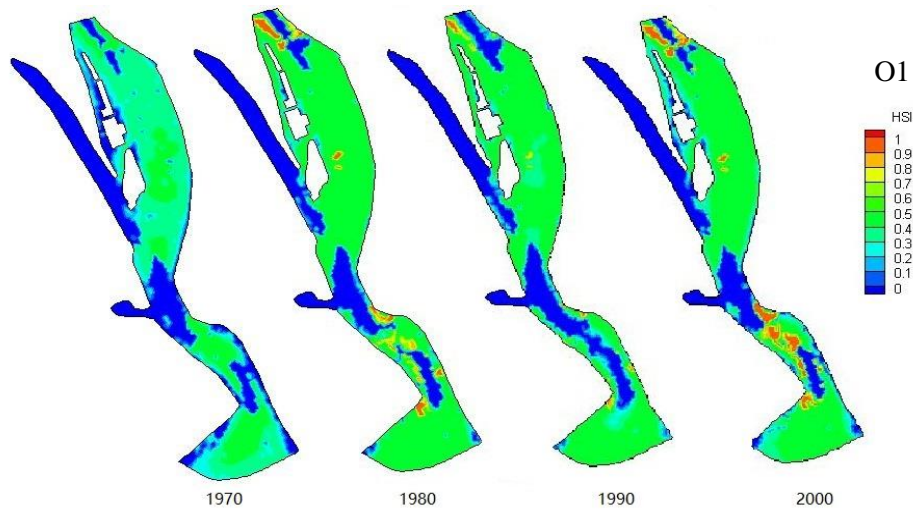


Figure 4.10: The HSI distribution at 1970, 1980, 1990, and 2000 for O1 and in scenario E2 based on spawning SI curves.

The WUA and OSI values based on spawning SI curves in scenario E1 showed exactly the same trends for the simulation period from 1970 to 2000. The simulated results for scenario E1 are shown in Figure 4.11. It can be noticed that there are no visible trends for WUA and OSI values fluctuations for O1, O2, O3 and O4 from 1970 to 2000. More specifically, the WUA value for O1 ranged from 39,325 m² to 60,982 m² while the WUA values for O3 and O4 were remained at the level of 13,690 m² and 9,950 m² respectively. The WUA values for O2 were much higher than the other computational options, with WUA values ranging from 83,608 m² to 106,128 m². Correspondingly, the OSI values for O1 fluctuated between 0.17 and 0.24 while the OSI values for O3 and O4 were remained at the level of 0.15 and 0.25 respectively. The OSI values for O2 ranged from 0.37 to 0.53.

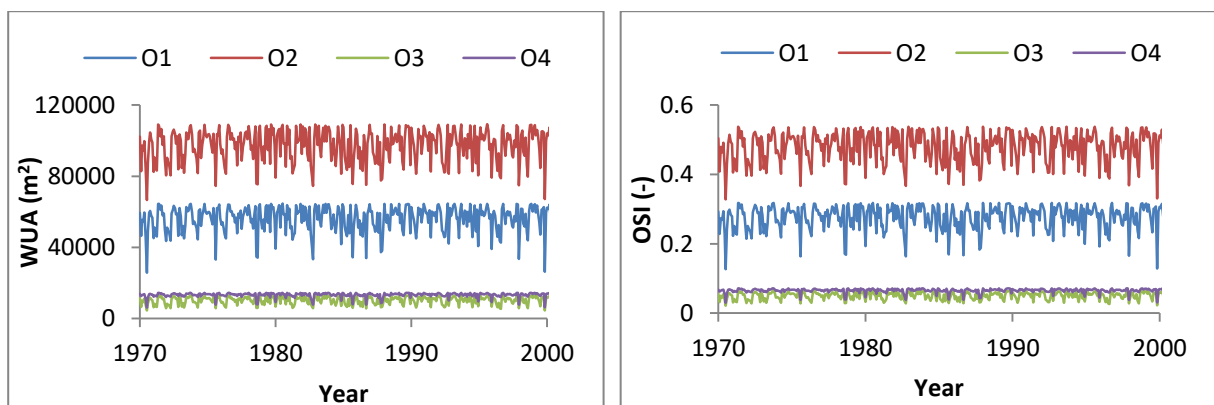


Figure 4.11: The WUA and OSI value fluctuations from 1970 to 2000 for O1, O2, O3, and O4 in scenario E1 based on spawning SI curves.

The WUA and OSI distribution of scenario E2 showed an different trend to scenario E1 (Figure 4.12). It can be noted that the WUA and OSI values showed a slightly increased trend from 1970 to 1980, and then remained stable. The WUA values for O1 and O2 in scenario E2 are slightly higher than the values for O1 and O2 in scenario E1. The OSI values for O1 and O2 in scenario E2 were also slightly higher than the values for O1 and O2 in scenario E1. In scenario E2, the WUA values for O1 mainly ranged from $4.7 \times 10^4 \text{ m}^2$ to $7.0 \times 10^4 \text{ m}^2$, and the corresponding OSI values ranged from 0.23 to 0.34. For O2, the WUA values changed between $1.1 \times 10^5 \text{ m}^2$ and $8.0 \times 10^4 \text{ m}^2$, and the corresponding OSI values changed between 0.44 and 0.55. The WUA and OSI values for O3 and O4 have the same trend. The WUA values fluctuated between $1.2 \times 10^4 \text{ m}^2$ and $2.3 \times 10^4 \text{ m}^2$ for O3 and O4, while OSI values changed between 0.047 and 0.1 for O3 and O4. The WUA and OSI value differences were also calculated and are shown in Figure 4.13. The WUA and OSI value differences for O1 and O2 were much higher than the values for O3 and O4. It can be seen that after 1985, the bigger differences were observed between these two scenarios regarding the WUA and OSI values for O1 and O2.

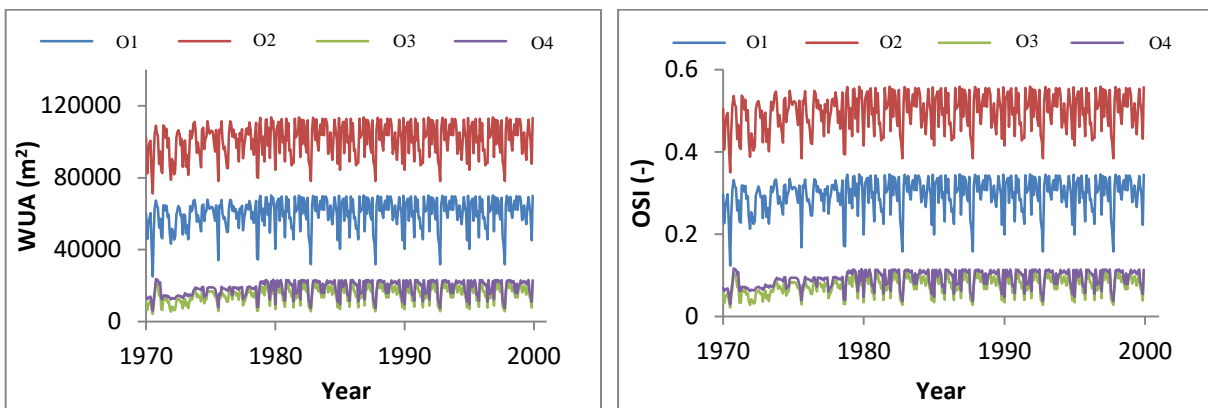


Figure 4.12: The WUA and OSI distribution from 1970 to 2000 for O1, O2, O3, and O4 in scenario E2 based on spawning SI curves.

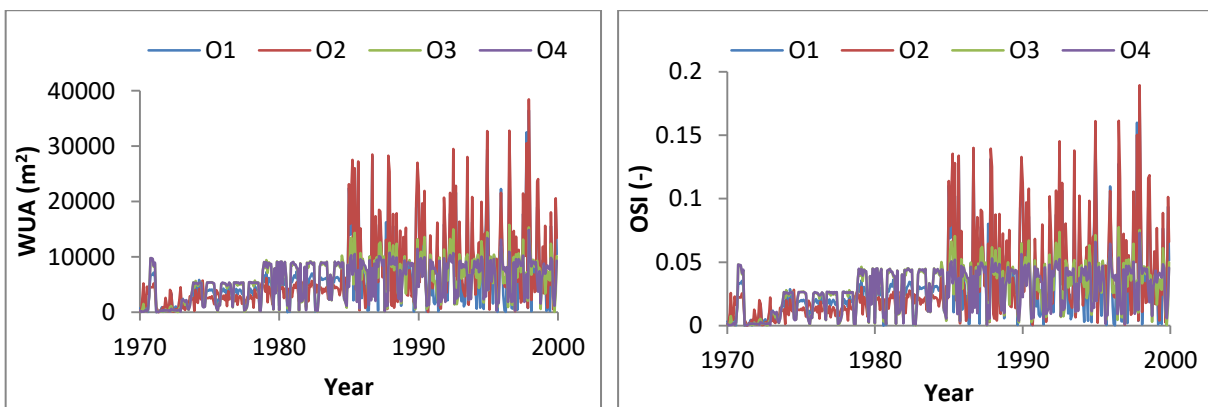


Figure 4.13: The WUA and OSI differences for O1, O2, O3, and O4 between scenario E1 and E2.

4.5.3 Population number analysis based on the logistic population model

After the habitat simulations were completed, the parameters required for population simulation were obtained. In scenario E1, the initial population number was set to 141,900. The empirical parameters α and β for the logistic population model were also settled (Equation 3-48). For O1, α and β have the same values, and are equal to 7 and 6 respectively. For O2, α and β are equal to 7 and 2 respectively. For O3, α and β are equal to 2 and 4 respectively. For O4, α and β are equal to 3 and 1.6 respectively. The general trend for the simulated number of fish from 1970 to 2000 declined from 1.4×10^5 in 1970 to around 2.5×10^4 in 2000 for O1, O2, O3, and O4. The measured fish numbers declined from 538 in 1970 to 28 in 2000 (Figure 4.14). Although there was a small mismatch in a few years, the simulated European grayling fish numbers in the Aare River matched well with the measured fish numbers. The results indicate that there were relative large fluctuations in fish numbers from 1970 to 2000 in O1 and O2 than that of in O3 and O4. This is because the fluctuation pattern in O1 and O2 are more significant than the fluctuation pattern in O3 and O4. It is also notable that the correlation coefficients between simulated European grayling population number and measured fish numbers are 0.73, 0.77, 0.67 and 0.40 for O1, O2, O3 and O4 respectively (Table 4.4).

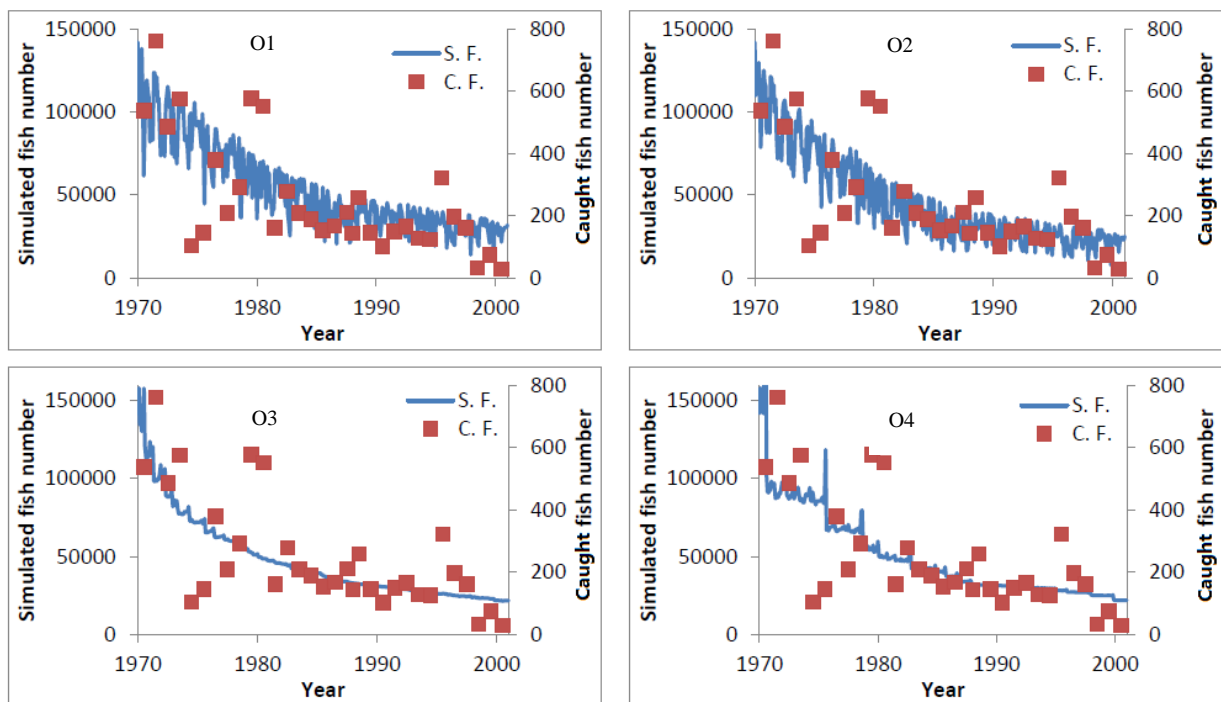


Figure 4.14: The European grayling simulated numbers based on the logistic population model in scenario E1.

Unlike E1, the scenario E2 includes the settings of dynamic changes in the riverbed substrate. The simulated European grayling fish numbers are shown in Figure 4.15 (scenario

E2). With a suitable empirical parameter setting for α and β in the logistic model (Equation 3-48), only a slight difference between the simulated fish number and the surveyed fish number was observed. The numerical model results also indicate that there were relative large fluctuations in fish numbers from 1970 to 2000 in O1 and O2. The simulated fish number fluctuations for O3 and O4 were insignificant when compared to the O1 and O2. For O1, O2, O3, and O4 in scenario E2, the simulated fish numbers decreased from 1.4×10^5 in 1970 to the level of 2.5×10^4 in 2000. It can be seen that the simulated number of European grayling showed reasonable agreement with the caught fish numbers for O1, O2, O3, and O4.

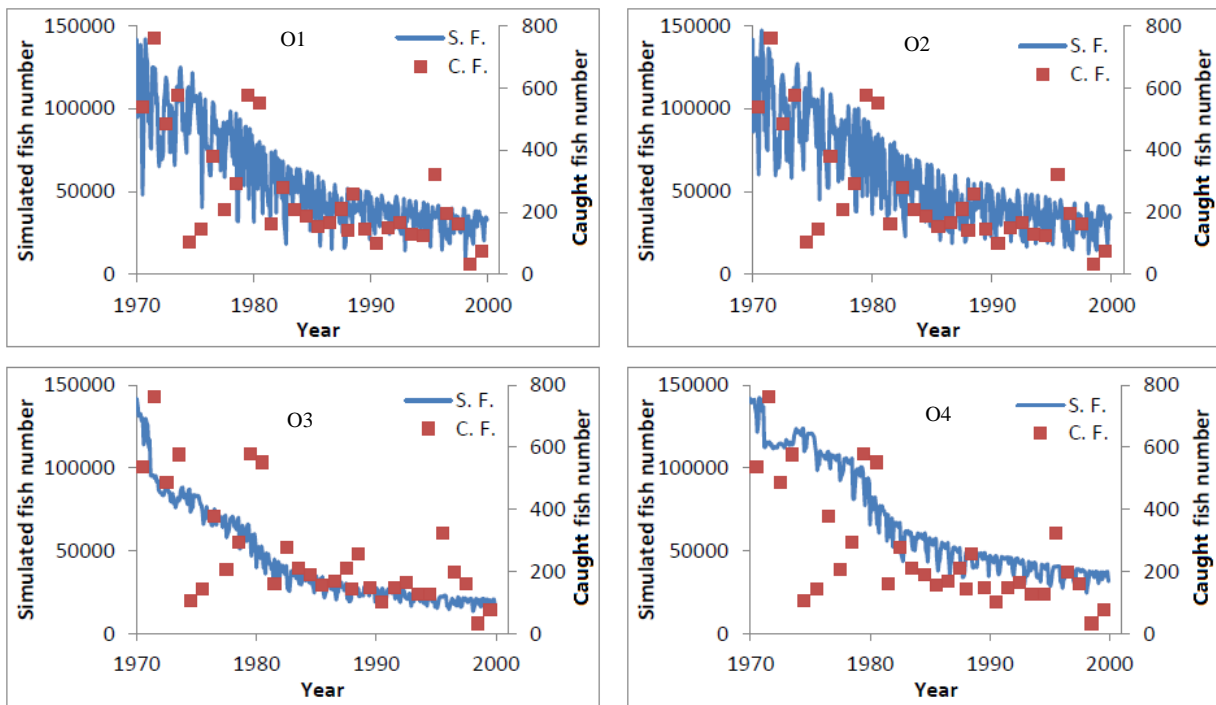


Figure 4.15: The European grayling simulated numbers based the logistic population model in scenario E2.

As shown in Figure 4.16, the fish population number differences between scenario E1 and scenario E2 were not significant for O1 and O3 from 1970 to 2000. For O2 and O4, the values of fish number differences between scenario E1 and E2 displayed a relatively large different compared to O1 and O3 during the simulation time. For O1 and O3, the trends for fish number differences between scenarios E1 and E2 for European grayling showed decreasing trends from 1970 to 1980, and then showed increasing trends from 1980 to 2000. However, the fish number differences between scenarios E1 and E2 showed increased trends from 1970 to 1980 and then showed decreasing trends for O2 and O4 from 1980 to 2000.

Table 4.4: Correlation coefficients between the simulated and measured fish numbers in the Aare River.

	Logistic		Matrix	
	E1	E2	E1	E2
O1	0.73	0.64	0.70	0.71
O2	0.77	0.65	0.70	0.71
O3	0.67	0.67	0.69	0.71
O4	0.40	0.64	0.71	0.71

It should be noticed that compared to scenario E1, scenario E2 is more realistic since both the riverbed evolution and riverbed substrates are considered in the whole model system. It seems that the hydromorphology model does not significantly affect the prediction of fish population number changes in this case study. However, this does not mean that the hydromorphology model should not be included in the ecohydraulic model system. The hydromorphology model is very important, and would affect predicted accuracy in some case studies (see Chapter 6). Overall, scenario E2 can be used to improve results at sites with higher fluctuations in sediment transport affecting the fish habitat and population status significantly (see Chapter 6). Scenario E1 can be used as an alternative for rivers and streams where riverbed deformation and riverbed substrate changes are less important.

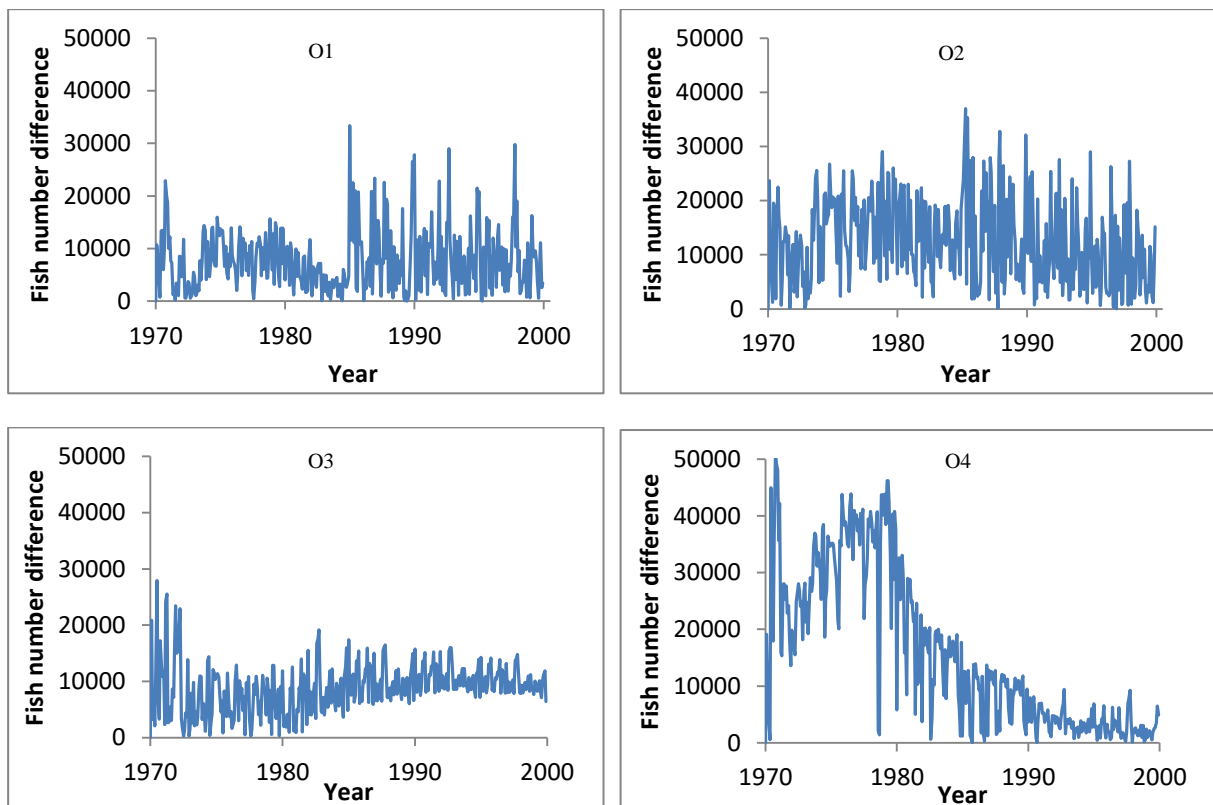


Figure 4.16: The European grayling simulated number differences between scenarios E1 and E2 for O1, O2, O3, and O4 based on the logistic population model.

4.5.4 Population density analysis based on the logistic population model

The calculated fish population density showed a decreasing trend from 1970 to 2000 for all four different computational options (Figure 4.17, Appendix Figures III.3a, 3b). For O1, high fish density values were observed in a large area of the computational domain except the areas near the inlet, tributary, and mid-length of the river. The maximum fish density for the European grayling was 55 fish per mesh cell in 1970, and the fish density decreased to 25 fish per mesh cell in 1980, and further decreased to 15 fish per mesh cell in 1990, finally dropping to 10 fish per mesh cell in 2000. For O2, the fish density distributions were more dispersed. The maximum fish density value in 1970 was 50 fish per mesh cell, while the values declined at all time levels and reached a density of 5 fish per mesh cell in 2000. The maximum fish density values obtained from O3 and O4 were higher than the maximum population density values calculated for O1 and O2. As shown in Appendix Figures III.3a and 3b, a very high fish density value (100 fish per mesh cell) was observed in three regions of the Aare River in 1970 when using computational options O3. However, the maximum value of the European grayling density decreased to a maximum value of 30 fish per mesh cell in 1980. The maximum fish density value further decreased from the 1980s to 1990s, and reached a value of 20 fish per mesh cell in 2000. For O4, the maximum fish density value in 1970 was 75 fish per mesh cell and then the maximum density value dropped to a value of only 10 fish per mesh cell in 2000.

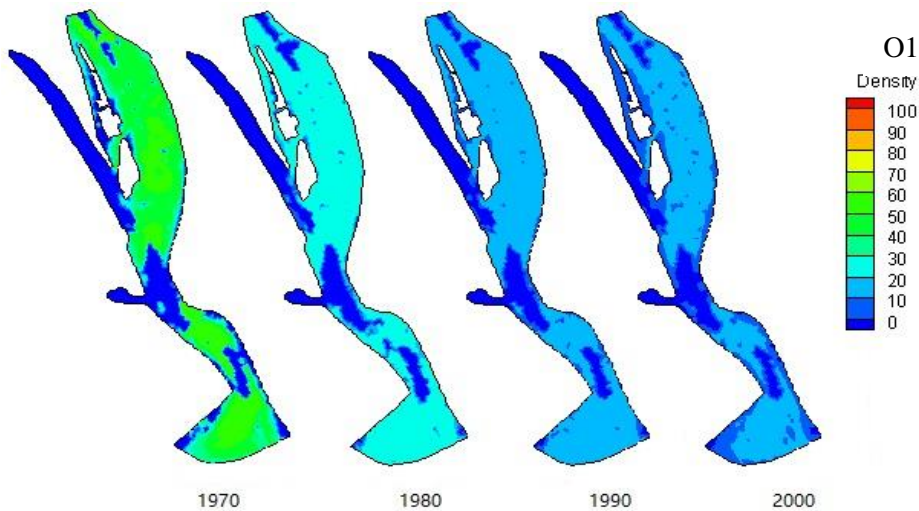


Figure 4.17: The European grayling density distributions for O1 in scenario E1 based on the logistic population model.

In scenario E2, the European grayling density distribution based on the logistic population model was calculated, and the results are shown in Figure 4.18, and Figures III.4a, 4b. In scenario E2, the fish population density distribution shows similar trends for O1, O2, O3, and O4. The maximum fish density values for O1, O2, O3, and O4 in scenario E2 were slightly higher than the respective maximum fish density values for O1, O2, O3,

and O4 in scenario E1. When using O1 in scenario E2, the maximum fish density value was shown to be 55 fish per mesh cell in 1970, and the maximum fish density decreased to 35 fish per mesh cell in 1980. Notably, the maximum fish density value in 1990 was similar to 1980, and the fish density distribution trend in 2000 was very similar to the distribution trend in 1990. When choosing O2 for fish density simulation in scenario E2, the fish density distribution showed similar trends at all times, with the maximum values of 50, 30, 30, and 20 fish per mesh cell for 1970, 1980, 1990, and 2000 respectively. Additionally, similar distribution trends in fish populations in most years were observed in O3 and O4, while the maximum fish density values in O3 was higher than the values in O4.

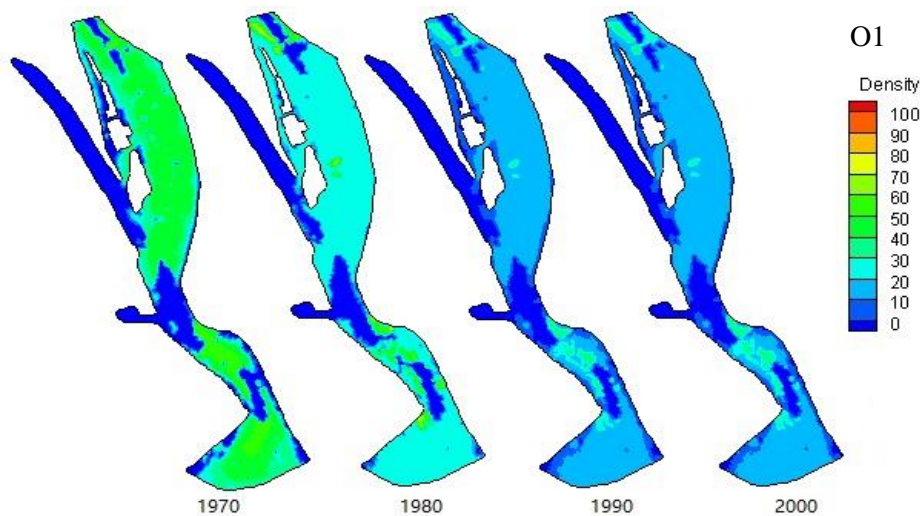


Figure 4.18: The European grayling density distributions for O1 in scenario E2 based on the logistic population model.

4.5.5 Population number analysis based on the matrix population model

By applying the matrix population model, all 9 life stages European grayling numbers were simulated in the Aare River. The OSI values were used as an input parameter for fish number simulation at all life stages.

The initial fish survival rate, fertility rate, and resulting life stage distributions were computed based on the Robson & Chapman method (1961), and the parameters used are shown in Table 4.1. In the surveyed fish sample, a catch curve from fish population is determined. Based on the catch curve, each life stage' proportions are obtained. The fish numbers of each life stage are equal to the proportions of each life stage multiplied by the total fish number. Similar to the two empirical parameters (α , β) in the logistic population model (Equation 3-48), two empirical parameters (a , b) are used in matrix population model (Equations 3-50, 3-51).

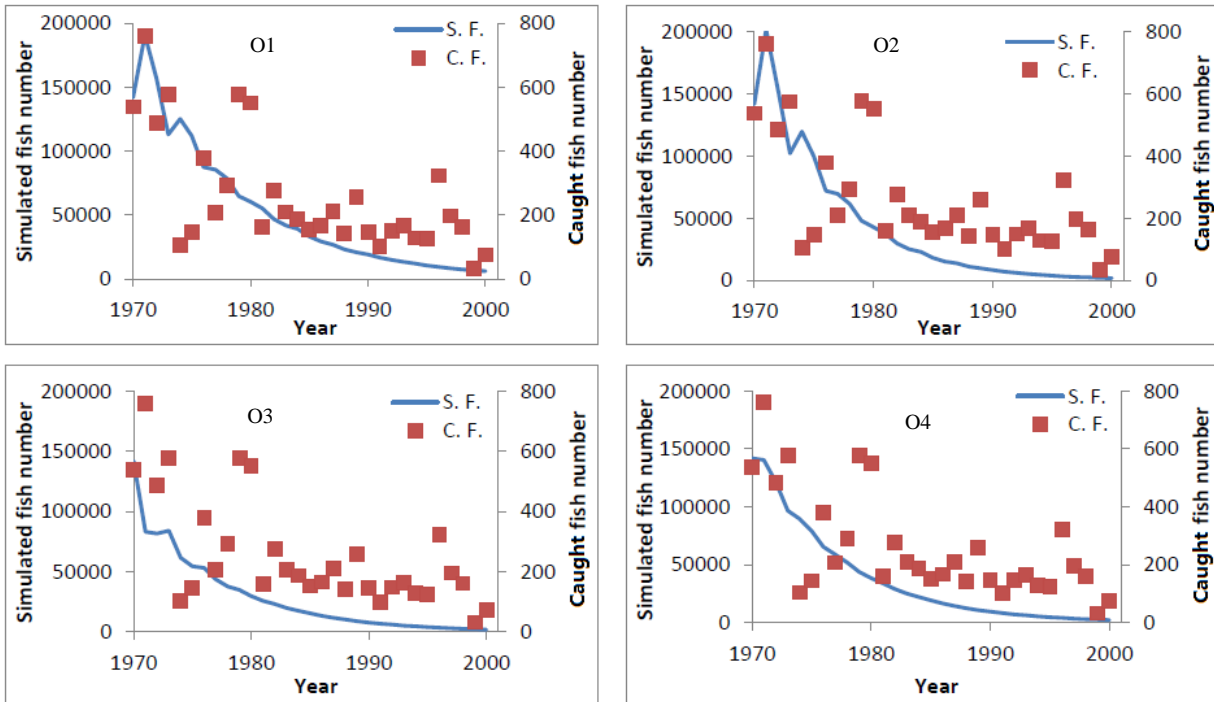


Figure 4.19: The simulated European grayling number based on the matrix population model in scenario E1.

In scenario E1, the values of empirical parameter a are 0.408, 0.599, 0.002, and 0.276 for O1, O2, O3, and O4 respectively. The values of empirical parameter b are settled as 0.406, 0.614, 0.002, and 0.274 for O1, O2, O3, and O4 respectively. For all four computational options, the numbers of European grayling in all nine life stages' were simulated, and the results are shown in Figures 4.19 and 4.20. It can be noticed that all four computational options for simulated total fish numbers have a reasonable agreement with the measured fish data (Figure 4.19). The correlation coefficients between simulated fish numbers and measured fish numbers are 0.70, 0.70, 0.69, and 0.71 for O1, O2, O3, and O4 respectively (Table 4.4). The simulated fish numbers increased from 141,900 in 1970 to 19,100 in 1971 and then declined to 5,970 in 2000 for O1. Similar to O1, the simulated fish numbers increased from 141,900 in 1970 to 20,200 in 1971 and then declined to 1,620 in 2000 for O2. The simulated fish number declined from 141,900 in 1970 to 2,160 in 2000 for O3, and to 2,390 in 2000 for O4 (Figure 4.19). For all nine life stages, a consistently decreasing trends from 1st to 9th life stages were observed. As shown in Figure 4.20, the fish numbers in the first life stage constituted a large proportion of the whole European grayling population numbers. Moreover, O1, O2, O3, and O4 have similar life stage distributions during the simulation times regarding fish age structure: the fish numbers in the early life stages significantly decreased compared to fish numbers in the other life stages during the simulation period (Figure 4.20).

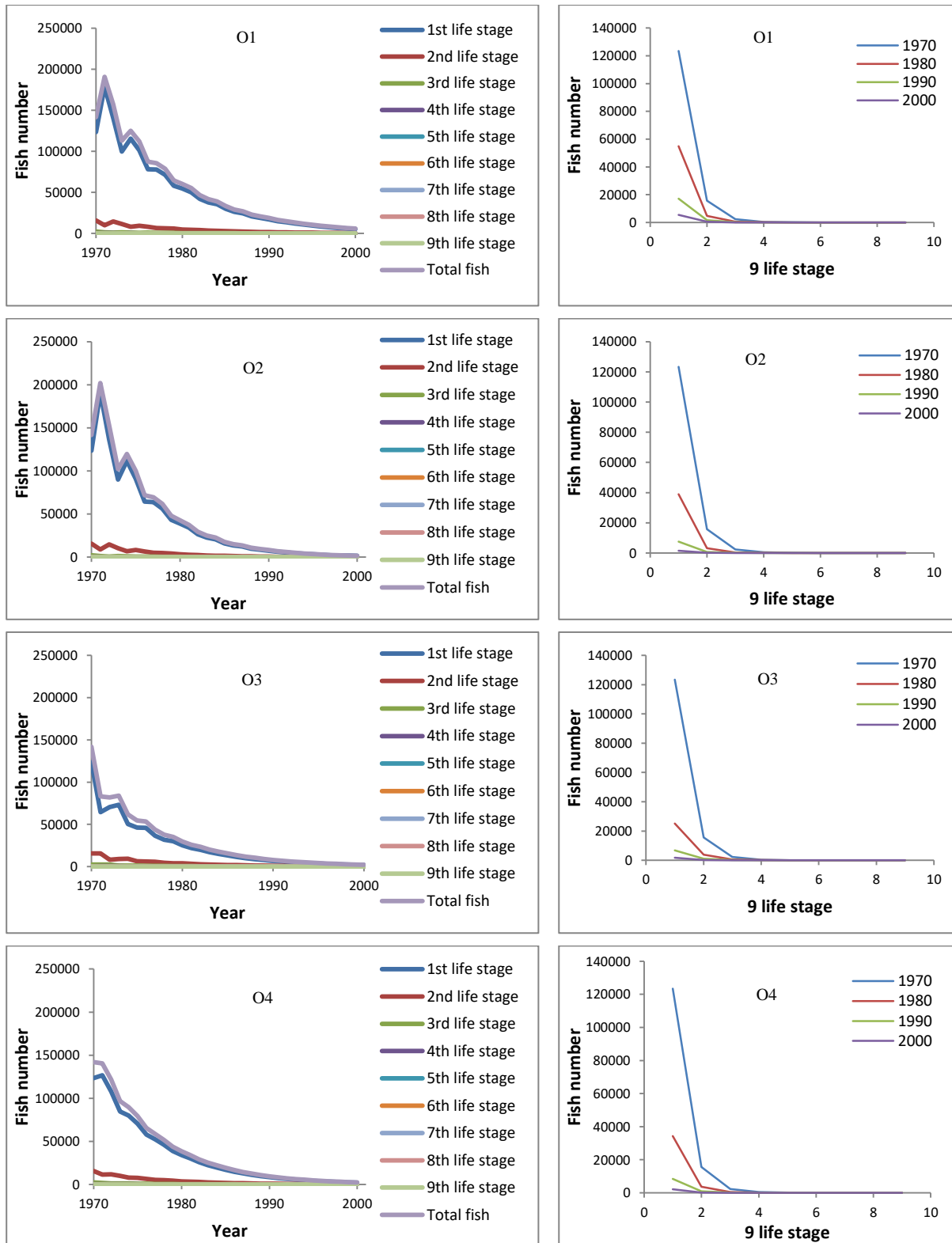


Figure 4.20: The European grayling population numbers of all life stages computed from the matrix population model in scenario E1.

In scenario E2, the values of empirical parameter a are 0.41, 0.60, 0.25, and 0.27 for O1, O2, O3, and O4 respectively (Equations 3-50, 3-51). The values of empirical parameter b settled as 0.41, 0.61, 0.25, and 0.27 for O1, O2, O3, and O4 respectively (Equations 3-39 to 3-42). The results of simulated fish numbers based on the matrix population model are shown in Figure 4.21. It can be seen that the correlation coefficients between simulated fish numbers and measured fish numbers are 0.69, 0.67, 0.70, and 0.70 for O1, O2, O3, and O4 respectively. Similar fish numbers for all four computational options were observed in scenario E2. Moreover, the total simulated fish numbers have good agreement with the measured fish data in O1, O2, O3 and O4.

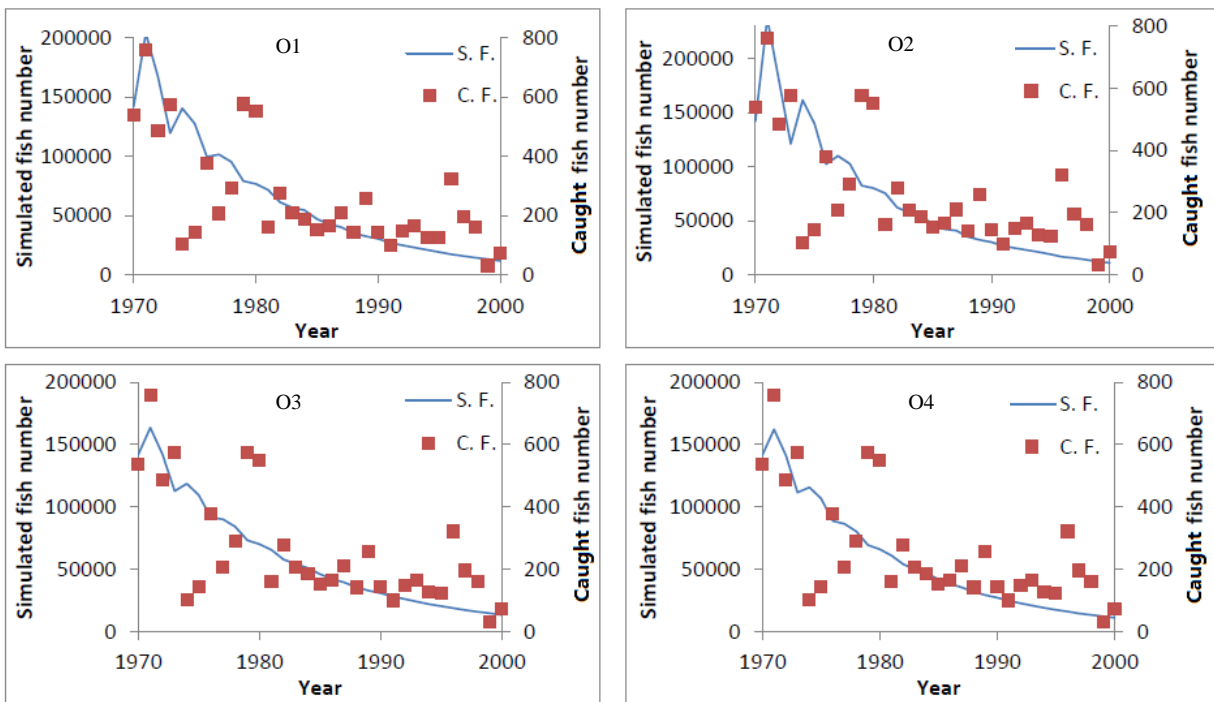


Figure 4.21: The simulated European grayling numbers based on the matrix population model in scenario E2.

In scenario E2, the simulation results of fish age structure distributions based on the matrix population model are shown in Figure 4.22. It can be noticed that the 1st life stage's fish population numbers showed an increasing trend from 1970 to 1972 for O1, O2, O3, and O4. The 1st life stage's fish population numbers decreased dramatically from 1972 to 2000 for O1, O2, O3, and O4. In contrast to the 1st life stage's fish numbers, the other fish life stages showed decreasing trends during the simulation times. The fish numbers in the 1st life stage represented a large proportion of the whole population numbers during the simulation times (from 1970 to 2000).

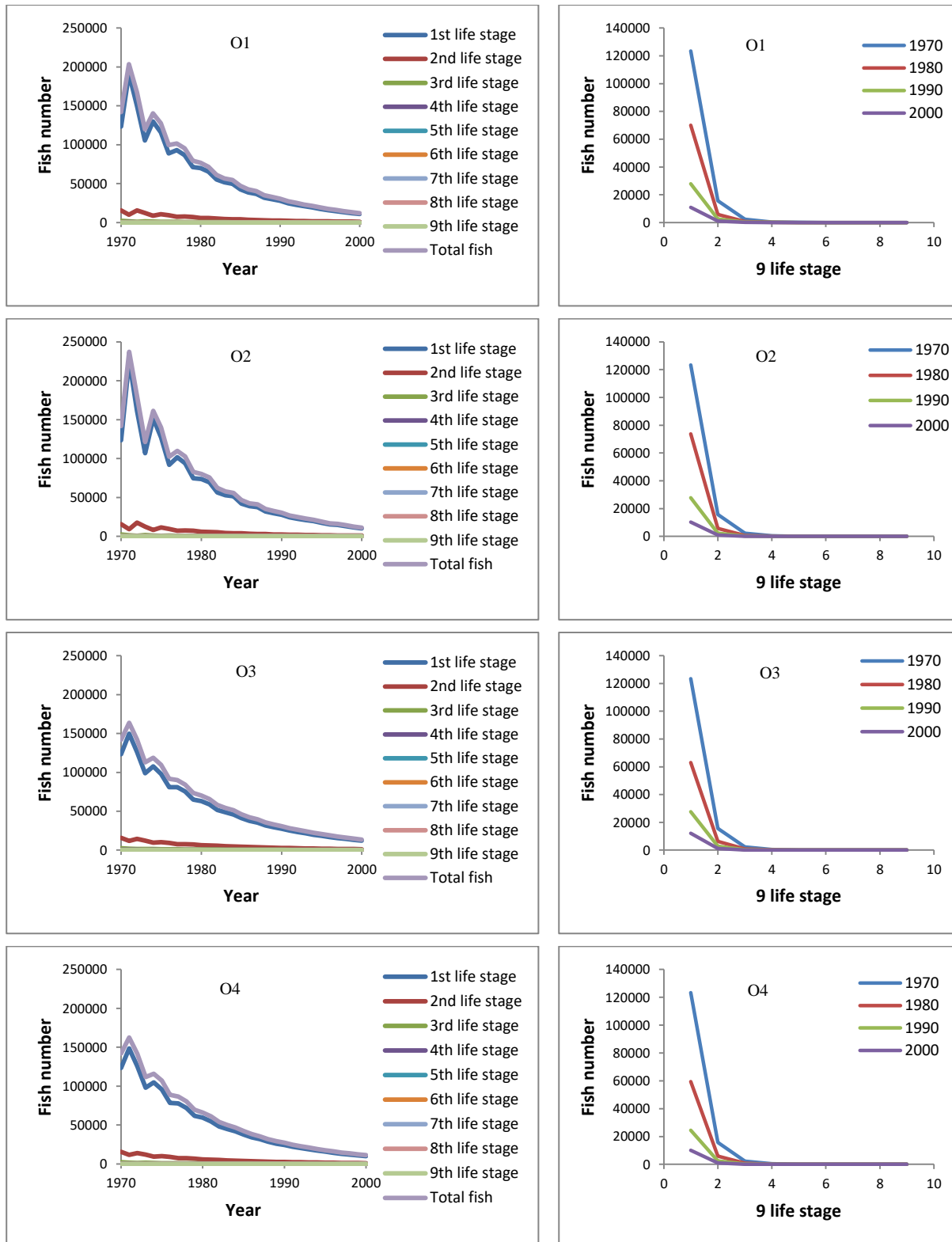


Figure 4.22: The European grayling population numbers and age structure based on the matrix population model in scenario E2.

The difference in fish numbers and fish age structure distributions between scenario E1 and E2 are shown in Figure 4.23. The significant fish number differences between scenarios E1 and E2 were observed in 1978, 1974, 1971, and 1976 for O1, O2, O3, and O4 respectively. The maximum values of fish number differences between scenario E1 and E2 for O1, O2, O3, and O4 are 1.6×10^4 , 4.0×10^4 , 8.2×10^4 , and 3.0×10^4 respectively. Among these, the values of fish number differences between scenario E1 and E2 for O3 display notable differences compared to the other three computational options, while the values of fish number differences among O1, O2, and O4 are relatively similar.

The values of fish number differences between scenarios E1 and E2 for European grayling life stage distribution showed an increasing trend from 1970 to 1980 with a maximum value of 1.2×10^4 in 1980 for the early life stage's fish (Figure 4.23). However, a decreasing trend was observed from 1980 to 2000 for the values of 1st life stage' fish number difference. The values of fish number difference in the 1st life stage were 1.5×10^4 for O1, 3.4×10^4 for O2, 3.8×10^4 for O3, and 2.5×10^4 for O4 in 1980. However, these values reduced to 5.0×10^3 for O1, 8.7×10^3 for O2, 1.0×10^4 for O3, and 1.4×10^3 for O4 in 1990, and continued declined to 5.0×10^4 for O1, 8.7×10^4 for O2, 1.0×10^4 for O3, and 7.9×10^3 for O4 in 2000.

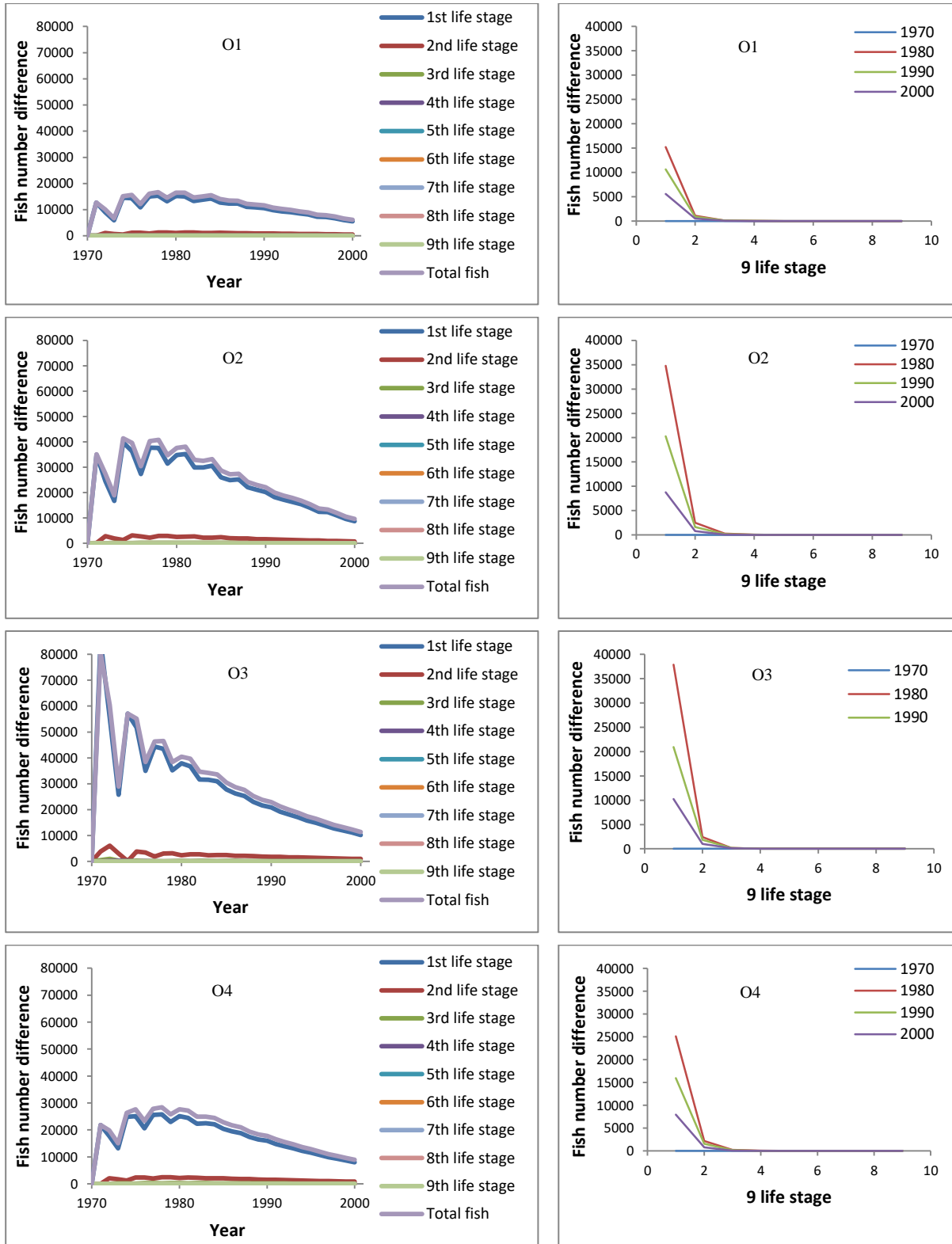


Figure 4.23: The population number and life stage distribution differences between the scenario E1 and scenario E2 based on the matrix population model.

4.5.6 Population density analysis based on the matrix population model

The European grayling population density computed from the matrix population model shows a decreasing trend for all four habitat computational options from 1970 to 2000 (Figure 4.24, Figures III.5a, 5b). For O1, the maximum fish density value was 85 fish per mesh cell in 1970, with the highest density along the river bank region. The density distribution trend in 1980 was similar to 1970, but the maximum population density declined to 35 fish per mesh cell in 1980. The maximum fish density further decreased to 10 fish per mesh cell in 1990 and to 7 fish per mesh cell in 2000. For O2, the maximum fish density was also located along the river bank, and fish density attained values of 70 fish per mesh cell in 1970, 40 fish per mesh cell in 1980, and 10 fish per mesh cell in 1990. The population density in 2000 declined to nearly 0 fish per mesh cell. The O3 and O4 displayed very similar fish density distributions. For O3 and O4, the maximum fish density values in 1970 were 100 fish per mesh cell and 80 fish per mesh cell. Respectively. The high density fish population was also mainly distributed along the river bank zones. However, the maximum fish density in both O3 and O4 decreased to 10 fish per mesh cell in 2000.

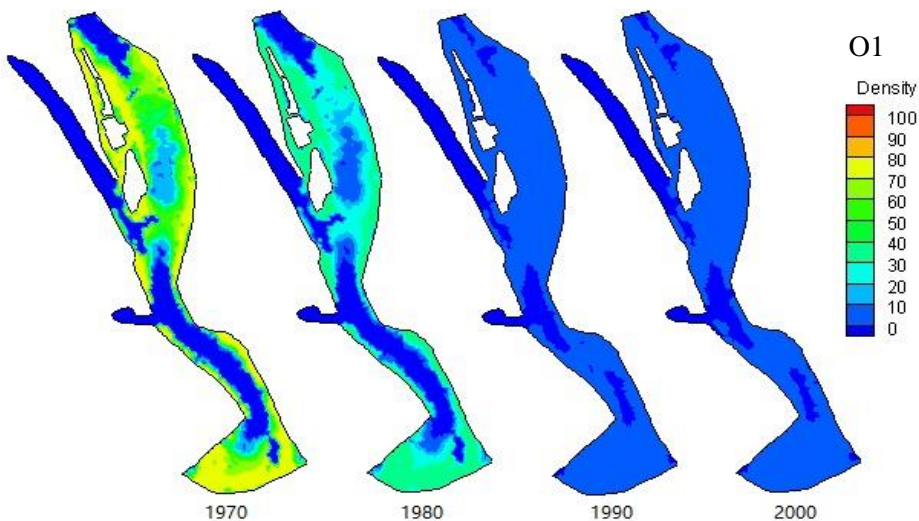


Figure 4.24: The European grayling population density variation based on the matrix population model in scenario E1.

Fish density distribution results in scenario E2 are shown in Figure 4.25 and Appendix Figures III.6a, 6b. The population density values display a decreasing trend for all four computational options. For O1, the high fish density values occurred mainly on the river bank areas with a maximum value of 100 fish per mesh cell in 1970. However, the maximum fish density value decreased to 30 fish per mesh in 1980, to 20 fish per mesh in 1990, and dropped to nearly 0 fish per mesh in 2000. For O2, the fish density distribution is more even distributed except the areas along the river tributary. The maximum fish

density values were 60 fish per mesh cell, 15 fish per mesh cell, 10 fish per mesh cell, and 8 fish per mesh cell in 1970, 1980, 1990, and 2000 respectively. For O3 and O4, the fish density distribution was mainly concentrated along the river bank and the downstream regions. The maximum fish density values for O3 and O4 were more than 100 fish per mesh in 1970, while the value decreased significantly, and dropped to nearly 0 fish per mesh in 2000.

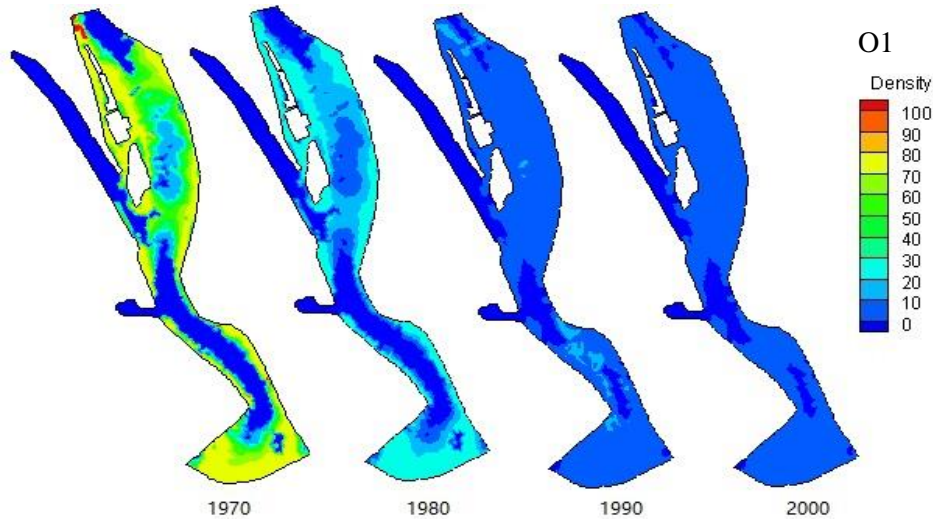


Figure 4.25: The European grayling density variation based on the matrix population model in scenario E2.

4.6 Discussion

The 2D ecohydraulic model system is applied for evaluating the European grayling habitats in the Aare River in this dissertation. The impact of the hydrodynamic, the hydromorphology, four habitat computational options, and the two population models are discussed. The possible solutions for restoring the European grayling population are also recommended in the following paragraphs.

The flow velocities, and water depths appear to be important variables for the European grayling. High SI values for the water depth lead to high HSI values for the majority of the computational domain and for almost all flow rate. Through the comparison of the four computational options, it can be seen that all four computational options can be used to represent the European grayling habitat quality, WUA and OSI values in the Aare River. When only considering the logistic and matrix population model simulation results, the hydromorphology model shows little impact for the European grayling population number changes in the Aare River. However, the hydromorphology model makes the model more adequate to predict habitat quality and fish populations in other places where the changes in riverbed and grain-size distributions are more pronounced (see Chapter 6).

Most models for population dynamic computations assume that the potential development of fish species is homogeneously distributed in large spatial areas (Fahrig & Merriam, 1985). In this case study, the distribution of fish density is related to the HSI distribution, which makes the population distribution more reliable and credible. Both the logistic population model and the matrix population model can simulate changes of fish numbers and trends in fish population distribution. However, there are some different characteristics between the logistic and the matrix population models (see Chapter 3). The matrix population model can provide details about the age structure of the selected fish. In addition, when comparing simulated results and the caught fish numbers, the correlation coefficients between predicted and observed results are in reasonable agreement for both the logistic population model and the matrix population model. More specifically, the fish numbers of all age classes and the fish density distributions can be simulated at each time step. This fish age structure information is extremely important for the case study with dam construction effects and with fish stocking effects (see Chapter 6).

In this case study, one possibility for restoring the European grayling population in the Aare River is the fish stocking strategy, which has been considered as a useful fish population restoration strategy in the Jiao-Mu River (see Chapter 6). In addition, adding the appropriate gravel in necessary areas of the river is also a suitable form of restoration management that improves the SI values for riverbed substrates. Furthermore, it is necessary to identify the critical periods, such as fish spawning season, periods of low flows, and high flows in order to effectively enhance the fish habitat. These periods should be focused on in the first instance (Armstrong et al., 2003). The fish stocking strategy and fish habitat improvement can also be evaluated and quantified by the ecohydraulic model system.

Moreover, adding deadwood structures in spawning areas is a good approach to restoring the fish populations. This solution has been documented and recommended by Guthruf (2005). Another potential strategy for European grayling population restoration could be changing the riverbed substratum. The change of the substratum may improve the fish fertility rate and the survival rate. These two parameters strongly influence fish population numbers and densities. However, the changes of the river substratum are not feasible for a large area.

Fish behavioral and ecological preferences are complex issues. In this case study, the European grayling are undoubtedly also influenced by other factors not accounted for in the ecohydraulic model system. The fairly good agreement between the simulation results and the caught fish numbers is not enough, and the model system needs to be calibrated with more data to evaluate its accuracy and efficiency. Thus, with more improvements to

the ecohydraulic model system, and with more data available to evaluate it, higher efficiency can be expected. Overall, despite the drawbacks and the shortcomings of the ecohydraulic model system, the data agreement between measurement and simulation gives us confidence to accept the model system's predictions.

4.7 Conclusion

In this case study, the impact of flow velocities, water depths, and substrates on the European grayling habitat and fish population in the Aare River were evaluated. The European grayling habitat quality, population numbers, and population distribution have been studied using a hydrodynamic, a hydromorphology, four different habitat computational options, and two different population models. The hydrodynamic and habitat models were validated in the first step against recorded data from a scientific report based on four flow discharges (namely 40 m³/s, 70 m³/s, 100 m³/s and 180 m³/s). In addition, the simulated fish numbers and the measured fish numbers in the Aare River were also compared. The comparison of results indicates that the ecohydraulic model system is satisfactory for simulating hydrodynamic variables, hydromorphologic variables, the European grayling habitats, and population status in the Aare River from 1970 to 2000.

The simulated results show that, firstly, the four habitat computational options successfully predicted the habitat suitability and the population development of the European grayling. The O2 results have the highest WUA and OSI values, and O1 results have the second highest WUA and OSI values. O3 and O4 have similar values for WUA and OSI, and the values are lower than for O2 and O1. Secondly, the logistic population model and the matrix population model achieve high accuracy for fish number simulations. The matrix population model can also predict fish age fluctuations and all fish age density distributions, which is especially important when the fish age structure must be dynamically identified in detail (see Chapter 6).

5 Model application in the Colorado River

5.1 Introduction

The Colorado River is an important water resource in the west of America, serving as the main source of drinking water for more than 25 million people and providing a unique ecosystem for the aquatic species living there. The Colorado River has been extensively engineered to meet these demands. There are 22 major storage reservoirs in the Colorado River Basin and eight major out-of-basin diversions. The two largest storage projects—Hoover and Glen Canyon Dams—are located on either end of Grand Canyon National Park. Glen Canyon Dam is located just north of the Grand Canyon National Park boundary, where it creates Lake Powell. At full capacity, Lake Powell was designed to hold 3.3×10^9 m³ of water and is the key storage unit within the Colorado River Storage Project (CRSP) (Gloss, et al., 2005).

The study case focuses on the river reach which extends from Lees Ferry to 50 km upstream of Lake Mead, at the State of Arizona, United States (latitude 35°30'N to 37°0'N, longitude 111°30'W to 114°0', see Figure 5.1). The case study has been divided into five subareas according to the U. S. Geological Survey's Grand Canyon Monitoring and Research Center. On each subarea, one segment was chosen to represent hydraulic and ecological status of the river stretch. The averaged values of the five subareas were used to represent the whole Colorado River reaches. In this case study, the hydrodynamics, the hydromorphology, the habitat quality, and the population numbers and densities for the years from 2000 to 2009 were simulated. The discharge in all subareas and elevation at outlet has been shown in Figure 5.2.

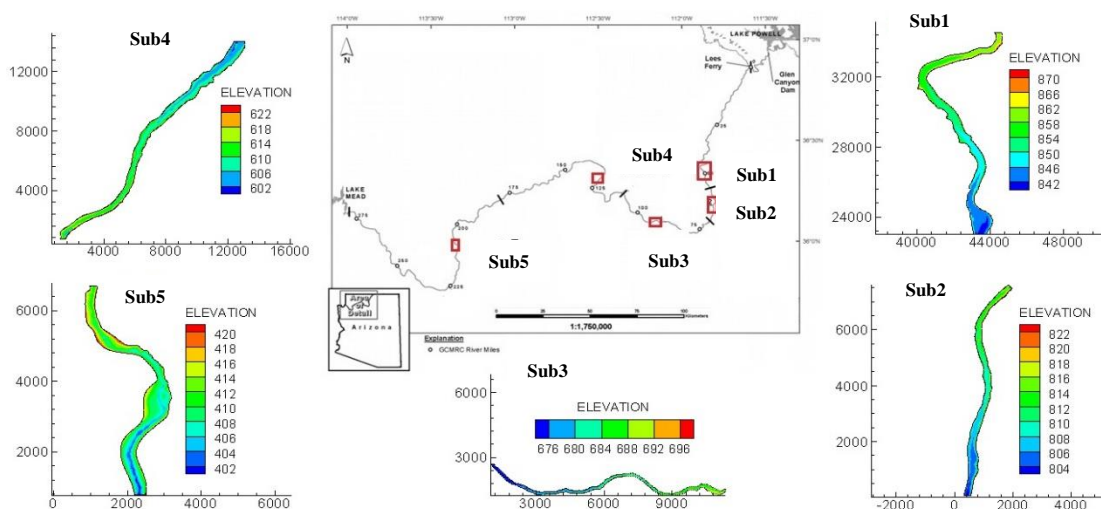


Figure 5.1: Map of the case study area in the Colorado River and computational domain of the meshes in the five subareas.

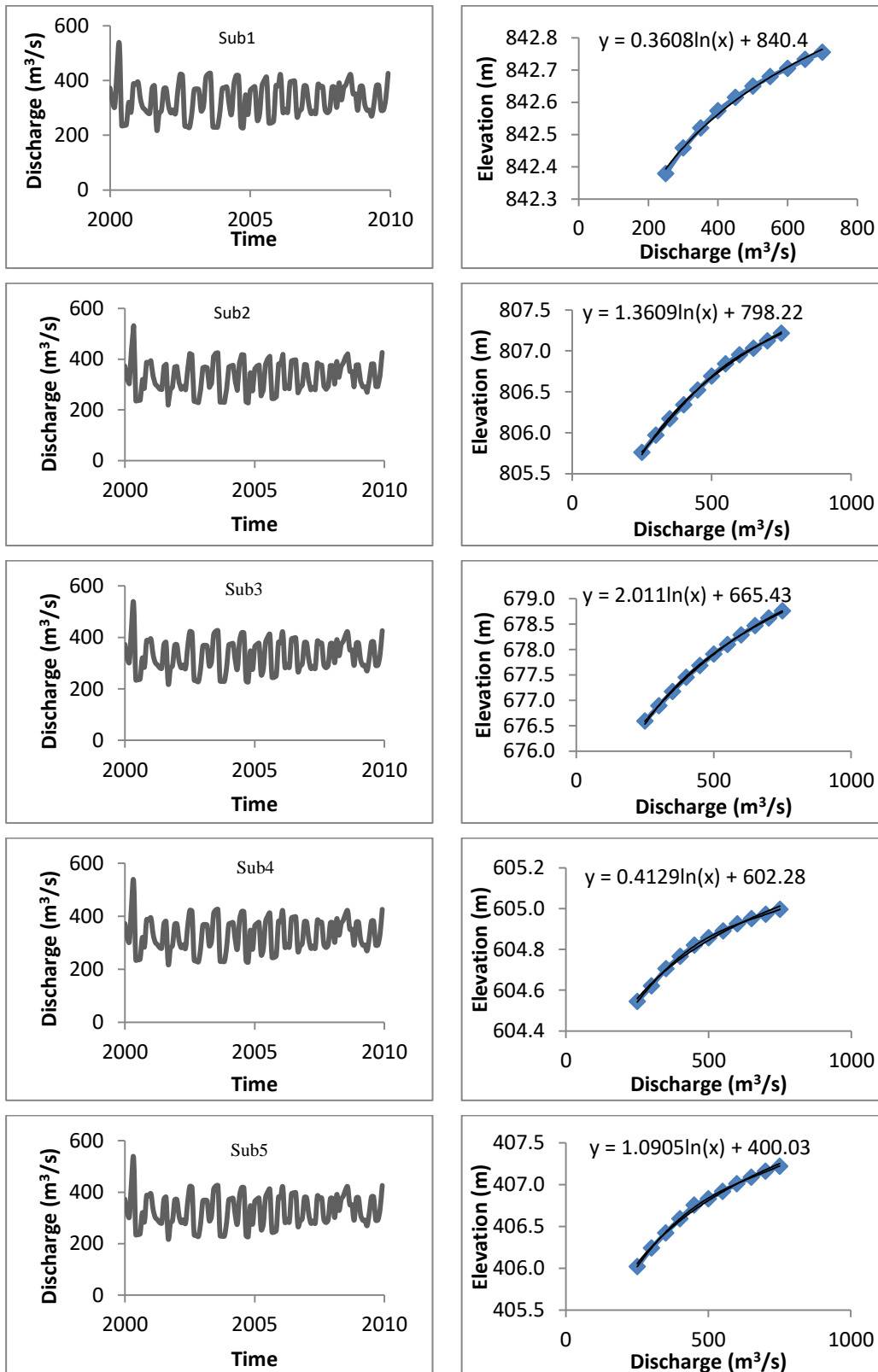


Figure 5.2: Discharge hydrograph at the inlet section and the stage curve at the outlet.

The selected areas have long, steep sections with quiet water separated by turbulent rapids. Periodic debris flows and frequent flash flooding originating in tributaries build debris fans at tributary mouths and deposit large boulders in the river (Cooley et al, 1977;

Webb et al, 1989; Melis et al, 1994; Webb, 1996). The areas selected are important geologically. Four types of surficial deposits are in the landscape of the Colorado River: (1) gravels in upper part of the Colorado River that were deposited in response to glacial activity in the Rocky Mountains; (2) terraces related to accumulation of sand in the channels of the Colorado, resulting from changes in stream flow and sediment load; (3) debris flow deposits at the mouths of relatively small tributaries that form bouldery fan-like surfaces; and (4) flood deposits of the Colorado River that were laid down by unusually large floods (Lucchitta, 1994; Kaplinski, et al., 2000). The particle size distribution and cross-section information were collected (Graf, 1995; Graf, et al., 1995; Flynn et al., 2003; Akahori, et al., 2008; Magirl et al., 2008). The flow discharges from 2000 to 2009 were also collected from the USGS data center (Hazel, et al., 2006).

The Colorado River is an important fish management area and conservationists have set up long-term fish monitoring in the river (Coggins, and Jr., 2008). For example, since the 1990s, several artificial flow tests have been conducted to the benefit of the endangered species and since 2000 two fish monitoring trips have been conducted each year (Makinster et al., 2010; Makinster et al., 2011). The fish monitoring in the Colorado River suggested that there are two types of fish existing in the rivers, two non-native fish species and one native species. The name of these fish species are the rainbow trout, the brown trout, the flannelmouth sucker, and the bluehead sucker. In this case study, we chose two non-native fish species (rainbow trout, brown trout) and one native fish species (flannelmouth sucker) as target fish to evaluate the ecohydraulic quality of the computational domains (Figure 5.3) (Melis, 2011).

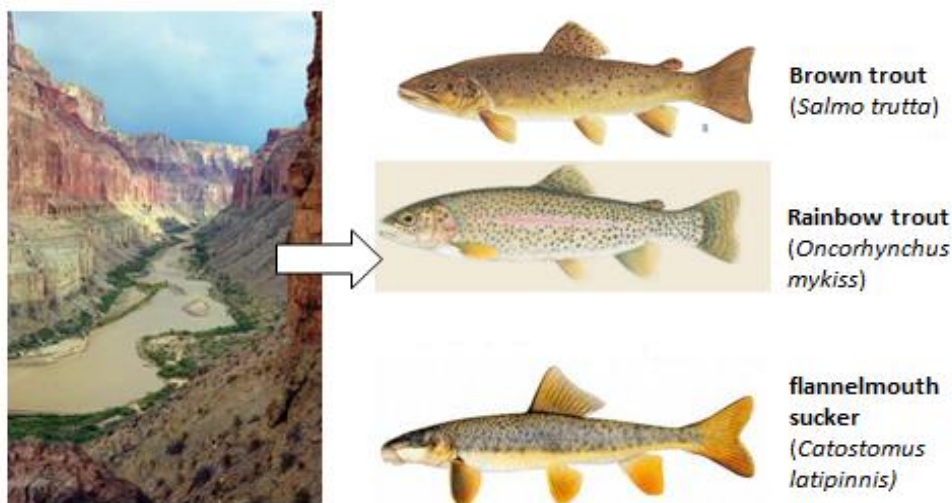


Figure 5.3: The three main fish species living in Colorado River.

The rainbow trout (*Oncorhynchus mykiss*), brown trout (*Salmo trutta*), and flannelmouth sucker (*Catostomus latipinnis*) were selected as targets species and divided into four life

stages: larvae, juvenile, adult, and spawning (Allen, 1983). The target fish species are being affected by dam-induced changes after the completion of Glen Canyon Dam and represent non-native and native fish species in the case study. The historical data of fish monitoring in the Colorado River indicates that the rainbow trout (*Oncorhynchus mykiss*), brown trout (*Salmo trutta*) are non-native and the most abundant fish species in the study river; while flannelmouth sucker (*Catostomus latipinnis*) are the typical native fish (Tyus & Saunders 2000; Minckley et al., 2003; Makinster et al., 2010). Flannelmouth sucker was historically the most abundant large fish species but declined dramatically and become an endangered fish species in the Colorado River Basin (Vanicek et al. 1970; Holden 1973; Minckley 1973; Holden and Stalnaker 1975; McAda 1977; Mueller and Wydoski 2004). Since the 1980s, scientists started efforts to recover endangered fish and started to investigate fish population response to the environmental parameters (Poff, et al., 1997; Melis, et al., 2011; Tyus & Saunders 2000).

In the current research a life stage assessment model was used to estimate population dynamics of target fish by fitting the model to a variety of data sources, including (1) fish number caught and fish length data collected from 2000 to 2009; (2) population estimates of target fish in the study case between 2000 and 2009. The targets fish species were captured two to four times per year in random sample sites by electrofishing before 2000, after that a new sample method was developed and sample site selection was relatively consistent and the targets fish were captured during spring. In order to determine the abundance and life stage of these target fish species, fish numbers, total lengths, and weights for all captured rainbow trouts, brown trouts, and flannelmouth suckers were recorded.

The purpose of this case study is to apply the ecohydraulic model system to evaluate the flow velocities, water depths, and sediment transport status. The ecohydraulic model system was also used to assess the habitat and population conditions of rainbow trout (*Oncorhynchus mykiss*), brown trout (*Salmo trutta*) and flannelmouth sucker (*Catostomus latipinnis*) based on historical flow and geometry records in the Colorado River for the period from 2000 to 2009. The other key objective of the modeling work presented here is to perform a parameter sensitivity analysis for the population model.

5.2 Model setup

5.2.1 Habitat model

Before the habitat suitability index can be calculated, the SI curves for physical parameters such as velocity, water depth, and substrates types were considered in the model. These described by the suitability curves, which can be derived based on field observations, literature review, professional judgment, and laboratory information on the effect of each parameter on rainbow trout (Bell et al., 1973; Erman & Hawthorne 1976; Raleigh et al., 1984; Maki-Petäys et al., 1997), brown trout (Raleigh et al., 1986; Jowett., 1990) and flannelmouth sucker (Cross, 1975; Valdez, R. A., 1990a, 1990b; Holden, 1977; Holden 1999; Mueller and Wydowski, 2004; Ryden 2005; Chart & Bergersen, 1992; Vanicek et al., 1970; Beyers et al., 2001; Mueller and Marsh, 2002; Weiss et al. 1998; Robinson et al. 1998; Brandenburg et al. 2005; Gido et al., 1997). The Figures 5.4a, b, and c show SI curves for the selected three fish species.

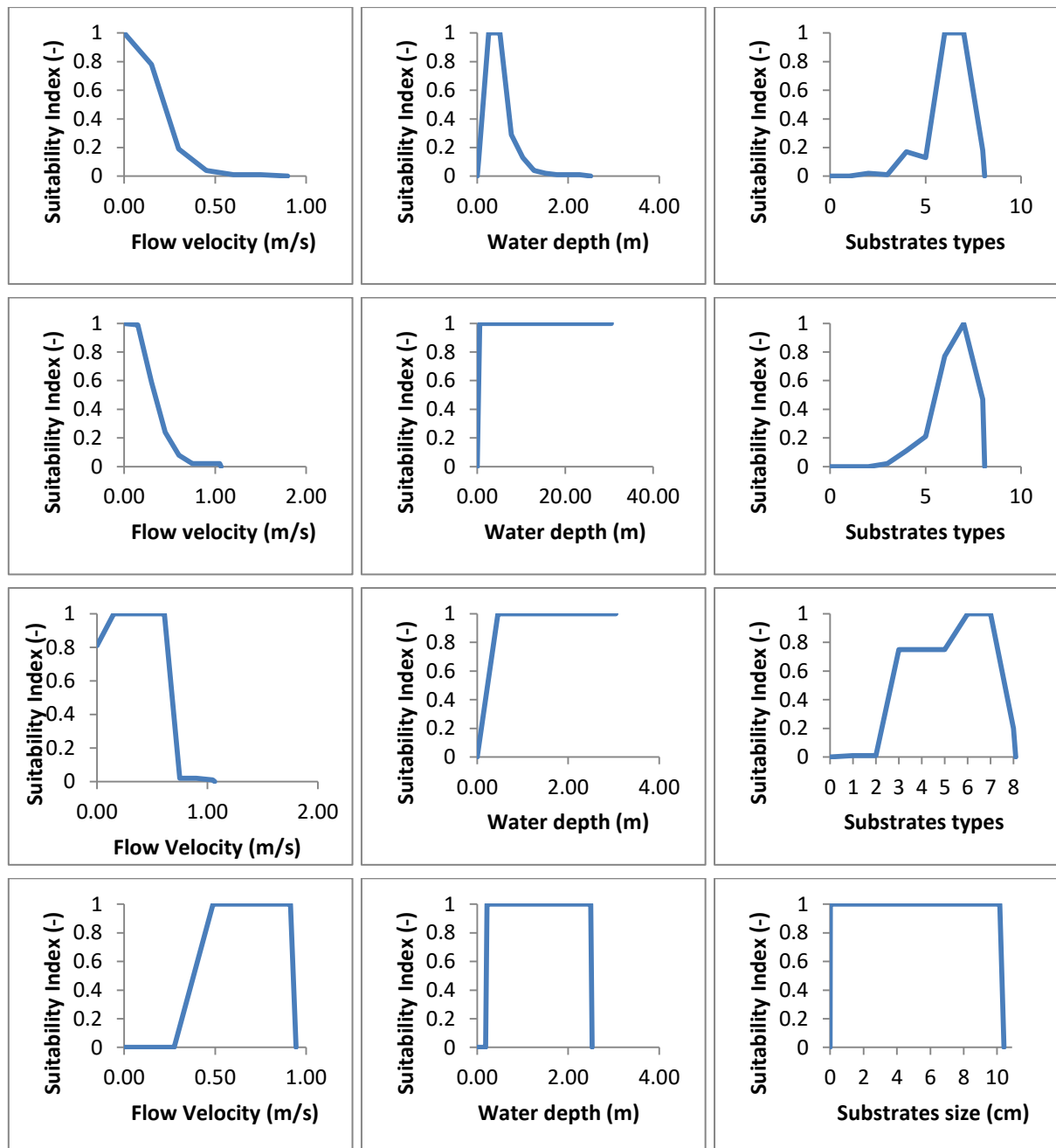


Figure 5.4a: Four life stages (Fry, Juvenile, Adult, and Spawning (from top to bottom)) fish SI curves of rainbow trout (Substrates types: 1 = plant detritus/organic material, 2 = mud/soft clay, 3 = silt (particle size < 0.062 mm), 4 = sand (particle size 0.062 to 2.000 mm), 5 = gravel (particle size 2.0 to 64.0 mm), 6 = cobble/rubble (particle size 64.0 to 250.0 mm), 7 = boulder (particle size 250.0 to 4000.0 mm), 8 = bedrock (solid rock)).

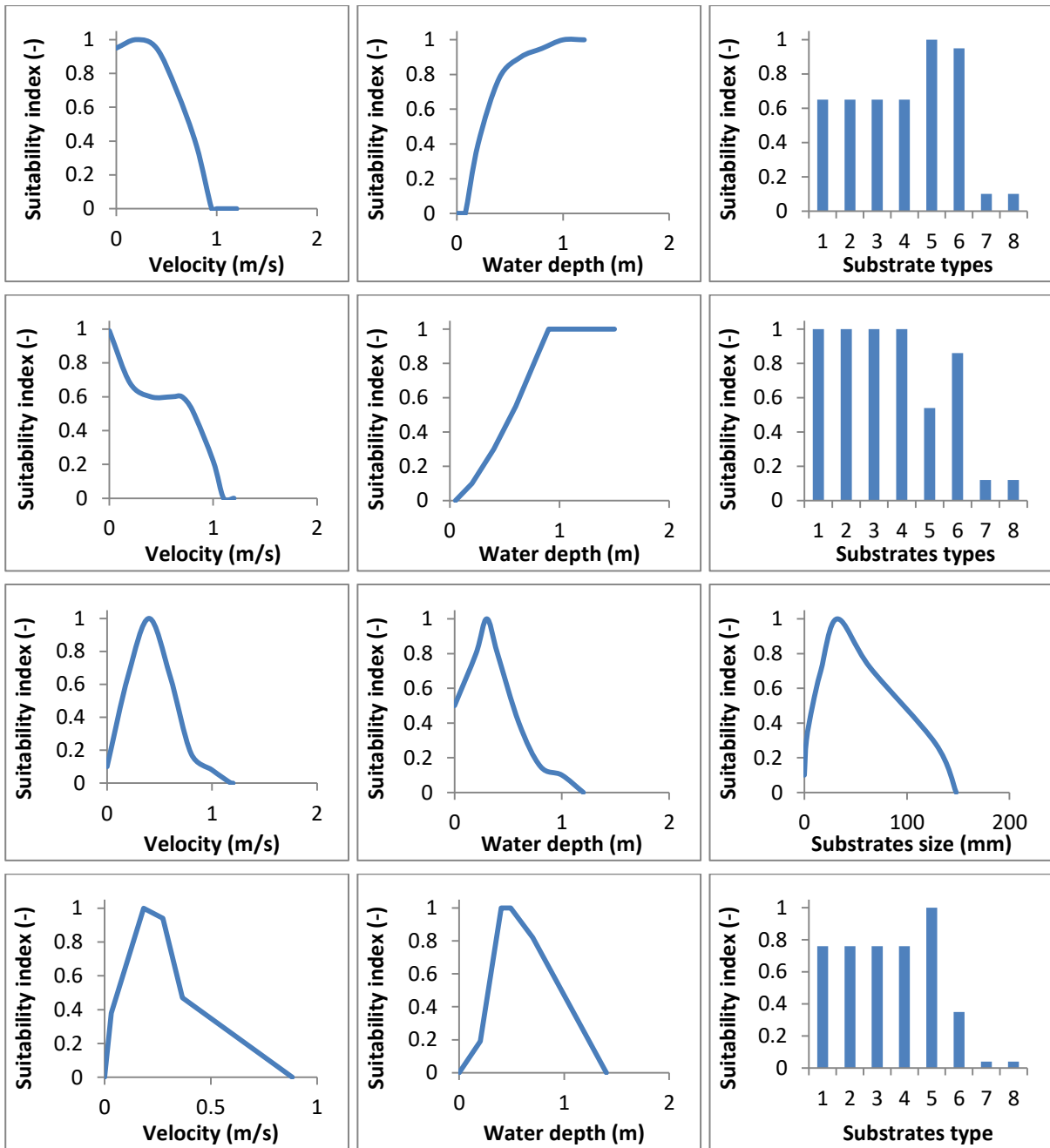


Figure 5.4b: Four life stages (Fry, Juvenile, Adult, and Spawning (from top to bottom)) fish SI curves of brown trout (Substrates types: 1 = plant detritus/organic material, 2 = mud/soft clay, 3 = silt (particle size < 0.062 mm), 4 = sand (particle size 0.062 to 2.000 mm), 5 = gravel (particle size 2.0 to 64.0 mm), 6 = cobble/rubble (particle size 64.0 to 250.0 mm), 7 = boulder (particle size 250.0 to 4000.0 mm), 8 = bedrock (solid rock)).

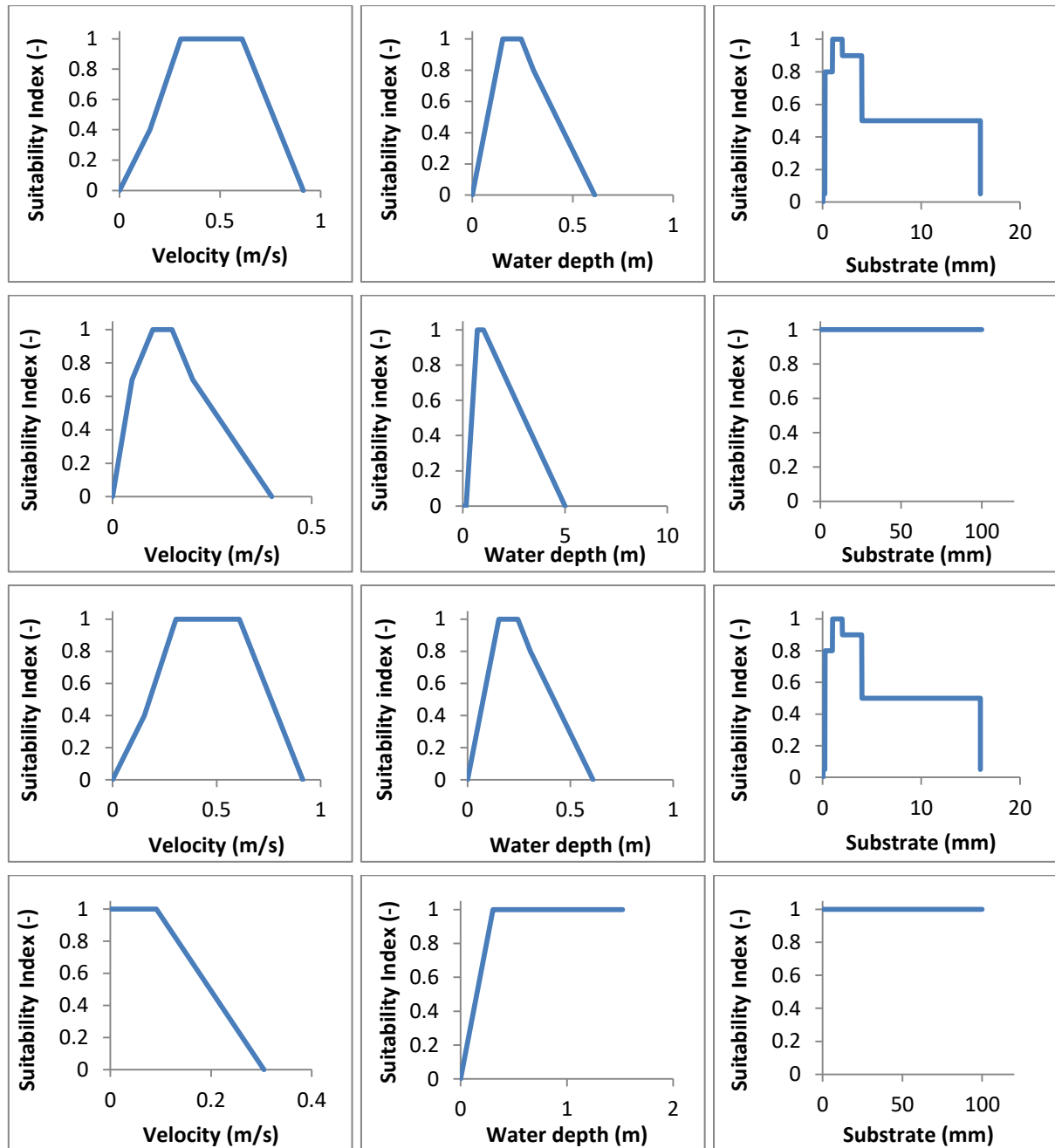


Figure 5.4c: Four life stages (Fry, Juvenile, Adult, and Spawning (from top to bottom)) fish SI curves of flannelmouth sucker.

The habitat suitability index (HSI) was used to evaluate the habitat quality, the available, and suitable areas. The approach provides a method for assessing the existing habitat conditions for fish within the case study by measuring how well each habitat variable meets the habitat requirements of the target species' life stage. The HSI was calculated for each mesh cell and each time step using Equation 3-39. The Equations 3-43 and 3-44 were used to calculate the weighted usable area (WUA) and the overall habitat suitability index (OSI) respectively.

5.2.2 Population model

The two robust population models, i.e. the logistic and matrix population models, were used to simulate and predict the fish population numbers and density changes with time. The logistic population model was calculated using Equation 3-48 obtaining directly the results for OSI and WUA in the habitat model.

Through the logistic population model, selected fish species number could be calculated. But, this model can only calculate the total fish number (Equation 3-48). If the fish number on each life stage needs to be considered, then the modified matrix population model should be applied (Equations 3-50, 3-51).

Due to the measured fish data types, it is difficult to know the fish age. The surveyed fish data mainly focus on fish length measurements and the lengths are attributed to a fish age. So, in order to fit the model with monitoring data, the matrix population model is converted to the fish length distribution model (Equation 3-52).

Table 5.1: The basic matrix parameters for three fish species used in Colorado River.

Life stage	Rainbow trout		Brown trout		Flannelmouth sucker	
	f	s	f	s	f	s
1	0	0.65	0	0.76	0	0.62
2	0	0.68	0	0.8	0	0.75
3	0	0.79	0	0.82	0	0.74
4	0	0.81	0	0.84	0	0.81
5	0	0.61	0	0.85	0	0.73
6	1.7	0.41	2.1	0.0255	0	0.63
7	7.5	0.126	26.8	0.0122	5.8	0.106
8	20.3	0.0112	43.7	0.0059	18.6	0.027
9	38.9	0.0075	65.5	0.0028	25.9	0.092
10	62.6	0.0075	73.7	0.0014	41.7	0.083
11	55.1	0.006	72.7	0.0006	41.7	0.009
12	51.7	0.006	72.7	0.0003	36.8	0.016
13	51.7	0.0002	72.7	0.0002	34.5	0.003
14	48.5	0.0002	72.7	0.0002	34.5	0.003

In this case study, the i and j for rainbow trout and brown trout are 3 and 8 respectively; i and j for flannelmouth sucker are 4 and 10 respectively (Equation 3-50). n is 14 for all 3 fish species. The basic matrix parameters and length definition for rainbow trout and brown trout and flannelmouth sucker are defined as given in Tables 5.1 and 5.2. The length life stage definition for three selected fish species determined by empirical experience, which considered the growth on the literature review (Glowacki, 2003; Makinster et al., 2010, 2011; Nuhfer, 1988; McAda & Wydoski, 1985; Lower Colorado River Multi-Species Conservation Program, 2008). The three target fish species' basic birth rate and basic survival rate are determined by the initial fish age structure, general fish birth rate

trends, fish survival rate, and the matrix model testing (Makinster et al., 2010, 2011; Glowacki, 2003; McAda & Wydoski, 1985; Mistak & Stille, 2008).

The method to determine the four life stages are defined as follows: rainbow trout and brown trout larval life stage lengths are defined below 150 mm and 180 mm respectively, juvenile rainbow trout life stage lengths are defined between 151 mm to 370 mm, adult rainbow trout life stage lengths are defined bigger than 370 mm. For brown trout juvenile fish life stage lengths are defined between 181 mm to 330 mm. Adult brown trout life stage lengths are defined longer than 331 mm (Gowing, 1986; Alexander, 1987; Nuhfer, 1988; Økland et al., 1993; Korman et al., 2010, 2011, 2012). Accordingly, for flannelmouth sucker, larval life stage length is below 150 mm, juvenile life stage length is between 151 and 380 mm, the flannelmouth sucker adult life stage length is bigger than 381 mm (Eddy and Underhill 1978, Holden 1977, Snyder et al., 2004, McAda 1977, McAda and Wydoski 1985; McKinney et al., 1999, Weiss et al. 1998). The adult fish will start spawning during the spawning season at age of six, six, and seven for rainbow trout, brown trout and flannelmouth sucker respectively.

Table 5.2: Length life stage definition for rainbow trout, brown trout and flannelmouth sucker.

Life stage	rainbow trout (mm)		brown trout (mm)		flannelmouth sucker (mm)	
1	50	larval	50	larval	40	larval
2	100		100		80	
3	150		180		120	
4	200	juvenile	250	juvenile	150	juvenile
5	240		270		210	
6	280		290		270	
7	330		310		300	
8	370		330		320	
9	390	adult & spawning	370	adult & spawning	350	adult & spawning
10	410		400		380	
11	430		440		410	
12	450		470		430	
13	470		510		450	
14	490+		540+		480+	

Population density

Through the logistic population model and matrix population model, we can calculate the selected fish species numbers. However, in order to consider the fish density distribution in the river, the fish population density equation is also applied (Equation 3-49).

The performance of logistic model is examined with the modified root mean square error (RMSE), mean absolute error (MAE) and percentage bias (PBIAS). This concept is learned from the basic concept of RMSE, MAE, and PBIAS.

$$MAE = \frac{\sum_{i=1}^n \left| \frac{P_{i,t}^{sim(F)}}{P_{max,t}^{sim(F)}} - \frac{P_{i,t}^{obs(F)}}{P_{max,t}^{obs(F)}} \right|}{n} \times 100\% \quad (5-5)$$

$$RMSE = \sqrt{\frac{1}{n-1} \sum_{i=1}^n \left(\frac{P_{i,t}^{sim(F)}}{P_{max,t}^{sim(F)}} - \frac{P_{i,t}^{obs(F)}}{P_{max,t}^{obs(F)}} \right)^2} \quad \text{for } i = 1, 2, \dots, n \quad (5-6)$$

$$PBIAS = \left[\frac{\sum_{i=1}^n \left(\frac{P_{i,t}^{sim(F)}}{P_{max,t}^{sim(F)}} - \frac{P_{i,t}^{obs(F)}}{P_{max,t}^{obs(F)}} \right) \times 100}{\sum_{i=1}^n \frac{P_{i,t}^{obs(F)}}{P_{max,t}^{obs(F)}}} \right] \quad (5-7)$$

Where n is the total number of data points in each case, $P_{i,t}^{sim(f)}$ is the i^{th} simulated data and $P_{i,t}^{obs(f)}$ is i^{th} observed data. $P_{max,t}^{sim(f)}$ is the maximum simulated data and $P_{max,t}^{obs(f)}$ is maximum observed data. The MAE can potentially identify the presence of bias. The RMSE gives an overall measure of the amount by which the data differ from the model predictions, whereas PBIAS is the deviation of data being evaluated, expressed in percentage.

5.2.3 Initial and boundary conditions for hydraulic and hydromorphology models

The five subareas of the computation domain represent areas of 7,732,385 m², 1,831,706 m², 1,459,146 m², 9,481,128 m², and 2,607,416 m² and they are named in the following Sub1, Sub2, Sub3, Sub4, and Sub5. The computational grid has been developed to cope with flow discharges ranging from 2000 to 2009. The grid system is composed by triangular grids with 5,709 mesh cells and 10,549 nodes for Sub1, with 6,059 mesh cells and 11,225 nodes for Sub2, with 6,216 mesh cells and 11,010 nodes for Sub3, with 6,858 mesh cells and 12,736 nodes for Sub4, and with 7,525 mesh cells and 14,260 nodes for Sub5.

The method for boundary conditions in this case study is exactly the same as the case study in the Aare River (see Chapter 4). The TELEMAC-2D hydrodynamics model has been used to calculate two physical parameters that can be used to determine the habitat suitability index: flow velocity and water depth. The SISYPHE hydromorphology model was used to calculate the riverbed deformation and the grain size distribution in the upper layer of the river bed. The velocities and water depths are also updated by the riverbed deformation. In order to achieve a stable flow and eliminate initially severe waves propagating in the domain for all five computational domains, a flow stabilization period of 48 hours has been applied. For obtaining an initial riverbed sediment distribution, a 30

days' simulation time has been set. When a stable riverbed has been obtained, the bed sediment distributions are used as initial bed fractions. When the model has been set up, the velocities, water depths and substrate distributions were simulated. The SI, HSI, WUA, OSI, P_t^F , $N_{t,d}$, $NL_{t,d}$ and $P_{t,d}$ values at each time step can be calculated.

5.3 Result and discussion

5.3.1 Hydrodynamic and hydromorphology simulations

Variations of the hydromorphologic processes, fish habitat quality, fish population numbers and their densities were predicted for all three selected fish species in the five computational subdomains in the time period from 2000 to 2009. The fish data surveyed were compared with the simulation results and used to validate the ecohydraulic model system.

As exemplary, the calculated flow velocities, water depths, bed elevation change, and grain size distributions in the years 2000, 2005 and 2009 are shown in Figures 5.5a to 5.5e. From the Figures, it can be noticed that in Sub1 the maximum velocity values range from 0.6 m/s to 1.2 m/s; the largest water depth values range from 1.5 m to 3 m. Riverbed substrates' diameters are between 1.5 mm and 5.5 mm. Compared with the simulation results in Sub1, the simulation results in Sub2 and Sub3 appear to be slightly different. More specifically, the maximum velocities range from 0.5 m/s to 1.5 m/s in Sub2, and range from 0.6 m/s to 1.6 m/s in Sub3. The largest water depths range from 2 m to 3.5 m in Sub2 and range from 3 m to 4.5 m in Sub3 respectively. In Sub2, the average grain sizes are between 4 mm and 36 mm. In Sub3, the average grain sizes range from 1 mm to 15 mm. The maximum velocities for both Sub4 and Sub5 range from 0.6 m/s and 1.8 m/s. The maximum water depths for both Sub4 and Sub5 are relatively higher than water depth for other subareas, with a maximum value of 4 m for Sub4, and with a maximum value of 8 m for Sub5. The average grain sizes range from 2 mm to 16 mm in Sub4, and range from 2 mm to 34 mm in Sub5.

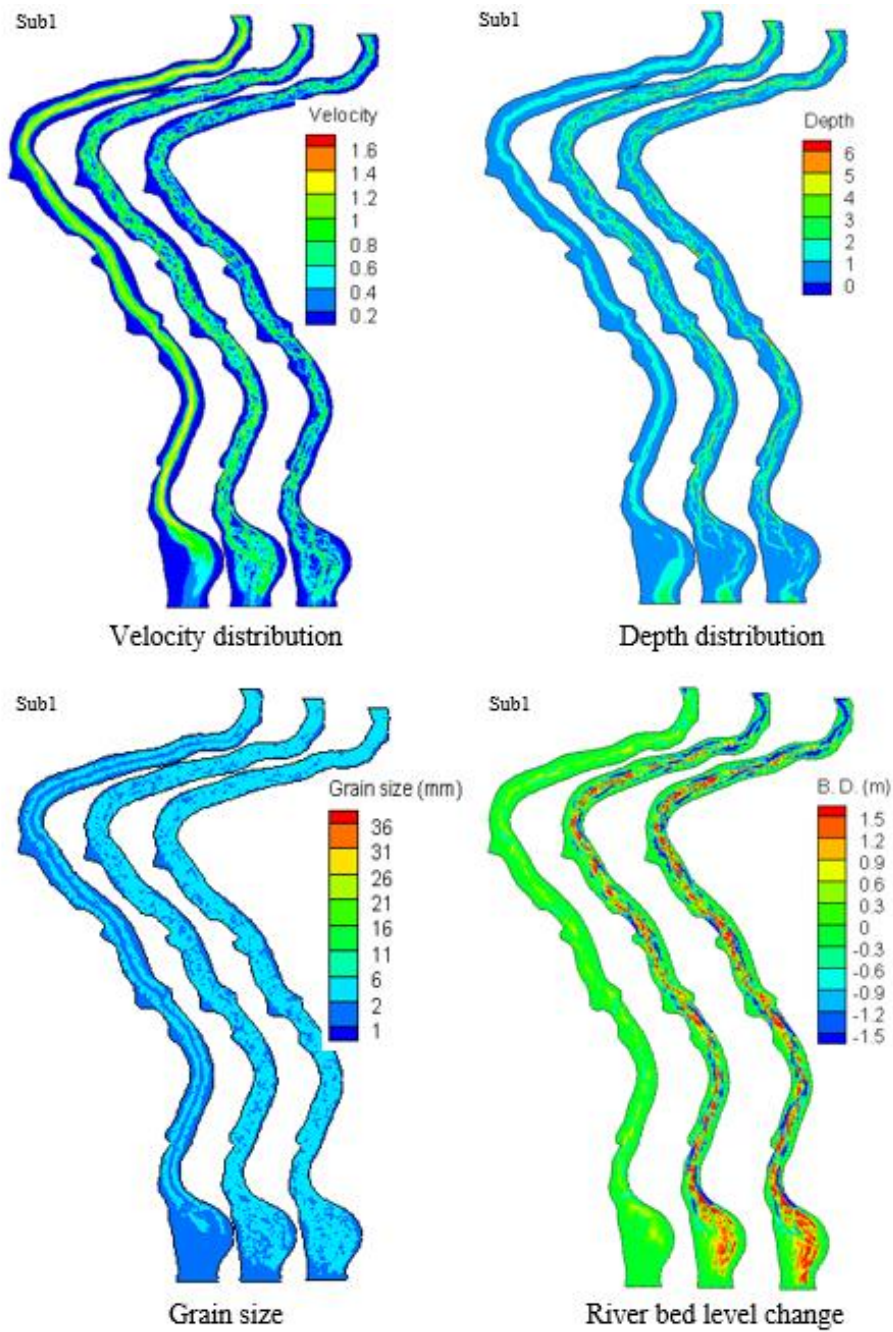


Figure 5.5a: The simulated velocity, water depth, substrate, and bed level changes in the Sub1 from 2000 to 2009 (from left to right: in 2000, 2005, and 2009).

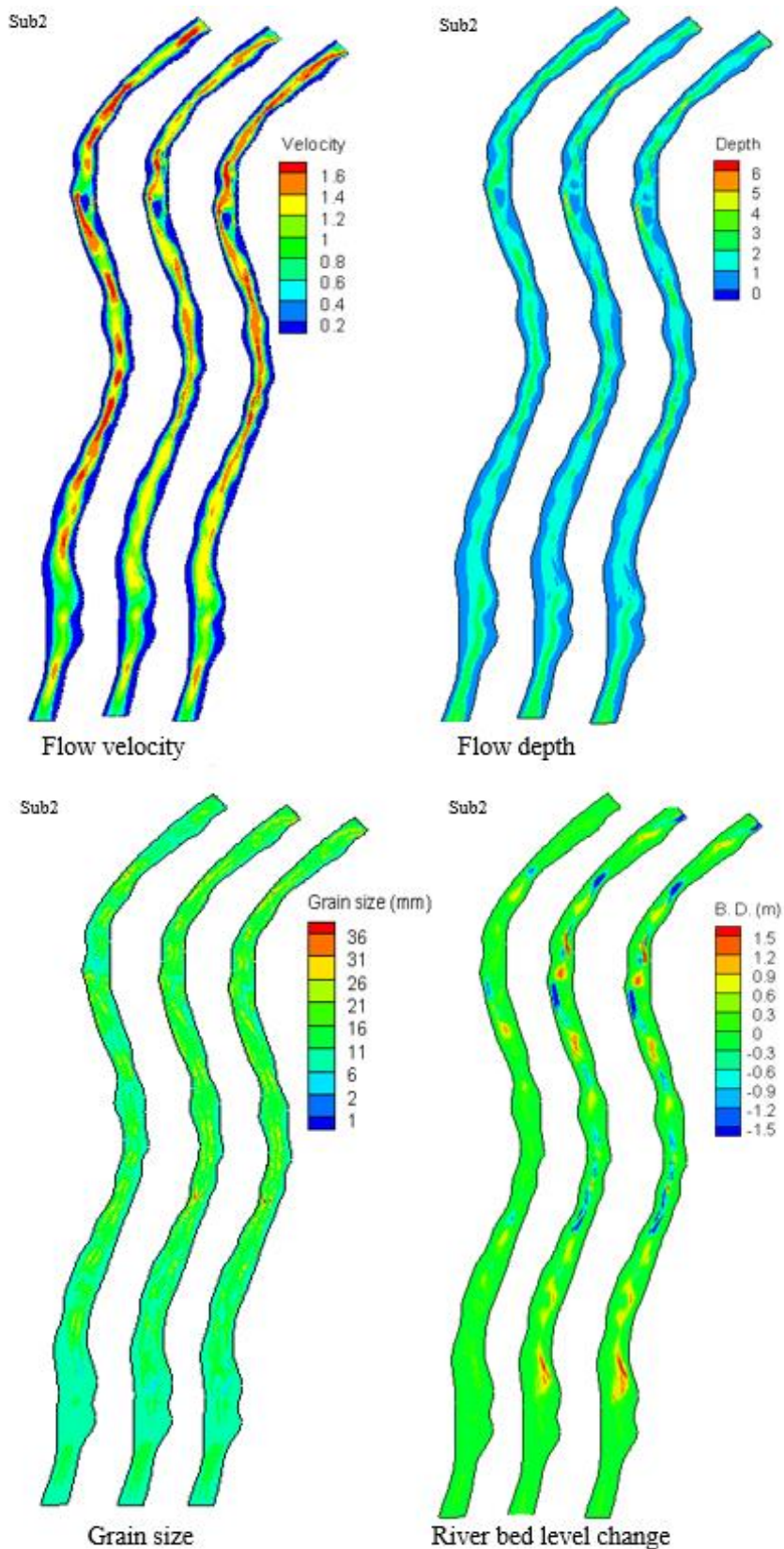


Figure 5.5b: The simulated velocity, water depth, substrate, and bed level changes in the Sub2 from 2000 to 2009 (from left to right: in 2000, 2005, and 2009).

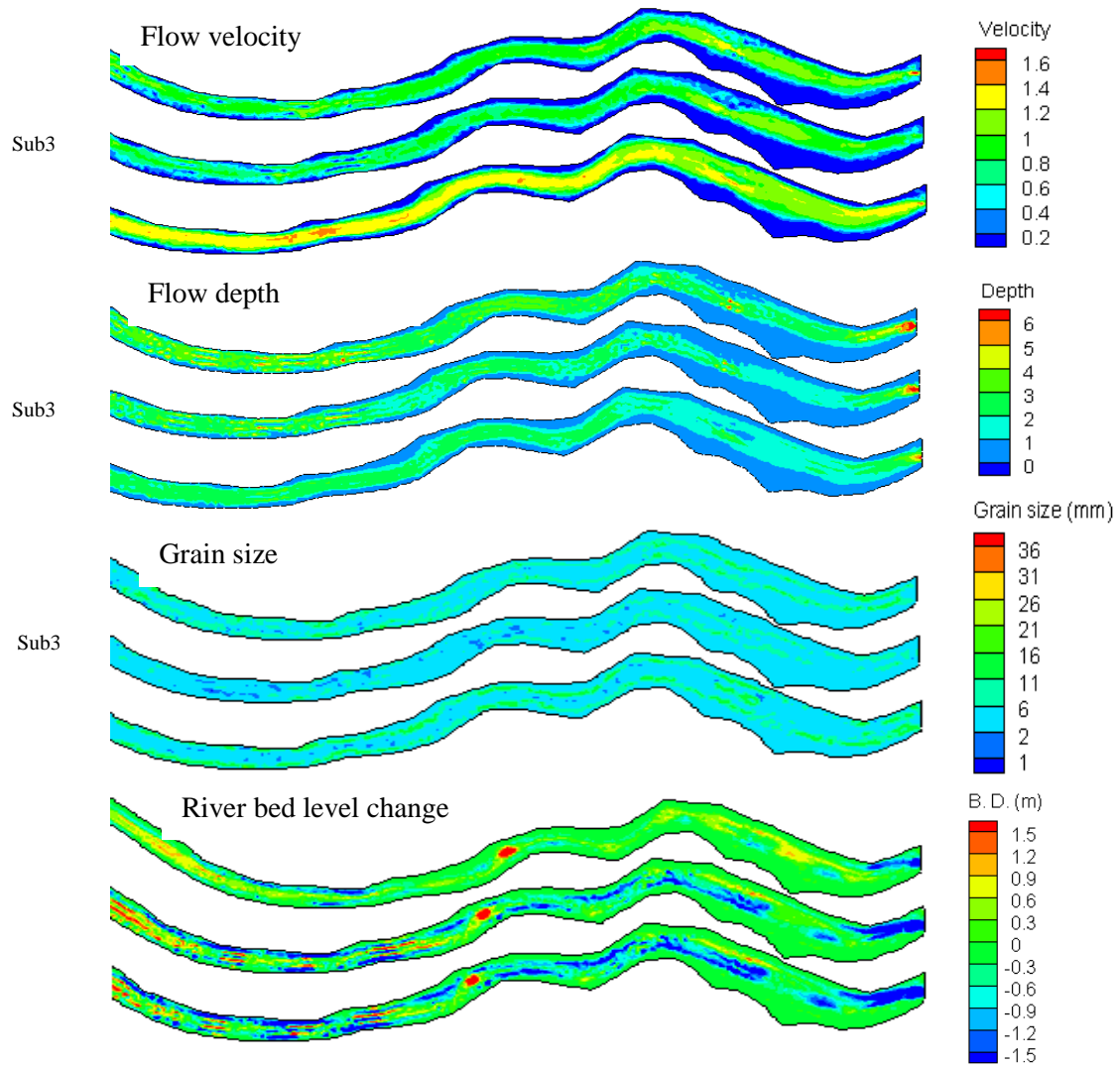


Figure 5.5c: The simulated velocity, water depth, substrate, and bed level changes in the Sub3 from 2000 to 2009 (from up to down: 2000, 2005, and 2009).

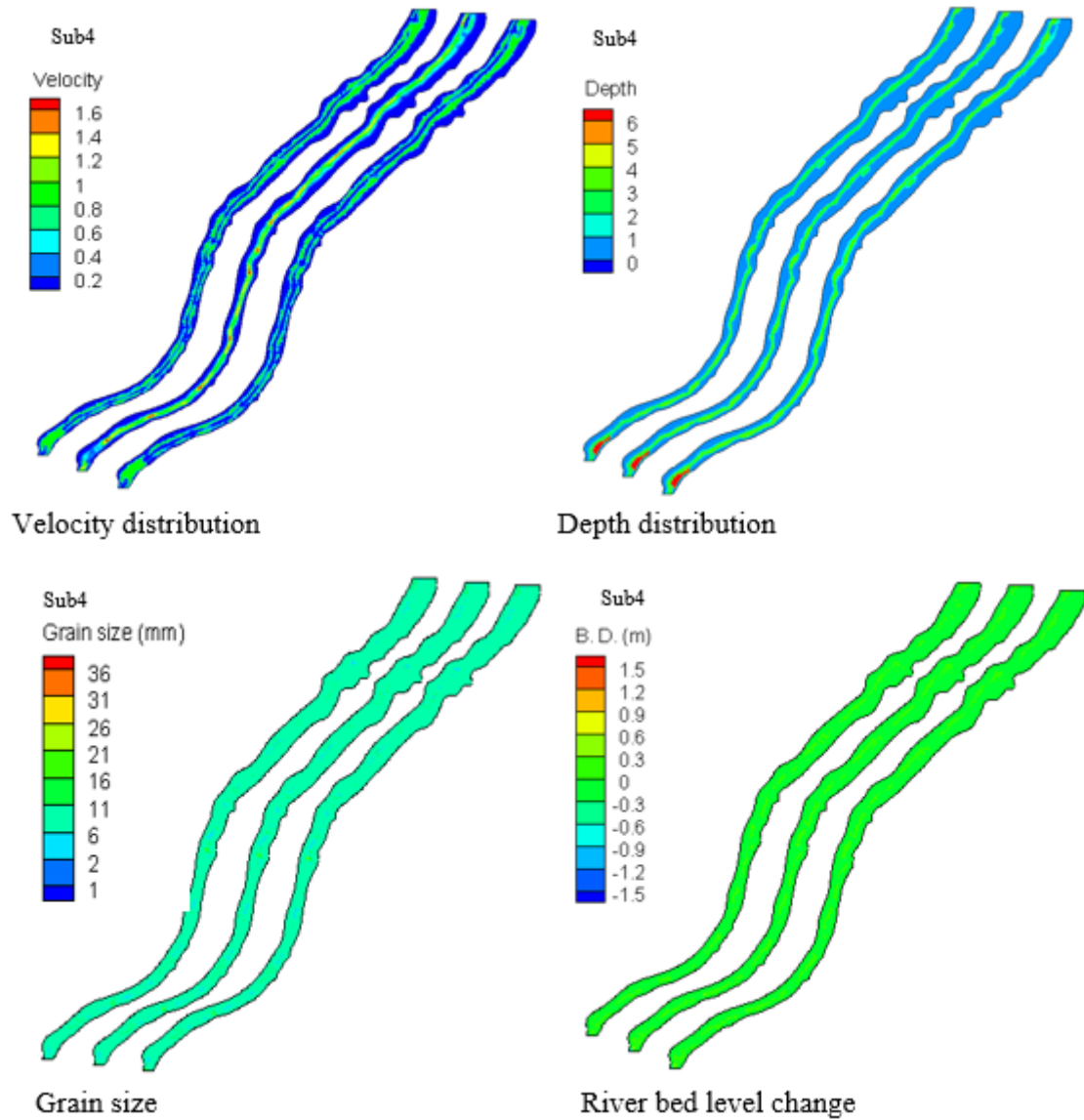


Figure 5.5d: The simulated velocity, water depth, substrate, and bed level changes in the Sub4 from 2000 to 2009 (from left to right: in 2000, 2005, and 2009).

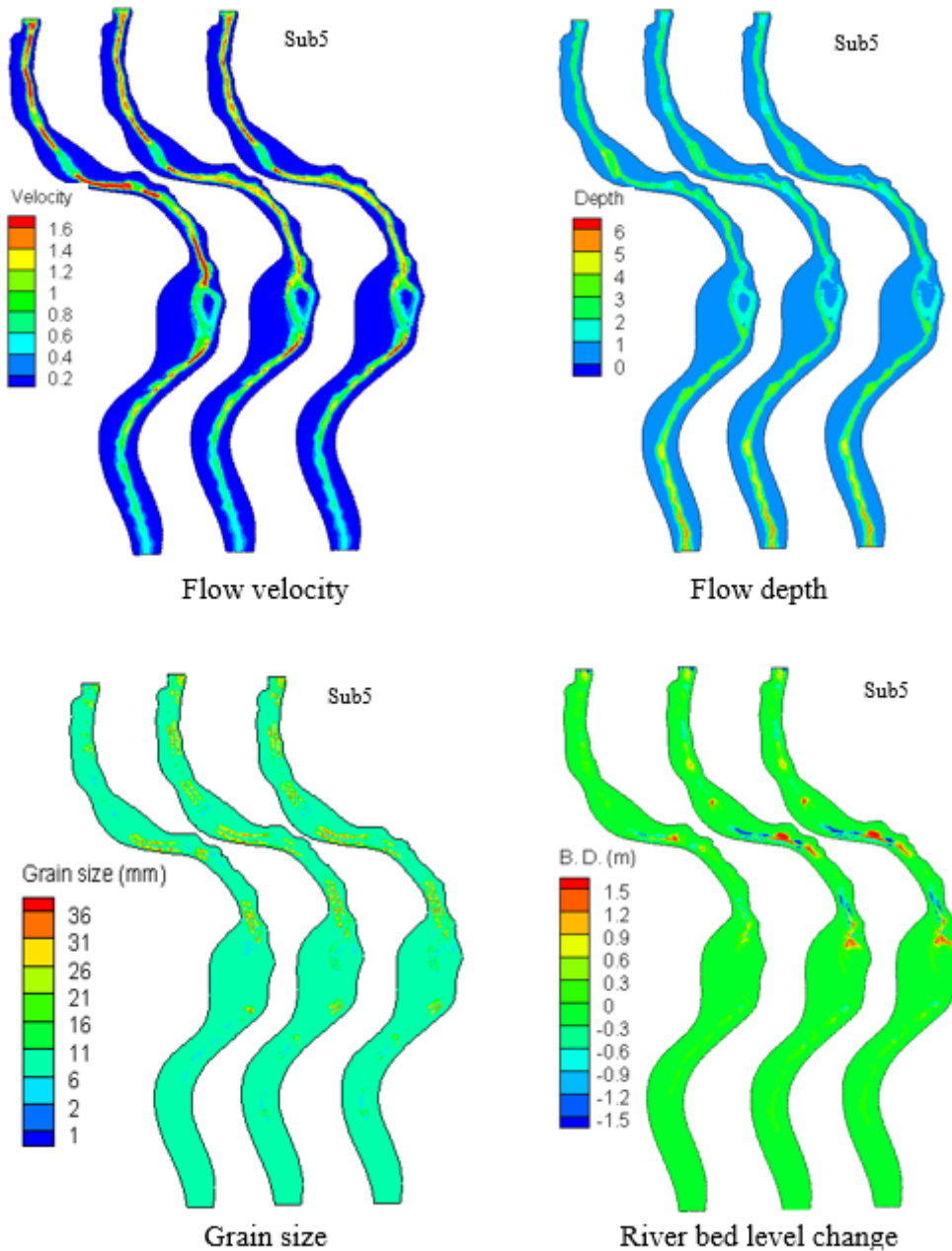


Figure 5.5e: The simulated velocity, water depth, substrate, and bed level changes in the Sub5 from 2000 to 2009 (from left to right: in 2000, 2005, and 2009).

Figure 5.5 also shows exemplary the riverbed deformation for all five subareas in the years 2000, 2005 and 2009. From the simulation results, it can be seen that during the simulation time period from 2000 to 2010, sediment erosion and deposition occurred over large areas of the Sub1 river stretch, with a discontinued pattern. The maximum sediment erosion and deposition values are 1.8 m and 2 m respectively. In the Sub2 river stretch, the riverbed substrates erosion is not significant, while the substrate deposition is sporadically distributed at several locations along the river stretch. The maximum sediment erosion and deposition values in Sub2 are 0.8 m and 2 m respectively during the simulation time. Similar to Sub2, the sediment deposition is more severe than erosion in Sub3, and

the sediment deposition is mainly focused on the middle and downstream of the river stretch, with a maximum value of 2.2 m. Compared to Sub1, Sub2, and Sub3, the sediment erosion and deposition are relatively small in the Sub4 river stretch. The maximum values for riverbed erosion and deposition are less than 1 m during the 10 years' simulation times. In Sub5, the sediment deposition is scattered over the narrowest part of the river stretch with the maximum value of 2.1 m in the year of 2010, and the maximum erosion value is 0.5 m during the simulation time.

5.3.2 Habitat quality simulation

The habitat suitability index values have been calculated by combining the suitability index curves for the flow velocities, water depths, and substrate types using Equation 3-39. In the Colorado River, the reason for choosing these three parameters is that the velocity, depth, and substrates override the role of other physical parameters and appear to have a critical impact on the three chosen target fish species living in the Colorado River. The HSI values for different life stages of rainbow trout, brown trout, and flannelmouth sucker have been simulated in all the five subareas. In Figures 5.6 to 5.10, the adult life stage has been chosen to illustrate the quality changes in the habitat of the three fish species from 2000 to 2009.

The HSI distributions for the adult life stages of rainbow trout, brown trout, and flannelmouth sucker in the river stretch Sub1 are shown in Figure 5.6. In 2000, it can be seen that the rainbow trout in the adult life stage had good habitat suitability conditions in the areas downstream near the outlet and along the riverbank. For the adult life stage of brown trout, the HSI values in the Sub1 is almost 0, except for a small area downstream near the outlet. The substrates are the main reason for the low HSI values for brown trout. The habitat suitability qualities for flannelmouth sucker have a similar trend as the rainbow trout habitat suitability qualities. However, the habitat quality was far from satisfactory with HSI distribution in most regions of this subareas.

In comparison with the habitat qualities in 2000, the HSI distribution in 2005 were relatively higher for the rainbow trout adult stage, with the whole river stretch in Sub1 filled with high HSI values. The adult brown trout still remained at a low HSI values, but with relatively higher values at the outlet of the river stretch Sub1. Compared with the adult brown trout habitat quality in 2000, the adult brown trout habitat quality was slightly higher in 2005. The velocity was the main reason for low HSI values for the brown trout in 2005. In 2005, adult flannelmouth sucker HSI values were more evenly distributed throughout the river stretch Sub2 and the habitat qualities were on the same level compared with the habitat quality in 2000.

At the end of the simulation time, it can be noted that the adult life stage of the rainbow trout was almost kept in a stable level compared the corresponding stage in 2005 except the areas along the riverbank. In 2009, the adult life stage of brown trout showed lower HSI values but the habitat quality was higher than the habitat quality in 2005. The flannelmouth sucker habitat quality was suitable for many areas in the river stretch Sub1, and also showed a slightly increasing trend as compared with the habitat quality in 2005.

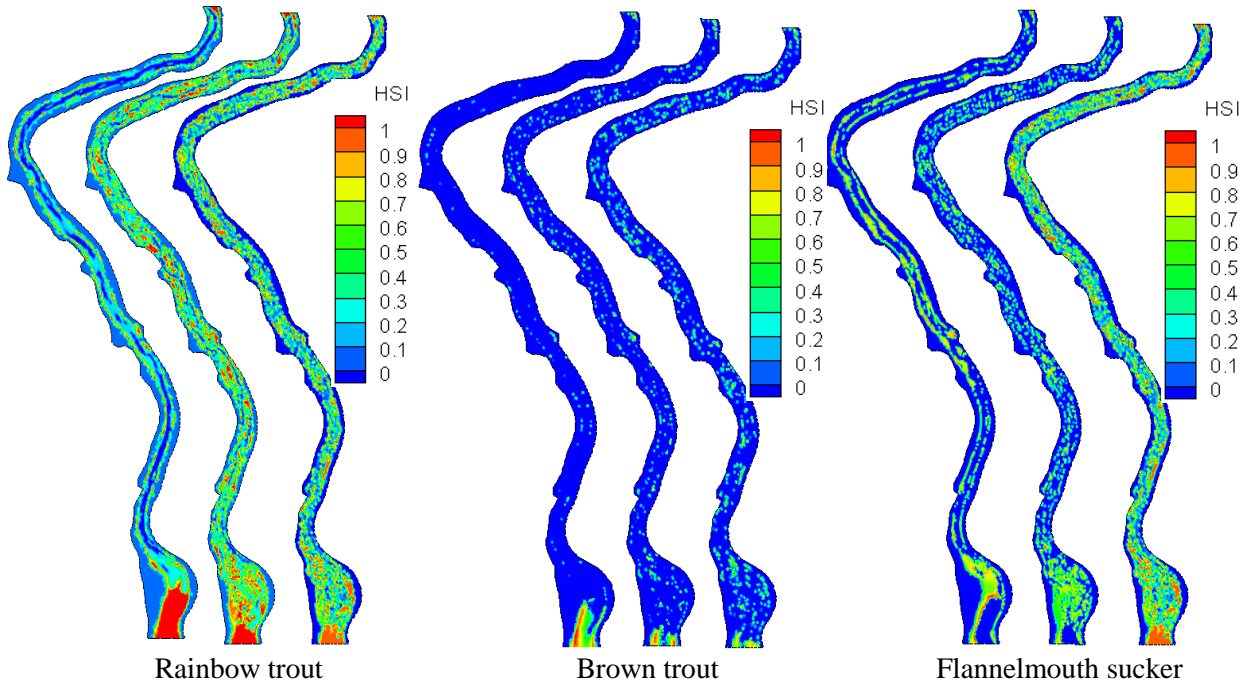


Figure 5.6: The simulated habitat suitability index distribution for the adult rainbow trout, brown trout, and flannelmouth sucker in the river stretch Sub1 (from left to right: in 2000, 2005, 2009).

The simulated HSI distributions for the adult life stages of rainbow trout, brown trout, and flannelmouth sucker in the river stretch Sub2 are shown in Figure 5.7. It can be seen that the adult life stage of rainbow trout habitat qualities are better than adult brown trout and flannelmouth sucker habitat qualities in all simulation times. Compared to the HSI values variations in the river stretch Sub1, the three fish species habitat quality remained at a stable level in the simulation time from 2000 to 2009. It is also noted that, in all simulation times, compared to rainbow trout habitat qualities, the brown trout and flannelmouth sucker habitat qualities in the river stretch Sub2 were not very suitable.

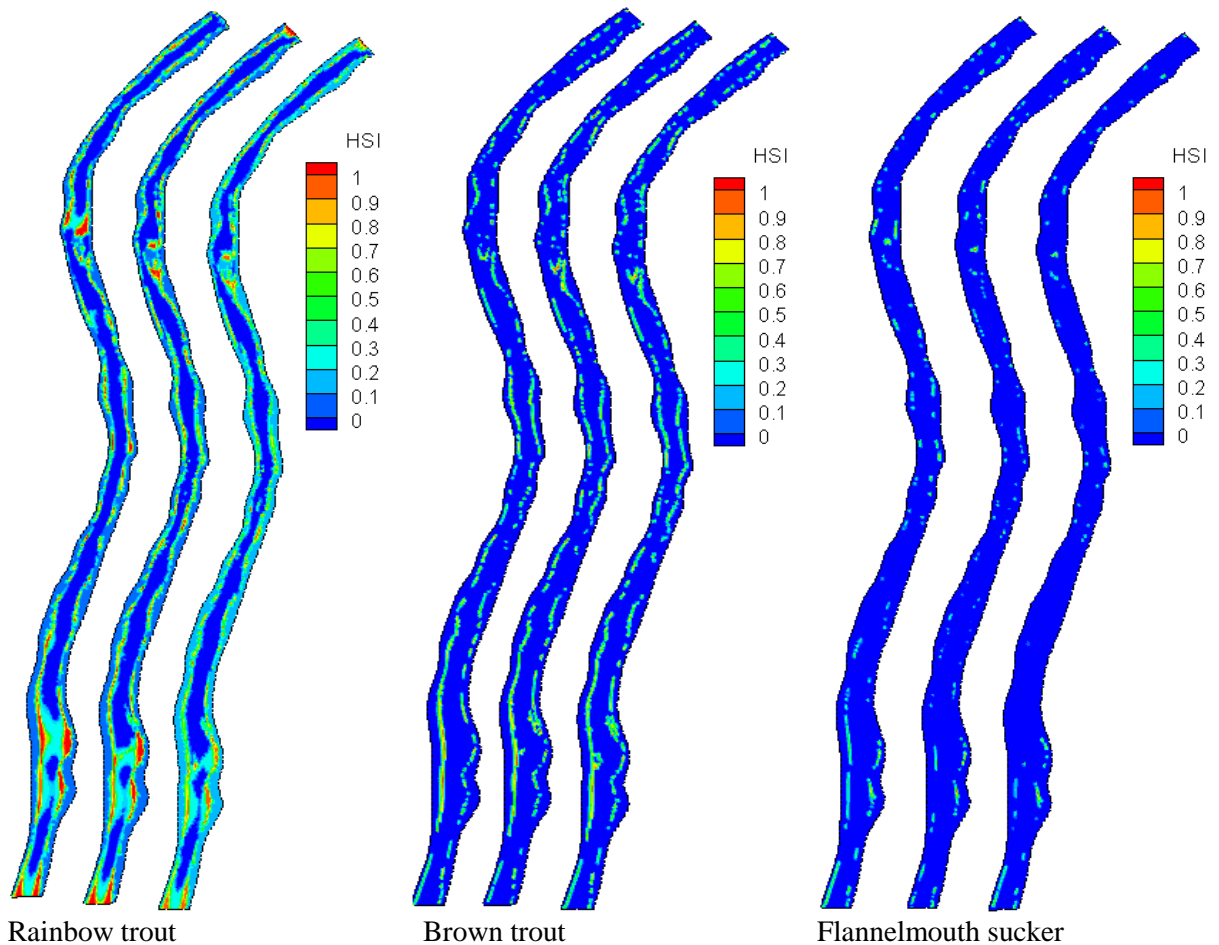


Figure 5.7: The simulated habitat suitability index distribution for the adult rainbow trout, brown trout, and flannelmouth sucker in the river stretch Sub2 (from left to right: in 2000, 2005, 2009).

The simulated habitat quality results for the selected life stage of the target fish species in the river stretch Sub3 are shown in Figure 5.8. Similar to the trend of the river stretch Sub2, the river stretch Sub3 rainbow trout adult life stage habitat qualities are better than that for the brown trout and flannelmouth sucker in 2000. The later simulation time of the habitat suitability index distribution showed a slightly increased trend. The brown trout adult life stage HSI values were unsuitable for a large area of the river stretch Sub3 and that values were stable from 2000 to 2009. Compared to the rainbow trout and brown trout, the flannelmouth sucker adult life stage HSI values had low values and were worse than that of the rainbow trout and brown trout during the simulation time from 2000 to 2009.

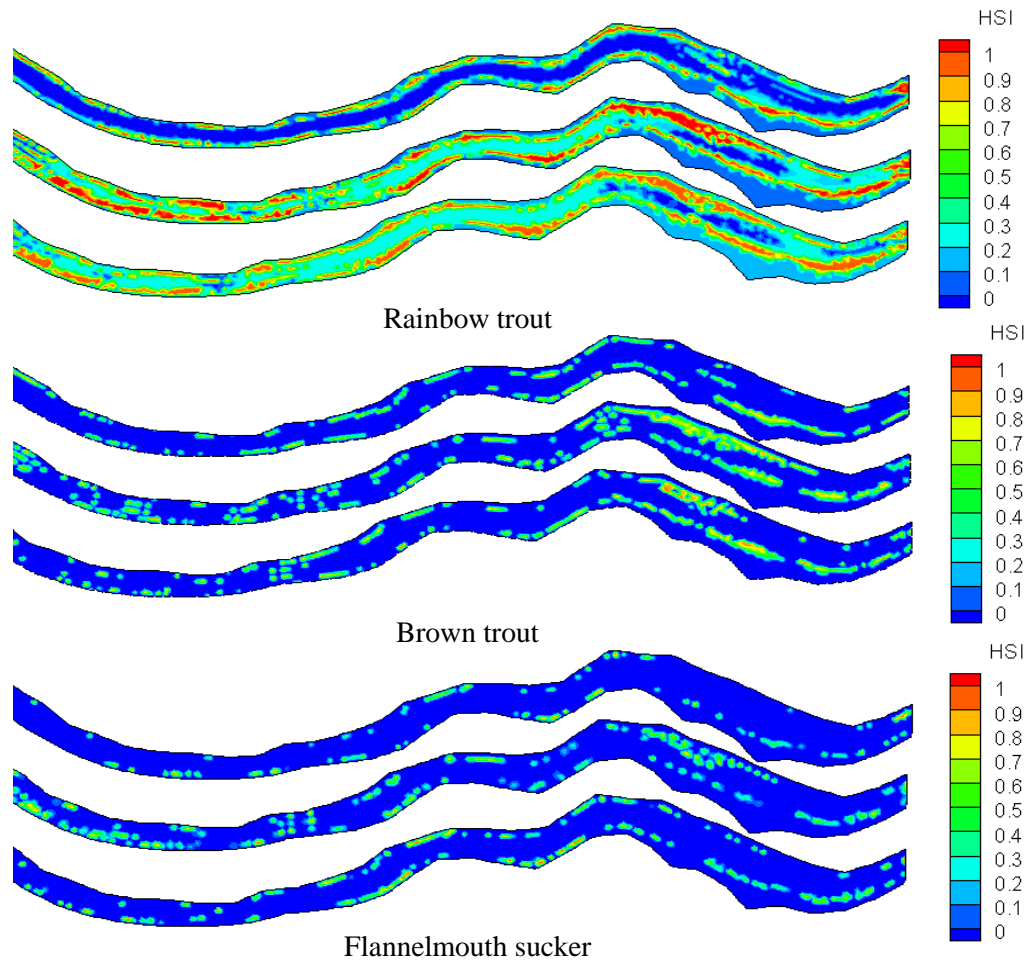


Figure 5.8: The simulated habitat suitability index distribution for the adult rainbow trout, brown trout, and flannemouth sucker in the river stretch Sub3 (from up to down: in 2000, 2005, 2009).

The habitat quality simulation results for adult life stages of the rainbow trout, brown trout and flannemouth sucker in the river stretch Sub4 are shown in Figure 5.9. It is shown that the rainbow trout HSI qualities are better than that of the brown trout and flannemouth sucker. The HSI along the river bank have higher values than HSI values in the middle of the river stretch. During the simulation time (from 2000 to 2009), the rainbow trout HSI values remain stable. The brown trout HSI distribution have high values downstream of Sub4 and the river bank also have higher values than the middle of the river; the flow velocity is the main reason for the low HSI in the middle of the river. For the adult life stage of flannemouth sucker in the river stretch Sub4, several areas with HSI values of 0.5 were scattered along the river bank.

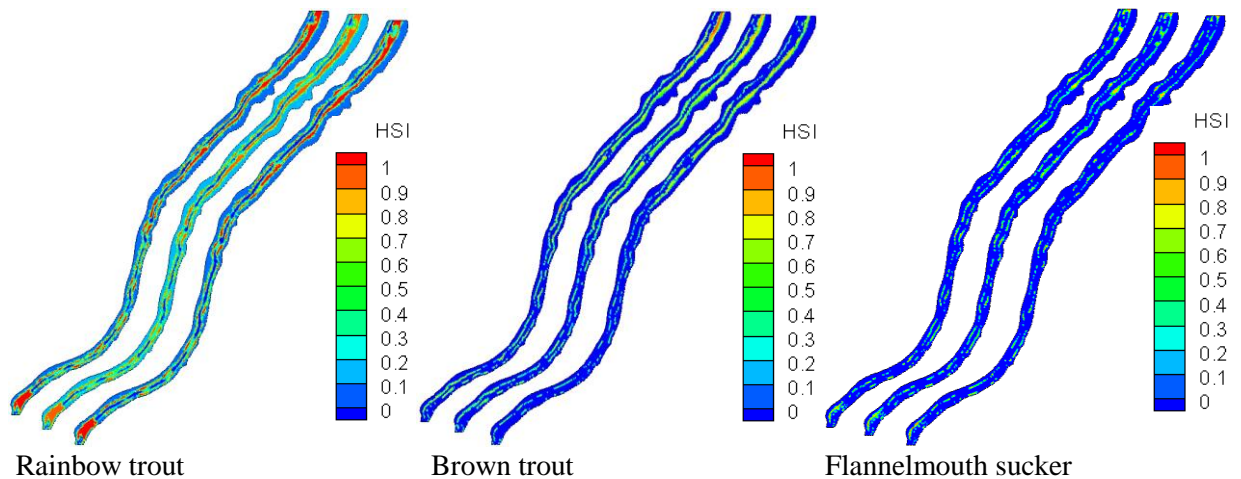


Figure 5.9: The simulated habitat suitability index distribution for the adult rainbow trout, brown trout, and flannemouth sucker in the river stretch Sub4 (from left to right: in 2000, 2005, 2009).

The HSI distribution results of the river stretch Sub5 are shown in Figure 5.10. During the simulation time, it is noted that the HSI distribution for rainbow trout adult life stage had insignificant variation during the simulation time. For brown trout, it appeared that the adult brown trout high HSI values were mainly focused along the river bank areas. The adult flannemouth sucker had the worst habitat quality with HSI values of nearly 0 in a large area. The adult habitat qualities remained unchanged during the simulation time.

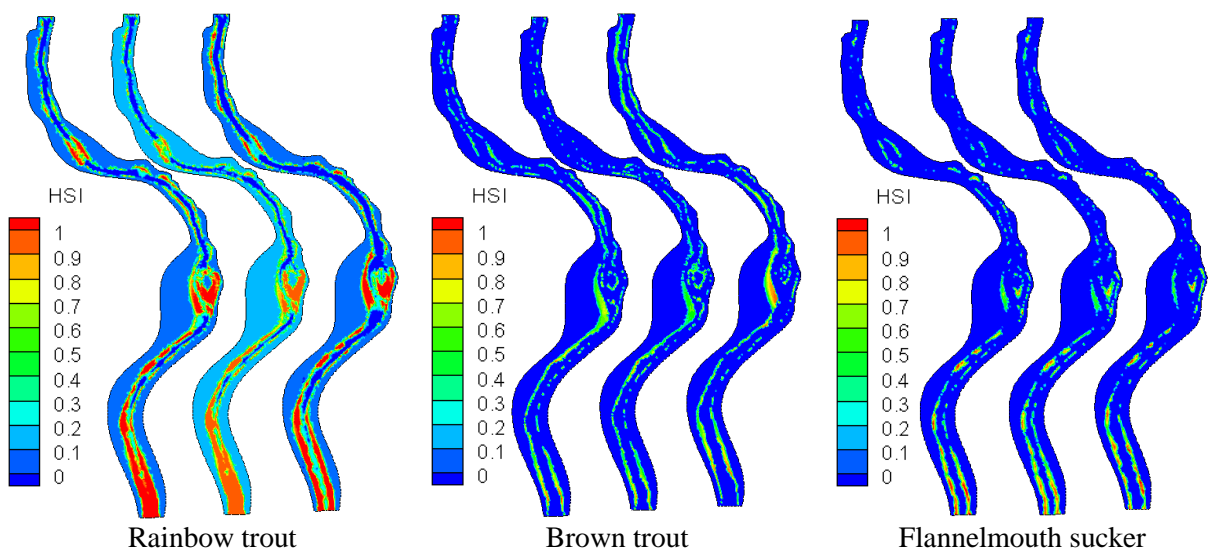


Figure 5.10: The simulated habitat suitability index distribution for the adult rainbow trout, brown trout, and flannemouth sucker in the river stretch Sub5 (from left to right: in 2000, 2005, 2009)

5.3.3 Habitat sensitivity analysis

Sensitivity analysis of the rainbow trout, brown trout and flannelmouth sucker habitat was based on the simulation results of WUA and OSI. The WUA and OSI calculations were according to the Equations of 3-43 and 3-44 which have been tested and verified by previous researchers (Moir et al., 2005, Mouton et al., 2007, Yi et al., 2010). It is noted that WUA and OSI values showed the exactly same trend while the OSI has different values at different life stages for the three selected fish species. In the river stretch Sub1, the WUA values for adult rainbow trout rose steadily with values from 1,959,144 m² in 2000 to 3,038,518 m² in 2005, and grew slightly until the end of 2009 with a value of 3,284,021 m². The adult rainbow trout OSI values increased from 2000 to 2005, and to 2009 with values of 0.25, 0.38 and 0.42 respectively. The adult brown trout WUA values grew from 2.5×10⁵ m² in 2000 to 4.7×10⁵ m² in 2009, and the corresponding OSI values were 0.031 and 0.061. The adult, flannelmouth sucker WUA values showed a great increasing trend at first and then showed slightly decreasing trend. The maximum WUA and OSI values for the adult flannelmouth sucker were 1.45×10⁶ m² and 0.18 respectively (Figure 5.11).

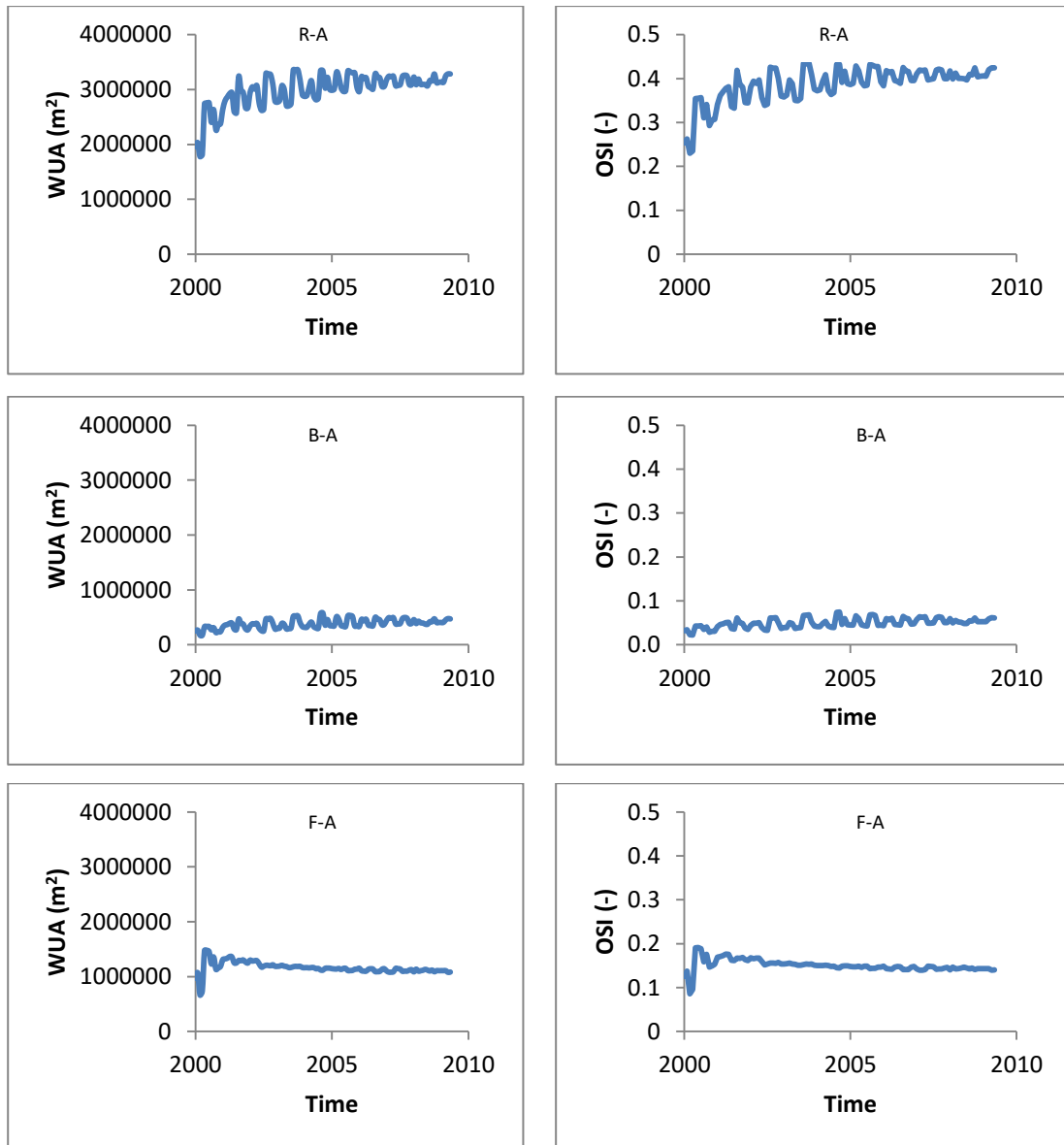


Figure 5.11: The WUA and OSI distribution for adult rainbow trout (R-A, upper), brown trout (B-A, middle), and flannelmouthsucker (F-A, lower) from 2000 to 2009 in the river stretch Sub1.

The adult life stage of rainbow trout, brown trout, and flannelmouth sucker habitat sensitivity analysis results of the Sub2 are shown in Figure 5.12. It can be noted that the adult rainbow trout WUA and OSI values were kept stable at around $3.8 \times 10^5 \text{ m}^2$ and 0.21 respectively. The adult brown trout WUA and OSI values were stable at the level of $1.15 \times 10^5 \text{ m}^2$ and 0.05 respectively. The adult flannelmouth sucker WUA and OSI values experienced a slightly decrease for the year 2000 and then showed an increase in later years. For the flannelmouth sucker, it was noted that the adult WUA and OSI values changed significantly in the years of 2008 and 2009.

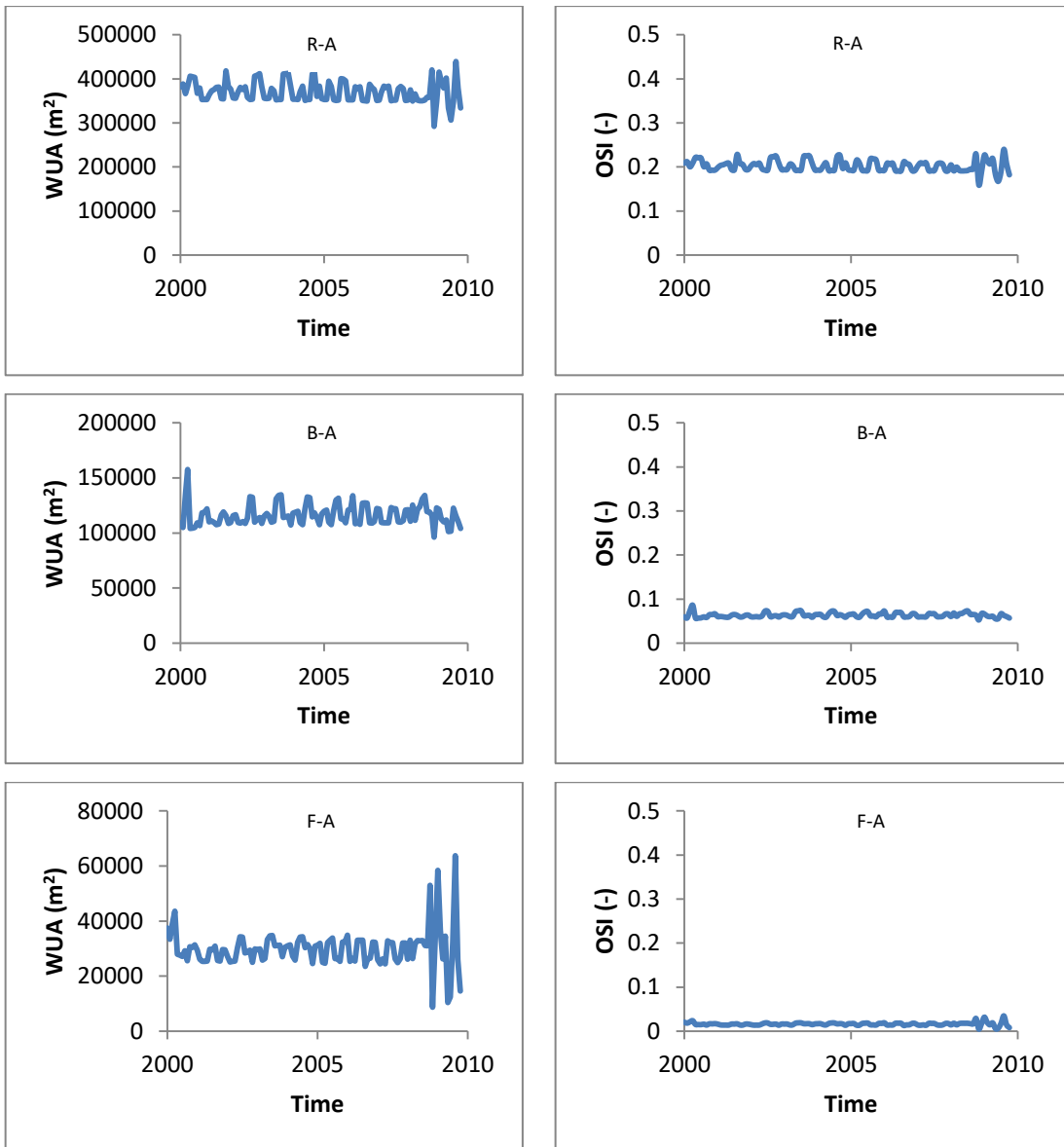


Figure 5.12: The WUA and OSI distribution for adult rainbow trout (R-A, upper), brown trout (B-A, middle) and flannelmouthsucker (F-A, lower) from 2000 to 2009 in the river stretch Sub2.

In the river stretch Sub3, the three selected fish species' WUA and OSI values are shown in Figure 5.13. It can be seen that the adult rainbow trout WUA and OSI values increased slightly over 10 simulation years. The adult brown trout WUA values showed the same trend with slightly increasing trend from 2000 to 2004 before decreasing from 2005 to 2009. The adult life stage of brown trout OSI values had exactly the same trend as the WUA values with average values of 0.06 over 10 simulation years. For the flannelmouth sucker, the adult WUA rose steadily from $4.0 \times 10^4 \text{ m}^2$ in 2000 to $6.4 \times 10^4 \text{ m}^2$ in 2007, and remained at the level of to $6.4 \times 10^4 \text{ m}^2$ in 2008, and decreased again with a value of $6.0 \times 10^4 \text{ m}^2$ before experienced a short increasing trend in 2009. The adult flannelmouth sucker OSI values increased from 2000 to 2007 and showed a decreasing trend in 2008,

and increased again in 2009 with values of 0.025, 0.045, 0.041, and 0.047 respectively (Figure 5.13).

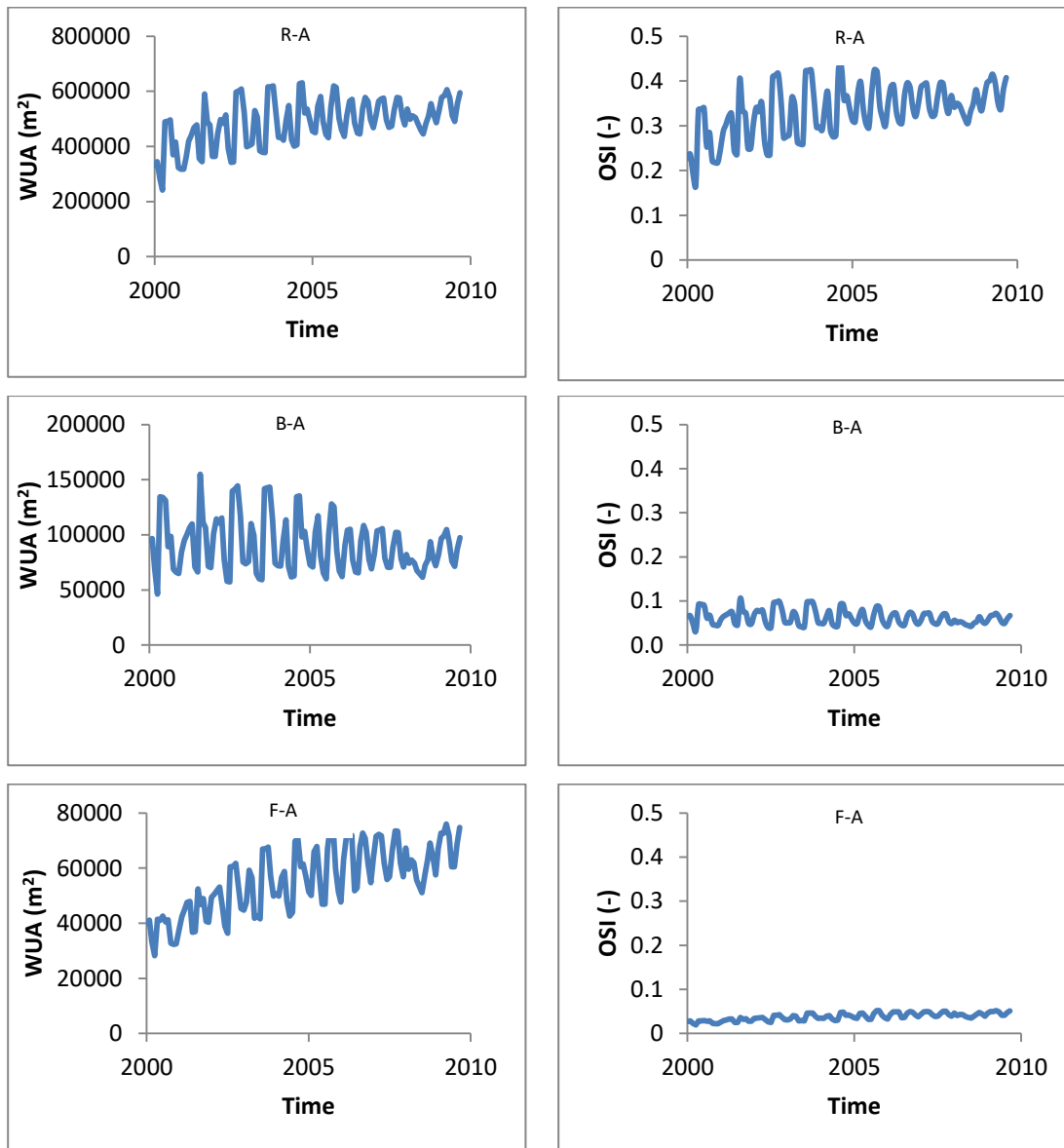


Figure 5.13: The WUA and OSI distribution for adult rainbow trout (R-A, upper), brown trout (B-A, middle) and flannelmouth sucker (F-A, lower) from 2000 to 2009 in the river stretch Sub3.

The adult life stage of rainbow trout, brown trout and flannelmouth sucker habitat sensitivity analysis results of the river stretch Sub4 are shown in Figure 5.14. It can be seen that the adult rainbow trout WUA and OSI values experienced a decreasing trend in 2000 and then experienced an increasing trend in the simulation time. After that, the WUA and OSI values remained at a stable level with an average value of $3.2 \times 10^6 \text{ m}^2$ and 0.33 respectively. The adult brown trout fish life stages' WUA values remained at the level of $6.0 \times 10^5 \text{ m}^2$, and the OSI values were nearly 0.055 over all simulation times. For the flannelmouth sucker, the adult WUA values were at the level of $1.2 \times 10^6 \text{ m}^2$ in most years.

The flannelmouth sucker adult OSI values remained at the value of nearly 0.13 over all simulation times.

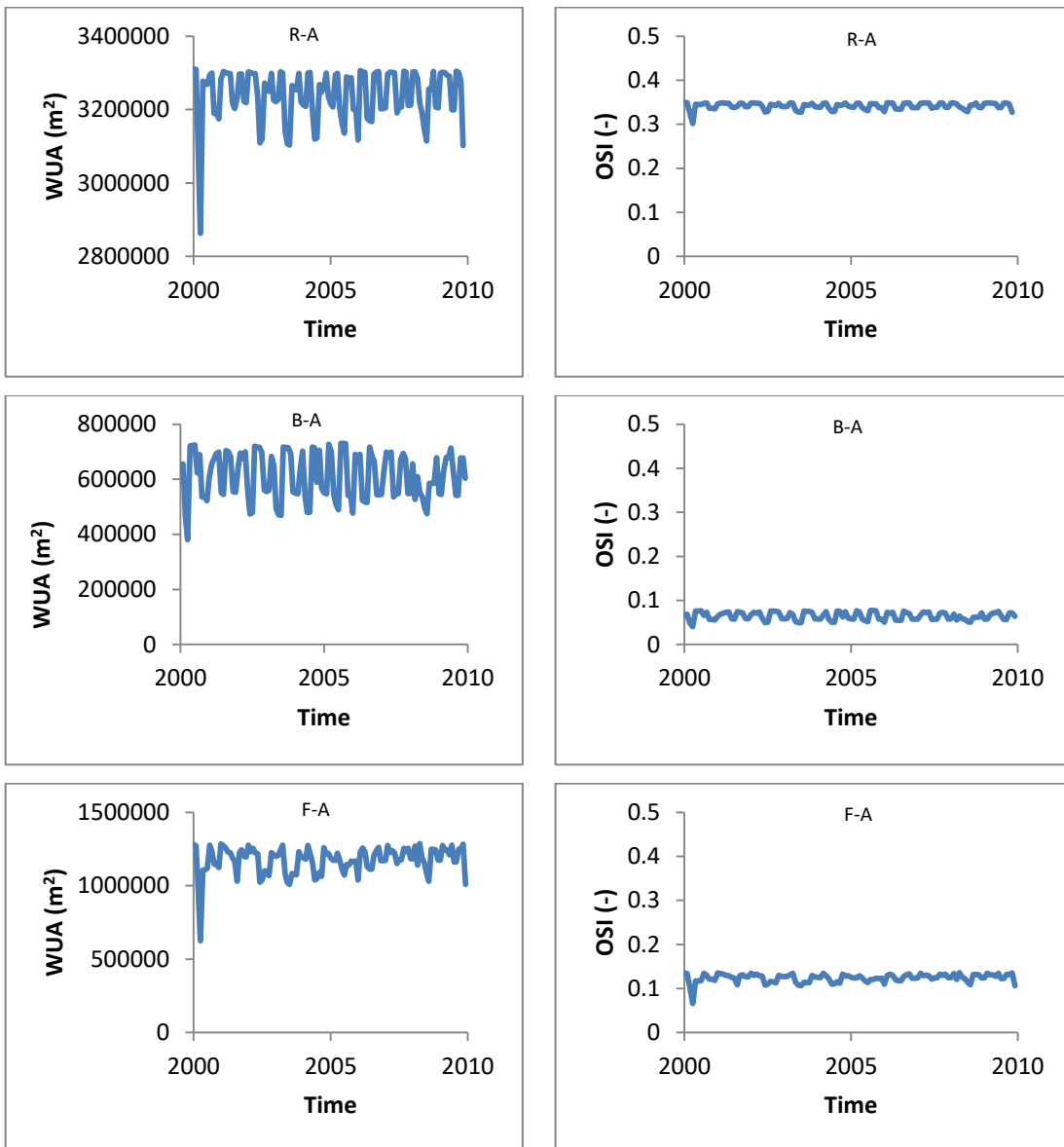


Figure 5.14: The WUA and OSI distribution for adult rainbow trout (R-A, upper), brown trout (B-A, middle), and flannelmouthsucker (F-A, lower) from 2000 to 2009 in the Sub4 river stretch.

In the river stretch Sub5, the adult WUA and OSI simulation results are shown in Figure 5.15. From the simulation results, it can be seen that the adult rainbow trout WUA values showed a decreasing trend from 2000 to 2009. The WUA values decreased from $7.6 \times 10^5 \text{ m}^2$ in 2000 to $7.2 \times 10^5 \text{ m}^2$ in 2009. The corresponding OSI values were also decreased from 0.3 in 2000 to 0.28 in 2009. The adult life stage of brown trout WUA values slightly fluctuated with mean value $1.4 \times 10^5 \text{ m}^2$ from 2000 to 2009. The corresponding OSI values had a relatively constant value of 0.055 from 2000 to 2009. The adult flannelmouth sucker WUA values stayed at the value of $1.4 \times 10^5 \text{ m}^2$ from 2000 to 2007 and then

changed between $1.2 \times 10^5 \text{ m}^2$ and $1.7 \times 10^5 \text{ m}^2$ in the later simulation times. The average adult flannemouth sucker OSI value was 0.05 from 2000 to 2009.

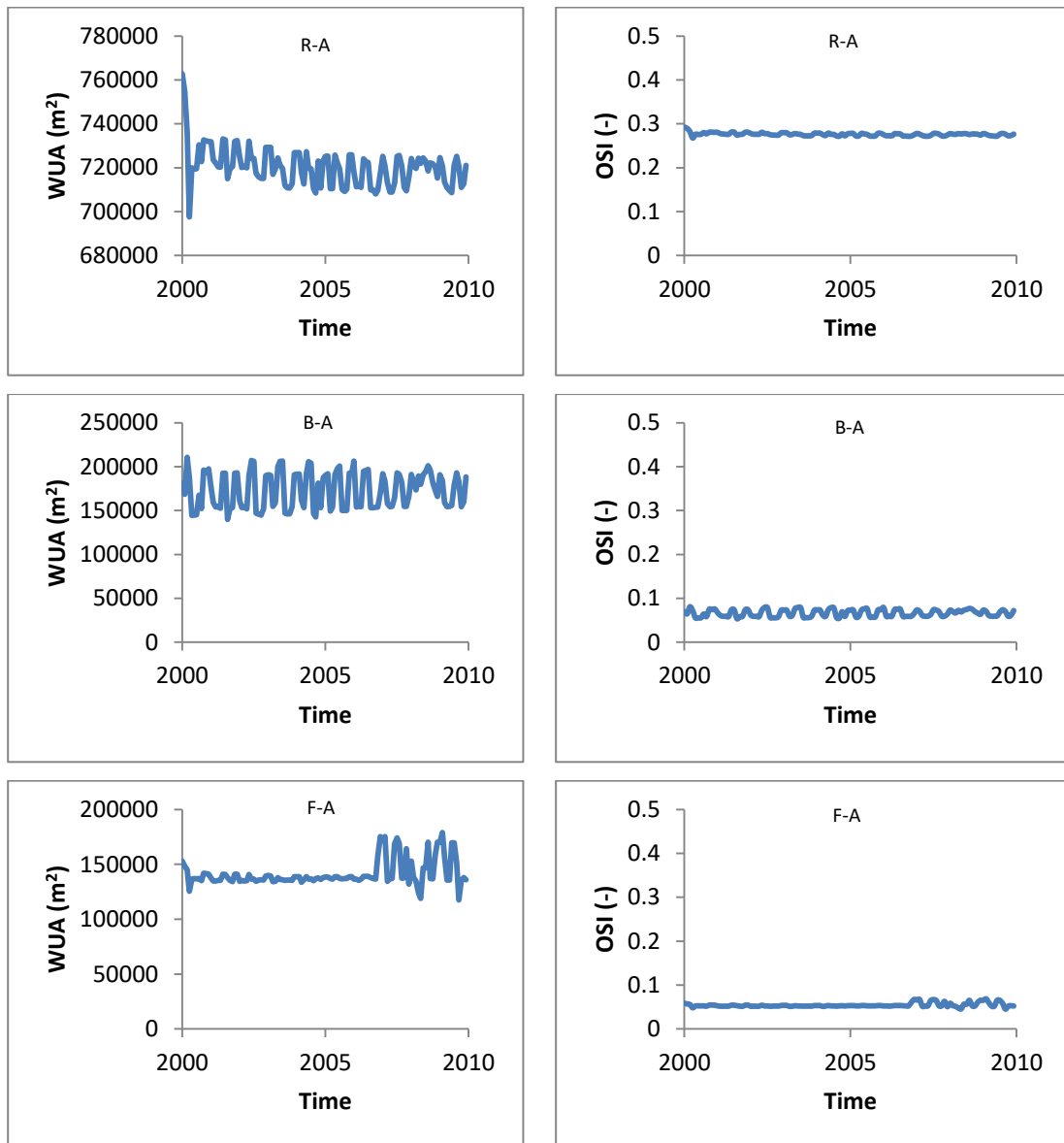


Figure 5.15: The WUA and OSI distribution for adult rainbow trout (R-A, upper), brown trout (B-A, middle) and flannemouthsucker (F-A, lower) from 2000 to 2009 in the river stretch Sub5.

The whole Colorado River, from Lees Ferry to 50 km upstream of Lake Mead, is represented by the average value of OSI in all five subareas at adult life stage. The WUA values for the whole Colorado River can be represented by the sum of WUA values in all five subareas. The WUA and OSI values for all of the Colorado River from 2000 to 2009 are shown in Figure 5.16. It can be seen that the rainbow trout's WUA and OSI values remained at a stable level during the simulation time from 2000 to 2009, with value of $6.7 \times 10^6 \text{ m}^2$ and 0.3 for WUA and OSI respectively. For the brown trout, the WUA and OSI values showed a slightly decreasing trend from 2000 to 2009. In contrast to the

brown trout, the flannelmouth sucker's WUA and OSI values showed increasing trends from 2000 to 2009, with maximum values of $3.4 \times 10^4 \text{ m}^2$ and 0.05 for WUA and OSI respectively.

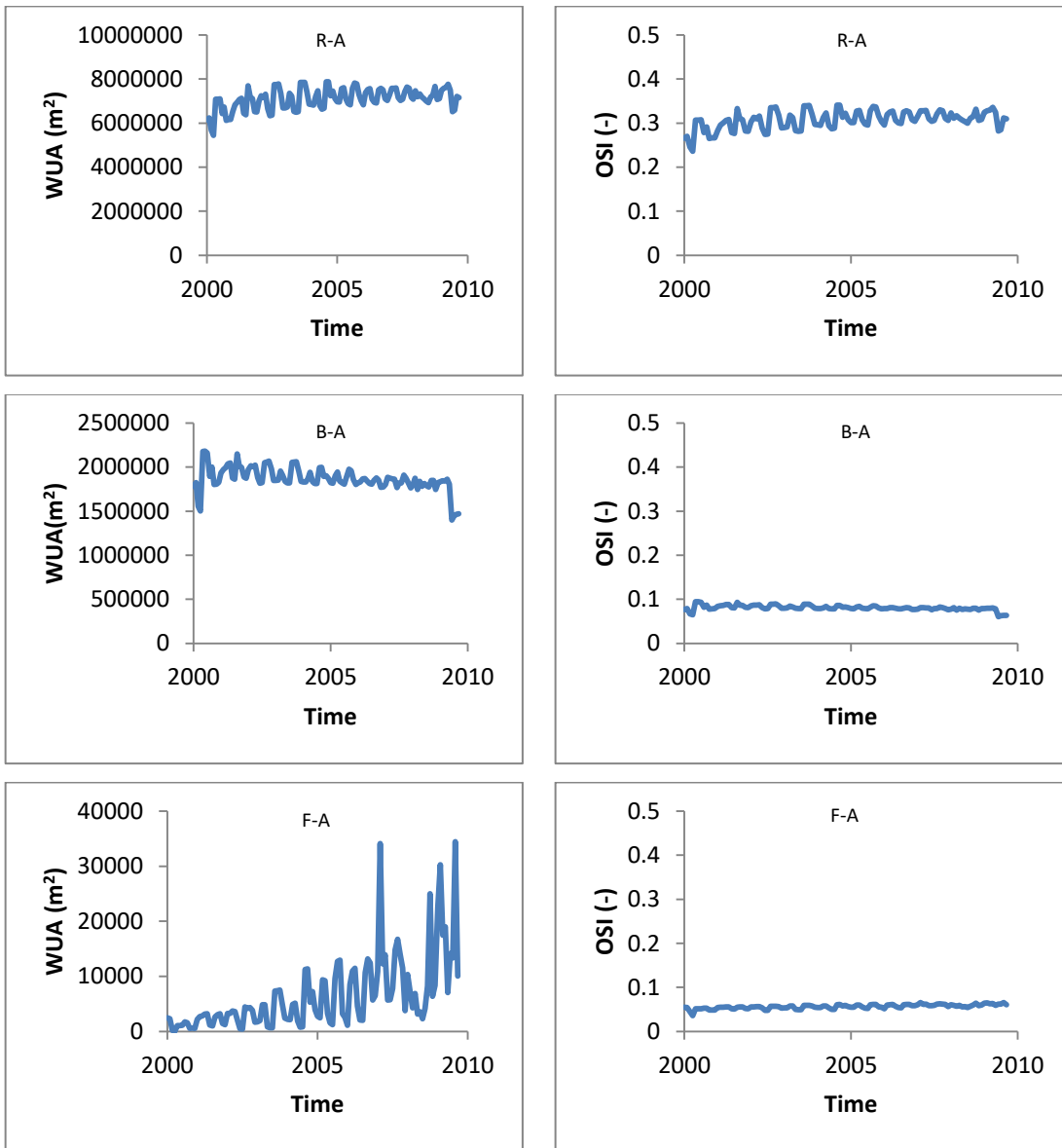


Figure 5.16: The WUA and OSI distribution for adult rainbow trout (R-A, upper), brown trout (B-A, middle) and flannelmouth sucker (F-A, lower) from 2000 to 2009 in the whole Colorado River.

5.3.4 Population number analysis based on the logistic population model

The logistic population model (Equation 3-48) is used to calculate the three fish species' population number in all five subareas and the whole river stretch of the Colorado River. The WUA and OSI values based on adult SI curves were set as inputs for the logistic population model. The initial fish population number has been set in Table 5.3. The initial fish number was determined by the total fish number, in this case study established by

USGS, and the proportion of each fish species (personal contact with Dr. Makinster). In the logistic population model time steps of one year and one month were used. The results using a one-year-time-step are presented in the Figures 5.17 to 5.22. The fish data measured, established by USGS, were compared with our simulation results and the performance of the logistic population model was examined with the root mean square error (RMSE), mean absolute error (MAE), and percentage bias (PBIAS) (Table 5.4).

Table 5.3: Fish population number used for simulation at five subareas in 2000.

	Rainbow trout	Brown trout	Flannelmouth sucker
Sub1	150,000	1,800	1,900
Sub2	62,000	800	3,000
Sub3	38,000	25,000	1,000
Sub4	8,000	5,100	51
Sub5	8,000	648	58
All reachers	805,775	213,946	110,079

The comparison of the simulated and surveyed results in the Sub1 river stretch are shown in Figure 5.17. It can be seen that (1) the rainbow trout number surveyed in 2009 (290 ± 35 CPUE) was the highest number observed during all simulation times. The rainbow trout numbers surveyed generally declined from 150 in 2000 to 50 in 2006, and then the fish number surveyed showed an increasing trend after 2006. The maximum rainbow trout numbers surveyed happened in 2009 with a value of 290. The simulation results in Sub1 showed that the rainbow trout number decreased from 2000 to 2007, and then remained at a stable level over the simulation time from 2007 to 2009. (2) The brown trout numbers surveyed in the Sub1 river stretch showed that: the brown trout declined from 2000 (1.8 ± 1.6 CPUE) to 2009 (0 ± 0 CPUE) except in the year 2004 (1.5 ± 0.7 CPUE). The simulated brown trout numbers increased from 2000 to 2001 and then showed a decreasing trend until the end of the simulation time. (3) The flannelmouth sucker numbers surveyed increased from 2000 to 2006, and then significantly declined in 2007 before slightly increasing again during the simulation time. The simulated flannelmouth sucker numbers also showed a similar trend with in the fish data surveyed.

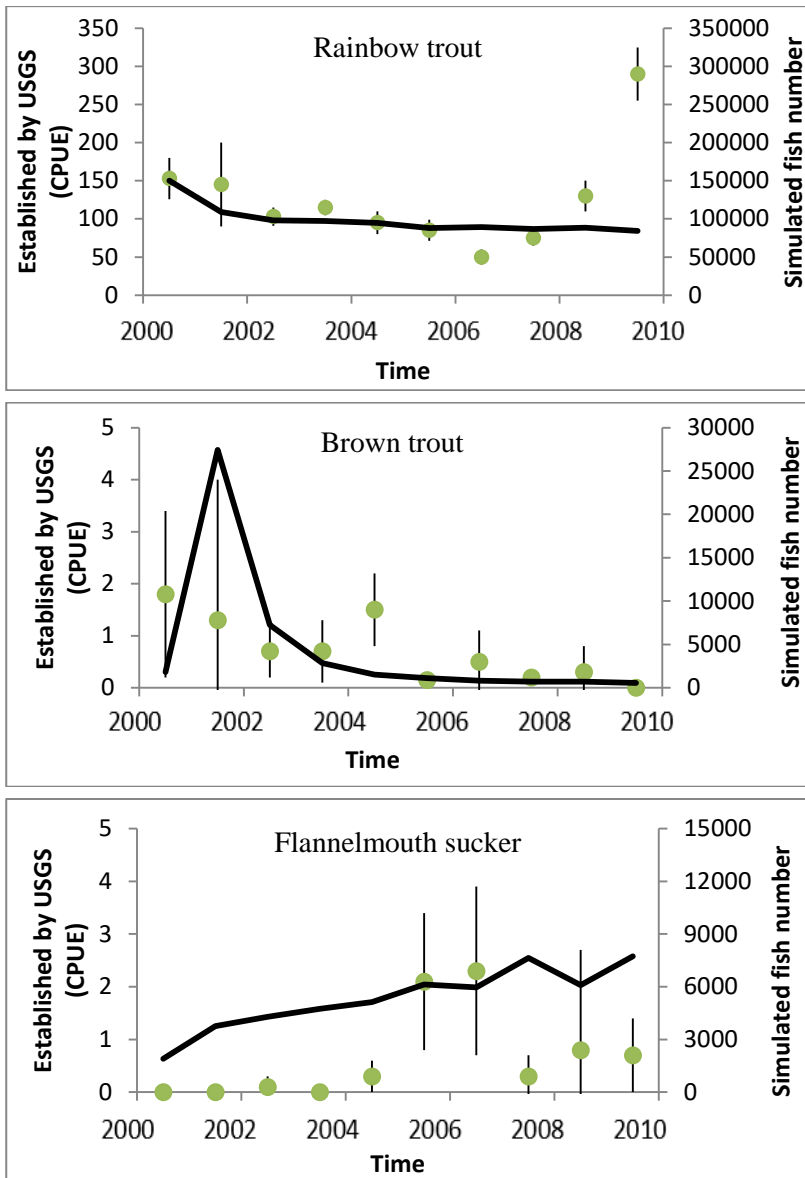


Figure 5.17: The variations of rainbow trout (upper), brown trout (middle) and flannelmouth sucker (lower) population numbers from 2000 to 2009 in the river stretch Sub1 (time step is one year; CPUE is the mean catch per unit effort; \blacklozenge is the USGS result; — is the simulated fish number).

In the river stretch Sub2, (1) the rainbow trout numbers surveyed in 2001 (70 ± 18 CPUE) were the highest observed fish numbers since 2000 (59 ± 15 CPUE). The surveyed rainbow trout numbers showed a slightly increasing trend from 2000 to 2001, and then the fish numbers declined from 2001 to 2006, and increased again from 2006 to 2009. The simulated rainbow trout numbers had a slightly different trend in these years from 2000 to 2002. (2) The surveyed brown trout fish numbers declined from 2001 (2.1 ± 1.6 CPUE) to 2006 (0 CPUE), and then remained in a relatively low level with a value of nearly 0. The simulated brown trout numbers remained relatively stable at the level of 1000, which does not match well with the fish numbers surveyed. (3) For the flannelmouth sucker in the river stretch Sub2, the fish numbers surveyed declined from 2000 (3 ± 2 CPUE) to

2004 (1 ± 0.4 CPUE), and then increased from 2004 to 2007 (7 ± 2.2 CPUE) before the fish numbers decreased again to 5.5 in 2009. The simulation flannelmouth sucker numbers showed the same trend as the fish number surveyed except for the years from 2006 to 2007 (Figure 5.18).

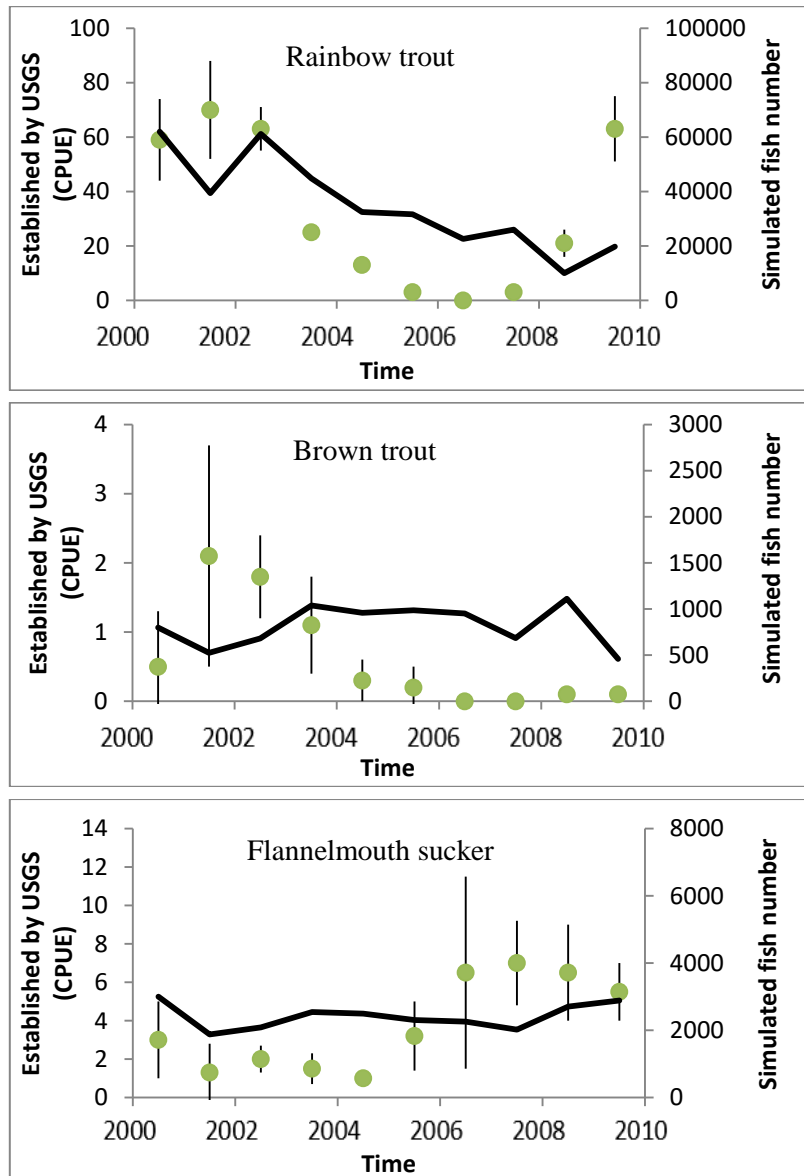


Figure 5.18: The variations of rainbow trout (upper), brown trout (middle) and flannelmouth sucker (lower) population numbers from 2000 to 2009 in the river stretch Sub2 (time step is one year; CPUE is the mean catch per unit effort; \blacklozenge is the USGS result; $-$ is the simulated fish number).

On the basis of the fish numbers surveyed in the river stretch Sub3, (1) the mean value of rainbow trout numbers also declined from 2001 to 2006 and increased from 2006 to 2009 (21 ± 7 CPUE) with the maximum value of 50 ± 13 CPUE in 2001. The simulated maximum rainbow trout numbers were in 2000 with a initial value of 38,000. The simulated rainbow trout number variations did not match well in 2007 and in 2009. (2) the

brown trout fish numbers surveyed declined from 2001 (30 ± 10 CPUE) to 2006 (1 ± 0.5 CPUE), and the fish numbers remained relatively low in 2006 and in 2007. After that the brown trout numbers dramatically increased in 2008 (13 ± 2 CPUE) and 2009 (20 ± 5 CPUE). The simulated brown trout numbers increased from 2000 (25,000 fish) to 2002 (36,365 fish), and then the fish numbers decreased before increased again in 2009 (23,602 fish). (3) The flannelmouth sucker numbers surveyed remained relatively low level from 2000 (1 ± 0.7 CPUE) to 2005 (1 ± 0.7 CPUE), and then the fish numbers dramatically increased in 2006 (5.3 ± 1.7 CPUE). After that, the mean surveyed numbers fluctuated between 3 and 5. The simulated flannelmouth sucker numbers variation trend matched well with fish data the surveyed, with the maximum fish number of 26,523 in 2009 (Figure 5.19).

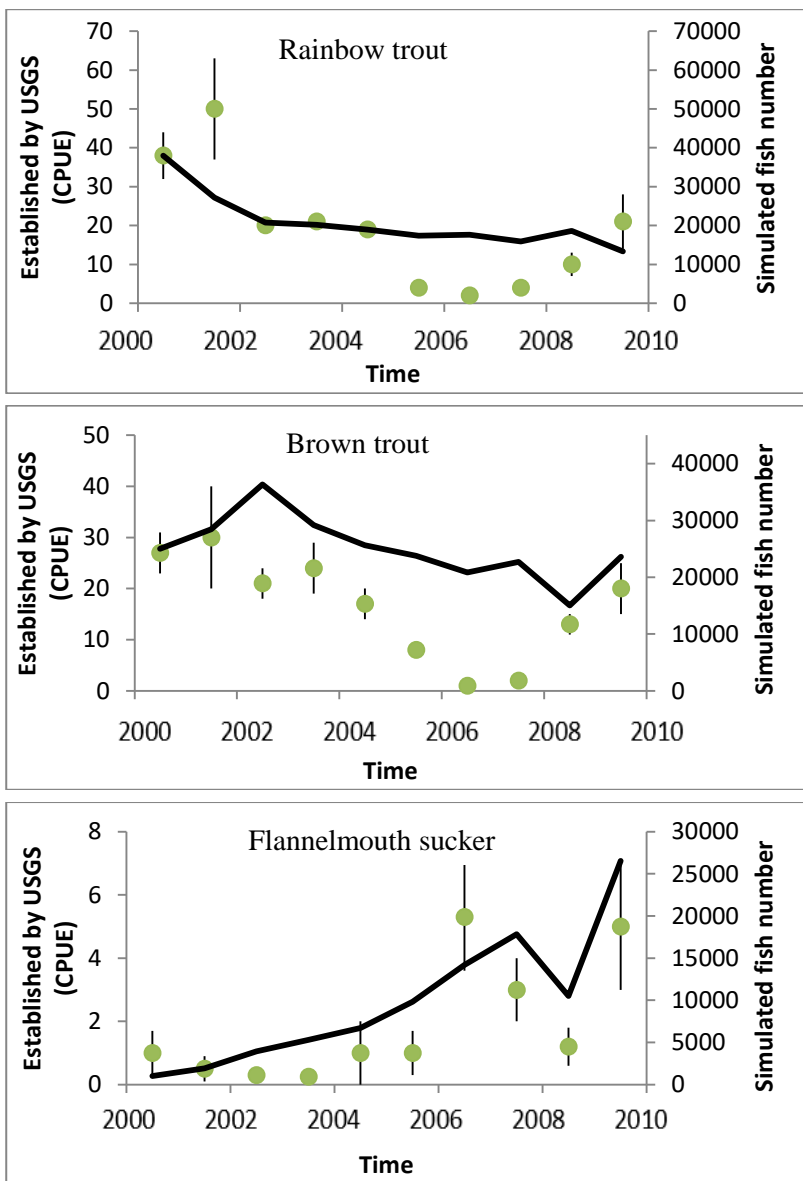


Figure 5.19: The variations of rainbow trout (upper), brown trout (middle) and flannelmouth sucker (lower) population number from 2000 to 2009 in the river stretch Sub3

(time step is one year; CPUE is the mean catch per unit effort; ♣ is the USGS result; – is the simulated fish number).

In the river stretch Sub4, (1) the rainbow trout numbers surveyed in 2001 (30 ± 8 CPUE) are the highest fish numbers of all simulation times. The rainbow trout surveyed fish numbers decreased from 2001 to 2007 (2 ± 0.5 CPUE), and then the fish numbers increased again in 2008 (10 ± 3 CPUE) and in 2009 (26 ± 6 CPUE). The simulated rainbow trout number demonstrated a similar trend as the fish numbers surveyed except in the years from 2005 to 2007. The maximum fish numbers were in 2001 with a value of 18,759. (2) The brown trout number surveyed increased from 2000 (2.5 ± 1.1 CPUE) to 2002 (6 ± 1.6 CPUE), but then decreased in later years and remained at a relative low value. In contrast to the surveyed brown trout numbers, the simulated fish numbers didn't change so dramatically, with a value of 7,903 in 2001 and 3,465 in 2008 respectively. (3) From 2000 to 2009, the flannelmouth sucker fish numbers increased from 2000 (1 ± 1 CPUE) to 2006 (23 ± 3 CPUE) and experienced a decreasing trend in later years, with a fish number of 12 in 2009. During the simulation time, the simulated fish number showed the same trend as in the surveyed data except in 2001. The maximum simulated fish number was 223 in 2001, and the minimum fish number was 75 in 2003 (Figure 5.20).

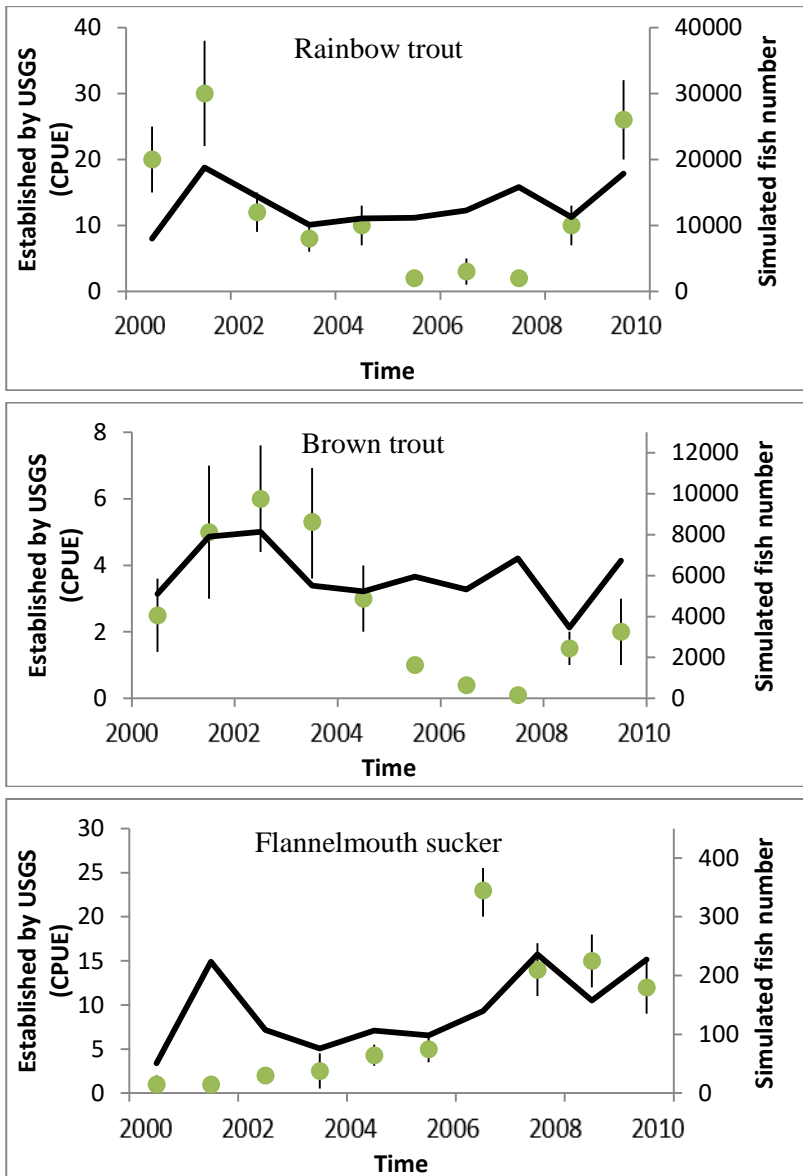


Figure 5.20: The variations of rainbow trout (upper), brown trout (middle) and flannelmouth sucker (lower) population numbers from 2000 to 2009 in the river stretch Sub4 (time step is one year; CPUE is the mean catch per unit effort; \blacklozenge is the USGS result; — is the simulated fish number).

In the river stretch Sub5, (1) the rainbow trout fish numbers surveyed remained at a relatively low value except in the years 2000 (7.5 ± 4.5 CPUE) and 2001 (6 ± 3 CPUE). The simulated rainbow trout fish numbers decreased from 2000 (8,000 fish) to 2009 (2,329 fish). (2) The brown trout numbers surveyed decreased from 2002 (0.9 ± 0.7 CPUE) to 2007 (0.05 ± 0.05 CPUE) with the highest value of 0.9 CPUE in 2002. In contrast to the surveyed data, the simulated brown trout number had the highest numbers in 2008 with a value of 1,210. (3) The flannelmouth sucker numbers surveyed remained at low values from 2000 (1 ± 1 CPUE) to 2007 (5 ± 1 CPUE), but then the fish numbers increased in 2008 and 2009. Simulated flannelmouth sucker numbers followed the same trend as the fish number surveyed, except in the year 2007 (Figure 5.21).

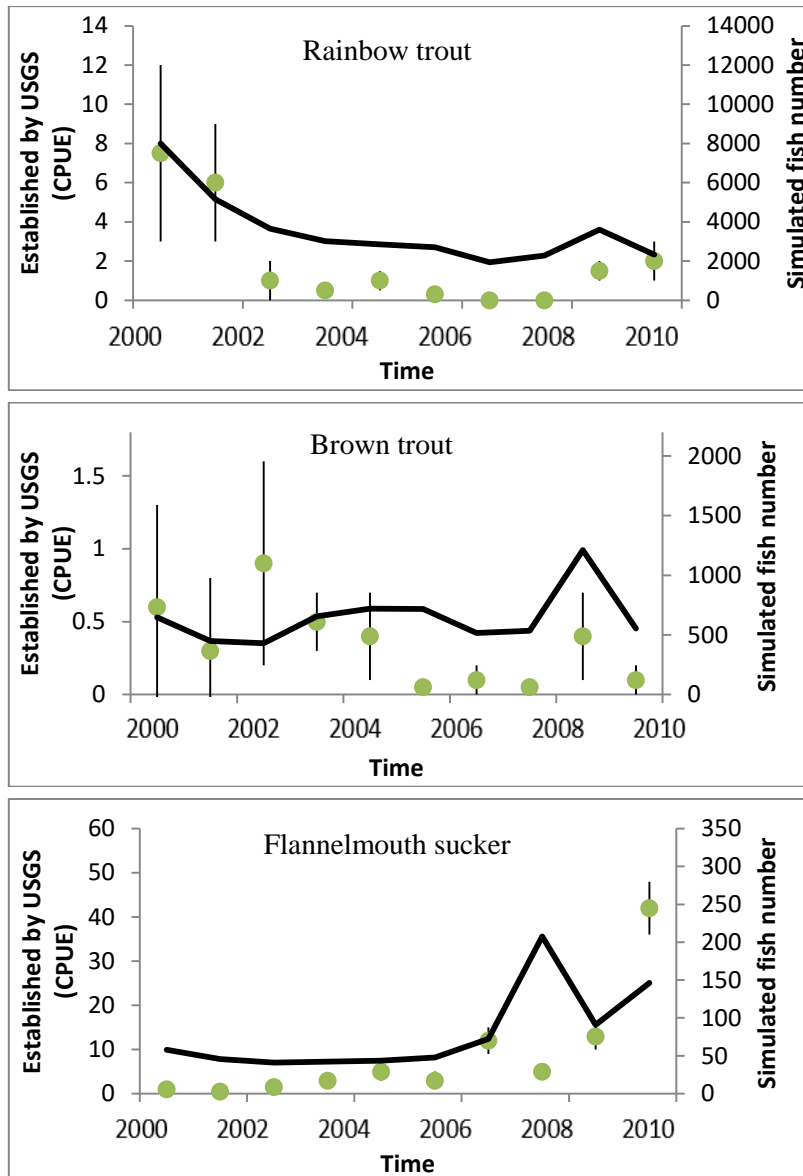


Figure 5.21: The variations of rainbow trout (upper), brown trout (middle) and flannelmouth sucker (lower) population numbers from 2000 to 2009 in the river stretch Sub5 (time step is one year; CPUE is the mean catch per unit effort; \blacklozenge is the USGS result; $-$ is the simulated fish number).

For the whole Colorado River, the rainbow trout, brown trout, and flannelmouth sucker simulated fish numbers matched well with the surveyed fish numbers established by USGS (personal contact with Dr. Makinster). (1) The highest surveyed rainbow trout numbers were in 2009 with a value of 62. The rainbow trout number surveyed declined from 2000 to 2006 and then the fish numbers increased after 2006. The rainbow trout fish numbers surveyed increased from 2008 to 2009 dramatically. The simulated rainbow trout population numbers showed exactly the same trend as the rainbow trout number surveyed. (2) In contrast to the rainbow trout numbers, which fluctuated from 2000 to 2009, both the surveyed brown trout number and the simulated brown trout number showed a decreasing trend during the simulation times. (3) In contrast to the brown trout, both the

surveyed flannelmouth sucker numbers and simulated flannelmouth sucker numbers showed an increasing trend from 2000 to 2009.

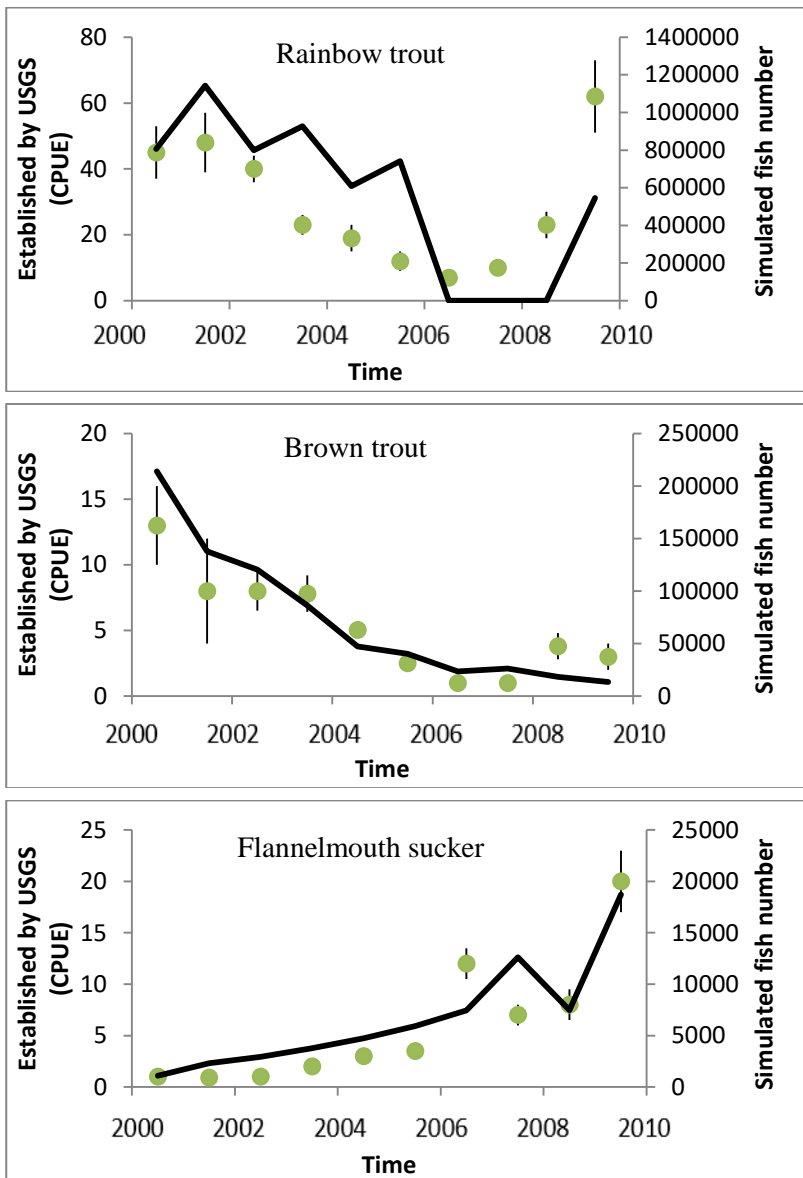


Figure 5.22: The variation of rainbow trout (upper), brown trout (middle) and flannelmouth sucker (lower) population number from 2000 to 2009 over the whole river stretch (time step is one year; CPUE is the mean catch per unit effort; ● is the USGS result; — is the simulated fish number).

Over the whole river stretch, based on the logistic population model when the simulated time step was changed to one month, the simulated fish numbers and the surveyed fish numbers from 2000 to 2009 are shown in Figure 5.23. It can be seen that the simulated fish numbers in the logistic model also agree quite well with the surveyed fish numbers (Figure 5.22, Figure 5.23).

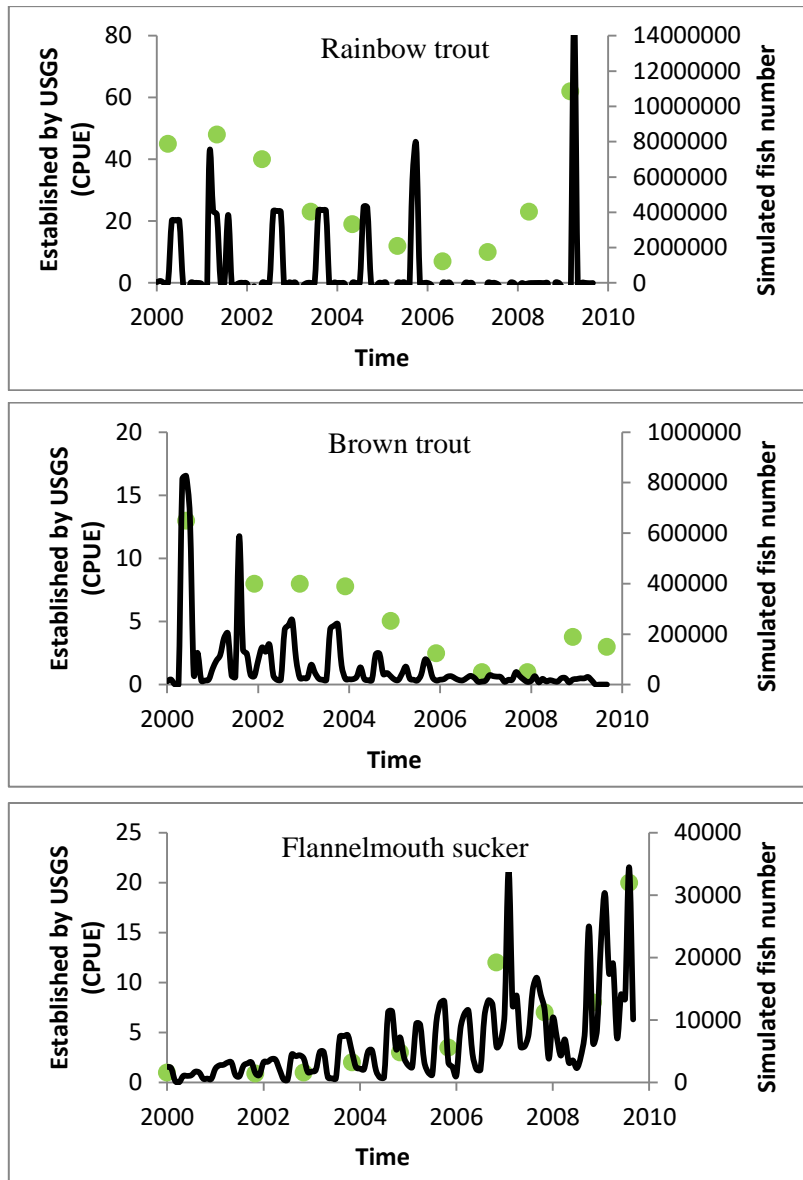


Figure 5.23: The variations of rainbow trout (upper), brown trout (middle) and flannelmouth sucker (lower) population number from 2000 to 2009 in the whole river stretch (time step is one month; CPUE is the mean catch per unit effort; ● is the USGS result; — is the simulated fish number).

5.3.5 Population density analysis based on the logistic population model

Based on the fish density distribution equation (Equation 3.49) in the logistic population model, the three selected fish population distributions were simulated. The rainbow trout, brown trout and flannelmouth sucker population densities in all five subareas from 2000 to 2009 are shown in Figure 5.24. From the Figure 5.24, it can be seen that the fish population density distribution showed trends very similar to the HSI distribution from 2000 to 2009 (Equation 3.49). Compared to the brown trout and flannelmouth sucker, the rainbow trout densities are higher than the fish densities of brown trout and flannelmouth sucker. When compared to the fish density in all five subareas, it can be seen that the

rainbow trout densities in the river stretch Sub1 were higher than the fish densities in other subareas. In the river stretch Sub1, the fish densities were relatively even distributed along the river stretch. The rainbow trout population densities have the highest value, and the brown trout densities have the lowest value. In the river stretch Sub2, the high fish population densities were mainly located along the river bank. In the river stretch Sub3, the population densities for rainbow trout and brown trout showed a decreasing trend from 2000 to 2009. Meanwhile, the flannelmouth sucker population densities were remained at a relatively stable level from 2000 to 2009. In the river stretches Sub4 and Sub5, the three fish population densities in the middle of the river are higher than the fish population densities along the river bank.

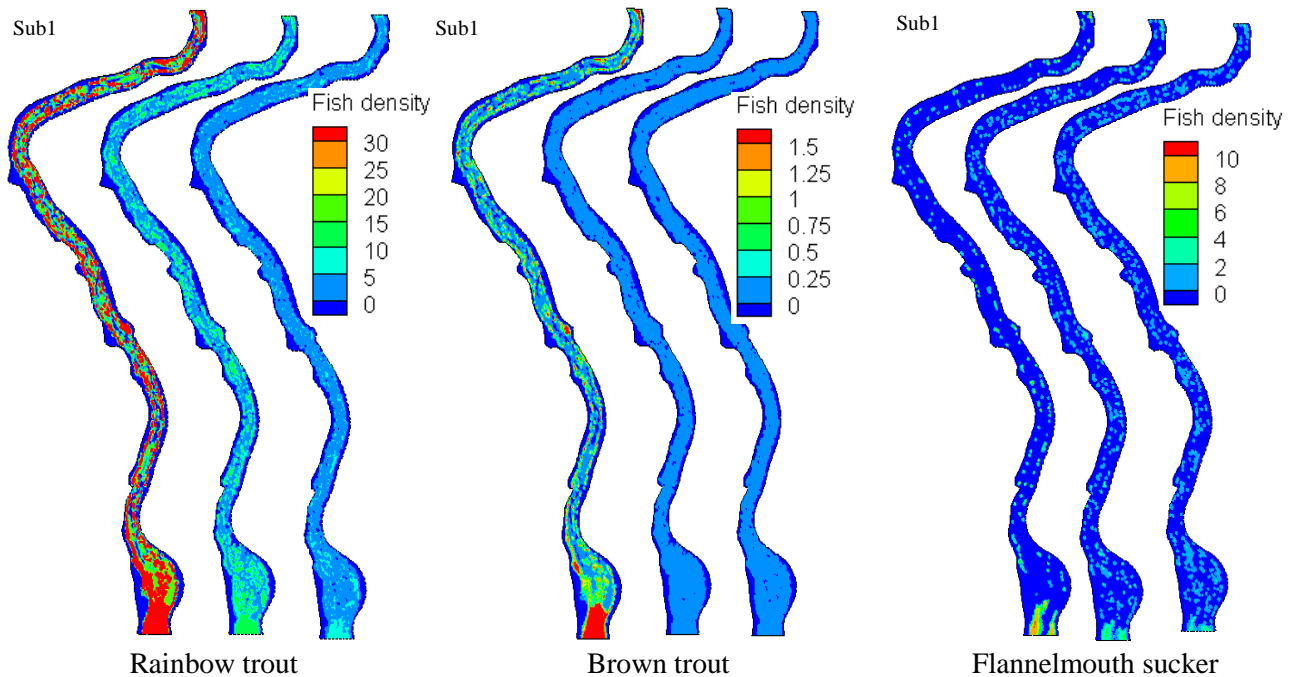


Figure 5.24a: The rainbow trout, brown trout and flannelmouth sucker population density distribution in the river stretch Sub1 (from left to right: in 2000, 2005 and 2009).

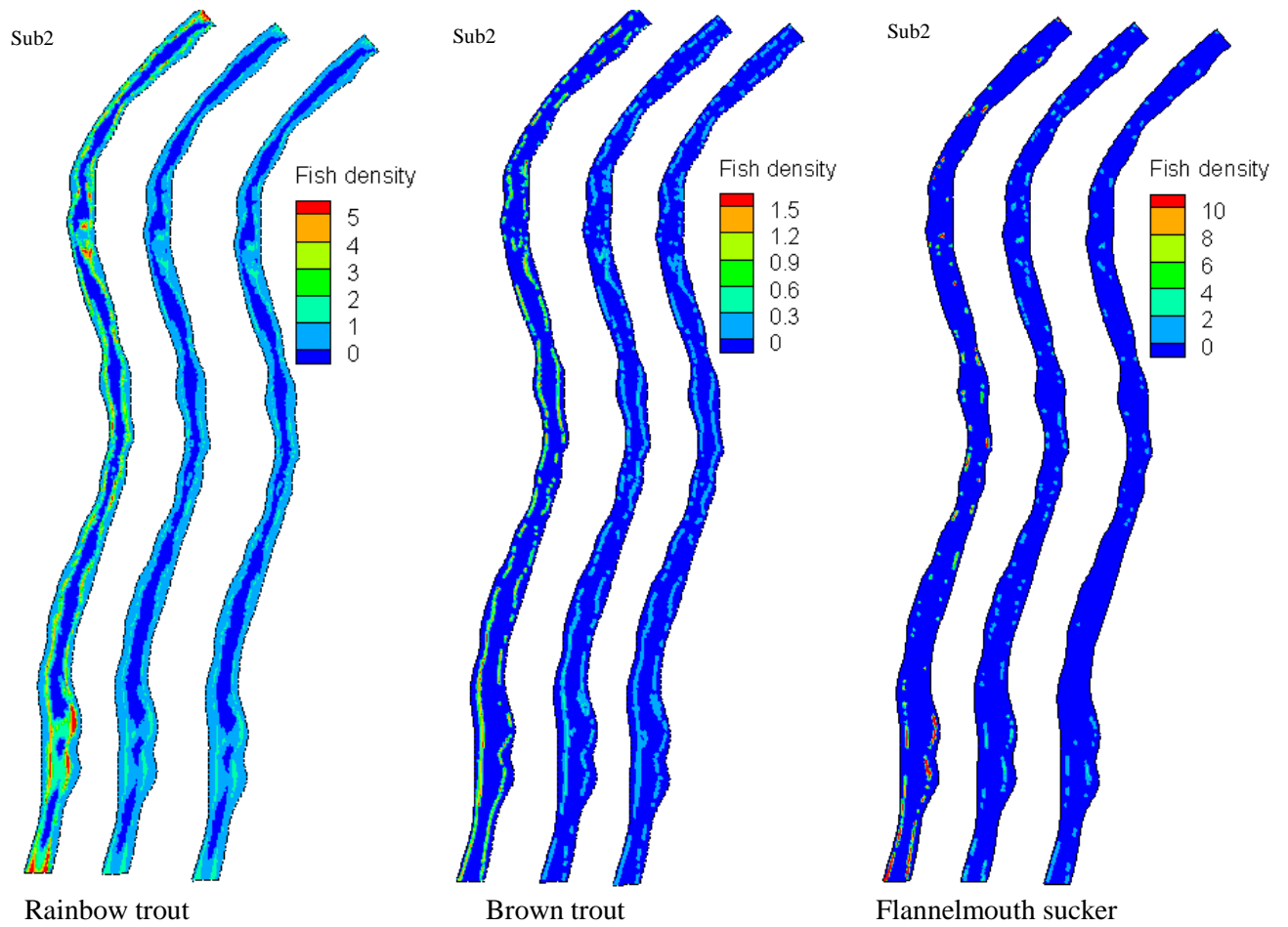


Figure 5.24b: The rainbow trout, brown trout and flannelmouth sucker population density distribution in the river stretch Sub2 (from left to right: in 2000, 2005 and 2009).

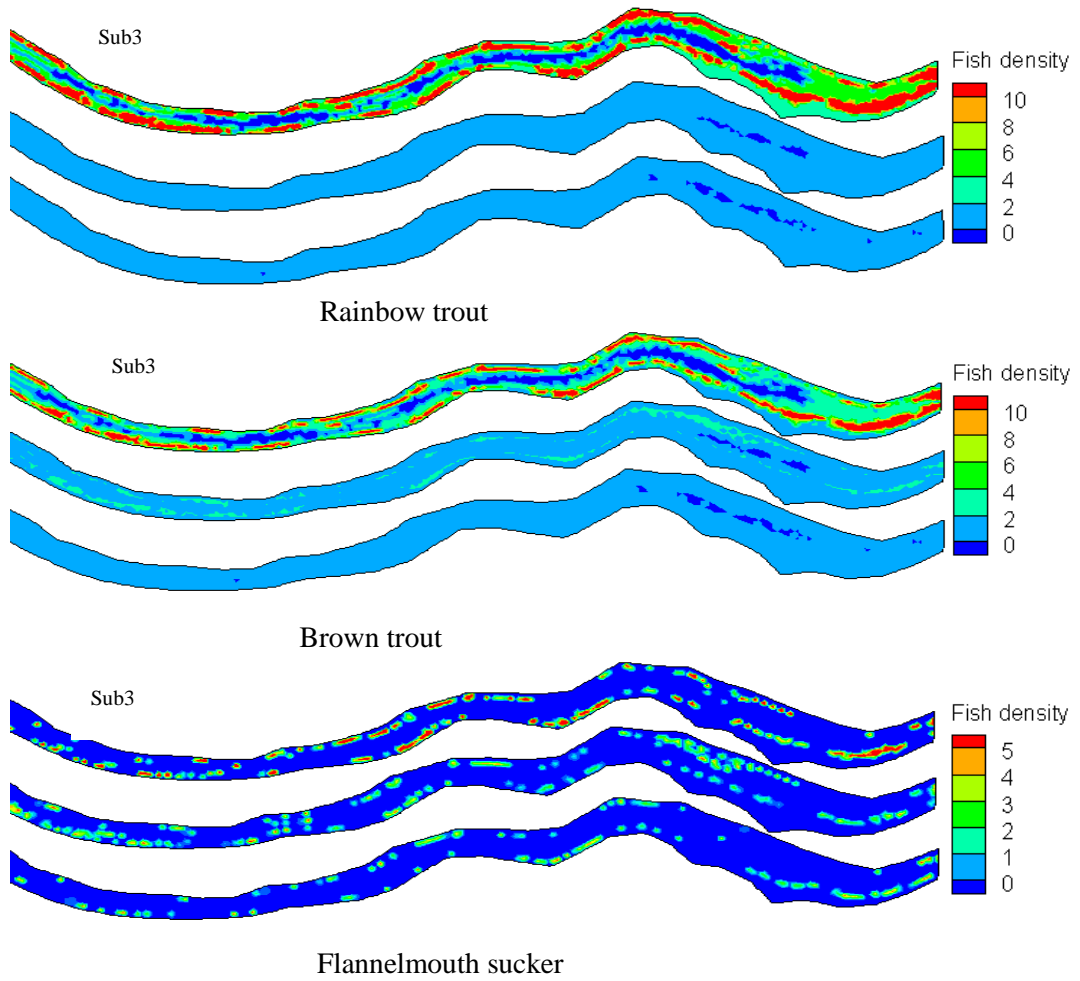


Figure 5.24c: The rainbow trout, brown trout and flannelmouth sucker population density distribution in the river stretch Sub3 (from up to down: in 2000, 2005 and 2009).

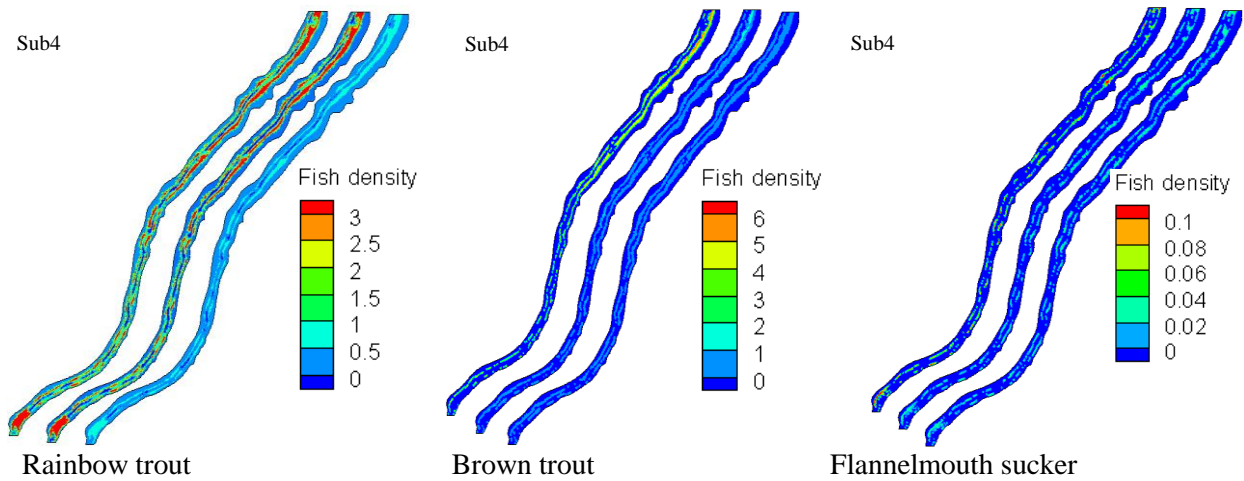


Figure 5.24d: The rainbow trout, brown trout and flannelmouth sucker population density distribution in the river stretch Sub4 (from left to right: in 2000, 2005 and 2009).

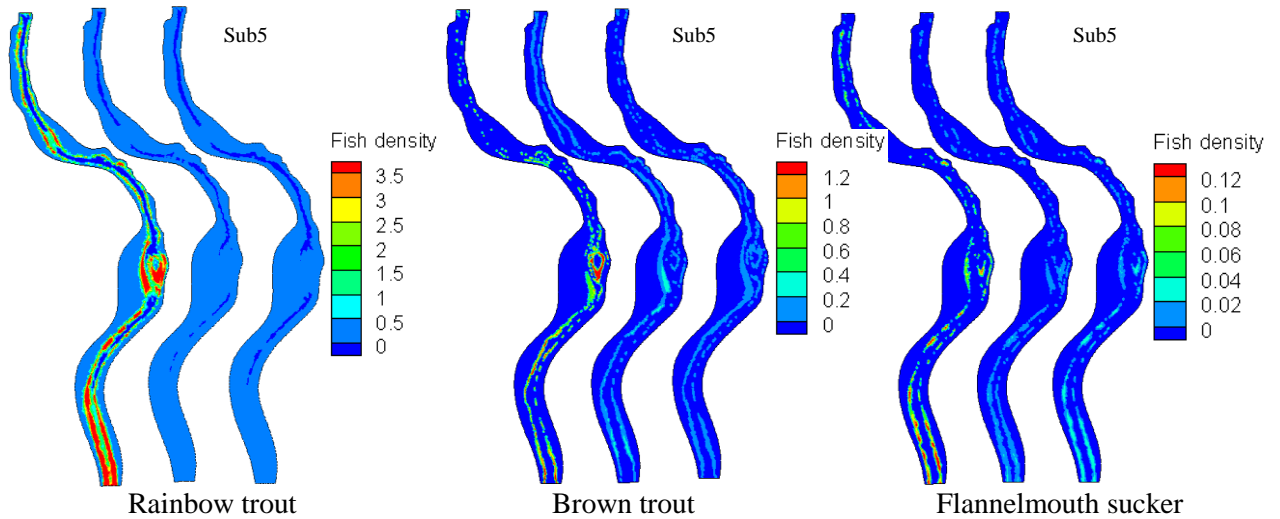


Figure 5.24e: The rainbow trout, brown trout and flannelmouth sucker population density distribution in the river stretch Sub5 (from left to right: in 2000, 2005 and 2009).

The performance of the logistic population model is presented in Table 5.4 through the MAE, RMSE and PBLAIS statistical indices. From Table 5.4 and Figures 5.17 to 5.23, it can be seen that the simulated fish population numbers in all five subareas of the Colorado River fit the fish numbers surveyed, while only a few simulation results do not match the fish data surveyed. MAE values are indicative of good logistic population model performance. The average values of MAE are 27%, 36% and 39% respectively for rainbow trout, brown trout, and flannelmouth sucker in all five subareas. The average values of RMSE are 0.29, 0.42, and 0.41 for rainbow trout, brown trout, and flannelmouth sucker respectively. The absolute value of PBIAS varied from 0.32 to 0.69 for the rainbow trout, varied from 3.4 to 0.49 for the brown trout, and varied from 0.26 to 0.93 for the flannelmouth sucker. Overall, the performance of the logistic model gives us the confidence to accept the model's simulation.

Table 5.4: Correlation coefficients between simulated and measured fish numbers in the five subareas of the Colorado River.

	Rainbow trout			Brown trout			Flannelmouth sucker		
	MAE	RMSE	PBLAS	MAE	RMSE	PBLAS	MAE	RMSE	PBLAS
Sub1	0.25	0.27	0.40	0.32	0.42	-3.45	0.43	0.44	0.45
Sub2	0.23	0.26	0.32	0.69	0.74	0.69	0.33	0.41	0.28
Sub3	0.24	0.27	0.49	0.25	0.32	0.36	0.53	0.56	0.26
Sub4	0.36	0.38	0.55	0.23	0.31	0.24	0.53	0.54	0.93
Sub5	0.26	0.26	0.69	0.29	0.33	0.49	0.11	0.12	0.37

5.3.6 Fish population analysis based on the fish length distribution model

In order to simulate the fish population number at each life stage, the matrix population model needs to be applied. In the matrix population model, the fry, juvenile, and spawning WUA and OSI for three selected fish species also needed to be simulated additionally and the simulation results are shown in Figures 5.26a, b, and c.

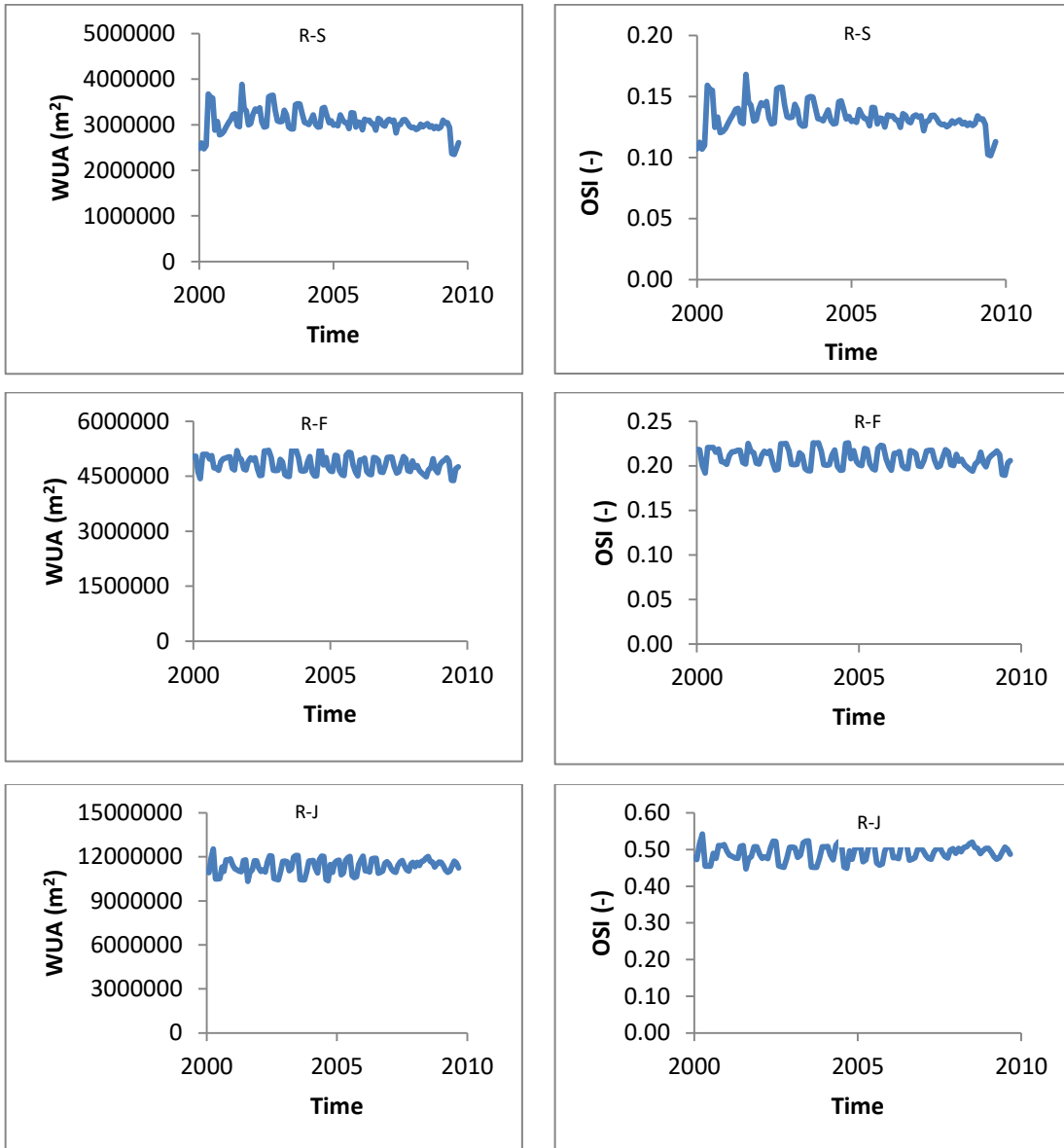


Figure 5.25a: The WUA and OSI distribution for spawning, fry, and juvenile rainbow trout (R-S is the rainbow trout spawning life stage; R-F is the rainbow trout fry life stage; R-J is the rainbow trout juvenile life stage).

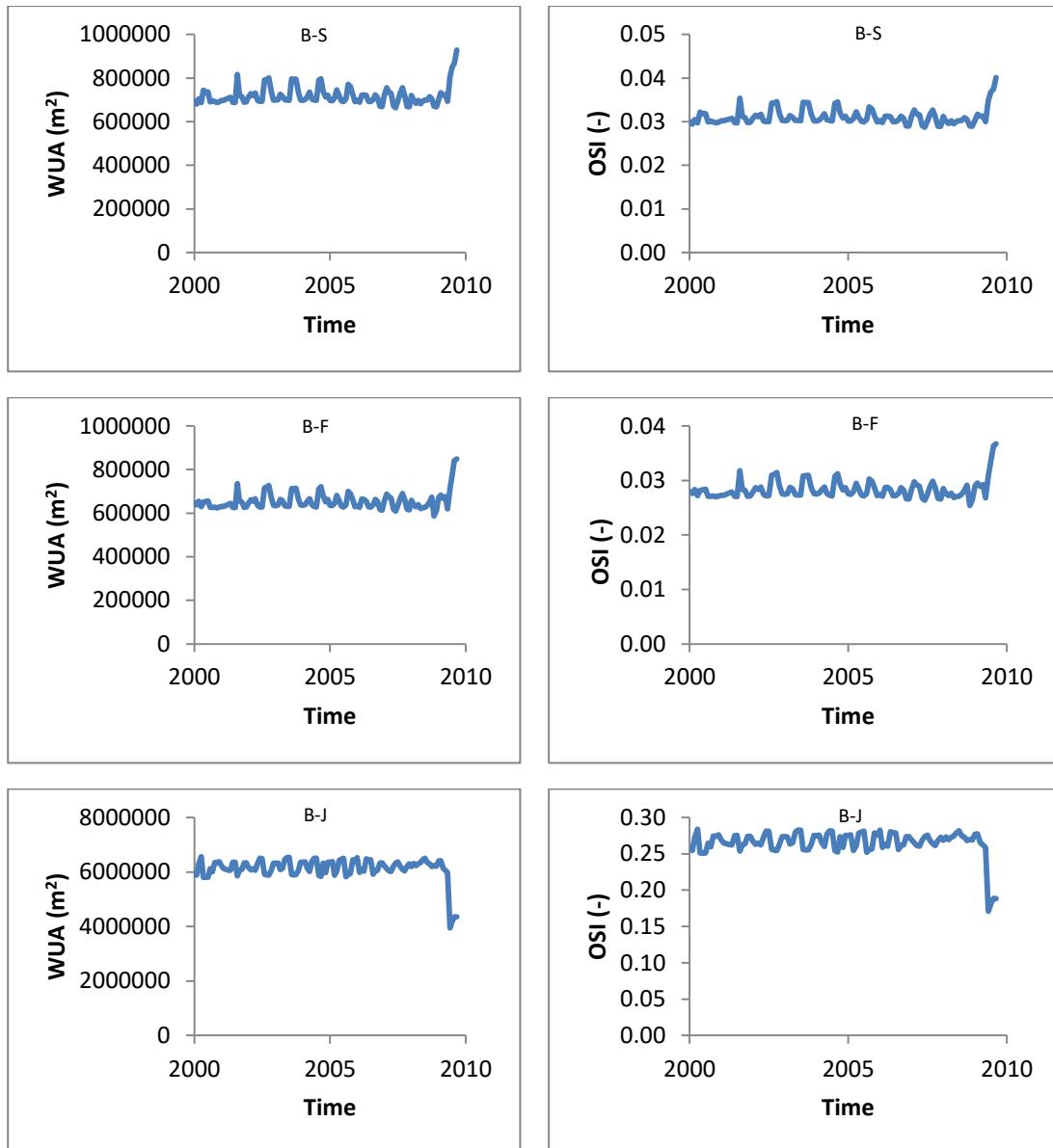


Figure 5.25b: The WUA and OSI distribution for spawning, fry, and juvenile brown trout (B-S is the brown trout spawning life stage; B-F is the brown trout fry life stage; B-J is the brown trout juvenile life stage).

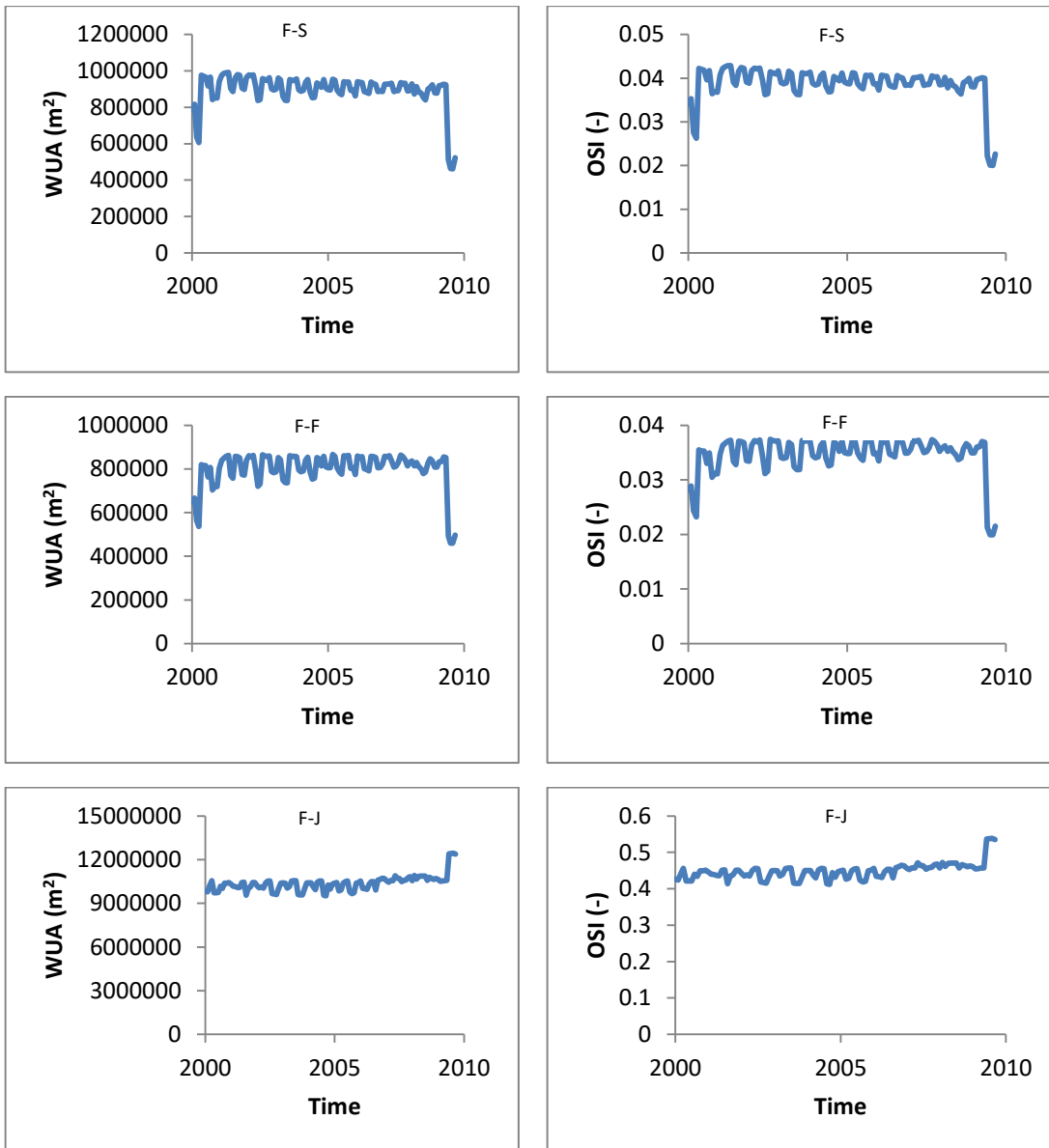


Figure 5.25c: The WUA and OSI distribution for spawning, fry, and juvenile flannelmouth sucker (F-S is the flannelmouth sucker spawning stage; F-F is the flannelmouth sucker fry life stage; F-J is the flannelmouth sucker juvenile life stage).

Based on the matrix population model (Equations 3-50, 3-51 and 3-52) and the OSI values, each length stage population numbers have been obtained. The total fish population numbers for the three selected fish species are shown in Figure 5.26. The specific length fish number variations for the three selected fish species are shown in Appendix IV. From the Figure 5.26, it can be seen that the general trends of the rainbow trout, brown trout, and flannelmouth sucker population numbers have a good agreement with the three surveyed fish number variations (Figure 5.26). However, for each life stage comparison based on the matrix population model, the agreement between simulation and the surveyed fish data is not quite good (see Appendix IV). The reasons for the divergences maybe due to the empirical parameter settings in the matrix population model are not

particularly suitable for these three fish species. It also could be the surveyed fish data cannot correctly represent the real fish length structure. Overall, despite the differences between the simulated results and the surveyed fish data, the ecohydraulic model system has proven to be quite useful in many case studies.

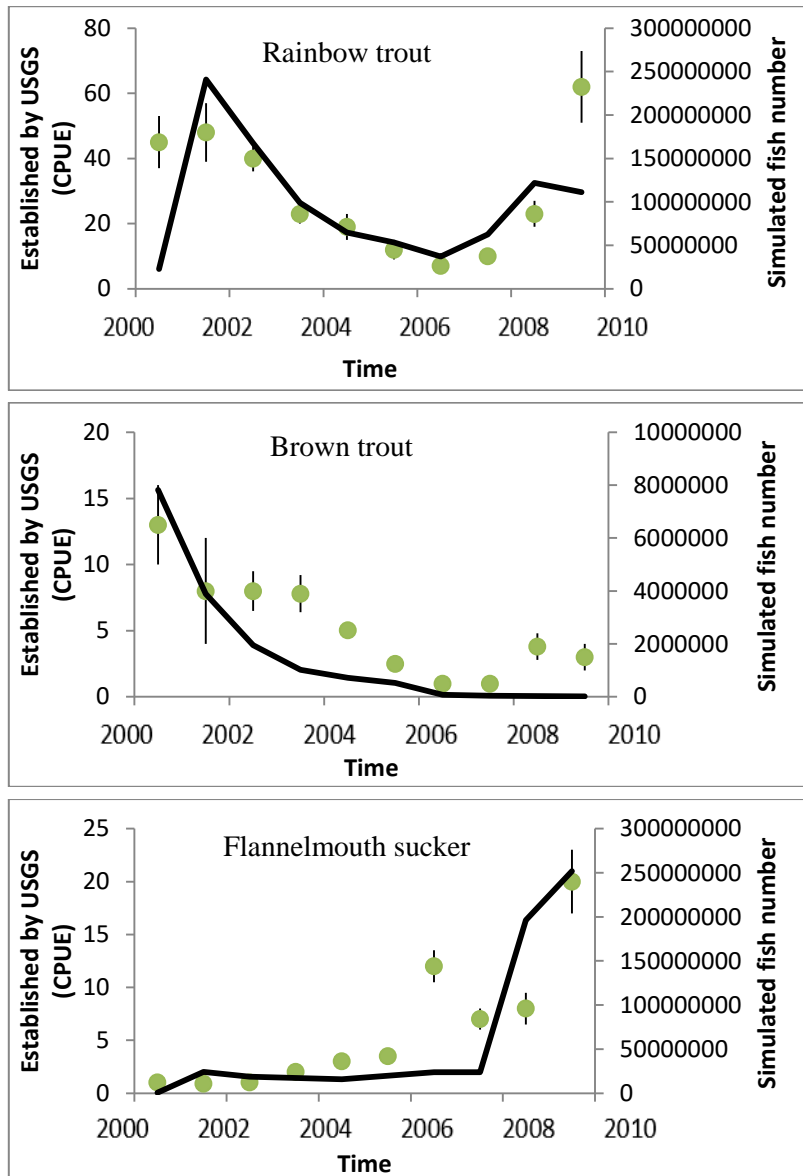


Figure 5.26: The variation of rainbow trout (upper), brown trout (middle) and flannelmouth sucker (lower) population numbers from 2000 to 2009 based on the matrix population model (CPUE is the mean catch per unit effort; \bullet is the USGS result; $-$ is the simulated fish number).

Through this case study, it is noted that compared to the logistic population model, the matrix population model can be used to calculate all life stages or all specific length fish number fluctuations. However, the accuracy of the matrix population model is relatively lower than that of the logistic model in this case study. It should be also noticed that the

values of logistic and matrix population models can serve as a useful tool to predict population changes. It also can be seen that the ecohydraulic model provides many advantages. It could be used to evaluate localized management actions, such as dam management, non-native fish control, and non-native and native fish stocking effects (see Chapter 6). The fish abundance distribution can also easily be used to indicate fish density in the computational domains. However, the change in simulated fish numbers may not fully represent the real fish number changes. This is because the settings of the empirical parameters in both the logistic and population models were not selected properly. It also may be due to the surveyed fish number, which are biased.

5.4 Conclusions

In this case study, 2D hydrodynamic, and sediment transport models were coupled with habitat and population models to investigate the rainbow trout, brown trout, and flannelmouth sucker fish number variation and fish density distribution change from 2000 to 2009 in the Colorado River. Three important physical indices, namely the velocity, water depth, and substrate of the riverbed were considered in this model. Model simulations were applied from 2000 to 2009 for the prediction of habitat and population status for three fish species and four representative life stages: larvae, juvenile, adult, and spawning.

During the simulation time, the model results showed that the ecohydraulic model system can correctly predict the habitat qualities and population number fluctuations in the Colorado River. Both the logistic population model and the matrix population model have a reasonable simulation accuracy. Both models indicate that the rainbow trout population numbers decreased from 2000 to 2007, and then the population numbers showed an increasing trend. It can also be seen that from 2000 and 2009, the non-native fish brown trout population numbers decreased steadily, while the native fish flannelmouth sucker population number increased slightly. It can be seen that in this case study, the logistic population model performed better than the matrix population model. It should be noted that in the logistic population model, it can be only simulated the total fish number and total fish density. However, the matrix population model can be simulated all life stage or all specific length fish number fluctuations and fish density variations.

It is worth noting that the simulations in this study are specific to the Colorado River and three target fish species, but this simulation technology and model system can easily be adapted to other river stretches, both natural rivers and rivers separated by hydraulic structures (Chapter 6). From the simulation results, it can be seen that this ecohydraulic model system provides very valuable information for river management and fish population management. However, a considerable amount of work collecting data is required to

validate the ecohydraulic model system. This is because precise and tested empirical parameters are very critical for the successful performance of the ecohydraulic model system.

6 Model application in the Jiao-Mu River

6.1 Introduction

Hydropower is a clean and renewable energy source and construction of hydropower plant has increased over the past 50 years to maximize hydropower energy. Hydropower is one of the leading renewables and a highly recommended energy source. However, hydropower construction may change riverbed shape, fish habitats and population status by altering flow discharge, velocity, sediment transport. These alterations can damage and deteriorate freshwater river and reservoir ecosystems (Willard & Marr, 1970; Rapport et al., 1998; Qin, 2001; Nilsson & Berggren, 2010). Damage to ecosystems may lead to an unsuitable environment for aquatic organisms to survive, or inability to support biodiversity in rivers and reservoirs (Eckholm, 1975; Kimer et al., 2008; Wang & Lin, 2013). For example, Corsica River in Chesapeake Bay, Maryland, U. S. A. was seriously affected by eutrophication and resulted in reduced submerged aquatic species, loss of marshes, degraded water quality, and increased hypoxia (Kemp et al., 2005; Palinkas, 2013). Due to mismanagement, Tai Lake which is one of the largest lake in China, has also been suffering from ecological degradation in the last 20 years (Zhu, 2008). Hydrological changes caused by massive dam construction could reduce the discharge and may concentrate pollutants downstream, which will result in habitat degradation and fish population decrease (Dudgeon, 2000; Nilsson & Berggren, 2000). The endangered fish species are especially sensitive and profoundly impacted by stream habitat degradation (Lammert & Allan, 1999; Lambert et al., 2014). Thus, in order to protect ecological factors in water resources, a certain number of effective stream restoration strategies must be implemented. Decreasing in endangered fish species has raised awareness for the importance of river habitats and the need for fish population analysis resulting from alteration in river ecosystems.

In the 1980s, ecologists and researchers have increasingly become concerned about the degradation of natural systems, and many of them are attempting to improve the related aquatic environment (Conroy et al., 1995). Stream and habitat restoration have become a multibillion dollar industry throughout the world. Restoration projects vary from single species at a small-scale to entire streams (Bernhardt et al., 2005; Brooks & Lake, 2007). Many of the streams and rivers have been chosen as targets for restoration, often with the aim of improving future restoration efforts through a restoration strategy. For example, in order to restore the habitat and ecosystem downstream Glen Canyon Dam, the adaptive management authority made a detailed scheme for the Dam operation and long-term ecological monitoring has been carried out in the Colorado River (Palinkas, 2013; Tyus et al., 1982, Tyus, 1989; Melis et al., 2012). Catchment Management Authorities are established in the state of Victoria in Australia and used to monitor the data of restoration

projects (Stewardson et al, 2002). Further, for river restoration, researchers and experts have found that freshwater fish status can be used to assess the ecological status of rivers and the richness of native fish is considered to be an indicator of aquatic ecosystem health (European Commission, 2000; Olaya-Marín et al., 2012). In addition, habitat suitability models were used as factors of fish abundance, and the ecological situation in stream and river systems (Hubert & Rahel, 1989; Zhou et al., 2014). Furthermore, researchers have recognized and emphasized the importance of the habitat models, and models have been widely used as a desirable application tool with a high degree of accuracy (Jowett & Davey, 2007). It is therefore necessary and important for restoration projects to be properly designed, effectively simulated and to evaluate whether the set goals are being met.

In China, the ecological evaluation of rivers and streams was started in the 21st century which is relatively late as compared to United States and European countries. In the past, Chinese ecological assessment was mainly focused on the reduction of soil erosion, elimination of debris flow, vegetation protection, and water quality monitoring. There was no focus on fish habitat and fish abundance fluctuation due to dam and river reconstructions (Jie et al., 2001; Wen et al., 2006). However, in recent years, Chinese water management authorities have paid much attention to the ecohydraulic evaluation, and have proposed many standards for ecohydraulic protection (Wang et al., 2013). For many rivers and streams, habitat quality evaluations are also being planned, especially those located in the 13 hydropower river basins. For example, in Yangtze River, Jinsha River, and Xiangxi River, the Chinese Sturgeon, Baiji (*Lipotes vexillifer*), and some migrating fish were studied. (Zhong et al., 1996; Xie et al., 2000; Li et al., 2009; Yi et al, 2010; Liu et al, 2011).

In this case study, the following important issues have been analysed and solved:

- Determining the fish species affected by Da-Wei dam construction and the related fish stocking strategies.
- 10 year's numerical analysis of dam construction effects on hydrodynamic and hydromorphology.
- Evaluation of the fish habitat quality in scenarios without dam construction, with dam construction, and with fish stocking.
- Evaluating two selected fish species number fluctuations and fish abundance changes in scenarios without dam construction, with dam construction, and with fish stocking based on the logistic population model and the matrix population model.
- Analysis the efficiency and sensitivity of three different fish stocking strategies in the Jiao-Mu River.

6.2 Study area and ecosystem situation in the Jiao-Mu River

China has a large number of rivers and streams; more than 50,000 covering a basin area over 100 km². Around 3,886 of these rivers have hydropower potential over 10 MW. During the last 50 years, investigations into China's hydro resources have been carried out, with a burgeoning in the field of hydro resources development (Water power, 2006; Huang & Yan, 2009). In order to fulfill industrial energy requirements, and to increase the share of renewable energy, China has proposed 13 river basins for hydropower construction since 1989, and these works are expected to be completed in 2050. The case study of the Jiao-Mu River belongs to one of the hydropower construction basins named Daduhe River basin. The other basins of hydropower construction are: The Northeast, Yellow River Main, Yellow River up reaches, Yalongjiang River, Yangtze River, Jinsha River, Nu River, Wu River, West Hunan, Fujian, Lancang-Mekong River, and Nanpang River (Figure 6.1) (Huang & Yan, 2009). The Jiao-Mu River originates in the Golog highlands (located in Qinghai, China) and extends 217 km. The Jiao-Mu River crosses the provinces of Qinghai, Sichuan, and Yunan. The computational domain in this case study is a river stretch of 20 km length, and 90 to 300 m width (E100°10'~102°00', N31°42'~33°37') (Figure 6.2).

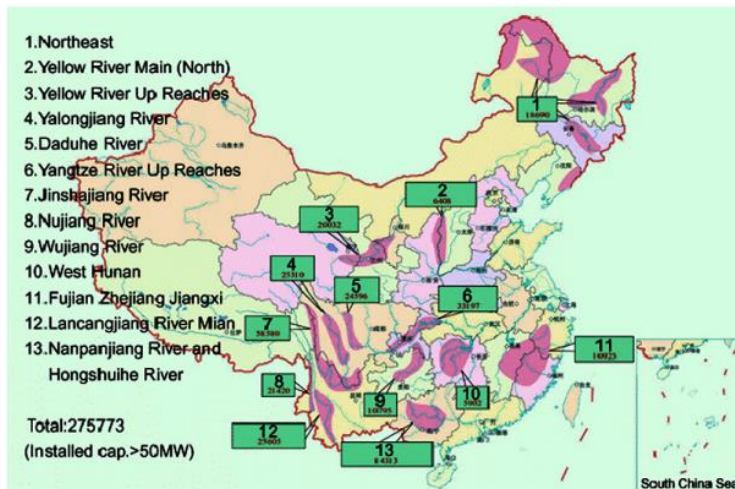


Figure 6.1: Local map of 13 river basins for hydropower construction in China (Huang & Yan, 2009).

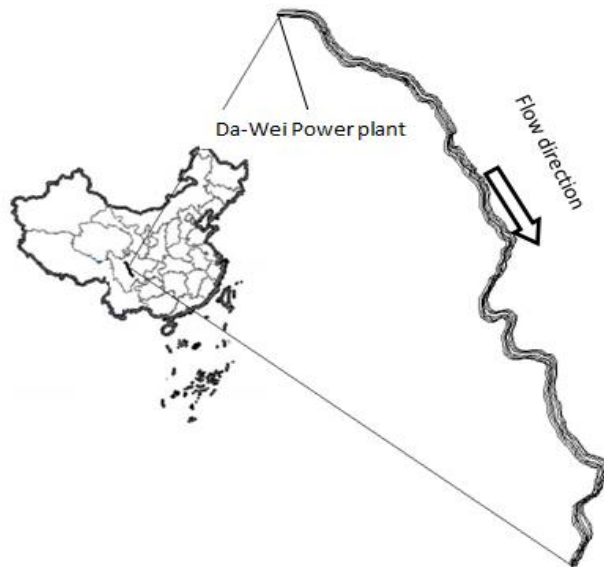


Figure 6.2: Location of the case study.

The Jiao-Mu River is a unique geological area. The computational domain in this case study focusses on the downstream of the Da-Wei dam (Figure 6.2). The riverbed elevation is from 2,590 m to 2,686 m with an average slope of 3.2 ‰ (Li et al., 2012). The representative monthly flow rate and bed-load are shown in Table 6.1. The stage-discharge relation of the outlet is shown in Table 6.2.

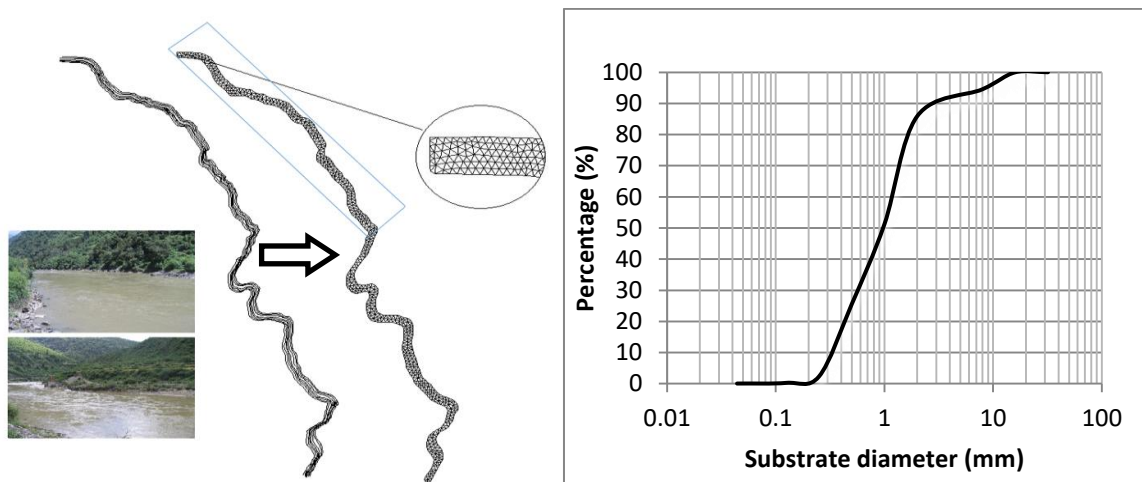


Figure 6.3: The computational domain and sediment grading curve of the Jiao-Mu River stretch.

The river has three types of geological materials, including conglomerates, cataclasites, and surficial deposits. The riverbed substrates formed due to stream flow, sediment transport, large floods, and glacial activity in the rocky mountains. The cross sections of the river are narrow with a steep slope of both river banks (40° to 70°). The geometrical shape of the cross section is of type V- shape or U- shape. The riverbed substratum is composed of bed rock (solid rock), boulder (250 to 4000 mm), cobble (64 to 250 mm),

gravel (2 to 64 mm), sand (0.3 to 2 mm), and silt & clay (0.03 to 0.045 mm) (Li et al., 2012). The riverbed sediment grading curve is shown in Figure 6.3.

Table 6.1: Discharge and sediment bed-load in the Jiao-Mu River stretch.

Month	1	2	3	4	5	6	7	8	9	10	11	12
Discharge ($\times m^3/s$)	46.6	44.5	55.2	100	201	390	470	324	396	284	124	67.2
Bed-load ($\times 10^4 t$)	0.00	0.00	0.00	0.92	6.91	34.2	67.4	17.3	33.5	8.58	0.00	0.00

The bed-load sediment transport and suspended transport data were obtained from the Jiao-Mu Hydrology Station which has the sediment data for 1967, and 1970 to 2006. The average value of the suspended sediment density is 257 g/m^3 , and the annual bed-load is $1.69 \times 10^9 \text{ kg}$.

Table 6.2: Stage-discharge relationship in the outlet section of the computational domain.

Water elevation (m)	Discharge (m^3/s)	Water elevation (m)	Discharge (m^3/s)
2596.1	0.00	2604.0	798
2596.5	0.535	2604.5	910
2597.0	3.40	2605.0	1030
2597.5	10.0	2605.5	1150
2598.0	21.6	2606.0	1280
2598.5	39.1	2607.0	1560
2599.0	63.6	2608.0	1860
2599.5	95.9	2609.0	2180
2600.0	137	2610.0	2530
2600.5	195	2611.0	2830
2601.0	261	2612.0	3170
2601.5	334	2613.0	3620
2602.0	413	2614.0	4100
2602.5	500	2615.0	4630
2603.0	593	2616.0	5180
2603.5	693		

The Jiao-Mu River ecosystem belongs to the Dadu River ecosystems, which have in China a unique ecology with hundreds of fish species living there (Appendix V). The Jiao-Mu River plays an important role in creating and maintaining diverse habitat conditions for fish species. The ecological and environmental situation in Jiao-Mu River is relatively fragile. The main fish species are schizothorax (*Racoma*), euchiloglanis davidi (*Sauvage*), schizothorax (*Schizothorax*), schizopygopsis malacanthus chengi (*Fang*), and euchiloglanis kishinouyei (*Kimura*).

The riverbed sediment distribution will greatly change after the Da-Wei dam construction.

The changes of riverbed substrates will result in the changes of fish habitat suitability conditions and fish abundance. According to the professional judgment by the Fish Research Institute in Sichuan province, ten fish species would be affected by dam construction (Table 6.3) (Li et al, 2012). In order to fulfill the ecological requirements and maintain suitable fish species abundance, the optimal fish stocking numbers need to be evaluated. In this case study, the schizothorax (*Schizothorax*) and schizothorax (*Racoma*) are chosen as target fish species. The schizothorax (*Schizothorax*) is the represented fish species with the largest population, and the schizothorax (*Racoma*) is the represented most endangered fish species.

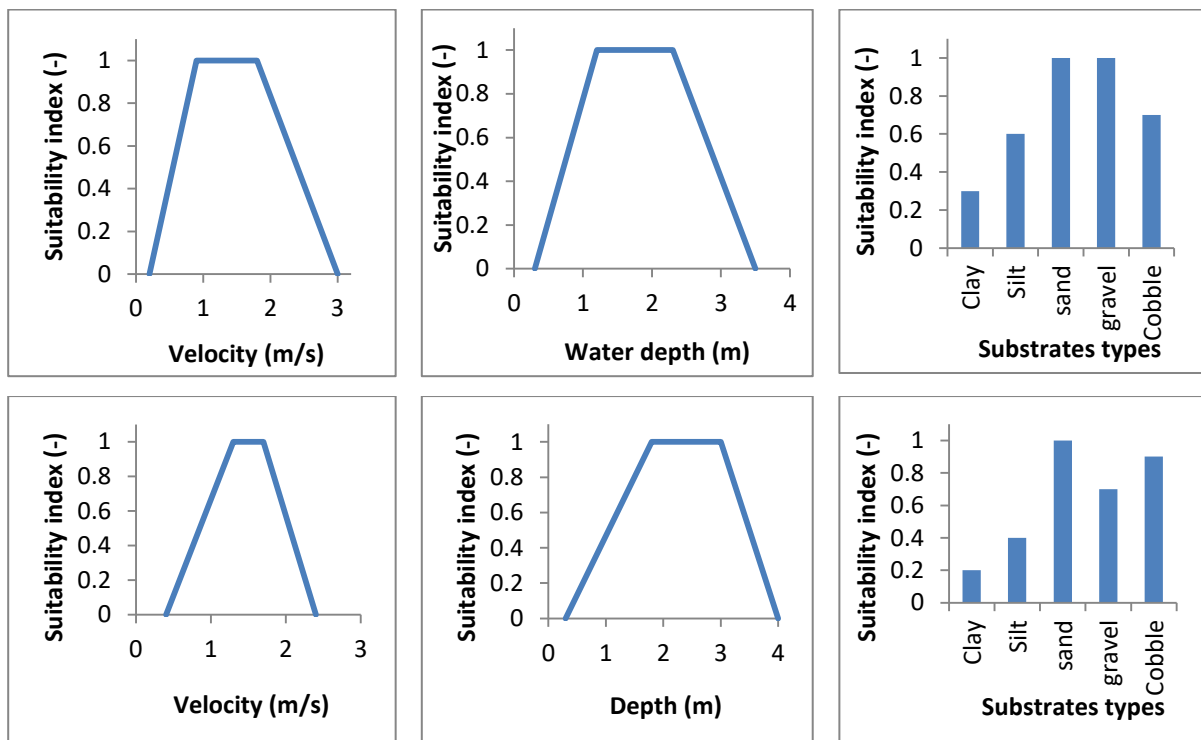


Figure 6.4: Schizothorax (*Schizothorax*) (upper) and schizothorax (*Racoma*) (lower) fish SI curves for velocity, water depth and riverbed substrates types.

The Jiao-Mu River stretch has spawning, overwinter, and feeding sites. For spawning sites, the coarse substrates such as gravel and cobble are preferred by fish. A high velocity is also preferred by fish. There are three spawning sites, named Ri-Bu, Kang-Mountain, and Royal Pearl. For overwinter sites, fish prefer low velocity, high water depth and mixed cobble and gravel. There are two overwinter sites, one located downstream of the dam and the other located in Kang-Mountain. The feeding sites are scattered throughout the Jiao-Mu River. Based on the fish observation at the spawning site, overwinter site, and feeding site, the fish SI curves are obtained. The fish SI curves are shown in Table 6.4 and Figure 6.4. The SI curves is used to predict the adult schizothorax (*Schizothorax*) (upper) and schizothorax (*Racoma*) habitat suitability index, WUA, and OSI. The WUA and OSI values from adult life stage are required by the logistic population model. Due

to lack of SI curves for fry, juvenile, and spawning life stages, and the OSI values calculated from these life stages are required by the matrix population model. So, in this case study, the OSI values calculated from adult life stage were used to represent the other three life stages.

Table 6.3: Fish species affected by dam construction (N. L. P. is national protection level; S. L. P. is state protection level; E. F. S. is endemic fish species; S. F. S. is survey fish species) (Li et al., 2012).

Number	Fish Latin name	N. L. P.;	S. L. P.;	E. F. S.;	S. F. S.
1	<i>Hucho bleereri</i> (Rimura)	II		●	
2	<i>Triplophysa markehencnsis</i> (Zhu et wu)				●
3	<i>Triplophysa brevicanda</i> (Herzenstein)				●
4	<i>Triplophysa stoliczkae</i> (Steindachner)				●
5	<i>Triplophysa slenura</i> (Herzenstein)				●
6	<i>Schizothorax</i> (<i>Schizothorax</i>)			●	●
7	<i>Schizothorax</i> (<i>Racoma</i>)		Δ	●	●
8	<i>Schizopygopsis malacanthus chengi</i> (Fang)			●	●
9	<i>Euchiloglanis davidi</i> (Sauvage)		Δ	●	●
10	<i>Euchiloglanis kishinouyei</i> (Kimura)			●	●

Table 6.4: Information sources of the SI curves for fish species schizothorax (*Schizothorax*) and schizothorax (*Racoma*).

Species	Index	Note
Schizotrax (<i>Schizothorax</i>)	Velocity	Optimal velocity is 0.9-1.8 m/s, <i>S. S.</i> prefers turbulent flow (Li et al., 2012).
	Water Depth	<i>S.S.</i> prefers deep water, with a minimum depth of 0.3m.
	Substrates	The <i>S. S.</i> prefers gravel and cobbles, and relies on the alga and the aquatic species there (Li et al., 2012).
Schizothrax (<i>Racoma</i>)	Velocity	<i>S. R.</i> prefers the range between laminar flow and turbulent flow (Li et al., 2012).
	Water Depth	The maximum depth for <i>S. R.</i> is 3m. <i>S. R.</i> prefers in deep water (Li et al., 2012).
	Substrates	The <i>S. R.</i> prefers the substrates sand, and cobbles (Li et al., 2012).

6.3 Model setup

In this case study, five different scenarios were chosen to simulate the dynamic fish habitat and fish population. The scenarios without dam construction (S1), with dam construction (S2), fish stocking strategy (S3), and the optimal fish stocking numbers (S3-2 and S3-3) are analyzed (Figure 6.5). In the cases of without considering dam effects and with considering dam effects, the flow rate is the same. The initial and boundary conditions at the outlet and the solid boundary condition is also the same. The boundary condition at the inlet are different. In the case of with considering dam effects, the time series discharge has been added. In the case of without considering dam building, beside the time series discharge has been added, the bed-load and suspended load material were added in inlet.

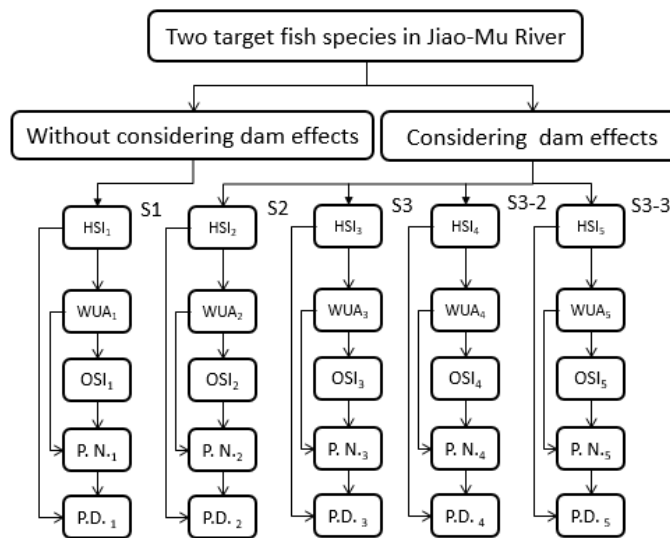


Figure 6.5: Flowchart of the case study in Jiao-Mu River.

6.3.1 Hydrodynamic and hydromorphology models

The hydrodynamics model is considered with reasonable accuracy and efficiency using the 2D shallow water equations. The $k-\varepsilon$ turbulence model is also considered (Equations 3-1 to 3-15). The Jiao-Mu River represents an area of 4,564,139 m². The computational grid is composed of triangular elements with 5,958 mesh cells and 10,606 nodes. Monthly flow discharge data, and sediment data are used, as shown in Figure 6.3 and Table 6.1. The three boundary condition types are applied to this model application: inlet boundary, outlet boundary, and solid wall boundary conditions. The inlet boundary condition was given by the discharge versus time relation. A stage-discharge relation was applied as outflow boundary condition, and zero gradient outlet boundaries were adapted for the turbulent kinetic energy. The solidwall boundary condition was applied on the river bank.

The initial condition was set by the steady flow discharge with constant velocities, depths, and riverbed substrates. The initial substrates distribution was the stable size-fraction for the whole domain. The mean grain size ranges from 0.13 mm to 15 mm.

The sediment transport estimation, and resulting riverbed changes were computed by the following formulae. The overall mass balance equation for bed-load sediment was employed to compute the bed evolution changes (Equation 3-38). The MPM equation, was used to determine the bed-load transport rate (Equation 3-20a, 3-20b).

In scenario without dam construction (S1), the Rouse number is lower than 0.8, which means the suspended load should be taken into consideration (Equation 3-28, 3-29). In scenario with dam construction (S2, S3, S3-2, and S3-3), the value of the Rouse number is bigger than 2, which means the suspended load would not be taken into consideration. The suspended sediment concentration calculation was based on Equation 3-30. The net exchange of sediment between suspended load and bed-load layer was calculated based on Equations 3-31 to 3-37.

6.3.2 Habitat model

The habitat suitability index (HSI) values were calculated for each mesh cell at each time step using Equation 3-39, and the fish SI curves as shown in Figure 6.4. The SI curves were created based on the observed fish data, scientific report and professional judgment (Table 6.4, Figure 6.4). In this case study, only three important indices were selected, which are: velocity, water depth, and substrate. The weighted usable area (WUA), overall suitability index (OSI), ideal habitat proportion (ISP), middle habitat proportion (MSP), and unsuitable habitat proportion (LSP) were also simulated in this model application based on Equation 3-43 to 3-47.

6.3.3 Population model

In this case study, two population models have been applied: these are the logistic population model and the matrix population model (Equation 3-50, 3-51). The population models were employed to evaluate the fish number changes and the fish density changes. The population models were also used to evaluate the effects of Da-Wei dam construction, and fish stocking strategies. They were also used to evaluate the efficiencies of three different examples of fish stocking strategies proposed by the river management authority.

In this model application, the schizothorax (*Schizothorax*) has been divided into eight life stages, and schizothorax (*Racoma*) has been divided into six life stages (Li et al., 2012). Because the survival rate and the birth rate data for the two selected fish species are very limited, the f_i and s_i are defined based on the method of Robson & Chapman (1961), and

the results are shown in Table 6.5. The fish population density was determined by the Equation 3-49.

Table 6.5: The empirical parameters used in the matrix population model (S. S. is schizothorax (*Schizothorax*); S. R. is schizothorax (*Racoma*)).

		1	2	3	4	5	6	7	8
S. S.	f_i	0	0	1	4	45	78	116	116
	s_i	0.104	0.179	0.401	0.248	0.042	0.020	0.004	0.001
S. R.	f_i	0	0	1	3	44	67	-	-
	s_i	0.0769	0.154	0.192	0.385	0.077	0.0001	-	-

6.3.4 Fish stocking strategy

Fish stocking strategies were determined by ecological engineering assessment. The fish stocking number was calculated from the following empirical function (Wang & Liang, 2005):

$$QN = \frac{F_T}{TW \times r} \quad (6-1)$$

Where the QN is the fish stocking number (-); TW is the fish stocking weight (kg) which is equal to 0.45 in this application; r is the survival rate (is equal to 8% based on the fish stocking experiment); F_T is fish stocking weight supported by the river system, which is determined by the following equations. It should be noticed that the dimension of F_T in Equation 6-1 is kg, but the dimension of F_T in Equation 6-2 is t .

$$F_T = F_p + F_a + F_s \quad (6-2)$$

Where F_p is fish stocking weight supported by river algae (t), F_a is fish stocking weight supported by river zooplankton (t), F_s is fish stocking weight supported by riverbed substrates materials (t).

$$F_p = \frac{B_G \times (P/B) \times c \times V \times 100}{k} \quad (6-3)$$

$$F_a = \frac{B_{zp} \times (P/B) \times c \times V \times 100}{k} \quad (6-4)$$

$$F_s = \frac{B_{zb} \times (P/B) \times c \times S}{k} \quad (6-5)$$

The related parameters are given in Table 6.6.

Table 6.6: The parameters applied in fish stocking.

F_p	B_G	P/B	c	V	k
	0.53	90	0.3	0.26	100
F_a	B_{zp}	P/B	c	V	k
	0.005	20	0.4	0.26	10
F_s	B_{zb}	P/B	c	S	k
	0.51	3	0.25	19.36	5

Where B_G is the mean phytoplankton density in the river (mg/L); B_{zp} is the mean zooplankton density in the river (mg/L); B_{zb} is the mean zoobenthos density in the river (mg/L); c is the fish utilization rate for phytoplankton, zooplankton, or zoobenthos (-); P/B is the ratio between total output and fish food density (-); V is the river water volume m^3 ; S is the effective water area m^2 ; k is the fish preference for the specific fish food types (-).

Table 6.7: Fish stocking established based on ecological engineering (Li et al, 2012).

Fish types	Length (cm)	Number ($\times 10^5$ /year)
Schizothorax (<i>Schizothorax</i>)	5~8	12
Schizothorax (<i>Racoma</i>)	5~8	3
Total		15

Based on these empirical equations, the F_p , F_a and F_s were determined with values of 3.7 t, 0.1 t, and 1.5 t respectively. The F is 5.3 t based on Equation 6-2. QN is equal to 1.47×10^6 . The fish stocking number 1.5×10^6 is used in this model application and it is shown in Table 6.7.

6.4 Result and discussion

The Jiao-Mu River velocities, water depths, and riverbed substrates changes were simulated for the duration of 10 years based on monthly flow rates. Then the corresponding fish habitat qualities for schizothorax (*Schizothorax*) and schizothorax (*Racoma*) were simulated. The two fish species population numbers, and population densities were also simulated for the scenarios without dam construction (S1), with dam construction (S2), and fish stocking (S3, S3-2, and S3-3). The simulations were performed by the TELEMAC-2D, SISYPHE software, a habitat model (Equation 3-39), logistic population model (Equations 3-48, 3-49), and a matrix population model (Equations 3-50, 3-51). The fish stocking effects were also considered and evaluated. The fish stocking number in scenario S3 is established by the empirical function, while the fish stocking number in scenario S3-2 and S3-3 were determined in order to establish the optimal fish stocking strategy.

6.4.1 Without considering Da-Wei dam construction effects

In scenario S1, the velocities, water depths, and substrates distribution simulation results are shown in Figure 6.6. It can be seen that the maximum velocities can reach a value upto 1.8 m/s. The simulated maximum water depths are between 3 m to 5m. The substrate distributions are kept stable with sediment ranges from 1 mm to 15 mm.

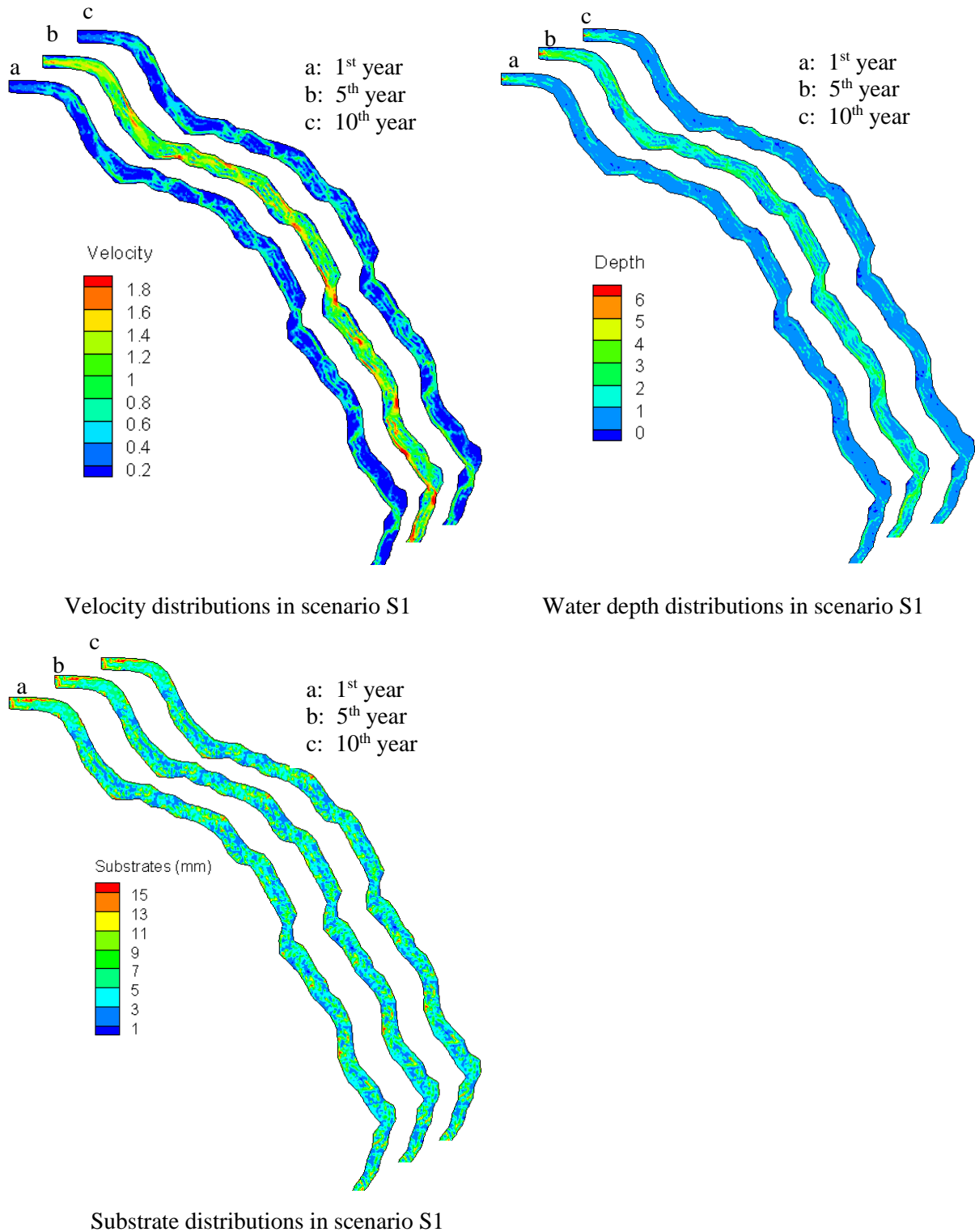


Figure 6.6: The velocities, depths, and substrates distribution in scenario S1.

In scenario S1, the HSI values for the schizothorax (*Schizothorax*) and schizothorax (*Racoma*) are determined by combining the velocity, depth, and substrates SI curves (Figure 6.4, Equation 3-39). Figure 6.7 shows the calculated HSI distribution for adult schizothorax (*Schizothorax*) and schizothorax (*Racoma*). In Figure 6.7, it is easily noticed that the habitat quality for adult schizothorax (*Schizothorax*) is better than the habitat quality for adult schizothorax (*Racoma*). Meanwhile, the WUA and OSI values in Figure 6.8 also indicate that the WUA and OSI values for adult schizothorax (*Schizothorax*) are better than WUA and OSI values for adult schizothorax (*Racoma*). For adult schizothorax (*Schizothorax*), it is shown that the WUA and OSI values periodically fluctuate, with maximum values of $2.3 \times 10^6 \text{ m}^2$ and 0.50 for WUA and OSI respectively. For adult schizothorax (*Racoma*), it is shown that the WUA and OSI values also periodically fluctuate with maximum WUA and OSI values of $1.1 \times 10^6 \text{ m}^2$ and 0.24 respectively.

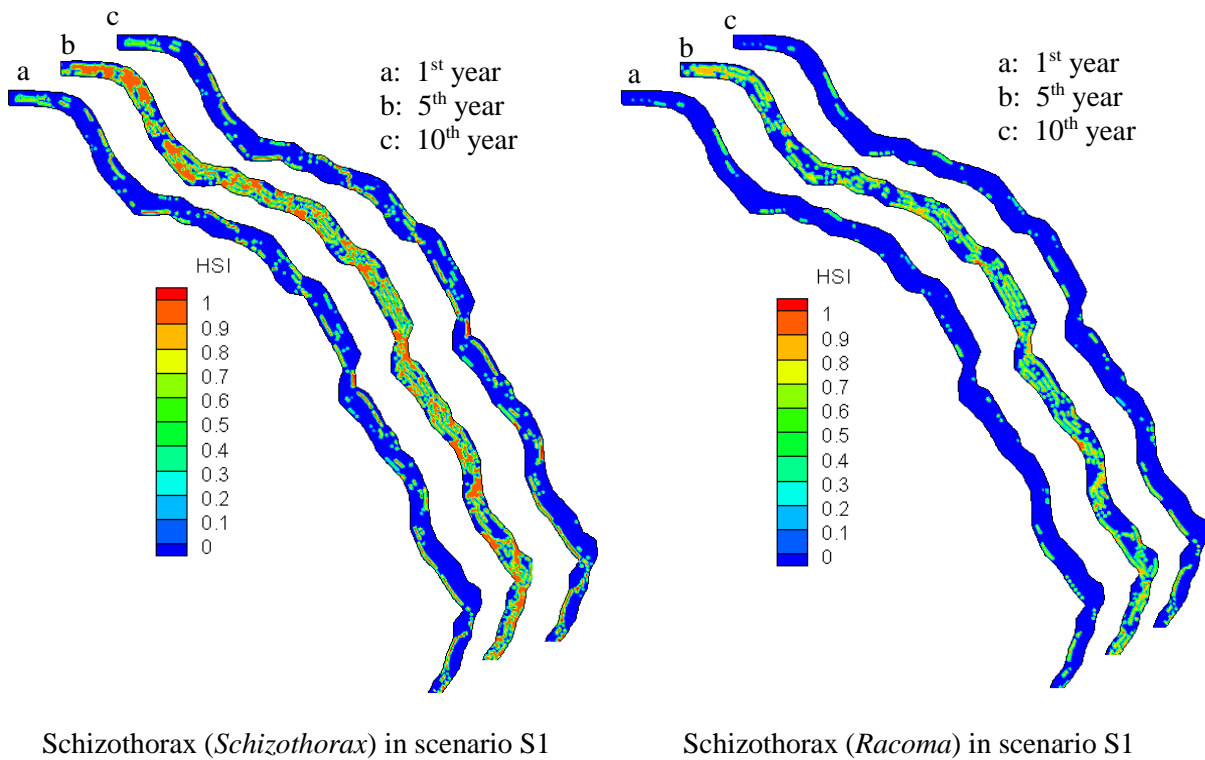


Figure 6.7: Adult schizothorax (*Schizothorax*) and schizothorax (*Racoma*) HSI distribution in scenario S1.

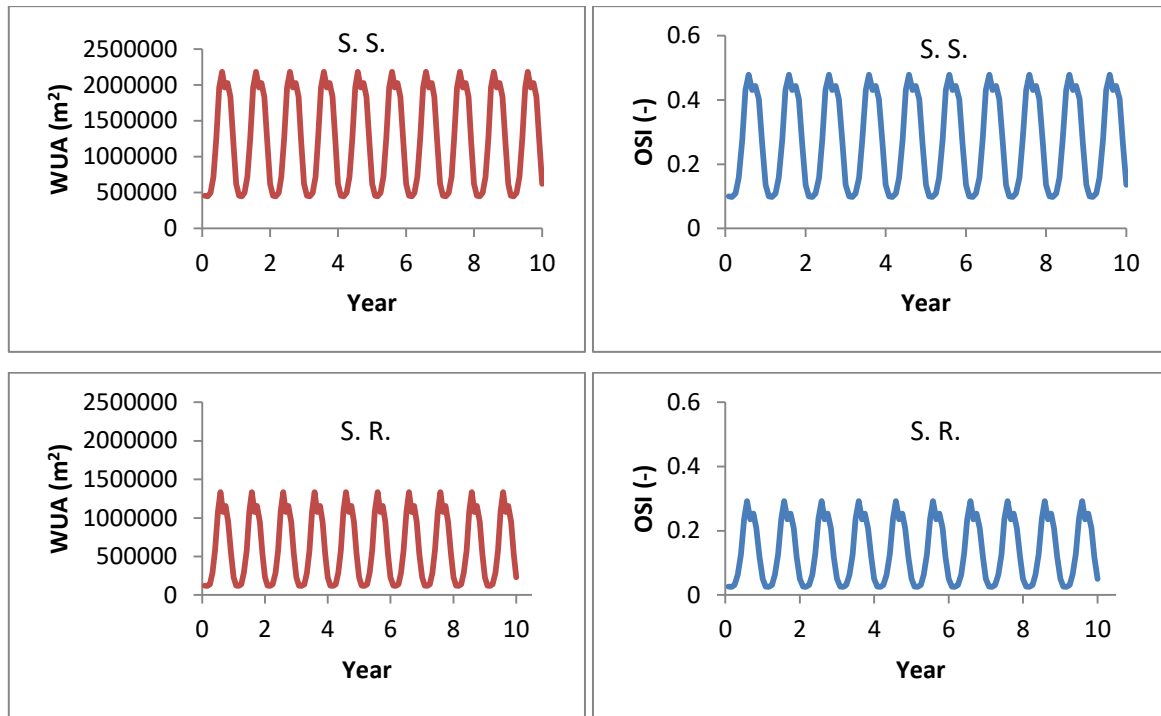


Figure 6.8: The WUA and OSI values for adult schizothorax (*Schizothorax*) (S. S.) and schizothorax (*Racoma*) (S. R.) in scenario S1.

6.4.2 With considering Da-Wei dam construction effects

In this case study, effects due to construction of the Da-Wei dam have been considered (S2), and the corresponding velocity, water depth, riverbed deformation, and the riverbed substrates changes are calculated. Figure 6.9 shows the simulated velocity, water depth, and riverbed substrate distribution at the beginning of the simulation time, at the middle of the simulation time, and at the end of the simulation time. It can be seen that the maximum velocity occurred at the location along the river bank at 5 km, 10 km and 17 km with a value of 3.3 m/s in discharge of 470 m³/s. The velocities in major computational domains range from 0.5 m/s to 1.6 m/s when using monthly flow rates. Water depths are also obtained from hydrodynamic simulation with a range of 1 m to 3.4 m. During the simulation time, the fractions of low grain size sediment also decreased. In scenario S2, the maximum erosion happened near the inlet, with a value of 6 m, while the maximum deposition happened in the middle of the river, with a value of 5.8 m. Compared to scenario S1, it can be seen that the maximum velocity values in scenario S2 are slightly smaller than the corresponding values in scenario S1. The maximum water depth and mean substrate values in scenario S2 are slightly bigger than the corresponding values in scenario S1.

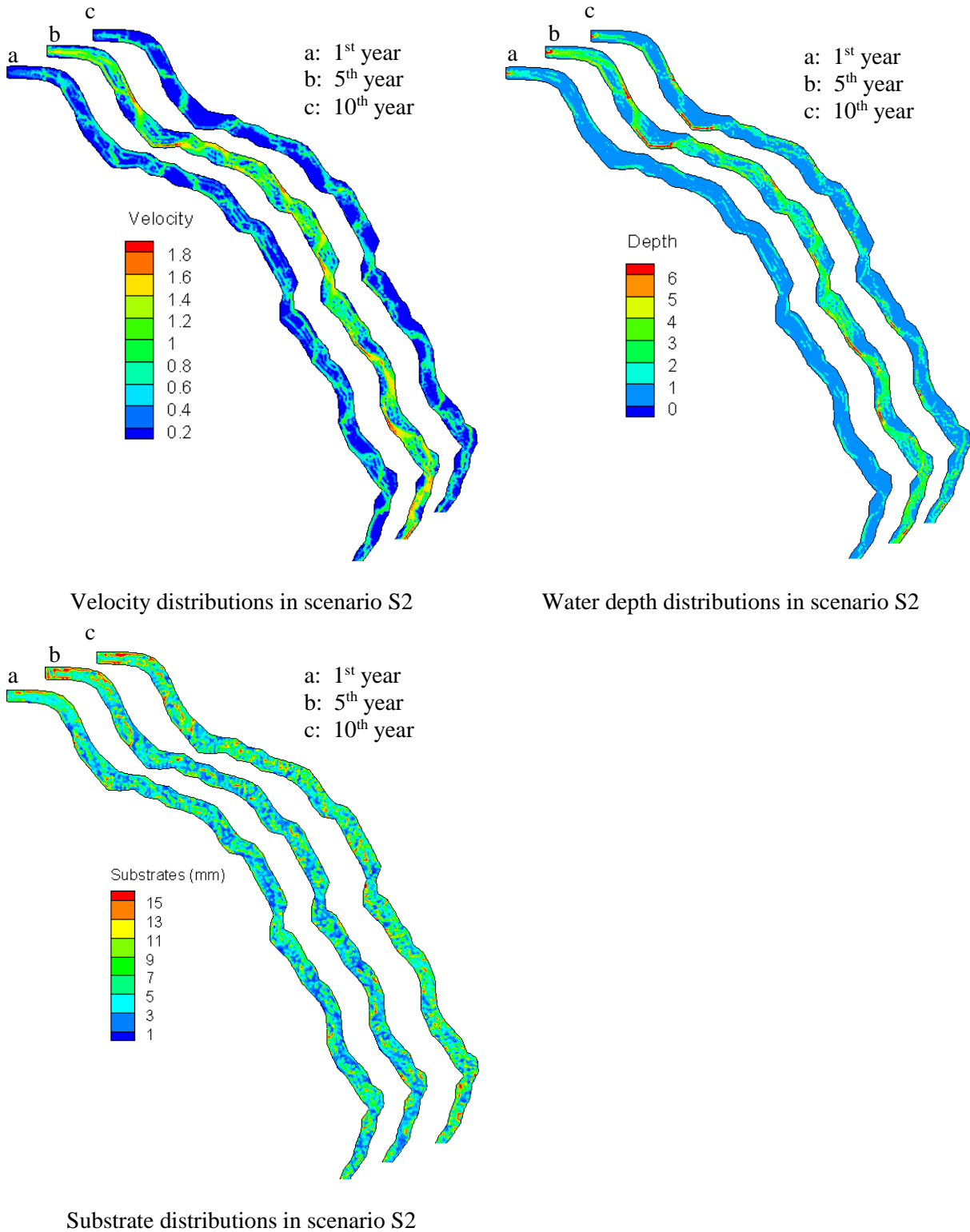


Figure 6.9: The velocity, depth, and substrate distribution in scenario S2.

Based on the habitat suitability analysis in scenario S2, it can be seen that (1) At the beginning of the simulation time, the adult schizothorax (*Schizothorax*) has an unsuitable

habitat quality in large areas of the computational domain. The suitable habitat quality is mainly concentrated along the riverbank rather than the river axis (Figure 6.10). The WUA and OSI values at the beginning of the simulation time are $4.7 \times 10^5 \text{ m}^2$ and 0.1 respectively. At the middle of the simulation time, the habitat quality is very suitable for adult schizothorax (*Schizothorax*) with high HSI values in large areas. The proportion of ISP, MSP and LSP values are 0.60, 0.03, and 0.37 respectively (Equations 3-45, 3-46, 3-47). At the middle of the simulation time, the WUA and OSI values are $1.65 \times 10^6 \text{ m}^2$ and 0.36 respectively. At the end of the simulation time, it was found that the habitat suitability conditions in the Jiao-Mu River are less satisfactory for adult schizothorax (*Schizothorax*). The water depth overriding the role of velocity and substrates appears to be the main reason for poor habitat suitability conditions. For adult schizothorax (*Schizothorax*), the ISP, MSP, and LSP values are 0.14, 0.04, and 0.82 respectively. The WUA and OSI values are $6.71 \times 10^5 \text{ m}^2$ and 0.15 respectively (Figure 6.11).

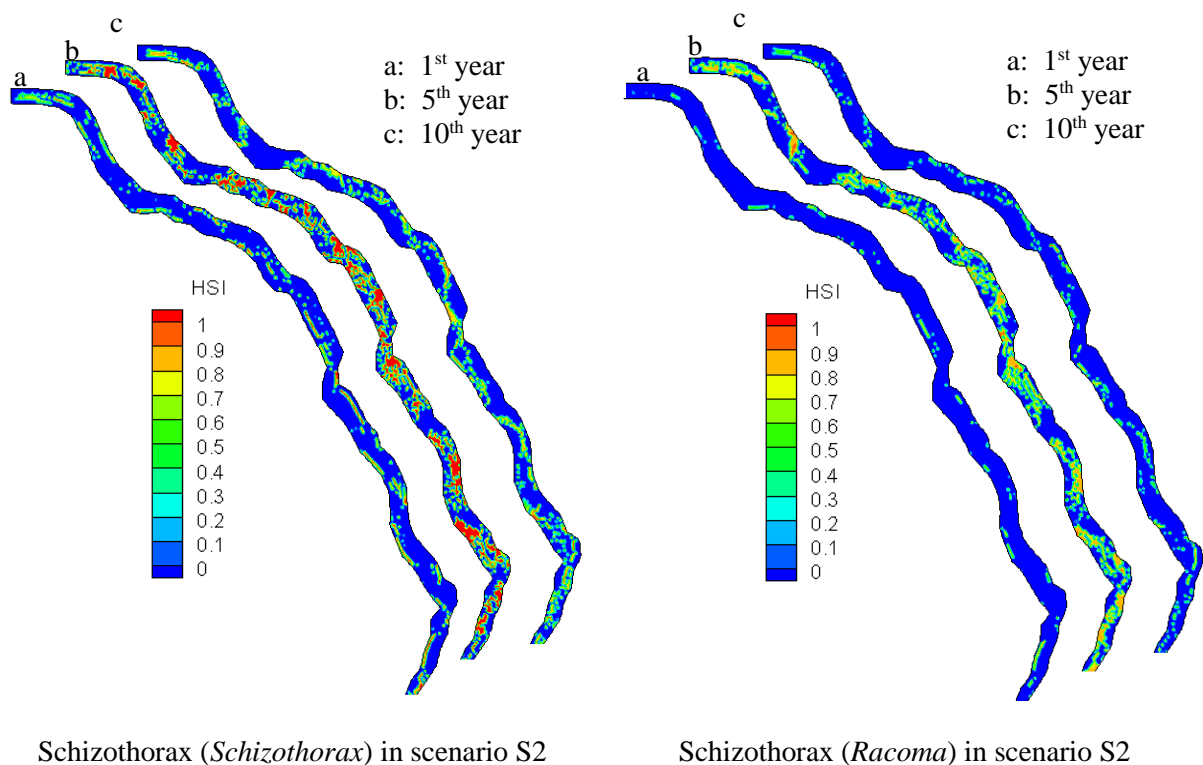


Figure 6.10: Adult schizothorax (*Schizothorax*) and schizothorax (*Racoma*) HSI distribution in scenario S2.

(2) Compared to the schizothorax (*Schizothorax*), it can be seen that the adult schizothorax (*Racoma*) habitat quality is worse than adult schizothorax (*Schizothorax*) habitat quality (Figures 6.10, 6.11). More specifically, at the beginning of simulation time, the majority of the river areas are not suitable for adult schizothorax (*Racoma*), and there are only a few areas scattered in the Jiao-Mu River with HSI values of approximately 0.5. At the middle of the simulation time, the adult schizothorax (*Racoma*) habitat quality is better than the habitat quality at the beginning of the simulation time. However, the adult

schizothorax (*Racoma*) habitat quality is still worse than the corresponding habitat quality of adult schizothorax (*Schizothorax*). For adult schizothorax (*Racoma*), the proportion of ISP, MSP and LSP for adult schizothorax (*Racoma*) are 0.28, 0.04, and 0.68 respectively. The WUA and OSI values are $1.13 \times 10^6 \text{ m}^2$ and 0.25 respectively. At the end of the simulation time, the habitat quality in the Jiao-Mu River is also less satisfactory for adult schizothorax (*Racoma*). It is noticeable that the ISP, MSP and LSP values are 0.03, 0.06, and 0.91 respectively. The simulation results of WUA and OSI values are $2.6 \times 10^6 \text{ m}^2$ and 0.06 respectively.

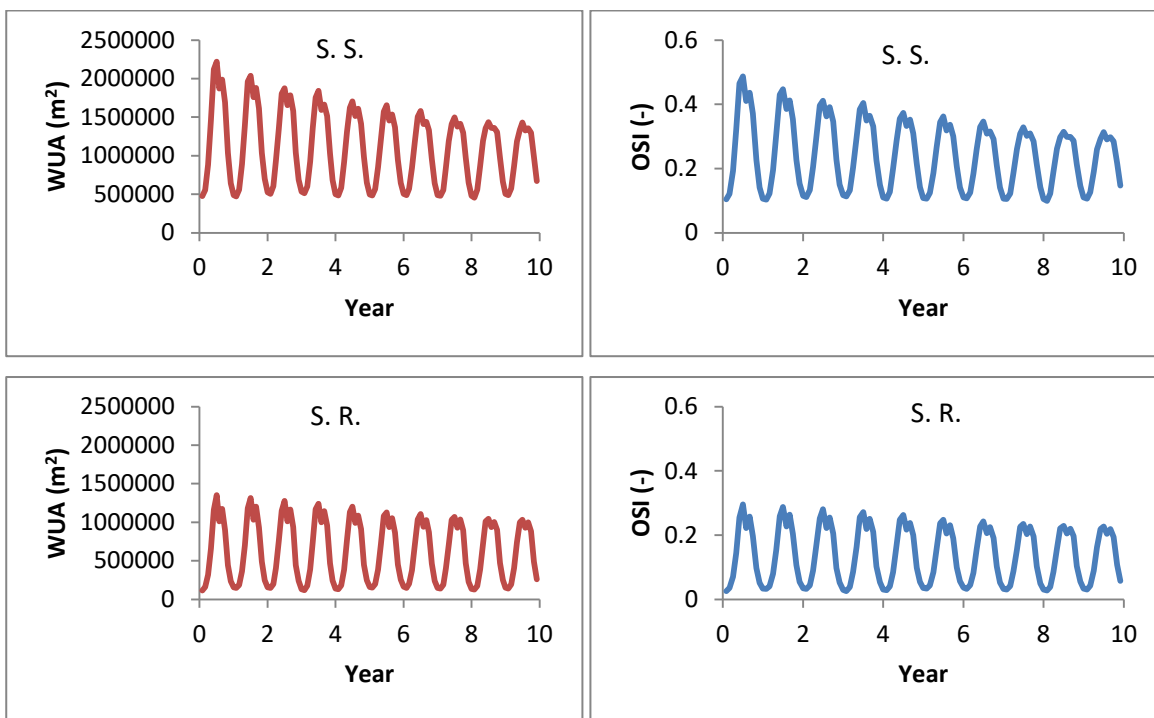


Figure 6.11: Adult schizothorax (*Schizothorax*) (S. S.) and schizothorax (*Racoma*) (S. R.) WUA and OSI distribution in scenario S2.

6.4.3 The logistic population model analysis for the five different scenarios

Equations 3-48 and 3-49 are used for calculating schizothorax (*Schizothorax*) and schizothorax (*Racoma*) population numbers and fish population density distribution in the Jiao-Mu River. Figure 6.12 shows the schizothorax (*Schizothorax*) population number changes in scenarios without considering the Da-Wei dam construction effects (S1), considering Da-Wei dam construction effects (S2), and considering fish stocking strategies based on empirical function (S3, S3-2, S3-3). It is noticeable that, in scenario S1, the schizothorax (*Schizothorax*) population number regularly fluctuated between 7.38×10^5 and 9.44×10^5 . It is also noticeable that when the Da-Wei dam construction effects have been considered (S2), the schizothorax (*Schizothorax*) population numbers show a decreasing trend with an annual number of 8.20×10^5 at the first year, and then the annual

fish numbers drop to 1.78×10^5 at the end of the simulation time. However, after the fish stocking strategy based on empirical function has been applied (S3) (Table 6.7), the schizothorax (*Schizothorax*) population numbers are relatively stable although the fish numbers showed a continuing declining trend in the first three years. The schizothorax (*Schizothorax*) population numbers decreased from 8.20×10^5 in the 1st year to 8.20×10^5 in the 3rd year. When the schizothorax (*Schizothorax*) stocking number changed to 1.0×10^5 per year (S3-2), the fish population numbers decreased from 4.89×10^6 in the 1st year to 3.4×10^6 in the 5th year, and then regularly fluctuated at a relatively stable level. When the schizothorax (*Schizothorax*) stocking number changed to 6.0×10^4 per year (S3-3), the fish population numbers started to show a decreasing trend until the 9th year. The schizothorax (*Schizothorax*) population numbers decreased from 4.89×10^6 in the 1st year to 2.8×10^6 in the 10th year. The simulation results indicate that based on the logistic population model, the optimal schizothorax (*Schizothorax*) stocking numbers are 1.2×10^5 per year.

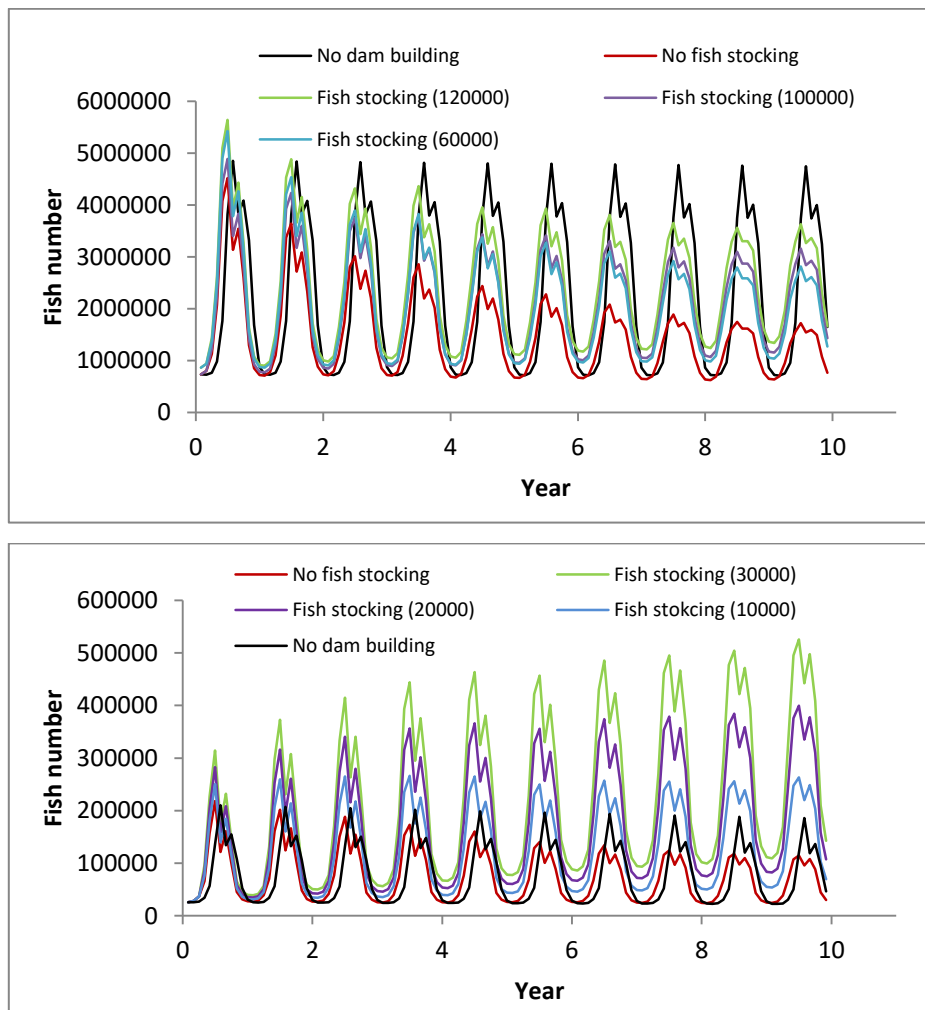


Figure 6.12: The population number of schizothorax (*Schizothorax*) (upper) and the schizothorax (*Racoma*) (lower) based on the logistic population model.

As seen in Figure 6.12, when the Da-Wei dam construction impacts were not considered (S1), similar to schizothorax (*Schizothorax*), the schizothorax (*Racoma*) population number also had a periodic fluctuation between 2.6×10^4 and 3.28×10^4 . When the Da-Wei dam construction effects are considered (S2), the schizothorax (*Racoma*) population number started to show a decreasing trend, and the fish numbers decreased from 1.16×10^5 in the 1st year to 6.79×10^4 in the 10th year. When the fish stocking strategy based on Table 6.7 is applied (S3), the simulated schizothorax (*Racoma*) population number showed an increasing trend, and at the end of the simulation time the fish numbers are increased to the level of 3.13×10^5 . When the schizothorax (*Racoma*) stocking number is 2×10^4 per year (S3-2), then the fish numbers also showed an increasing trend and stayed at the level of 2.24×10^5 at the end of the simulation time. When the schizothorax (*Racoma*) stocking number change to 1×10^4 per year (S3-2), then this stocking strategy was able to keep the fish population numbers at a stable level, with the value 1.47×10^5 in all simulation times (Figure 6.12). The simulation results indicate that based on the logistic population model, the optimal schizothorax (*Racoma*) stocking numbers are 1.0×10^4 per year.

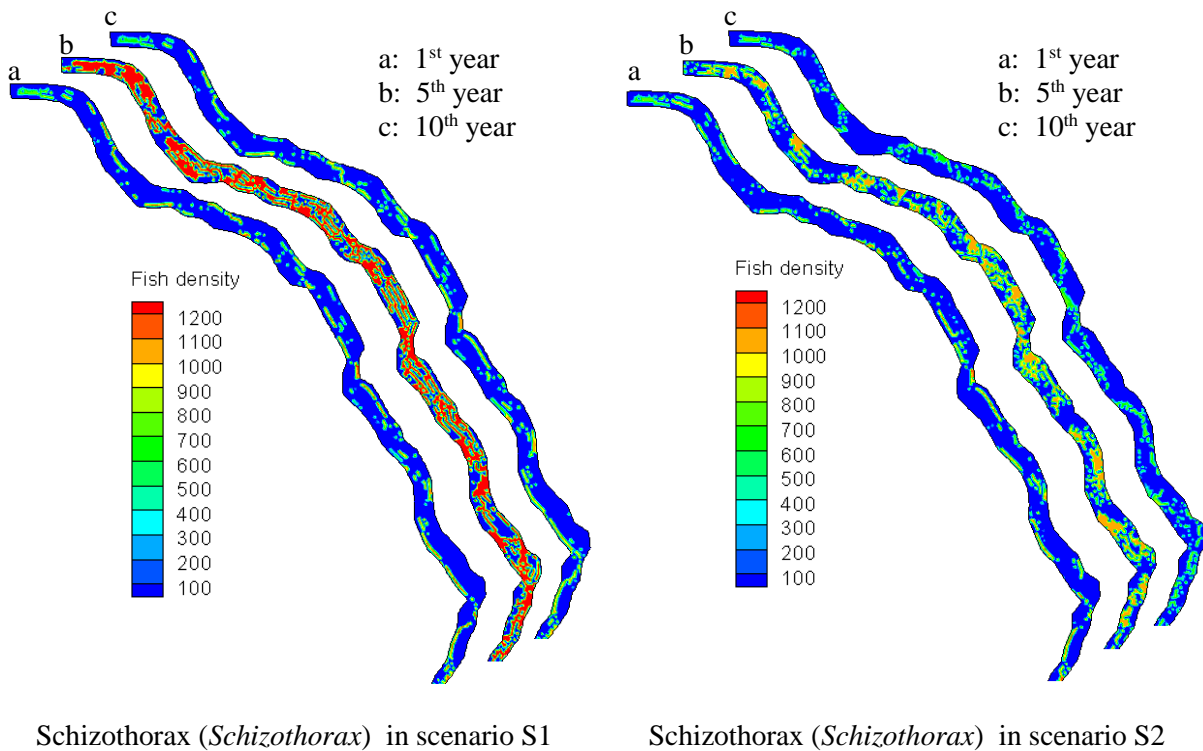


Figure 6.13a: Schizothorax (*Schizothorax*) population density based on the logistic population model in scenarios without dam construction effects (S1), and with dam construction effects (S2).

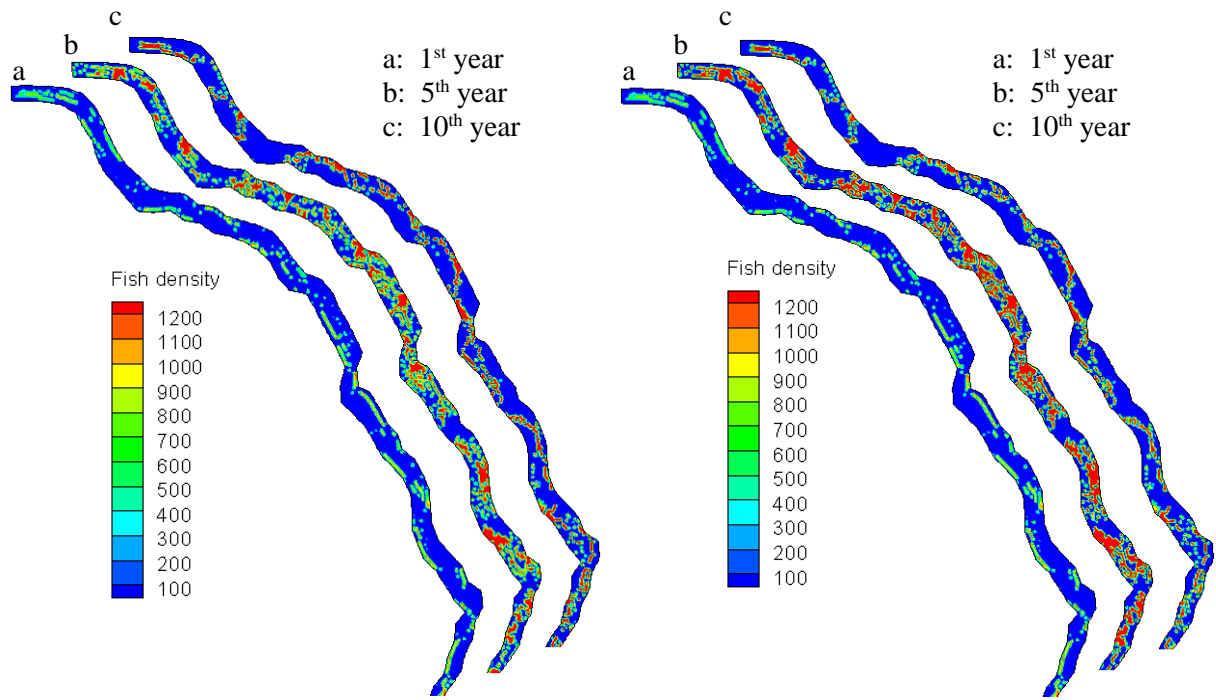
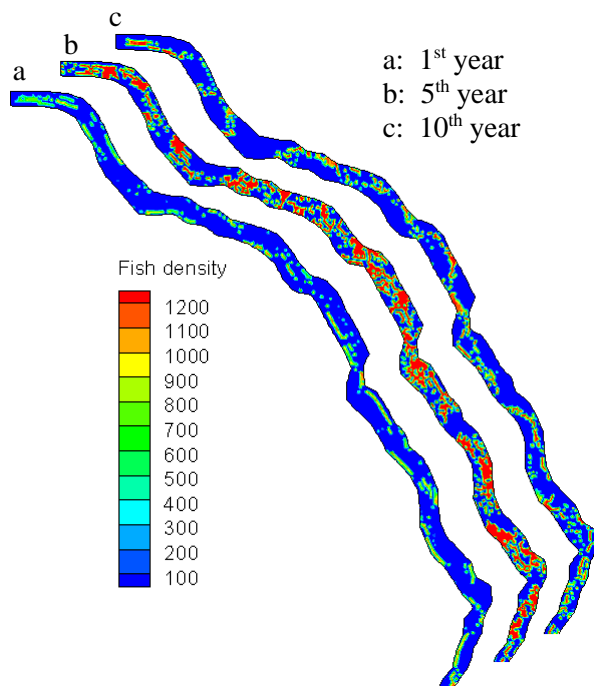
Schizothorax (*Schizothorax*) in scenario S3Schizothorax (*Schizothorax*) in scenario S3-2Schizothorax (*Schizothorax*) in scenario S3-3

Figure 6.13b: Schizothorax (*Schizothorax*) population density based on the logistic population model in scenarios with fish stocking numbers 1.2×10^5 (S3), with fish stocking numbers 1.0×10^5 (S3-2), and with fish stocking numbers 6.0×10^4 (S3-3).

Figures 6.13a, and 6.13b show the schizothorax (*Schizothorax*) population density distribution in scenarios without dam construction effects (S1), with dam construction effects (S2), with fish stocking numbers 1.2×10^5 (S3), with fish stocking numbers 1.0×10^5 (S3-2), and with fish stocking numbers 6.0×10^4 (S3-3). From Figure 6.13, it can be seen that the schizothorax (*Schizothorax*) density ranges from 100 fish per mesh cell to 1200 fish per mesh cell. At the beginning of the simulation time, all scenarios show the same fish density distribution, with 100 fish per mesh in larger areas of the river. The maximum fish density is 950 fish per mesh cell for schizothorax (*Schizothorax*) at the beginning of the simulation time. At the middle of the simulation time, it can be seen that the scenario S1 has the highest fish density value, and the scenario S2 has the lowest fish density value. In scenarios S3, S3-2, and S3-3, the fish density values are slightly smaller than the scenario S1, but the values are much higher than scenario S2. In scenario S2, the fish density values remain at the lowest level at the end of the simulation time. In scenarios S3, S3-2, and S3-3, the fish density values are higher than the values in scenarios S2, and S1.

Figures 6.14a and 6.14b show the schizothorax (*Racoma*) population density distribution in scenarios S1, S2, S3, S3-2, and S3-3. It can be recognized that the schizothorax (*Racoma*) population density values are much smaller than the schizothorax (*Schizothorax*) population density values. In scenario S1, the mean value of schizothorax (*Racoma*) density remains at a level of 90 fish per mesh cell. In scenario S2, the mean value of schizothorax (*Racoma*) has declined from 90 fish per mesh cell to 60 fish per mesh cell, with maximum values 90 fish per mesh cell. From Figure 6.14, it can be seen that with the fish stocking strategy (S3, S3-2, S3-3), the schizothorax (*Racoma*) density values are better than the fish density values in scenarios S1 and S2. It can be also seen that when the fish stocking number slightly decreased, the fish density was not significantly affected. The maximum schizothorax (*Racoma*) population density for all scenarios is 150 fish per mesh cell.

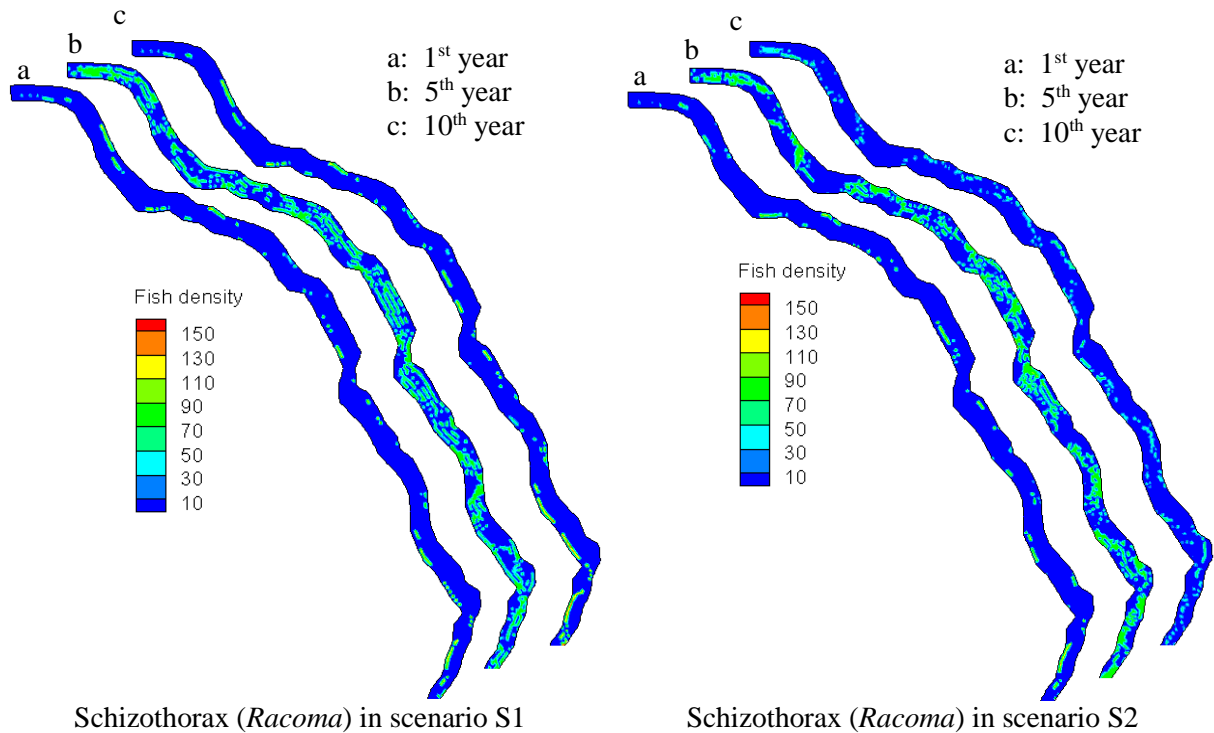


Figure 6.14a: Schizothorax (*Racoma*) population density based on the logistic population model in the scenarios: without dam construction effects (S1), with dam construction effects (S2),

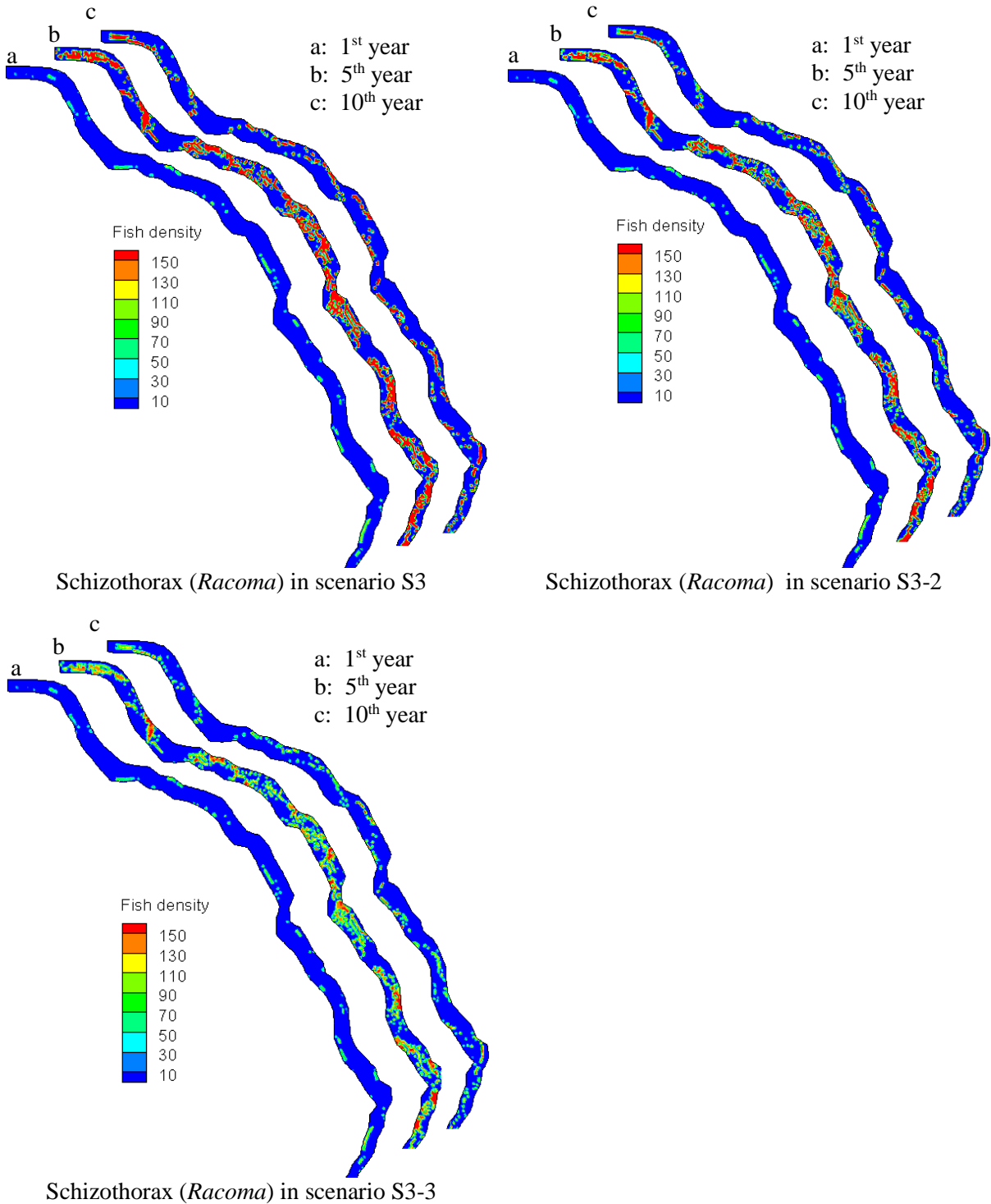


Figure 6.14b: Schizothorax (*Racoma*) population density based on the logistic population model in the scenarios: with fish stocking numbers 3.0×10^4 (S3), with fish stocking numbers 2.0×10^4 (S3-2), and with fish stocking numbers 1.0×10^4 (S3-3).

6.4.4 The matrix population model analysis for the five different scenarios

In the logistic population model, only the whole population number and density variations can be simulated. However, in the matrix population model, all life stages' fish population numbers and density can be simulated. The matrix population model was applied for all life stages' of schizothorax (*Schizothorax*) and schizothorax (*Racoma*) population numbers, and population density distribution. Based on the matrix population model, all five scenarios for both selected fish species simulation results are shown in Figures 6.15, 6.16, 6.17, and 6.18.

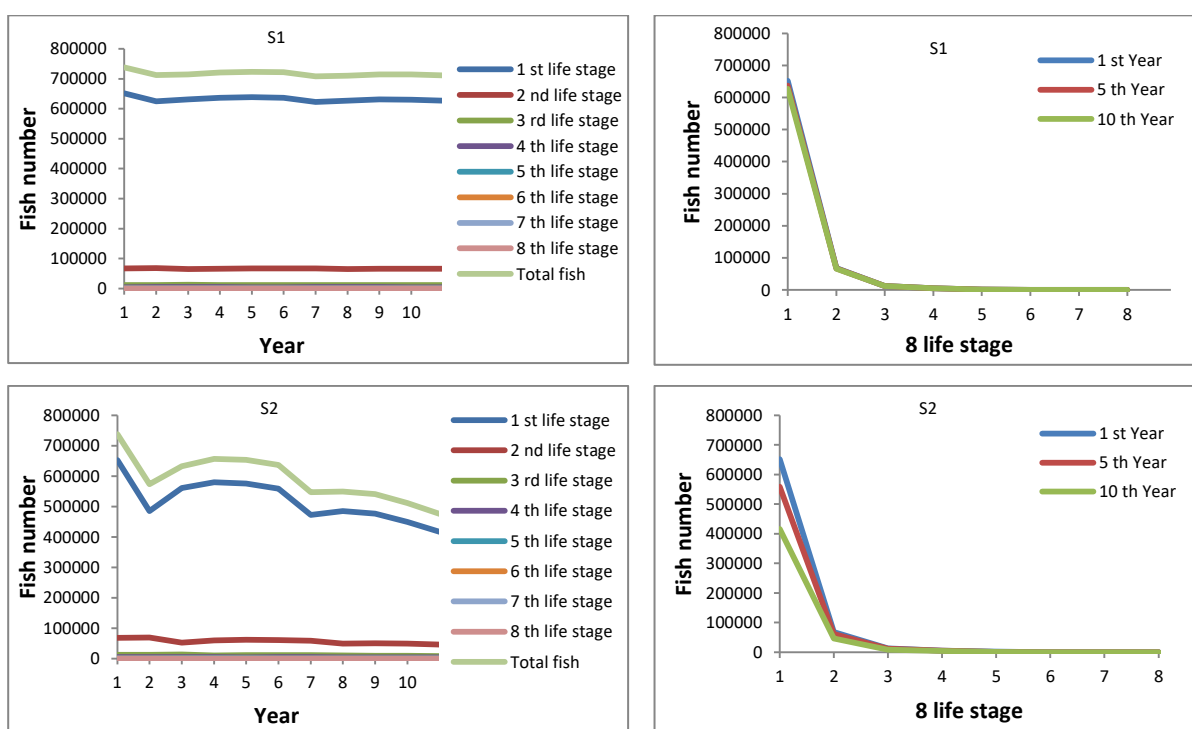


Figure 6.15a: Schizothorax (*Schizothorax*) population number based on the matrix population model in scenarios: without dam construction effects (S1), with dam construction effects (S2).

From Figures 6.15a and 6.15b, in scenario S1, the calculated total schizothorax (*Schizothorax*) population numbers slightly decreased in the first year, and then fish numbers remained stable at the level of 7.1×10^5 . In scenario S1, all eight life stages' number distributions also remained unchanged at all simulation times (Figure 6.15). In scenario S2, schizothorax (*Schizothorax*) total fish numbers showed a decreasing trend in the simulation period, with the number 7.3×10^5 in the 1st year decreased to 6.3×10^5 in the 5th year, and further decreased to 4.7×10^5 in the 10th year. The eight life stages' fish numbers also showed a decreasing trend. In scenario S2, the early life stages' schizothorax (*Schizothorax*) numbers decreased faster than other life stages. In scenario S3, when the fish stocking number 1.2×10^5 per year is applied, the schizothorax (*Schizo-*

thorax) total fish number, and all eight fish life stages' numbers showed slightly increasing trend. In scenarios S3-2 and S3-3, the fish stocking numbers are 1.0×10^5 and 6.0×10^4 per year respectively. It can be seen that when the fish stocking number is 1.0×10^5 per year (S3-2), the schizothorax (*Schizothorax*) total fish numbers and the eight fish life stages could be kept at a stable level. However, when the fish stocking number was reduced to 6.0×10^4 per year (S3-3), the schizothorax (*Schizothorax*) numbers show a slightly decreasing trend. In scenario S3-3, there is a minor decrease in the schizothorax (*Schizothorax*) early life stage numbers. Based on the matrix population model simulation result, the optimal schizothorax (*Schizothorax*) fish stocking number is 1.0×10^5 per year.

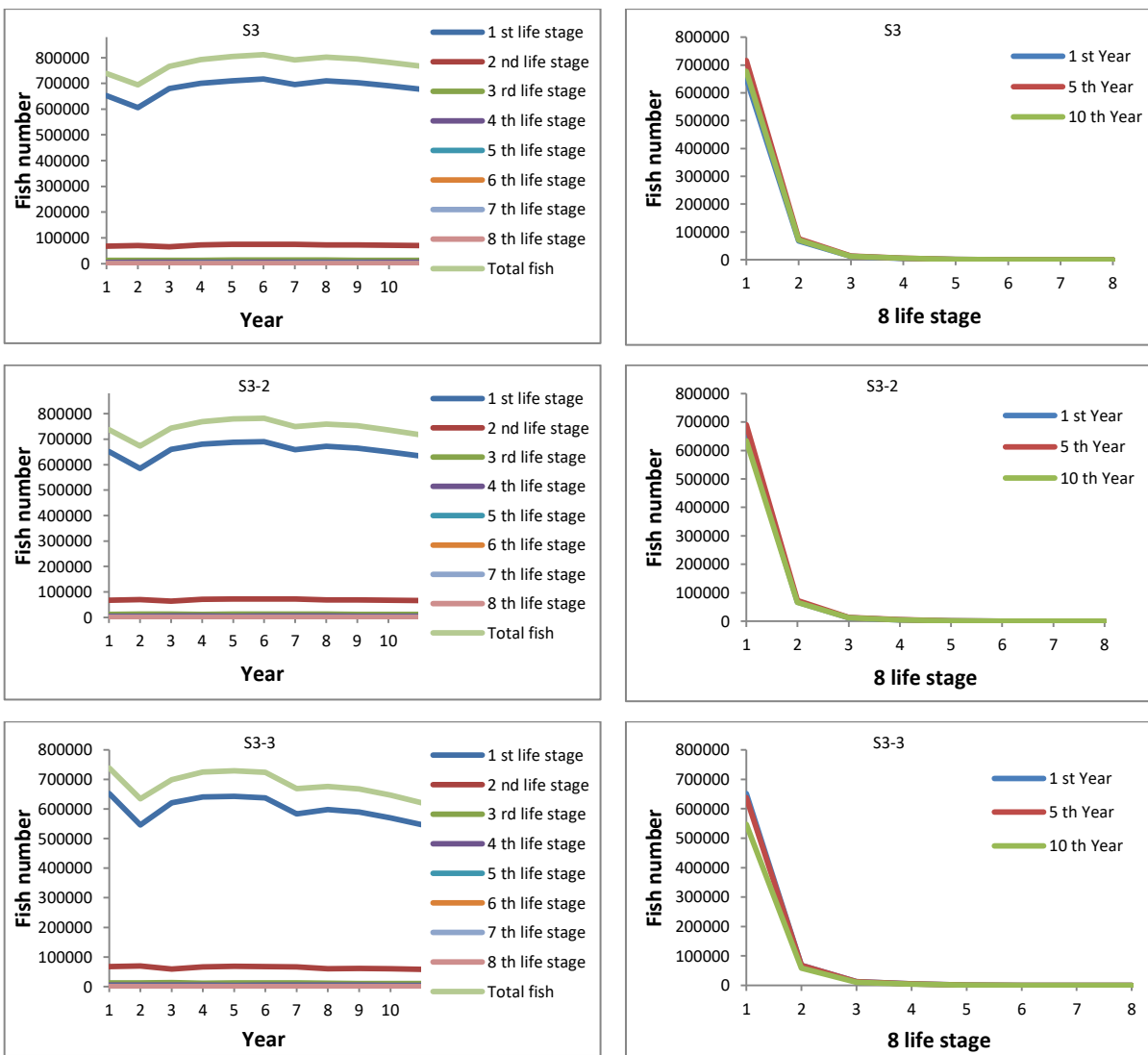


Figure 6.15b: Schizothorax (*Schizothorax*) population number based on the matrix population model in scenarios: with fish stocking number of 1.2×10^5 (S3), with fish stocking number of 1.0×10^5 (S3-2), and with fish stocking number of 6.0×10^4 (S3-3).

The schizothorax (*Racoma*) total population numbers, and six life stages' population numbers in scenarios S1, S2, S3, S3-2, and S3-3 are shown in Figures 6.16a and 6.16b. During the simulation time, in scenario S1, it can be seen that the schizothorax (*Racoma*) has a stable total population level with a value of 2.5×10^4 , and the 1st year fish numbers are much higher than other fish life stages' numbers. In scenario S1, all six life stages' numbers distribution are also associated with a consistently stable value during the simulation time. In scenario S2, the schizothorax (*Racoma*) population number showed a significant downward trend with the number decreased from 2.6×10^4 in the 1st year to 5.4×10^2 in the 10th year. The early life stage numbers of schizothorax (*Racoma*) also significantly decreased. In scenario S3, when the fish stocking number 3×10^4 per year is applied, the schizothorax (*Racoma*) population numbers show an increasing trend, with a number increased from 2.5×10^4 in the 1st year to 4.3×10^4 at the end of the simulation time. In scenario S3, the early life stages' schizothorax (*Racoma*) number increase faster than other life stages. In scenario S3, it can be seen that the fish stocking strategy was more successful than expected. Thus, in order to optimize the fish stocking numbers, another two fish stocking strategies with fish stockings number of 2×10^4 per year (S3-2) and 1×10^4 per year (S3-3) were also applied. From the simulation results, it can be noticed that the fish stocking number 2×10^4 per year is good enough to keep the schizothorax (*Racoma*) population number stable and life stage distribution stable. However, with the fish stocking numbers of 1×10^4 per year (S3-3), the schizothorax (*Racoma*) population numbers show a decreasing trend, with total fish numbers decreased from 2.5×10^4 in the 1st year to 1.3×10^4 in the 10th year. In scenario S3-3, the early life stages' schizothorax (*Racoma*) number decline is faster than other life stages fish numbers. Based on the matrix population model simulation result, the optimal schizothorax (*Racoma*) fish stocking numbers are 2.0×10^4 per year.

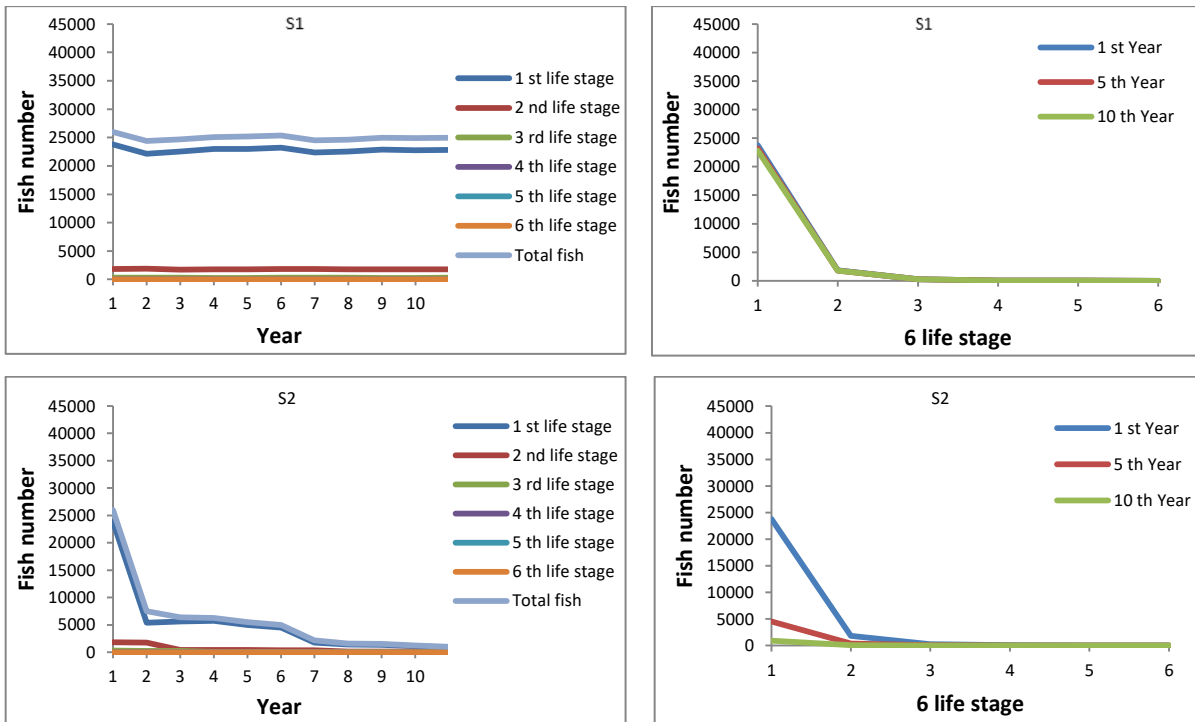


Figure 6.16a: Schizothorax (*Racoma*) population number based on the matrix population model in the scenarios without dam construction effects (S1), with dam construction effects (S2).

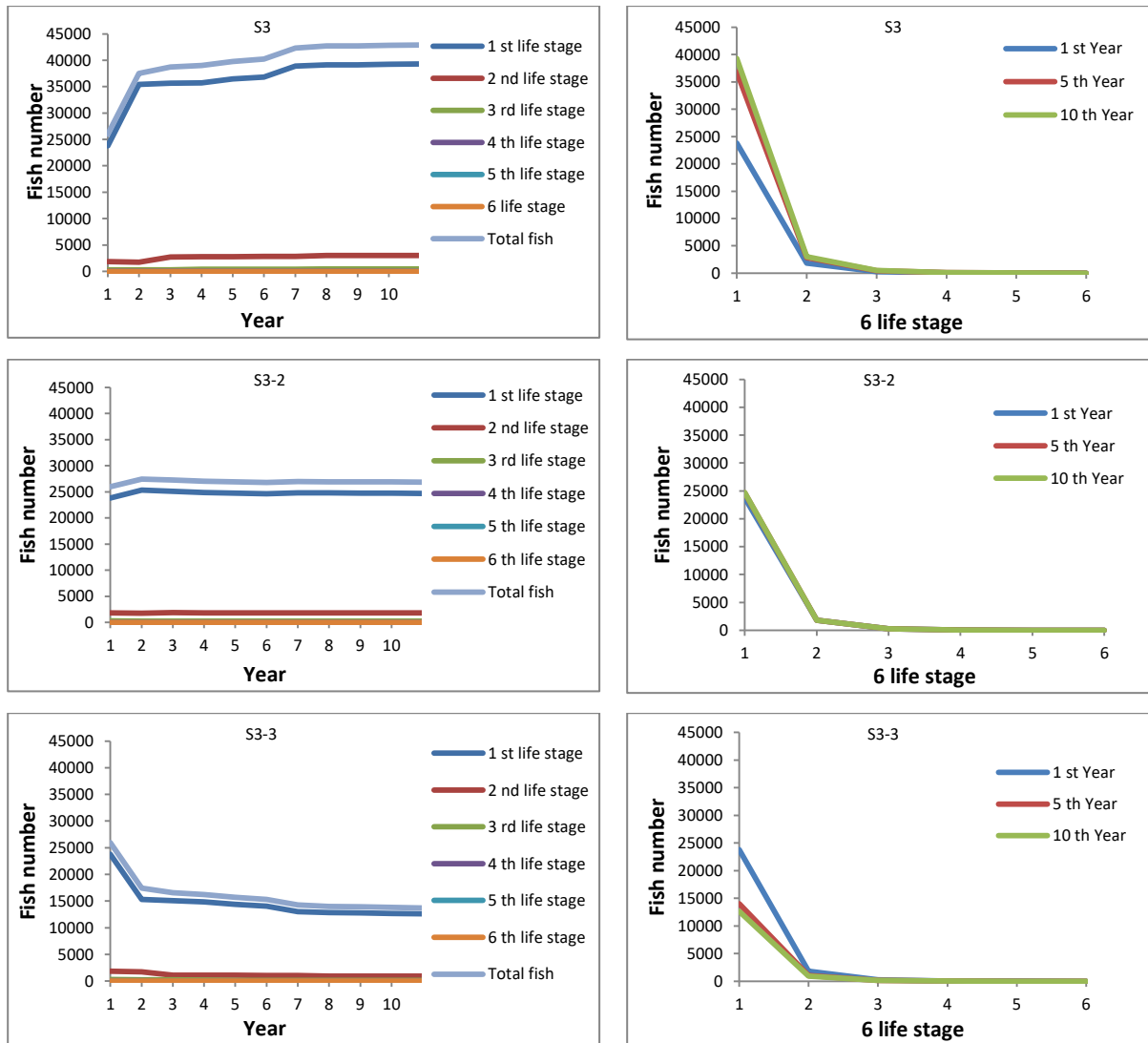
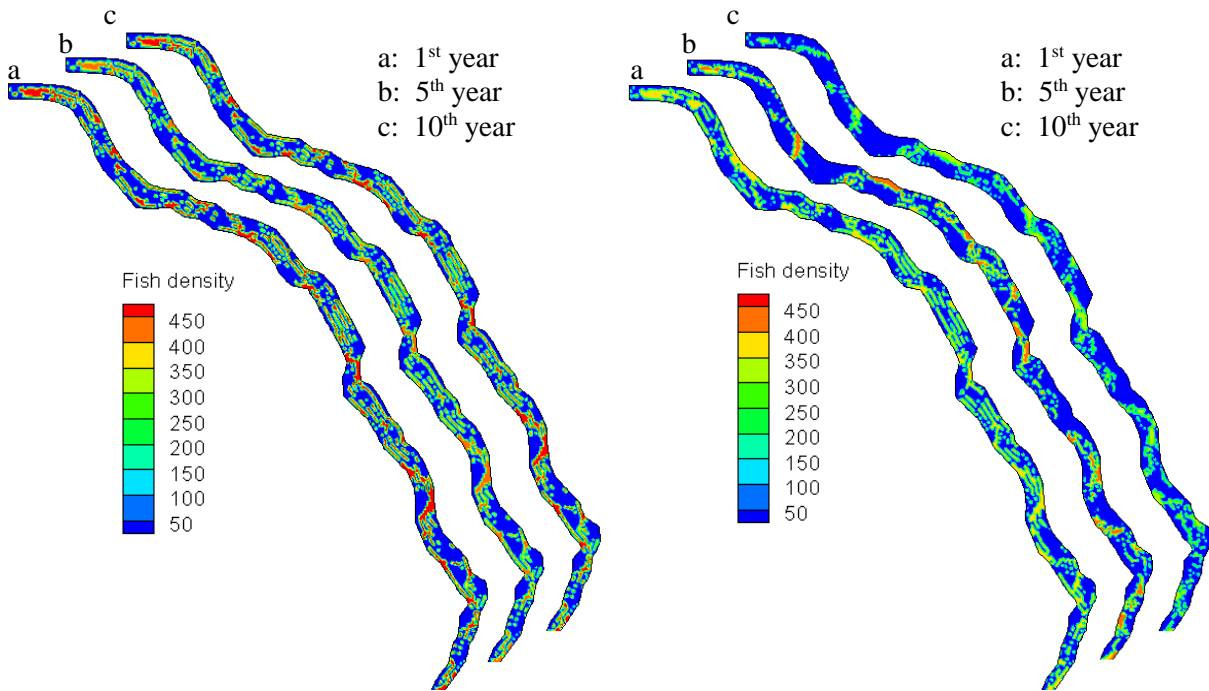


Figure 6.16b: Schizothorax (*Racoma*) population number based on the matrix population model in the scenarios with fish stocking numbers 3.0×10^4 (S3), with fish stocking numbers 2.0×10^4 (S3-2), and with fish stocking numbers 1.0×10^4 (S3-3).

Figure 6.17 shows the schizothorax (*Schizothorax*) population density distribution in scenarios without dam construction effects (S1), with dam construction effects (S2), with fish stocking numbers 1.2×10^5 (S3), with fish stocking numbers 1.0×10^5 (S3-2), and with fish stocking numbers 6.0×10^4 (S3-3). It can be noticed that compared to the logistic population model, the maximum fish population density based on the matrix population model is relatively lower, and the simulated fish numbers fluctuated less. The maximum fish density for schizothorax (*Schizothorax*) is 450 fish per mesh cell. In scenario S1, from Figure 6.17, it is noted that the schizothorax (*Schizothorax*) densities are constant during all the simulation time. In scenario S2, it can be seen that the schizothorax (*Schizothorax*) density values are lower than the fish density values in scenario S1, with a maximum fish density of 350 fish per mesh cell. In scenario S2, the fish density also shows a decreasing trend. With fish stocking strategies applied (scenario S3, S3-2, and S3-3), it can be seen

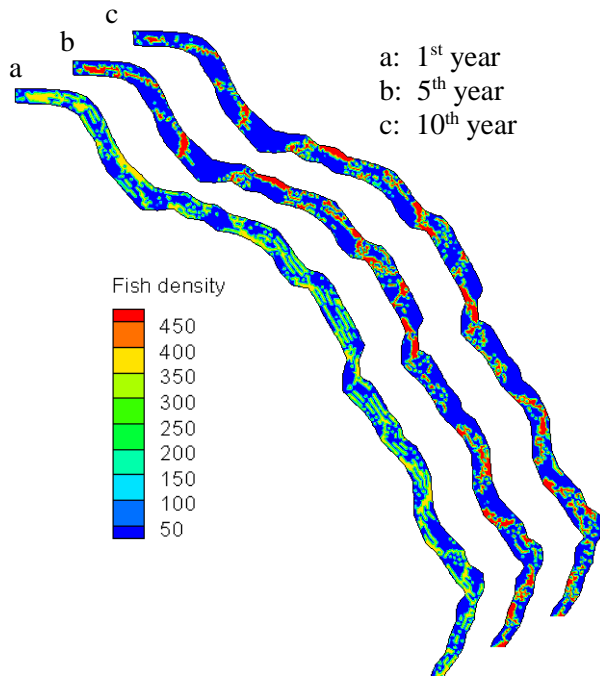
that the schizothorax (*Schizothorax*) density values remained stable in the computational domain. This shows a slightly increasing trend with the stocking numbers 1.2×10^5 per year (S3) and 1.0×10^5 per year (S3-2).



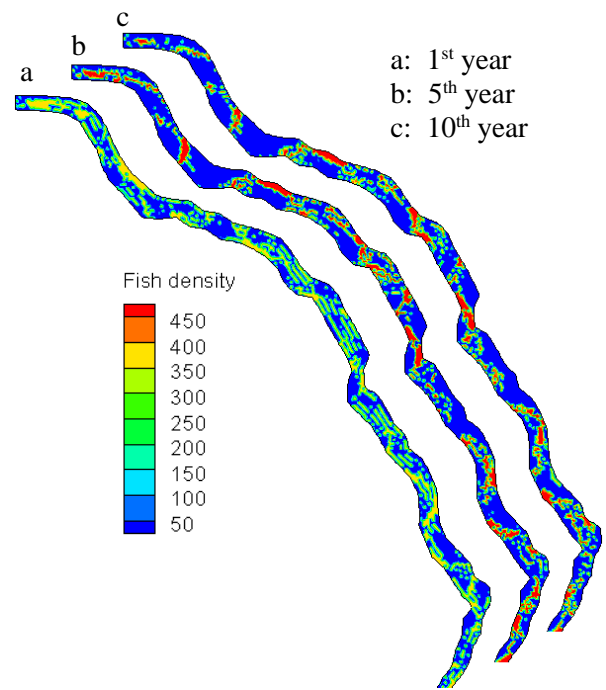
Schizothorax (*Schizothorax*) in scenario S1

Schizothorax (*Schizothorax*) in scenario S2

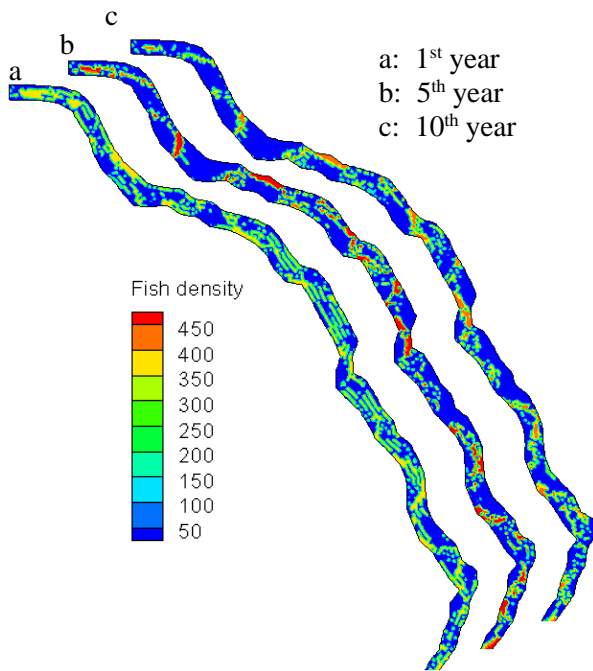
Figure 6.17a: Schizothorax (*Schizothorax*) population density based on the matrix population model in scenarios S1 and S2.



Schizothorax (*Schizothorax*) in scenario S3



Schizothorax (*Schizothorax*) in scenario S3-2



Schizothorax (*Schizothorax*) in scenario S3-3

Figure 6.17b: Schizothorax (*Schizothorax*) population density based on the matrix population model in scenarios S3, S3-2 and S3-3.

Figure 6.18 shows the schizothorax (*Racoma*) population density distribution in scenarios without dam construction effects (S1), with dam construction effects (S2), with the fish stocking numbers 3.0×10^4 (S3), 2.0×10^4 (S3-2), and 1.0×10^4 (S3-3). It can be seen that the maximum schizothorax (*Racoma*) population density value is 42 fish per mesh cell. It can be also seen that the schizothorax (*Racoma*) population density values are much

smaller than the schizothorax (*Schizothorax*) population density values. In scenario S1, the schizothorax (*Racoma*) density values remained at a level of 25 fish per mesh cell. In scenario S2, the schizothorax (*Racoma*) declined from 25 fish per mesh cell in the 1st year to nearly 0 fish per mesh cell in the 10th year. In scenario S3, schizothorax (*Racoma*) density distribution showed an increasing trend during the simulation time, with the maximum fish density at 50 fish per mesh cell. In scenarios S3 and S3-2, the schizothorax (*Racoma*) density values are higher than the values in scenarios S2 and S1. In scenario S3-3, the schizothorax (*Racoma*) density distribution showed a slightly decreasing trend during the simulation time.

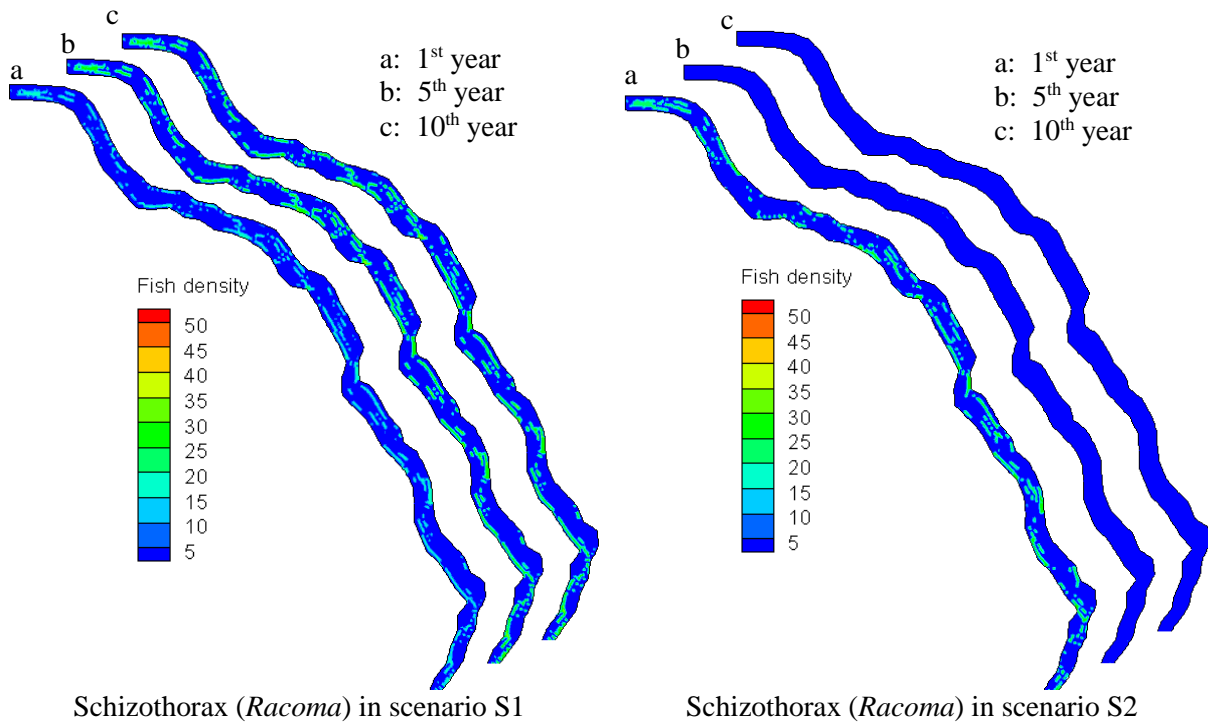


Figure 6.18a: Schizothorax (*Racoma*) population density distribution based on the matrix population model in scenarios S1 and S2.

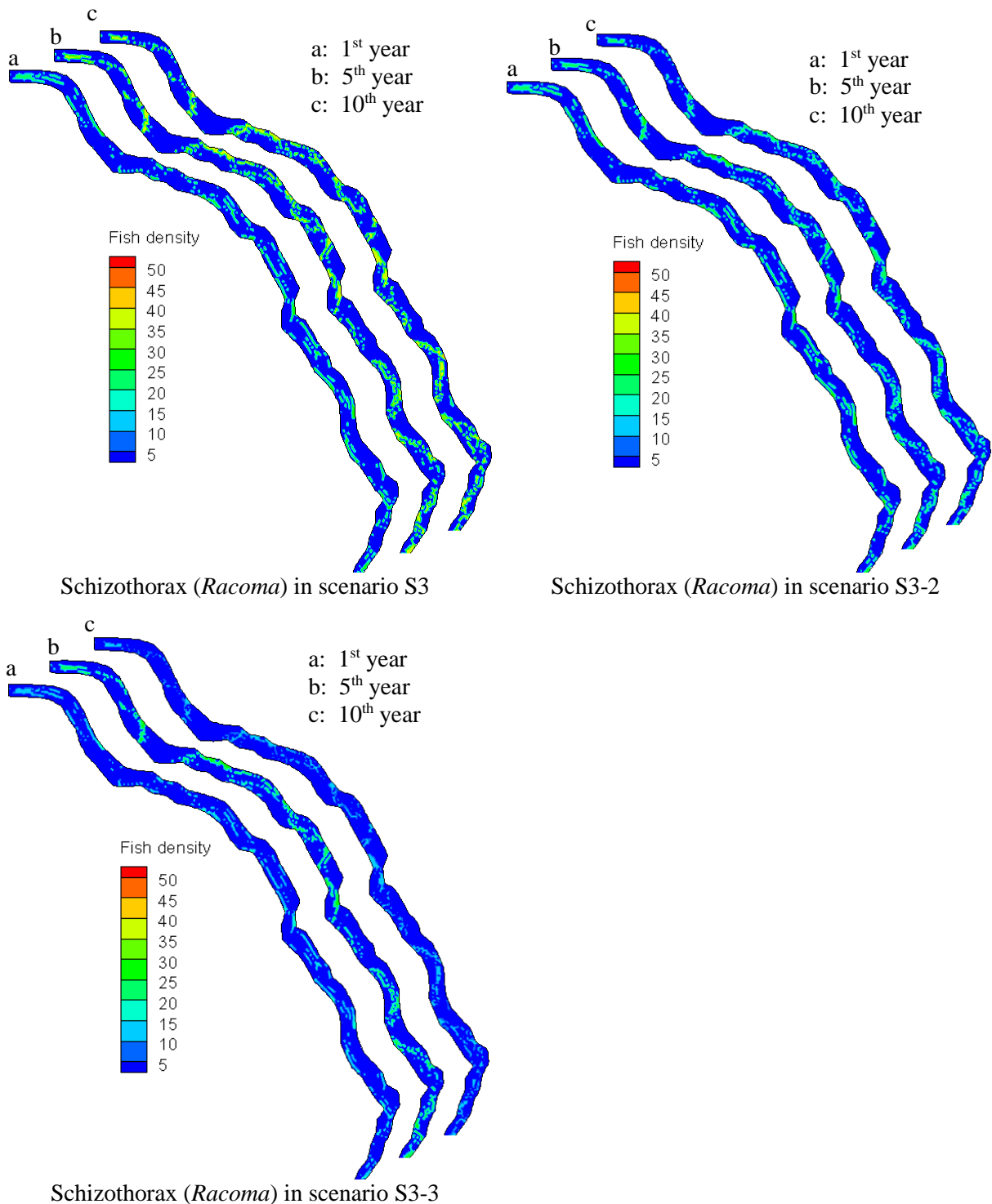


Figure 6.18b: Schizothorax (*Racoma*) population density distribution based on the matrix population model in scenarios S3, S3-2, and S3-3.

In this case study, the simulation results indicate that both selected fish species namely schizothorax (*Schizothorax*) and schizothorax (*Racoma*) would decrease, considering Da-Wei dam construction effects. The simulation results also indicate that the fish stocking strategies can prevent the two fish species population declining. From the simulation

results, it can be seen that based on the logistic population model, the optimal fish stocking numbers are 1.2×10^5 per year and 1.0×10^4 per year for schizothorax (*Schizothorax*) and schizothorax (*Racoma*) respectively. However, based on the matrix population model, the optimal fish stocking numbers are different. The most suitable fish stocking numbers are 1.0×10^5 per year and 2.0×10^4 per year for schizothorax (*Schizothorax*) and schizothorax (*Racoma*) respectively.

It should be noted that, in order to monitor the fish stocking effects and calibrate the model system, a long-term monitoring program needs to be set up. Data such as hydrology, hydraulics, riverbed substrates, fish species composition, fish population age structure, and fish population dynamics should be monitored.

It should also be noted that there are several aspects of the model system which could be further improved. Among other things, the empirical formula in the hydromorphology model may need to be improved. For the habitat model, if possible, each life stage for fish preference should be determined. For the population model, more fish field data are required for evaluating both the logistic and matrix population models. In addition, the fluctuations for the logistic population model are higher than the fluctuations for the matrix population model, which could be improved by further improving the logistic model.

6.5 Conclusion

In the Jiao-Mu River, development of the ecohydraulic model system is essential in order to protect and maintain the ecosystem. With the use of the ecohydraulic model system, the fish number variations, fish density changes, and fish age structure were simulated. This case study evaluated the Da-Wei dam construction effects and fish stocking effects on two selected fish species in the Jiao-Mu River. The physical habitat quality was evaluated in the Jiao-Mu River, and selected fish species abundance variations were also simulated. The efficiencies in scenarios without considering dam building (S1), considering dam construction (S2), and considering fish stocking (S3, S3-2 and S3-3) were evaluated. In addition, stocking sensitivity analyses were also considered in this case study.

The model results indicate that when the Da-Wei dam construction effects were included, the habitat quality, the population number, and population density of the schizothorax (*Schizothorax*) and the schizothorax (*Racoma*) would decrease. However, the schizothorax (*Schizothorax*) and the schizothorax (*Racoma*) population status could be restored by the fish stocking strategies. In the logistic population model, the optimal fish stocking numbers are 1.2×10^5 per year and 1.0×10^4 per year for schizothorax (*Schizothorax*) and schizothorax (*Racoma*) respectively. In the matrix population model, the optimal fish stocking numbers are 1.0×10^5 per year and 2.0×10^4 per year for schizothorax (*Schizothorax*) and schizothorax (*Racoma*) respectively.

Part D: Conclusions and suggestions for further research

7 Conclusions

7.1 Summary of the work

The ecohydraulic model system described in the present dissertation provides an ecosystem methodology which concerns both ecology and hydraulic engineering. The ecohydraulic model system constitutes four models: a hydrodynamic model, a hydromorphology model, a habitat model, and a population model including the logistic population model concept and the matrix population model concept. Three study areas with differing fish species were used to generate habitat suitability index, weighted usable area, overall suitability index, fish population number and density. Each specific case study and selected target fish were separately discussed according to the engineering demand. The ecohydraulics model was applied to support ecological assessments of rivers, and to protect and maintain the ecosystem of the river.

The Aare River, the Colorado River Basin, and the Jiao-Mu River were chosen as case studies. The European grayling (*Thymallus thymallus*. L.) in the Aare River; rainbow trout (*Oncorhynchus mykiss*), brown trout (*Salmo trutta*); and flannelmouth sucker (*Catostomus latipinnis*) in the Colorado River; schizothorax (*Schizothorax*) and schizothorax (*Racoma*) in the Jiao-Mu River were selected as target fish species.

In the case study of the Aare River, the European grayling (*Thymallus thymallus*) was selected as a target fish and the fluvial geomorphology from 1970 to 2000 were studied. Dynamic changes in the habitat of the European grayling (*Thymallus thymallus*) were studied based on two scenarios, namely the model system without hydromorphology model (E1) and with hydromorphology model (E2). The corresponding fish population number and density distribution were also investigated based on the logistic and the matrix population models. The surveyed fish data was used to evaluate the population model's performance. The differences for habitat calculation and population simulation based on different habitat options were compared. The results indicate that the model simulation shows good agreement with the surveyed data according to the EAWAG (2002). The application results also indicate that the ecohydraulic model system can correctly predict the European grayling habitat and population status in the Aare River. For the matrix population model, the population simulation results show also a fairly good agreement with the observed data.

In the case study of the Colorado River, the ecohydraulic model system was used to investigate the rainbow trout, brown trout, and flannelmouth sucker fish number fluctuation

and fish density distribution changes from 2000 to 2009. Three important physical indices, including velocity, water depth and substrates of the river bed were considered in this case study. Five subareas in the Colorado River were chosen as computational domains. Model simulations were calculated from 2000 to 2009 for the habitat and population situation of three fish species with four representative life stages: larvae, juvenile, adult and spawning. Simulation results show that the habitat quality varied on three fish species at four life stages. The rainbow trout population number had fluctuations between 2000 and 2009. It can also be seen that brown trout decreased steadily while the flannel-mouth sucker increased slightly. The surveyed total number of fish has a good agreement with the logistic model prediction.

In the case study of the Jiao-Mu River, the ecohydraulic model system has been proposed to evaluate the effects of the Da-Wei dam construction and the optimum numbers for fish stocking. Two fish species schizothorax (*Schizothorax*) and schizothorax (*Racoma*) were selected as target fish species in this study. Three fish stocking strategies were proposed and evaluated by the ecohydraulic model system. The results indicate that before building dam construction the habitat quality and population number for schizothorax (*Schizothorax*) and schizothorax (*Racoma*) fluctuated regularly. After taking account of the dam construction effects, both target fish population numbers decreased. When the empirical fish stocking strategy is factored in, both target fish population numbers might stabilize. The optimal fish stocking number with the logistic population model for schizothorax (*Schizothorax*) and schizothorax (*Racoma*) are respectively 1.2×10^5 and 1×10^4 per year. The optimal fish stocking number with the matrix population model for schizothorax (*Schizothorax*) and schizothorax (*Racoma*) are respectively 1×10^5 and 2×10^4 per year.

By employing these case studies and the results obtained, the physical factors that determine the target fish habitat and population abundance can be highlighted. The case studies also explain how dam construction effects and the fish stocking strategies influence river ecosystems. The ecohydraulic model system has also been recognized as an increasingly useful tool for successful river management. The advantage of the model system is that it can predict the river's hydrodynamic, hydromorphology, fish habitat, and fish population status. The model system is also important for future research and engineering applications, providing decision-makers with useful information for optimizing their choices.

7.2 Final remark and future research

Water resources development and aquatic ecosystems in freshwater river basins constitute a novel, dynamic, and efficient approach to maintaining and managing healthy fish populations. Freshwater aquatic ecosystem inter-relationships are very complex, and current knowledge about this area is limited. However, researchers and experts' efforts are required for further development and improved accuracy (Janauer, 2000; Newson, & Newson, 2000; Nestler et al., 2008; Katopodis, 2012).

Additional efforts should also be undertaken to evaluate the multiple species habitat and population modeling frameworks with regarding to combining hydrodynamic, hydromorphology, and fish SI curves. Habitat quality could be determined by the classic method, the fuzzy method, or other methods such as support vector machine (SVM). Using SI curves habitat model, SI curves should be more precise. With respect to the fuzzy logic habitat model, the fuzzy rules need more testing. In addition, in the habitat model, other parameters such as water temperature, flow oxygen density distribution etc. should also be taken into consideration.

In addition, extra attention should be given in the area of sediment transport and grain sorting calculations, which is a bottle neck in this model system. Another important development that could be undertaken in the area, would be combining the habitat and population model with multiple dam operation, which would have particular significance in countries with many large dams such as China and India. For a river with multi hydroelectric stations, resources operation plays a vital role in managing the local ecosystem. Ecohydraulic modeling may be used as an optimal tool for planning and better operation of water resources without damaging the freshwater ecosystem.

Ecohydraulics would benefit from more collaborations between researchers, engineers and biologists to quantify the interaction between hydraulics and ecology, particularly biota behavior. Long-term monitoring programs are also needed to conduct the observed data to calibrate and to verify the ecohydraulic model systems.

Acknowledgements

Whenever I try to write a list of people to acknowledge, I may forget someone important. I therefore express my apologies and thanks to the numerous individuals who helped me make this dissertation a reality but that I failed to mention in here.

For the successful completion of this dissertation, I would like to express my sincere gratitude to my doctoral supervisor, Prof. Dr.sc.techn. Peter Rutschmann and Dr-Ing. Minh Duc Bui, for your insightful comments encouragement, but also for your valuable guidance and concrete help during my research and stay in the University from various perspectives. I would like to express my sincere thanks to Prof. Kinzelbach Wolfgang for heartfelt suggestions for doing research and overcoming cultural barrier, and also thanks as the examiners in the examination committee. I also want to thanks Prof. Liqiu Meng for visiting my previous university (Northwest A & F University) in 2010 which give me the chance to know TUM and also give me the motivation to come Germany. I also want to thanks Prof. Liqiu Meng for being the chairman of the examination committee.

My sincere thanks also goes to Dr. Makinster, Dr. Telis and U.S. Geological Survey, who provide detailed information for the data on Colorado River and precious suggestions. I am grateful to Dr. Matthias Schneider and Mr. Lucas Pfister who provided the data on Aare River. I want to say thanks to China Hydro Cooperation for kindness providing the data of Jiao-Mu River. Without these help and suggestions, Subject work would not to be finished. I also thank to all my colleagues in Munich and Obernach Hydraulic Laboratory for the stimulating discussions, especially, Dr. Arnd, Dr. Knapp, Dr. Richard, Dr. Zunic, Ms. Dorothea, Ms. Machauer, Ms. Stögmüller, Anna, Ateeq, Daniel, Nguyen, Duong, Florian, Franz, Jingbo, Julien, Kaveh, Kordula, Marcela, Markus, Reisenbüchler Markus, Mathilde, Michi, Nikos, Sebastian, Shokry, Stephan, Giehl Stefan, Schäfer Stefan, Tatiana and Tobias and many other friends. I really appreciate for all the happy time together and the sleepless nights we were working together before deadlines, and for all the fun we had together.

I am also thankful to CSC (China Scholarship Council) scholarship, for providing me the four years' doctoral scholarship and also the teachers and the ambassador selfless help and assistant. Thanks Mr. Jiqiang Dai, Ms. Chongling Huang help since the first day I came to Germany and all the time in Munich.

Finally, I want to express my sincere gratitude to the fellowship, my parents, my sister, and my girlfriend: Yu Zhong for the encouragement and support and also for overcoming the difficult time together. My special thanks goes to Jeff Gale, I really miss the time we reading together and enhance my faith.

Munich, Germany, July, 2016

Weiwei Yao

List of Figures

Figure 2.1: Model structure of the SALMOD	10
Figure 2.2: The daily action of the InSTREAM	11
Figure 3.1 The flowchart of the ecohydraulic modeling.....	13
Figure 3.2: Factors affecting the habitat suitability	25
Figure 3.3: An example of habitat suitability curves for selected fish	26
Figure 3.4: The flowchart of fuzzy logic based habitat model	27
Figure 3.5: Membership functions for the input variables and the output variable.	27
Figure 3.6: Illustration of the fuzzy rule settings	28
Figure 3.7: Output for habitat suitability index (HSI) after defuzzification.	28
Figure 3.8: Flowchart of the habitat model.....	30
Figure 3.9: Length-at-age relation for a fish species.....	34
Figure 4.1: Computation domain and substrate types.....	38
Figure 4.2: Flow hydrograph of the Aare river from 1970 to 2000.....	38
Figure 4.3: Flowchart of the ecohydraulic model system structure for European grayling in the Aare river.....	39
Figure 4.4: Extent of the computational river stretch and the generated mesh.....	40
Figure 4.5: Fry, juvenile, and adult European grayling SI curves for velocity, water depth and substrate types.....	42
Figure 4.6: The WUA values comparison for four habitat computational options and the EAWAG report.....	45
Figure 4.7: The WUA comparison based six different methods.....	45
Figure 4.8a: The velocity distribution at 1970, 1980, 1990, and 2000 in scenario E1 and E2.....	49
Figure 4.8b: The water depth distribution at 1970, 1980, 1990, and 2000 in scenario E1 and E2.....	49
Figure 4.8c: The substrates distribution at 1970, 1980, 1990, and 2000 in scenario E1 and E2.....	49
Figure 4.9: The HSI distribution at 1970, 1980, 1990, and 2000 for O1 and in scenario E1 based on spawning SI curves.	50
Figure 4.10: The HSI distribution at 1970, 1980, 1990, and 2000 for O1 and in scenario E2 based on spawning SI curves.	50
Figure 4.11: The WUA and OSI value fluctuations from 1970 to 2000 for O1, O2, O3, and O4 in scenario E1 based on spawning SI curves.	51
Figure 4.12: The WUA and OSI distribution from 1970 to 2000 for O1, O2, O3, and O4 in scenario E2 based on spawning SI curves.....	51
Figure 4.13: The WUA and OSI differences for O1, O2, O3, and O4 between scenario E1 and E2.....	52
Figure 4.14: The European grayling simulated numbers based on the logistic population model in scenario E1	53

Figure 4.15: The European grayling simulated numbers based on the logistic population model in scenario E2	54
Figure 4.16: The European grayling simulated number difference between scenarios E1 and E2 for O1, O2, O3, and O4 based on the logistic population model.....	55
Figure 4.17: The European grayling density distributions for O1 in scenario E1 based on the logistic population model.	56
Figure 4.18: The European grayling density distributions for O1 in scenario E2 based on the logistic population model..	57
Figure 4.19: The simulated European grayling number based on the matrix population model in scenario E1.	58
Figure 4.20: The European grayling population numbers of all life stage structure based on the matrix population model.....	59
Figure 4.21: The simulated European grayling numbers based on the matrix population model in scenario E2.	60
Figure 4.22: The European grayling population number and age structure based on the matrix population model in scenario E2.	61
Figure 4.23: The population number and life stage distribution difference between the scenario E1 and scenario E2 based on the matrix population model.	63
Figure 4.24: The European grayling population density variation based on the matrix population model in scenario E1.	64
Figure 4.25: The European grayling population density variation based on the matrix population model in scenario E2.	65
Figure 5.1: Map of case study area in the Colorado River and computational results for the meshes in the five subarea.	68
Figure 5.2: Discharge hydrograph at the inlet section and the stage curve at the outlet.	69
Figure 5.3: The three main fish species living in colorado river.	70
Figure 5.4a: Four life stages fish SI curves of rainbow trout.....	73
Figure 5.4b: Four life stages fish SI curves of brown trout.	74
Figure 5.4c: Four life stages fish SI curves of flannelmouth sucker.....	75
Figure 5.5a: The simulated velocity, water depth, substrate, and bed level changes in the Sub1 from 2000 to 2009.	80
Figure 5.5b: The simulated velocity, water depth, substrate, and bed level changes in the Sub2 from 2000 to 2009.	81
Figure 5.5c: The simulated velocity, water depth, substrate, and bed level changes in the Sub3 from 2000 to 2009.	82
Figure 5.5d: The simulated velocity, water depth, substrate, and bed level changes in the Sub4 from 2000 to 2009.	83
Figure 5.5e: The simulated velocity, water depth, substrate, and bed level changes in the Sub5 from 2000 to 2009.	84
Figure 5.6: The simulated habitat suitability index distribution for adult rainbow trout, brown trout and flannelmouth sucker in the river stretch Sub1.	86

Figure 5.7: The simulated habitat suitability index distribution for adult rainbow trout, brown trout and flannelmouth sucker in the river stretch Sub2.	87
Figure 5.8: The simulated habitat suitability index distribution for adult rainbow trout, brown trout and flannelmouth sucker in the river stretch Sub3.	88
Figure 5.9: The simulated habitat suitability index distribution for adult rainbow trout, brown trout and flannelmouth sucker in the river stretch Sub4.	89
Figure 5.10: The simulated habitat suitability index distribution for adult rainbow trout, brown trout and flannelmouth sucker in the river stretch Sub5.	89
Figure 5.11: The WUA and OSI distribution for adult rainbow trout, brown trout, and flannelmouthsucker from 2000 to 2009 in the river stretch Sub1.	91
Figure 5.12: The WUA and OSI distribution for adult rainbow trout, brown trout, and flannelmouthsucker from 2000 to 2009 in the river stretch Sub2.	92
Figure 5.13: The WUA and OSI distribution for adult rainbow trout, brown trout, and flannelmouthsucker from 2000 to 2009 in the river stretch Sub3.	93
Figure 5.14: The WUA and OSI distribution for adult rainbow trout, brown trout, and flannelmouthsucker from 2000 to 2009 in the river stretch Sub4.	94
Figure 5.15: The WUA and OSI distribution for adult rainbow trout, brown trout, and flannelmouthsucker from 2000 to 2009 in the river stretch Sub5.	95
Figure 5.16: The WUA and OSI distribution for adult rainbow trout, brown trout, and flannelmouthsucker from 2000 to 2009 in the whole Colorado River.	96
Figure 5.17: The variations of rainbow trout, brown trout and flannelmouth sucker population number from 2000 to 2009 in the river stretch Sub1.	98
Figure 5.18: The variations of rainbow trout, brown trout and flannelmouth sucker population number from 2000 to 2009 in the river stretch Sub2.	99
Figure 5.19: The variations of rainbow trout, brown trout and flannelmouth sucker population number from 2000 to 2009 in the river stretch Sub3.	100
Figure 5.20: The variations of rainbow trout, brown trout and flannelmouth sucker population number from 2000 to 2009 in the river stretch Sub4.	102
Figure 5.21: The variations of rainbow trout, brown trout and flannelmouth sucker population number from 2000 to 2009 in the river stretch Sub5.	103
Figure 5.22: The variations of rainbow trout, brown trout and flannelmouth sucker population number from 2000 to 2009 over the whole river stretch.	104
Figure 5.23: The variations of rainbow trout, brown trout and flannelmouth sucker population number from 2000 to 2009 in the the river stretch.	105
Figure 5.24a: The rainbow trout, brown trout and flannelmouth sucker population density distribution in the river stretch Sub1.	109
Figure 5.24b: The rainbow trout, brown trout and flannelmouth sucker population density distribution in the river stretch Sub2.	109
Figure 5.24c: The rainbow trout, brown trout and flannelmouth sucker population density distribution in the river stretch Sub3.	109

Figure 5.24d: The rainbow trout, brown trout and flannelmouth sucker population density distribution in the river stretch Sub4.....	109
Figure 5.24e: The rainbow trout, brown trout and flannelmouth sucker population density distribution in the river stretch Sub5.....	109
Figure 5.25a: The WUA and OSI distribution for spawning, fry and juvenile rainbow trout.....	110
Figure 5.25b: The WUA and OSI distribution for spawning, fry and juvenile brown trout	110
Figure 5.25c: The WUA and OSI distribution for spawning, fry and juvenile flannelmouth sucker	111
Figure 5.26: The variation of rainbow trout, brown trout and flannelmouth sucker population numbers from 2000 to 2009 based on the matrix population model....	113
Figure 6.1: Local map of 13 hydropower construction base in China.	118
Figure 6.2: Location of the study area in this case study.	119
Figure 6.3: The computation domain and the sediment grading curve of the Jiao-Mu River.	119
Figure 6.4: Schizothorax (<i>schizothorax</i>) and schizothorax (<i>racoma</i>) fish SI curves for velocity, water depth and riverbed substrates types.	121
Figure 6.5: Flowchart of the model applicaion in Jiao-Mu River.....	123
Figure 6.6: The velocity, depth, and substrates distribution in scenario S1	127
Figure 6.7: Schizothorax (<i>schizothorax</i>) and schizothorax (<i>racoma</i>) HSI distribution in scenario S1.....	128
Figure 6.8: The WUA and OSI values for schizothorax (<i>schizothorax</i>) and schizothorax (<i>racoma</i>) in scenario S1.....	129
Figure 6.9: The velocity, depth, and substrate distribution in scenario S2	130
Figure 6.10: Schizothorax (<i>schizothorax</i>) and schizothorax (<i>racoma</i>) HSI distribution in scenario S2.....	131
Figure 6.11: Schizothorax (<i>schizothorax</i>) and schizothorax (<i>racoma</i>) WUA and OSI distribution in scenario S2.	132
Figure 6.12: Population number of schizothorax (<i>schizothorax</i>) and the schizothorax (<i>racoma</i>) based on the logistic population model.	133
Figure 6.13a: Schizothorax (<i>schizothorax</i>) population density based on the logistic population model in scenarios without dam construction effects (S1), with dam construction effects (S2).....	135
Figure 6.13b: Schizothorax (<i>schizothorax</i>) population density based on the logistic population model in scenarios with fish stocking number 1.2×10^5 (S3), fish stocking number 1.0×10^5 (S3-2) and fish stocking number 6.0×10^4 (S3-3).	135
Figure 6.14a: Schizothorax (<i>racoma</i>) population density based on the logistic population model in scenarios without dam construction effects (S1), with dam construction effects (S2).....	135

Figure 6.14b: Schizothorax (<i>racoma</i>) population density based on the logistic population model in scenarios with fish stocking number 3.0×10^4 (S3), fish stocking number 2.0×10^5 (S3-2) and fish stocking number 1.0×10^4 (S3-3).....	136
Figure 6.15a: Schizothorax (<i>schizothorax</i>) population number based on the matrix population model in scenarios without dam construction effects (S1), with dam construction effects (S2).....	140
Figure 6.15b: Schizothorax (<i>schizothorax</i>) population number based on the matrix population model in scenarios with fish stocking number 1.2×10^5 (S3), fish stocking number 1.0×10^5 (S3-2) and fish stocking number 6.0×10^4 (S3-3).....	140
Figure 6.16a: Schizothorax (<i>racoma</i>) population density based on the matrix population model in scenarios without dam construction effects (S1), with dam construction effects (S2)	142
Figure 6.16b: Schizothorax (<i>racoma</i>) population density based on the matrix population model in scenarios fish stocking number 3.0×10^4 (S3), fish stocking number 2.0×10^4 (S3-2) and fish stocking number 1.0×10^4 (S3-3)).	142
Figure 6.17a: Schizothorax (<i>schizothorax</i>) population density based on the matrix population model in scenarios S1 and S2.....	145
Figure 6.17b: Schizothorax (<i>schizothorax</i>) population density based on the matrix population model in scenarios S3, S3-2 and S3-3.....	145
Figure 6.18a: Schizothorax (<i>racoma</i>) population density based on the matrix population model in scenarios S1 and S2.	147
Figure 6.18b: Schizothorax (<i>racoma</i>) population density based on the matrix population model in scenarios S3, S3-2 and S3-3.....	147

List of Tables

Table 3.1: Manning coefficient useable range for channel types and materials.	16
Table 3.2: Validity range of the sediment transport formulae	19
Table 4.2: The survival rate and birth rate of the European grayling for matrix population model.	43
Table 4.2: The parameter descriptions for suitability index class.....	43
Table 4.3: The parameter for WUA comparison.....	43
Table 4.4: Correction coefficients between simulated and measured fish number in Aare river.....	56
Table 5.1: The basic matrix parameter for three fish species used in Colorado River. ..	76
Table 5.2: Length life stage definition for rainbow trout, brown trout and flannelmouth sucker.....	77
Table 5.3: Fish population number used for simulation at five subareas in 2000.	97
Table 5.4: Correlation coefficients between simulated and measured fish numbers in the five subareas of the Colorado River.	109
Table 6.1: Discharge and sediment bed-load in the Jiao-Mu River stretch.	120
Table 6.2: Water elevation and discharge relationship in the outlet of computational domain.	120
Table 6.3: Fish species affected by dam construction.....	122
Table 6.4: Information sources of SI curves for fish species schizothorax (<i>schizothorax</i>) and schizothorax (<i>racoma</i>).	122
Table 6.5: The empirical parameters used in the matrix population model.	125
Table 6.6: The parameter applied in fish stocking.....	126
Table 6.7: Fish stocking established based on ecological engineering.....	126

Reference

- Acreman, M. C., and Ferguson, A. J. D. (2010). Environmental flows and the European water framework directive. *Freshwater Biology*, 55(1), 32-48.
- Alfredsen, K., and Killingtveit, A. (1996). The habitat modelling framework: a tool for creating habitat analysis programs. In: Leclerc, M., Capra, H., Valentin, S. Boudreault, A., Cote, Y. (Eds.), *Proceedings of the Second International Symposium on Habitat Hydraulics*, vol. B. Quebec City, Canada, pp. 215–227.
- Almeida, G., and Rodríguez, J. (2009). Integrating sediment dynamics into physical habitat models. 18th World Imacs/ModSim Congress, Cairns, Australia: 2258–2264.
- Armstrong, J. D., Kemp, P. S., Kennedy, G. J. A., Ladle, M., and Milner, N. J. (2003). Habitat requirements of Atlantic salmon and Brown trout in rivers and streams. *Fisheries Research*, 62(2), 143-170.
- Armstrong, J.D., Kemp, P.S., Kennedy, G.J.A., Ladle, M., and Milner, N.J. (2003). Habitat requirements of Atlantic salmon and Brown trout in rivers and streams, *Fisheries Research*, Volume 62, Issue 2, Pages 143-170,
- Armstrong, J. D., Kemp, P. S., Kennedy, G. J. A., Ladle, M., and Milner, N. J. (2003). Habitat requirements of Atlantic salmon and Brown trout in rivers and streams. *Fisheries research*, 62(2), 143-170.
- Ackers, P., and White, W. R. (1973). Sediment transport: New approach and analysis. *Journal of the Hydraulics Division, American Society of Civil Engineers*, Vol. 99, No. HY 11, pp. 2040-2060.
- Alexander, G. R. (1987). Comparative growth and survival potential of Brown trout (*Salmo trutta*) from four wild stocks and one domestic stock. *Michigan Academician* 19:109-119.
- Allen, A. W. (1983). Habitat suitability index models: beaver. Western Energy and Land Use Team, Division of Biological Service, Research and Development, Fish and Wildlife Service, US Department of the Interior.
- Akahori, R., Schmeckle, M. W., Topping, D. J. and Melis, T. S. (2008). Erosion properties of cohesive sediments in the Colorado River in Grand Canyon. *River Research and Applications*, 24(8), 1160-1174.
- Aziz-Alaoui, M. A. (2002). Study of a Leslie–Gower-type tritrophic population model. *Chaos, Solitons & Fractals*, 14(8), 1275-1293.
- Bailard, J. A., and Inman, D. L. (1981). An energetics bedload model for a plane sloping beach: local transport. *Journal of Geophysical Research: Oceans* (1978–2012), 86(C3), 2035-2043.
- Ballard, C. M. (2012). *RiverFLO-2D and the Surfacewater Modeling System (SMS)* (Doctoral dissertation, Brigham Young University).
- Bartholow, J.M., Laake, J. L., Stalnaker, C. B. and Williamson S. (1993). A salmonid population model with emphasis on habitat limitations. *Rivers*, 4: 265–279.

Bartholow, J. M. (1996). Sensitivity of a salmon population model to alternative formulations and initial conditions. *Ecological Modeling*, 88 (1–3), 215–226.

Bartholow J. (2001). SALMOD a population model for salmonids users' manual. U.S. Geological Survey Midcontinent Ecological Science Center.

Baxter, P. W., Mccarthy, M. A., Possingham, H. P., Menkhorst, P. W., and Mccarthy, N. (2006). Accounting for management costs in sensitivity analyses of matrix population models. *Conservation Biology*, 20(3), 893-905.

Bell, M. C. (1973). Fisheries handbook of engineering requirements and biological criteria. U.S. Army Corps Engineers, North Pacific Div. Contract DACW57-68-C-0086. 92 pp.

Berkers, F (1993). Traditional ecological knowledge in perspective. *Traditional ecological knowledge: Concepts and cases*, 1-9.

Bernhardt, E. S., Palmer, M., Allan, J. D., Alexander, G., Barnas, K., Brooks, S., ... & Sudduth, E. (2005). Synthesizing U. S. river restoration efforts. *Science(Washington)*, 308(5722), 636-637.

Beyers, D. W., Sodergren, J. M. Bundy, and Bestgen, K. R. (2001). Habitat use and movement of bluehead sucker, Flannelmouth sucker, and roundtail chub in the Colorado River. Final Report to Colorado Division of Wildlife. Contribution 21, Larval Fish Laboratory, Department of Fishery and Wildlife Biology, Colorado State University, Fort Collins. 30 p.

Bijker, E. W. (1971). Longshore transport computations. *Journal of the Waterways, Harbors and Coastal Engineering Division*, 97(4), 687-701.

Blackburn, J., and Steffler, P. M. (2002). River 2D two dimensional depth averaged model of river hydrodynamics and fish habitat. *River2D Tutorials*, University of Alberta.

Bovee, K. D. (1982). A Guide to Stream Habitat Analysis Using the Instream Flow Incremental Methodology. *Instream Flow Information Paper No. 12 US Fish and Wildlife Service, Fort Collins, Colorado* 248 pp.

Bovee, K. D. (1986). Development and evaluation of habitat suitability criteria for use in the instream flow incremental methodology. *instream flow information paper no. 21, US Fish and Wildlife Service Biological Report*, 86 (7) Washington, DC.

Bovee, K. D., Waddle, T. J., Talbert, C., Hatten, J. R., and Batt, T. R. (2008). Development and application of a decision support system for water management investigations in the upper Yakima River, Washington. *US Geological Survey*.

Brandenburg, W. H., Farrington, M. A. and Gottlieb, S. J. (2005). Colorado pikeminnow and razorback sucker larval fish survey in the San Juan River during 2004. *San Juan River Basin Recovery Implementation Program, U.S. Fish and Wildlife Service, Albuquerque, New Mexico*.

Bratrich, C., Truffer, B., Jorde, K., Markard, J., Meier, W., Peter, A., and Wehrli, B. (2004). Green hydropower: a new assessment procedure for river management. *River Research and Applications*, 20(7), 865-882.

- Brauer, F., Castillo-Chavez, C., and Castillo-Chavez, C. (2001). *Mathematical models in population biology and epidemiology* (Vol. 1). New York: Springer.
- Brooks, R. P. (1997). Improving habitat suitability index models. *Wildlife Society Bulletin*, 163-167.
- Brooks, S. S., and Lake, P. S. (2007). River restoration in Victoria, Australia: change is in the wind, and none too soon. *Restoration Ecology*, 15(3), 584-591.
- Brown, C. B. (1950). *Sediment Transport. Engineering Hydraulics*, Ch. 12.
- Brunner, G. W. (2005). *Sediment Transport Modeling in HEC RAS*.
- Brunner, G. W. (2010). *HEC-RAS River Analysis System User Manual Version 3.1. CPD68*. US Army Corps of Engineers, Institute for Water Resources, Hydrologic Engineering Center: Davis, California, 790.
- Bryant, E. H. (1973). Habitat selection in a variable environment. *Journal of theoretical biology*, 41(3), 421-429.
- Bui, M. D., Wenka, T., and Rodi, W. (2004). Numerical modeling of bed deformation in laboratory channels. *Journal of Hydraulic Engineering*, 130(9), 894-904.
- Bui, M. D., and Rutschmann, P. (2010). Numerical modelling of non-equilibrium graded sediment transport in a curved open channel. *Computers & Geosciences*, 36(6), 792-800.
- Bui MD, Abdelaziz S, Rutschmann P (2013) Numerical Modeling of Hydromorphological Change and Fish Habitat in the Rhine River. *HydroVision 2013. Proc. of the HydroVision International Conference, July 23-26, 2013, Session 5J1: Environmental Aspects of Hydropower Development*, 14 pages, Denver, USA 7
- Burnhill, T. J. (2009). *Modelling the cumulative barrier and passage effects of mainstream hydropower dams on migratory fish populations in the Lower Mekong Basin*. Mekong River Commission.
- Caswell, H. (2001). *Matrix population models*. John Wiley & Sons, Ltd.
- Chart, T. E., and Bergersen, E. P. (1992). Impact of mainstream impoundment on the distribution and movements of the resident Flannelmouth sucker (*Catostomidae: Catostomus latipinnis*) population in the White River, Colorado. *Southwestern Naturalist* 37:9-15.
- CHC. (2011) *Blue Kenue reference manual*. Canadian hydraulics center.
- Coggins, L. G. (2008). *Active adaptive management for native fish conservation in the Grand Canyon—Implementation and evaluation*: Gainesville, University of Florida, Ph.D. dissertation, 173 p.
- Coggins, L. G., and Walters, C. J. (2009) *Abundance trend and status of the Little Colorado River population of humpback chub; an update considering data from 1989-2008*: U.S. Geological Survey Open-File Report 2009-1075, 18p.
- Coleman, S. E., and Nikora, V. I. (2009). Exner equation: A continuum approximation of a discrete granular system. *Water Resources Research*, 45(9).

Commission, E. (2000): Directive 2000/60/EC. Establishing a framework for community action in the field of water policy, Luxembourg: European Commission, PE-CONS 3639/1/100 Rev 1.

Conroy, M. J., Cohen, Y., James, F. C., Matsinos, Y. G., and Maurer, B. A. (1995). Parameter estimation, reliability, and model improvement for spatially explicit models of animal population. *Ecological Applications*, 5(1), 17-19.

Conway, C. J., Nadeau, C. P., and Piest, L. (2010). Fire helps restore natural disturbance regime to benefit rare and endangered marsh birds endemic to the Colorado River. *Ecological Applications*, 20(7), 2024-2035.

Cooley, M. E., Aldridge, B. N. and Euler. R. C. (1977). Effects of the catastrophic flood of December, 1966, North Rim area, eastern Grand Canyon, Arizona, U.S. Geological Survey Professional Paper 980, 43 p.

Cross, J. N. (1975). Ecological distribution of the fish of the Virgin River. M.S. Thesis, University of Nevada, Las Vegas. 187 p.

Deangelis, D. L., and Gross, L. J. (1992). Which individual-Based approach is most appropriate for a given problem? *Individual-Based Models and Approaches in Ecology*. pp. 67-87.

Dibajnia, M., and Watanabe, A. (1996). A transport rate formula for mixed-size sands. *Coastal Engineering Proceedings*, 1(25).

Dobler, W., Baran, R., Steinbacher, F., Ritter, M., and Aufleger, M. (2014, May). Using high resolution bathymetric lidar data for a Telemac2D simulation. In *EGU General Assembly Conference Abstracts* (Vol. 16, p. 1026).

Dudgeon, D. (2000). Large-Scale Hydrological Changes in Tropical Asia: Prospects for Riverine Biodiversity The construction of large dams will have an impact on the biodiversity of tropical Asian rivers and their associated wetlands. *BioScience*, 50(9), 793-806.

Dunbar, M. J., Elliott, C. R. N., Acreman, M. C., and Gustard, A. (1996). Ecologically acceptable flows phase II, Volume 1: Habitat time series analysis. Environment Agency R&D Technical Report W19.

Dunning, J. B., Stewart, D. J., Danielson, B. J., Noon, B. R., Root, T. L., Lamberson, R. H., and Stevens, E. E. (1995). Spatially explicit population models: current forms and future uses. *Ecological Applications*, 5(1), 3-11.

EAWAG (Swiss Federal Institute for Environmental Science and Technology) (2002). *Fischereiliches Gutachten über die Aarebaggerung in Thun*. Forschungsanstalt des ETH-Bereichs, Kastanienbaum, Switzerland, 201 pp. (in German).

Eckholm, E. P. (1975). The Deterioration of Mountain Environments Ecological stress in the highlands of Asia, Latin America, and Africa takes a mounting social toll. *Science*, 189(4205), 764-770.

Einstein, H. A. (1942). Formulae for transportation of bed-load, *Trans. ASCE*, 107, 561-577.

- Eddy, S., and Underhill, J. C. (1978). *How to know the freshwater fishes?* 3rd edition. WCB/ McGraw-Hill, Boston, Massachusetts.
- Edwards, E. A., Gebhart, G., and Maughan, O. E. (1983). *Habitat suitability information: smallmouth bass*. Oklahoma cooperative fish and wildlife research unit still water.
- Engelund, F. and Hansen, E. (1967). *A monograph on sediment transport in alluvial streams*, Teknisk Forlag, Copenhagen, Denmark.
- Erman, D. C., and Hawthorne, V. M. (1976). The quantitative importance of an intermittent stream in the spawning of Rainbow trout. *Transactions of the American Fisheries Society*. 105:675-681.
- European Commission. (1992). Council Directive 92/43/EEC of 21 May 1992 on the conservation of natural habitats and of wild fauna and flora. *Official Journal of the European Communities*, L 206. 1992. p. 7. 22.7.
- Fahrig, L., and Merriam, G. (1985). Habitat patch connectivity and population survival. *Ecology*, 1762-1768.
- Flynn, M. E. and Hornewer, N. J. (2003). Variations in sand storage measured at monumented cross sections in the Colorado River between Glen Canyon Dam and Lava Falls Rapid, northern Arizona, 1992-99. U.S. Geological Survey Open-File Report: 2003 - 4104.
- Fox Jr, W. and William W. (1970). An exponential surplus-yield model for optimizing exploited fish population. *Transactions of the American Fisheries Society*, 99(1), 80-88.
- Freeman, M. M. (1992). The nature and utility of traditional ecological knowledge. *Northern Perspectives*, 20(1), 9-12.
- Fu, X. L., Li, D. M., and Jin, G. Y. (2007). Calculation of flow field and analysis of spawning sites for Chinese sturgeon in the downstream of Gezhouba Dam. *Journal of Hydrology*, 19, 78-83.
- Gabl, R., Gems, B., De Cesare, G., and Aufleger, M. (2013). Anregungen zur Qualitätssicherung in der 3-D-numerischen Modellierung mit FLOW-3D. Eingereicht bei der WasserWirtschaft.
- Gard, M. (2009). Comparison of spawning habitat predictions of PHABSIM and River2D models. *International Journal of River Basin Management*, 7(1), 55-71.
- Gard, M. (2010). Response to Williams (2010) on Gard (2009). Comparison of spawning habitat predictions of PHABSIM and River2D models. *International Journal of River Basin Management*, 8(1), 121-125.
- Gido, K. B., Propst, D. L., and Molles Jr, M. C. (1997). Spatial and temporal variation of fish communities in secondary channels of the San Juan River, New Mexico and Utah. *Environmental Biology of Fish* 49:417-434.
- Ginot, V. (1995). EVHA, a Windows software for fish habitat assessment in streams. *Bulletin Francais de la Peche et de la Pisciculture* (France).
- Gloss, S. P., Lovich, J. E., and Melis, T. S. (2005). The state of the Colorado River ecosystem in Grand Canyon: U.S. Geological Survey Circular 1282, 220 p.

- Glowacki, S. C. (2003). A comparison of growth rates of wild Rainbow trout (*Oncorhynchus mykiss*) in the upper Sacramento River before and after the Cantara Spill of 1991 (Master dissertation, Humboldt State University).
- Gowing, H. (1986). Survival and growth of matched plantings of Assinica strain brook trout and hybrid brook trout (Assinica male x Domestic female) in six small Michigan lakes. *North American Journal of Fisheries Management* 6:242-251.
- Gönczi, A. P. (1989). A study of physical parameters at the spawning sites of the European grayling (*Thymallus thymallus* L.). *Regulated Rivers: Research & Management*, 3(1), 221-224.
- Graf, J. B. (1995). Measured and predicted velocity and longitudinal dispersion at the steady and unsteady flow, Colorado River, Glen Canyon Dam to Lake Mead: *Water Resources Bulletin*, V. 31, no. 2, P. 265-281.
- Graf, J. B., Marlow, J. E., Fisk, G. G. and Jansen, S. M. (1995). Sand-storage changes in the Colorado River downstream from the Paria and Little Colorado Rivers, June 1992 to February 1994. U.S. Geological Survey Open-File Report: 95-446.
- Grimm, V. (1999). Ten years of individual-based modelling in ecology: what have we learned and what could we learn in the future? *Ecological modelling*, 115(2), 129-148.
- Guthruf, J. (2005) Äschenlaichplätze Aare Thun, Planung und Erfolgskontrolle, Aquatica GmbH, Büro für Gewässerökologie und Wassertechnik, Switzerland, 50 pp. (in German).
- Hall, A. J., McConnell, B. J., Rowles, T. K., Aguilar, A., Borrell, A., Schwacke, L., and Wells, R. S. (2006). Individual-based model framework to assess population consequences of polychlorinated biphenyl exposure in bottlenose dolphins. *Environmental Health Perspectives*, 114, 60.
- Harvey, B. C., Jackson, S. K., and Lamberson, R. H. (2009). InSTREAM: the individual-based stream trout research and environmental assessment model (Vol. 218). US Department of Agriculture, Forest Service, Pacific Southwest Research Station.
- Hauer, C., Unfer, G., Holzmann, H., Schmutz, S., and Habersack, H. (2013). The impact of discharge change on physical instream habitats and its response to river morphology. *Climatic change*, 116(3-4), 827-850.
- Hazel, Joseph, E., Jr., Kaplinski, M., Parnell, R., Kohl, K., and Topping, D. J. (2006). Stage-Discharge Relations for the Colorado River in Glen, Marble, and Grand Canyons, Arizona: U.S. Geological Survey Open-File Report 2006-1243, 7 p.
- Hering, D., Borja, A., Carstensen, J., Carvalho, L., Elliott, M., Feld, C. K., and Bund, W. V. (2010). The European Water Framework Directive at the age of 10: a critical review of the achievements with recommendations for the future. *Science of the Total Environment*, 408(19), 4007-4019.
- Hess, G. R. (1996). Linking extinction to connectivity and habitat destruction in meta-population models. *American Naturalist*, 226-236.

- Holden, P. B. (1977). A study of the habitat use and movement of the rare fish in the Green River from Jensen to Green River, Utah, August and September, 1977. Final Report for Western Energy and Land-use Team, Contract 14-16-0009-77-050, BIO-WEST, Logan, Utah.
- Holden, P. B. (editor). (1999). Flow recommendations for the San Juan River. San Juan River Basin Recovery Implementation Program, U.S. Fish and Wildlife Service, Albuquerque, New Mexico.
- Huang, G., Chen, Q., and Jin, F. (2010). Implementing eco-friendly reservoir operation by using genetic algorithm with dynamic mutation operator. In *Life System Modeling and Intelligent Computing* (pp. 509-516). Springer Berlin Heidelberg.
- Huang, H., and Yan, Z. (2009). Present situation and future prospect of hydropower in China. *Renewable and Sustainable Energy Reviews*, 13(6), 1652-1656.
- Hubert, W. A., and Rahel, F. J. (1989). Relations of physical habitat to abundance of four nongame fish in high-plains streams: a test of habitat suitability index models. *North American Journal of Fisheries Management*, 9(3), 332-340.
- Hunziker R.P. (1995). *Fraktionsweiser Geschuebetransport*, Ph.D. thesis, Mitteilungen Nr 138 der Versuchsanstalt für Wasserbau, Hydrologie und Glaziologie, ETH Zurich, Switzerland.
- Hunziker, R. P., and Jaeggi, M. N. (2002). Grain sorting processes. *Journal of Hydraulic Engineering*, 128(12), 1060-1068.
- Ibrahim, L., Preuss, T. G., Schaeffer, A., and Hommen, U. (2014). A contribution to the identification of representative vulnerable fish species for pesticide risk assessment in Europe—A comparison of population resilience using matrix models. *Ecological Modelling*, 280, 65-75.
- Ingram, A., Ibbotson, A., and Gallagher, M. (2000). The ecology and management of the European grayling *Thymallus thymallus* (Linnaeus). Interim report. East Stoke, UK, Institute of Freshwater Ecology, 91pp.
- Jacobsen, N. G., Fuhrman, D. R., and Fredsøe, J. (2012). A wave generation toolbox for the open-source CFD library: OpenFoam. *International Journal for Numerical Methods in Fluids*, 70(9), 1073-1088.
- Janauer, G. A. (2000). Ecohydrology: fusing concepts and scales. *Ecological Engineering*, 16(1), 9-16.
- Jie, F. B., Hua, L. G., Ding, C. L., Ming, M. K., and Ran, L. J. (2001). Scheme of ecological regionalization in China. *Acta Ecologica Sinica*, 1000.
- Jones, N.E., Tonn, W.M., Scrimgeour, G.J., and Katopodis, C. (2003). Productive capacity of an artificial stream in the Canadian Arctic: assessing the effectiveness of fish habitat compensation. *Canadian Journal of Fisheries and Aquatic Sciences*. 60, 849–863.
- Jorde, K., and Bratrich, C. (2000). Ecological evaluation of Instream Flow Regulations based on temporal and spatial variability of bottom shear stress and hydraulic habitat quality. In *Ecohydraulics, 2nd International Symposium on Habitat Hydraulics*. Quebec City, Canada.

- Jowett, I. G. (1997). Instream flow methods: a comparison of approaches. *Regulated Rivers* 13, 115–127.
- Jowett, I. G. (1990). Factors related to the distribution and abundance of brown and Rainbow trout in New Zealand clear-water rivers. *New Zealand journal of marine and freshwater research*, 24(3), 429-440.
- Jowett, I. G., and Davey, A. J. (2007). A comparison of composite habitat suitability indices and generalized additive models of invertebrate abundance and fish presence–habitat availability. *Transactions of the American Fisheries Society*, 136(2), 428-44
- Judd, S. (2010). *The MBR book: principles and applications of membrane bioreactors for water and wastewater treatment*. Elsevier, Nov 26.
- Kaplinski, M., Hazel, J.E., Jr., Parnell, R., Breedlove, M., Kohl, K. and Gonzales, M. (2009). Monitoring fine-sediment volume in the Colorado River ecosystem, Arizona; bathymetric survey techniques: U.S. Geological Survey Open-File Report 2009-1207, 33 p.
- Katopodis, C. (2005). Developing a toolkit for fish passage, ecological flow management and fish habitat works. *Journal of Hydraulic Research*. 43, 451–467.
- Katopodis, C. C. (2012). Ecohydraulic approaches in aquatic ecosystem: Integration of ecological and hydraulic aspects of fish habitat connectivity and Suitability. *Ecological Engineering*, 48, 1-7.
- Katopodis, C., and Gervais, R. (2012). Ecohydraulic analysis of fish fatigue data. *River Research and Applications*. 28, 444–456.
- Kemp, W. M., Boynton, W. R., Adolf, J. E., Boesch, D. F., Boicourt, W. C., Brush, G., ... and Stevenson, J. C. (2005). Eutrophication of Chesapeake Bay: historical trend and ecological interactions. *Marine Ecology Progress Series*, 303(21), 1-29.
- Kemp, P. S. (2012). Bridging the gap between fish behaviour, performance and hydrodynamics: an ecohydraulics approach to fish passage research. *River Research and Applications*, 28(4), 403-406.
- Kirmer, A., Tischew, S., Ozinga, W. A., Von Lampe, M., Baasch, A., and Van Groenendael, J. M. (2008). Importance of regional species pools and functional traits in colonization processes: predicting re-colonization after large-scale destruction of ecosystem. *Journal of Applied Ecology*, 45(5), 1523-1530.
- Knapp, R. A. (2005). Effects of nonnative fish and habitat characteristics on lentic herpetofauna in Yosemite National Park, USA. *Biological Conservation*, 121(2), 265-279.
- Knapp, R. A., Boiano, D. M., and Vredenburg, V. T. (2007). Removal of nonnative fish results in population expansion of a declining amphibian (mountain yellow-legged frog) (*Rana muscosa*). *Biological Conservation*, 135(1), 11-20.
- Koch F.G. and Flokstra C. (1981). Bed level computations for curved alluvial channels, XIXth Congress of the International Association for Hydraulic Research, New Delhi India.

- Korman, J., Yard, M., Walters, C., and Coggins, L. G. (2009). Effects of fish size, habitat, flow, and density on capture probabilities of age-0 Rainbow trout estimated from electrofishing at discrete sites in a large river. *Transactions of the American Fisheries Society*, 138(1), 58-75.
- Korman, J., Kaplinski, M, and Melis, T.S. (2010). Effects of high-flow experiments from Glen Canyon Dam on abundance, growth, and survival rate of early life stages of Rainbow trout in the Lees Ferry reach of the Colorado River: U.S. Geological Survey Open-File Report 2010-1034, 31p.
- Korman, J., Kaplinski, M., and Melis, T. S. (2011). Effects of fluctuating flows and a controlled flood on incubation success and early survival rate and growth of age-0 Rainbow trout in a large regulated river. *Transactions of the American Fisheries Society*, 140(2), 487-505.
- Korman, J., Martell, S. J., Walters, C. J., Makinster, A. S., Coggins, L. G., Yard, M. D., and Persons, W. R. (2012). Estimating recruitment dynamics and movement of Rainbow trout (*Oncorhynchus mykiss*) in the Colorado River in Grand Canyon using an integrated assessment model. *Canadian Journal of Fisheries and Aquatic Sciences*, 69(11), 1827-1849.
- Lambert, G. I., Jennings, S., Kaiser, M. J., Davies, T. W., and Hiddink, J. G. (2014). Quantifying recovery rates and resilience of seabed habitats impacted by bottom fishing. *Journal of Applied Ecology*.
- Lammert, M., and Allan, J. D. (1999). Assessing biotic integrity of streams: effects of scale in measuring the influence of land use/cover and habitat structure on fish and macroinvertebrates. *Environmental Management*, 23(2), 257-270.
- Lancaster, J., and Downes, B. J. (2010). Linking the hydraulic world of individual organisms to ecological processes: putting ecology into ecohydraulics. *River Research and Applications*, 26(4), 385-403.
- Lancaster, J., and Downes, B. J. (2010). Ecohydraulics needs to embrace ecology and sound science, and to avoid mathematical artefacts. *River research and applications*, 26(7), 921-929.
- Li, F., Cai, Q., Fu, X., and Liu, J. (2009). Construction of habitat suitability models (HSMs) for benthic macroinvertebrate and their applications to instream environmental flows: a case study in Xiangxi River of Three Gorges Reservoir region, China. *Progress in Natural Science*, 19(3), 359-367.
- Li, H., Shen, D., Lai, J., Zhou, J., and Gong, Q. (2012) Aquatic Ecosystem Impact Assessment Report for Da-Wei power plant building in Jiao-Mu River (unpublished report, in Chinese).
- Ligon, F. K., Dietrich, W. E., and Trush, W. J. (1995). Downstream ecological effects of dams. *BioScience*, 183-192.
- Liu, F. Y., Zhang, Z. X., Wang, X. Q., Li, K., Sun, Y., and Zhang, C. (2011). Effects of habitat heterogeneity on early growth of *Quercus franchetii* natural regeneration seedlings in the Jinsha River Dry-hot Valley. *Chinese Journal of Applied & Environmental Biology*, 17(3), 338-344.

- Loranger, E. J., and Kenner, S. (2005). Comparison of One-and Two Dimensional Hydraulic Habitat Models for Simulation of Trout Stream Habitat (Doctoral dissertation, South Dakota School of Mines and Technology, Rapid City).
- Lower Colorado River Multi-Species Conservation Program. (2008). Lower Colorado River Multi-Species Conservation Program Draft Final Science Strategy. Bureau of Reclamation, Lower Colorado Region, Boulder City, NV.
- Lucchitta, Ivo. (1994). Topographic map of the Lees Ferry area, Arizona: U.S. Geological Survey Open-File Report, M (200) R29o no.94-411.
- Magirl, C. S., Breedlove, M. J., Webb, R. H. and Griffiths, P. G. (2008). Modeling Water-Surface Elevations and Virtual Shorelines for the Colorado River in Grand Canyon, Arizona. U.S. Geological Survey Open-File Report: 2008-5075.
- Maki-Petäys, A., Muotka, T., Huusko, A., Tikkanen, P., and Kreivi, P. (1997). Seasonal changes in habitat use and preference by juvenile Brown trout, *Salmo trutta*, in a northern boreal river. *Canadian Journal of Fisheries and Aquatic Sciences*, 54(3), 520-530.
- Makinster, A. S., Persons, W. R., Avery, L. A. and Bunch, A. J. (2010). Colorado River fish monitoring in Grand Canyon, Arizona; 2000 to 2009 summary: U.S. Geological Survey Open-File Report. 2010-1246, 26 p.
- Makinster, A. S., Persons, W. R. and Avery, L. A. (2011). Status and trend of the Rainbow trout population in the Lees Ferry reach of the Colorado River downstream from Glen Canyon Dam, Arizona, 1991–2009: U.S. Geological Survey Scientific Investigations Report 2011–5015, 17 p.
- McAda, C. W. (1977). Aspects of the life history of three catostomids native to the upper Colorado River basin. M.S. Thesis. Utah State University, Logan. 116 p.
- McAda, C.W., and Wydoski, R.S. (1985). Growth and reproduction of the Flannelmouth sucker, *Catostomus latipinnis* in the upper Colorado River Basin 1975-76. *Great Basin Naturalist* 45:281-286.
- McKinney, T., Persons, W.R. and Rogers, R.S. (1999). Ecology of Flannelmouth sucker in the Lee's Ferry tailwater, Colorado River, Arizona. *Great Basin Naturalist* 59:259-265.
- McMahon, T. E., Terrell, J. W., and Nelson, P. C. (1984). Habitat suitability information: walleye. FWS/OBS (USA).
- Melis, T.S., R.H. Webb, P.G. Griffiths, and Wise, T.J. (1994). Magnitude and frequency data for historic debris flows in Grand Canyon National Park and vicinity, Arizona, U.S. Geological Survey Water Resources Investigations Report 94-4214. 285 p.
- Melis, T. S. (2011). Effects of three high-flow experiments on the Colorado River ecosystem downstream from Glen Canyon Dam, Arizona: U.S. Geological Survey Circular 1366, 147p.
- Melis, T. S., Korman, J., and Kennedy, T. A. (2012). Abiotic & biotic responses of the Colorado River to controlled floods at Glen Canyon Dam, Arizona, USA. *River Research and Applications*, 28(6), 764-776.
- Mendel, J. (1995). Fuzzy logic systems for engineering: a tutorial. *Proceedings of the IEEE*, 83(3):345-377.

- Meyer-Peter, E., and Müller, R. (1948). Formulas for bed-load transport. In Proceedings of the 2nd Meeting of the International Association for Hydraulic Structures Research (pp. 39-64).
- Milhous, R. T., Wegner, D. L., and Waddle, T. (1984). 'User's guide to the Physical Habitat Simulation System (PHABSIM)', U.S. Fish and Wildlife Service, Instream Flow Info. Pap., 11, FWS/OBS-81/43, Washington, D.C.
- Milhous, R. T., Updike, M. A., Schneider, D. M. (1989). Physical Habitat simulation system reference Manual; Version II, Instream Flow information paper No. 26; US Fish and wildlife service, Biological Report 89(16).
- Miller, S. W., Budy, P., and Schmidt, J. C. (2010). Quantifying Macroinvertebrate Responses to In-Stream Habitat Restoration: Applications of Meta-Analysis to River Restoration. *Restoration Ecology*, 18(1), 8-19.
- Mistak, J. L., and Stille, D. A. (2008). Regional Hydraulic Geometry Curve for the Upper Menominee River. Michigan department of natural resources fisheries division. pp 21.
- Mitsch, W. J. (2012). What is ecological engineering? *Ecological Engineering*, 45, 5-12.
- Moir, H. J., Gibbins, C. N., Soulsby, C., and Youngson, A. F. (2005). PHABSIM modelling of Atlantic salmon spawning habitat in an upland stream: testing the influence of habitat suitability indices on model output. *River research and applications*, 21(9), 1021-1034.
- Morris, W.F., and Doak, D.F., (2002). *Quantitative Conservation Biology: The Theory and Practice of Population Viability Analysis*. Sinauer Associates, Sunderland, USA.
- Mouton, A. M., Schneider, M., Depestele, J., Goethals, P. L., and De Pauw, N. (2007): Fish habitat modelling as a tool for river management. *Ecological engineering*, 29(3), 305-315.
- Mouton, A. M., Schneider, M., Peter, A., Holzer, G., Müller, R., Goethals, P. L., and De Pauw, N. (2008). Optimization of a fuzzy physical habitat model for spawning European grayling (*Thymallus thymallus* L.) in the Aare river (Thun, Switzerland). *Ecological modelling*, 215(1), 122-132.
- Mouton, A. M., De Baets, B., and Goethals, P. L. (2009). Knowledge-based versus data-driven fuzzy habitat suitability models for river management. *Environmental Modelling & Software*, 24(8), 982-993.
- Mouton, A. M., Alcaraz-Hernández, J. D., De Baets, B., Goethals, P. L., and Martínez-Capel, F. (2011). Data-driven fuzzy habitat suitability models for brown trout in Spanish Mediterranean rivers. *Environmental Modelling & Software*, 26(5), 615-622.
- Mueller, G. A., and Wydoski, R. (2004). Reintroduction of the Flannelmouth sucker in the lower Colorado River. *North American Journal of Fisheries Management*. 24:41-46.
- Mueller, G. A., and Marsh, P. C. (2002). Lost, a desert and its native fish: A historical perspective of the lower Colorado River. Information and Technology Report USGS/BRD/ITR— 2002-0010. U.S. Government Printing Office, Denver, Colorado, 69 p.

- Murdoch, W. W., McCauley, E., Nisbet, R. M., Gurney, S. C., and Roos, A. M. (1992). *Individula-based models: combining testability and generality*. New York, pp.18-35.
- Nagaya, T., Shiraishi, Y., Onitsuka, K., Higashino, M., Takami, T., Otsuka, N., Akiyama, J., and Ozeki, H. (2008). Evaluation of suitable hydraulic conditions for spawning of Ayu with horizontal 2D numerical simulation and PHABSIM. *Ecological modelling*, 215(1), 133-143.
- Naghibi, A., and Lence, B. (2012). Assessing impacts of high flow events on fish population: Evaluation of risk-based performance measures. *Ecological Modelling*, 240, 16-28.
- Nykänen, M., Huusko, A., and Mäki - Petäys, A. (2001). Seasonal changes in the habitat use and movements of adult European grayling in a large subarctic river. *Journal of Fish Biology*, 58(2), 506-519.
- Nykänen, M., and Huusko, A. (2004). Transferability of habitat preference criteria for larval European grayling (*Thymallus thymallus*). *Canadian Journal of Fisheries and Aquatic Sciences*, 61(2), 185-192.
- Nelson, P. C. (1984). Suitability index curves for use in the instream flow incremental methodology, a handy pocket guide. Instream Flow and Aquatics Systems Group, Western Energy and Land Use Team, US Fish and Wildlife Service.
- Newson, M. D., and Newson, C. L. (2000). Geomorphology, ecology and river channel habitat: mesoscale approaches to basin-scale challenges. *Progress in Physical Geography*, 24(2), 195-217.
- Nestler, J. M., Goodwin, R. A., Smith, D. L., and Anderson, J. J. (2008). A mathematical and conceptual framework for ecohydraulics. *Hydroecology and ecohydrology: Past, present and future*.
- Nielsen, P. (1992). *Coastal Bottom Boundary Layers and Sediment Transport*. World Scientific, Vol 4
- Nilsson, C., and Berggren, K. (2000). Alterations of Riparian Ecosystem Caused by River Regulation Dam operations have caused global-scale ecological changes in riparian ecosystem. How to protect river environments and human needs of rivers remains one of the most important questions of our time. *Bio Science*, 50(9), 783-792.
- Nuhfer, A. J. (1988). A comparison of growth of brown trout from selected western rivers with growth of brown trout from Michigan rivers. Michigan Department of Natural Resources. Fisheries Division, Technical Report, 88-6.
- Noonan, M. J., Grant, J. W., and Jackson, C. D. (2012). A quantitative assessment of fish passage efficiency. *Fish and Fisheries*, 13(4), 450-464.
- Olaya-Marín, E. J., Martínez-Capel, F., Soares Costa, R. M., and Alcaraz-Hernández, J. D. (2012). Modelling native fish richness to evaluate the effects of hydromorphological changes and river restoration (Júcar River Basin, Spain). *Science of the Total Environment*, 440, 95-105.

- Økland, F., Jonsson, B., Jensen, A. J., and Hansen, L. P. (1993). Is there a threshold size regulating seaward migration of Brown trout and Atlantic salmon? *Journal of Fish Biology*, 42(4), 541-550.
- Palinkas, C. M. (2013). Seasonal and interannual patterns of sedimentation in the Corsica River (MD): Evaluating the potential influence of watershed restoration. *Estuarine, Coastal and Shelf Science*, 127, 37-45.
- Palmer, M. A., Menninger, H. L., and Bernhardt, E. (2010). River restoration, habitat heterogeneity and biodiversity: a failure of theory or practice? *Freshwater biology*, 55(s1), 205-222.
- Panfil, M. S. and Jacobson R. B. (1999). Hydraulic modeling of in-channel habitats in the Ozark Highlands of Missouri: Assessment of habitat sensitivity to environmental change. US Geological Survey, Columbia Environmental Research Center. <http://www.cerc.usgs.gov/rss/rfmodel/> (Accessed in 11.02.2015).
- Panfil, M. S., and Jacobson, R. B. (2000). Hydraulic modeling of in-channel habitats in the Ozark Highlands of Missouri: Assessment of physical habitat sensitivity to environmental change, U.S. Geological Survey, Columbia Environmental Research Center website at <http://www.cerc.usgs.gov/rss/rfmodel/>, (Accessed in 28.05.2014).
- Parasiewicz, P. (2001). MesoHABSIM: A concept for application of instream flow models in river restoration planning. *Fisheries*, 26(9), 6-13.
- Parasiewicz, P. (2003). "Upscaling: integrating habitat model into river management." *Canadian Water Resources Journal* 28.2: 283-299.
- Parasiewicz, P. (2007). "The MesoHABSIM model revisited." *River Research and Applications* 23.8: 893-903.
- Peck, M. A., and Hufnagl, M. (2012). Can IBMs tell us why most larvae die in the sea? Model sensitivities and scenarios reveal research needs. *Journal of Marine Systems*, 93, 77-93.
- Piegorsch, W. W., Weinberg, C. R., and Taylor, J. A. (1994). Non-hierarchical logistic models and case-only designs for assessing susceptibility in population-based case-control studies. *Statistics in medicine*, 13(2), 153-162.
- Qin, B. (2001). Approaches to mechanisms and control of eutrophication of shallow lakes in the middle and lower reaches of the Yangze River. *Journal of Lake Sciences*, 14(3), 193-202.
- Raleigh, R. F., T. Hickman, R. C. Solomon, and P. C. Nelson. (1984). Habitat suitability information: Rainbow trout. U.S. Fish Wildl. Servo FWS/OBS-82/10.60. 64 pp.
- Raleigh, R. F., L. D. Zuckerman, and P. C. Nelson. (1986). Habitat suitability index models and instream flow suitability curves: Brown trout, revised. U.S. Fish Wildl. Servo Biol. Rep. 82(10.124). 65 pp. [First printed as: FWS/OBS-82/10.71, September 1984].
- Rapport, D. J., Costanza, R., and McMichael, A. J. (1998). Assessing ecosystem health. *Trend in Ecology & Evolution*, 13(10), 397-402.
- Rashleigh, B., Barber, M. C., Cyterski, M. J., Johnston, J. M., Parmar, R., and Mohamoud, Y. (2004). Population models for stream fish response to habitat and hydrologic

alteration: the CVI Watershed Tool. Research Triangle Park (NC): USEPA. EPA/600/R-04/190.

Reid, H. E., Brierley, G. J., and Boothroyd, I. K. G. (2010). Influence of bed heterogeneity and habitat type on macroinvertebrate uptake in peri-urban streams. *International Journal of Sediment Research*, 25(3), 203-220.

Renshaw, E. (Ed.). (1993). *Modelling biological population in space and time* (Vol. 11). Cambridge University Press.

Riadh A., Cedric G., and Jean M. H. (2014) Telemac modeling system: 2d hydrodynamics telemac-2d software release 7.0 User manual. R&D, Electricite de France, Paris, 134.

Retout, S., Mentré, F., and Bruno, R. (2002). Fisher information matrix for non-linear mixed-effects models: evaluation and application for optimal design of enoxaparin population pharmacokinetics. *Statistics in medicine*, 21(18), 2623-2639.

Rice, S. P., Little, S., Wood, P. J., Moir, H. J., and Vericat, D. (2010). The relative contributions of ecology and hydraulics to ecohydraulics. *River Research and Applications*, 26(4), 363-366.

Rijn, L. C. V. (1984b). Sediment transport, part II: suspended load transport. *Journal of hydraulic engineering*, 110(11), 1613-1641.

Robson, D. S., and Chapman, D. G. (1961). Catch curves and mortality rates. *Transactions of the American Fisheries Society*, 90(2), 181-189.

Robinson, A.T., R.W. Clarkson, and R.E. Forrest. (1998). Dispersal of larval fish in a regulated river tributary. *Transactions of the American Fisheries Society*. 127:772-786.

Robins, P. E., and Davies, A. G. (2011). Application of Telemac-2D and Sisyphe to complex estuarine regions to inform future management decisions. XVIIIth Telemac & Mascaret User Club Chatou, France, 19-21.

Rodi, W. (1993). *Turbulence models and their application in hydraulics*. CRC Press.

Russ, G. R., and Alcala, A. C. (2004): Marine reserves: long-term protection is required for full recovery of predatory fish population. *Oecologia*, 138(4), 622-627.

Rutschmann, P., Bui, M. D., Abdelaziz, S., Yao, W., Rutschmann, B., and Geiger, F. (2014). Ökologische Modellierungen–drei Fallbeispiele. 37th Dresdner Wasserbaukolloquium.

Ryden, D. W. (2005). Long-term monitoring of sub-adult and adult large-bodied fish in the San Juan River: 2004. San Juan River Basin Recovery Implementation Program, U.S. Fish and Wildlife Service, Albuquerque, New Mexico.

Schaefer, M. B. (1954). Some aspects of the dynamics of population important to the management of the commercial marine fisheries. *Inter-American Tropical Tuna Commission Bulletin*, 1(2), 23-56.

Schneider, M., Noack, M., Gebler, T., and Kopecki, L. (2010). Handbook for the habitat simulation model CASiMiR. Module CASiMiR-Fish. Base version. SJE–Schneider & Jorde Ecological Engineering GmbH. LWW–Institut für Wasserbau, Universität Stuttgart.

- Sempeski, P., and Gaudin, P. (1995). Habitat selection by grayling - II. Preliminary results on larval and juvenile daytime habitats. *Journal of Fish Biology*, 47(2), 345-349.
- Shepherd, J. J., and Stojkov, L. (2007): The logistic population model with slowly varying carrying capacity. *ANZIAM Journal*, 47, C492-C506.
- Silva, A. T., Santos, J. M., Ferreira, M. T., Pinheiro, A. N., and Katopodis, C. (2011). Effects of water velocity and turbulence on the behaviour of Iberian barbel (*Luciobarbus bocagei*, Steindachner 1864) in an experimental pool-type fish way. *River research and applications*, 27(3), 360-373.
- Snyder, D.E., R.T. Muth, and C.L. Bjork. (2004). Catostomid fish larvae and early juveniles of the upper Colorado River basin-morphological descriptions, comparisons, and computer-interactive key. Contribution 139 of the Larval Fish Laboratory, Colorado State University. Technical Publication No. 42, Colorado Division of Wildlife, Fort Collins, Colorado.
- Spence, R., and Hickley, P. (2000). The use of PHABSIM in the management of water resources and fisheries in England and Wales. *Ecological Engineering*, 16(1), 153-158.
- Steeb, W. H. (2011). *The nonlinear workbook: chaos, fractals, cellular automata, neural networks, genetic algorithms, gene expression programming, support vector machine, wavelets, hidden Markov models, fuzzy logic with C++, Java and SymbolicC++ programs*. World Scientific.
- Steffler, P. and Blackburn J., (2002). *River2D Two-Dimensional Depth Averaged Model of River Hydrodynamics and Fish Habitat. Introduction to Depth Averaged Modeling and User's Manual*. University of Albert, Canada, P120.
- Stewardson, M., I. Rutherford, P. Cottingham, and E. S. G. Schreiber. (2002). Evaluating the effectiveness of stream habitat reconstruction in the Murray Darling Basin. Final report of MDBC Project R10008, Stage 1. Murray Darling Basin Commission, Canberra, Australia.
- Stohlgren, T.J., P. Ma, S. Kumar, M. Rocca, J.T. Morissette, C.S. Jarnevich, and N. Benson. (2010). Ensemble habitat mapping of invasive plant species. *Risk Analysis* 30(2): 224-235.
- Talbert, C. B. and Talbert, M. K. (2012). *User Manual for SAHM package for VisTrails*. Fort Collins, CO: US Geological Survey, Fort Collins Science Center. 72 p.
- Tassi P., Villaret C. (2014). *Sisyphé V6.3 User's Manual*. R&D, Electricite de France, Paris, 76.
- Te Chow, V. (1959). *Open channel hydraulics*.
- Tomsic, C. A., Granata, T. C., Murphy, R. P., and Livchak, C. J. (2007). Using a coupled eco-hydrodynamic model to predict habitat for target species following dam removal. *Ecological Engineering*, 30(3), 215-230.
- Tyus, H. M., Burdick, B. D., Valdez, R. A., Haynes, C. M., Lytle, T. A., and Berry, C. R. (1982). *Fish of the upper Colorado River basin: distribution, abundance, and status. Fish of the upper Colorado River system: present and future*. Western Division, American Fisheries Society, Bethesda, Maryland, 12-70.

- Tyus, H. M. (1989). Habitat use and streamflow needs of rare and endangered fish, Yampa River, Colorado (No. FWS-89/14). Fish and wildlife service vernal UT.
- USFWS (U.S. Fish and Wildlife Service) (1980). Habitat as a basis for environmental assessment. USFWS, Report 101 ESM, Fort Collins, CO.
- Usher, P. J. (2000). Traditional ecological knowledge in environmental assessment and management. *Arctic*, 183-193.
- Valdez, R. A., Holden, P. B., and Hardy, T. B. (1990). Habitat Suitability Index Curves for Humpback Chub of the Upper Colorado River Basin. *Rivers*, 1(1.), 31-42.
- Valdez, R. A. (1990). The endangered fish of Cataract Canyon. Final Report of Bio/West, Inc., Logan, Utah, to US Bureau of Reclamation, Salt Lake City, Utah.
- Van Rijn, L. C. (1984). Sediment transport, part I: bed load transport. *Journal of hydraulic engineering*, 110(10), 1431-1456.
- Van Rijn, L. C. (1993). Principles of sediment transport in rivers, estuaries and coastal seas (Vol. 1006). Amsterdam: Aqua publications.
- Vanicek, C. D., R.H. Kramer, and Franklin, D.R. (1970). Distribution of Green River fish in Utah and Colorado following closure of Flaming Gorge Dam. *Southwestern Naturalist* 14:297-315.
- Vaughan, I. P., Diamond, M., Gurnell, A. M., Hall, K. A., Jenkins, A., Milner, N. J., ... and Ormerod, S. J. (2009). Integrating ecology with hydromorphology: a priority for river science and management. *Aquatic Conservation: Marine and Freshwater Ecosystem*, 19(1), 113.
- Verhulst, P.F., 1838. Notice sur la loi que la population suit dans son accroissement. *Correspondance Mathématique et Physique*, 10, 113-117.
- Waddle, T. (2001). PHABSIM for Windows user's manual and exercises (No. 2001-340, pp. 0-288).
- Wampler P. L. (1985). Habitat preference curves for hatchery-reared juvenile fall Chinook salmon in a small western Washington stream. U.S. Fish and Wildlife service fisheries assistant office Olympia, WA.
- Wang, F., and Lin, B. (2013). Modelling habitat suitability for fish in the fluvial and lacustrine regions of a new Eco-City. *Ecological Modelling*, 267, 115-126.
- Wang J., and Liang, Y.L. (2005). Explore the Wu-chang Lake silver carp and bighead carp fingerlings stocking production potential and estimated production of phytoplankton with Fisheries Technology, 5 (4), 343-350.
- Wang, Y., and Xia, Z. (2009). Assessing spawning ground hydraulic suitability for Chinese sturgeon (*Acipenser sinensis*) from horizontal mean vorticity in Yangtze River. *Ecological Modelling*, 220(11), 1443-1448.
- Wang, Z., Lee, J. H., and Xu, M. (2013). Eco-hydraulics and eco-sedimentation studies in China. *Journal of hydraulic research*, 51(1), 19-32.

- Webb, R. H., P. T. Pringle, and Rink, G.R. (1989). Debris flows from tributaries of the Colorado River, Grand Canyon National Park, Arizona, U.S. Geological Survey Professional Paper 1492.
- Webb, R. H. (1996). *Grand Canyon, a Century of Change*, University of Arizona Press, Tucson.
- Weiss, S.J., Otis, E.O. and Maughan, O.E. (1998). Spawning ecology of Flannelmouth sucker, *Catostomus latipinnis* (Catostomidae), in two small tributaries of the lower Colorado River. *Environmental Biology of Fish* 52:419-433.
- Wen, X., Xi, Y., Zhang, L., and Lu, X. (2006). Analysis of community structure of Rotifera and ecological assessment of water quality in Lake Jinghu, Wuhu city. *Acta hydrobiologica sinica/Shuisheng Shengwu Xuebao*, 30(2), 152-158.
- Wheaton, J. M., Pasternack, G. B., and Merz, J. E. (2004). Spawning habitat rehabilitation-II. Using hypothesis development and testing in design, Mokelumne river, California, USA. *International Journal of River Basin Management*, 2(1), 21-37.
- White, G. C., and Burnham, K. P. (1999). Program MARK: survival estimation from population of marked animals. *Bird study*, 46(S1), S120-S139.
- Wilcock, P. R., and Crowe, J. C. (2003). Surface-based transport model for mixed-size sediment. *Journal of Hydraulic Engineering*, 129(2), 120-128.
- Willard, B. E., and Marr, J. W. (1970). Effects of human activities on alpine tundra ecosystem in Rocky Mountain National Park, Colorado. *Biological Conservation*, 2(4), 257-265.
- Wu, W., Rodi, W., and Wenka, T. (2000). 3D numerical modeling of flow and sediment transport in open channels. *Journal of Hydraulic Engineering*. 126(1), 4-15.
- Wu, R., and Mao, C. (2007). The assessment of river ecology and habitat using a two-dimensional hydrodynamic and habitat model. *Journal of Marine Science and Technology*, 15(4), 322-330.
- Wu, W. (2008). *Computational river dynamics*. CRC Press.
- Wu W. (2014) Stream fish habitat suitability. (<http://adweb.clarkson.edu/~wwu/topics.Html>) (accessed 5th May, 2015)
- Weiss, S.J., Otis, E.O. and Maughan, O.E. (1998). Spawning ecology of Flannelmouth sucker, *Catostomus latipinnis* (Catostomidae), in two small tributaries of the lower Colorado River. *Environmental Biology of Fish* 52:419-433.
- Xie, S., Cui, Y., Zhang, T., Fang, R., and Li, Z. (2000). The spatial pattern of the small fish community in the Biandantang Lake—a small shallow lake along the middle reach of the Yangtze River, China. *Environmental Biology of Fish*, 57(2), 179-190.
- Yao, W., Bui, M.D. and Rutschmann, P. (2014). Application of habitat and population modeling in river management. – In *Internationales Symposium Wasser- und Flussbau im Alpenraum 25.-27. in Zürich*. Veranstalter: Versuchsanstalt für Wasserbau, Hydrologie und Glaziologie (VAW), ETH Zürich. In Zusammenarbeit mit: Institut für Wasserbau und Wasserwirtschaft, Technische Universität Graz und Lehrstuhl und Versuchsanstalt für Wasserbau und Wasserwirtschaft, Technische Universität München.

Hrsg.: R.M. Boes. Zürich: VAW, ETH Zürich, S. 207 – 216, (Band 1: VAW-Mitteilungen; 227).

Yi, Y., Yang, Z., and Zhang, S. (2010). Ecological influence of dam construction and river-lake connectivity on migration fish habitat in the Yangtze River basin, China. *Procedia Environmental Sciences*, 2, 1942-1954.

Yi, Y., Wang, Z. and Yang, Z. (2010). Effects of High-Flow. Two-dimensional habitat modeling of Chinese sturgeon spawning sites. *Ecological Modelling*, 221(5), 864-875.

Zadeh, L. A. (1965). Information and control, Fuzzy sets. 8(3), 338-353.

Zhang, J., Mauzerall, D. L., Zhu, T., Liang, S., Ezzati, M., and Remais, J. V. (2010). Environmental health in China: progress towards clean air and safe water. *The Lancet*, 375(9720), 1110-1119.

Zhong, Y., and Power, G. (1996). Environmental impacts of hydroelectric projects on fish resources in China. *Regulated Rivers: Research & Management*, 12(1), 81-98.

Zhou, J., Zhao, Y., Song, L., Bi, S., and Zhang, H. (2014). Assessing the effect of the Three Gorges reservoir impoundment on spawning habitat suitability of Chinese sturgeon (*Acipenser sinensis*) in Yangtze River, China. *Ecological Informatics*, 20, 33-46.

Zhu G. (2008). The Taihu Lake eutrophication problem and the solution for it. *Lake science* 20(1), 21-26 (In Chinese).

Zyserman, J. A., and Fredsøe, J. (1994). Data analysis of bed concentration of suspended sediment. *Journal of Hydraulic Engineering*, 120(9), 1021-1042.

Notations

The following symbols are used in this dissertation:

a, b	Emperical parameters for the matrix population model.
B	The ratio between the ripple roughness and water depth
B_G	The mean phytoplankton density in the river
B_{zp}	The mean zooplankton density in the river
B_{zb}	The mean zoobenthos density in the river
c	The fish utilization rate for phytoplankton, zooplankton, or zoo-benthos
C	Suspending sediment concentration
C_f	Bottom friction
C_f'	The bottom friction used in the hydromorphology model
C_h	Chezy coefficient
C_r	Quadratic friction
C_{eq}	Suspended load mass concentration at reference lever under equilibrium conditions
C_{ref}	Suspended load concentration at reference lever
C_{veq}	Suspended load volume concentration at reference lever under equilibrium conditions
D	Particle size parameter
D^*	Non dimensional particle size parameter
D_{50}	Particle size parameter in 50 percent
E	The suspension rate
E-D	The net exchange of sediment between suspended load and bed-load layer
F	The ratio between the reference and depth-average concentration
F_T	Fish stocking weight supported by the river system
F_p	Fish stocking weight supported by river algae
F_a	Fish stocking weight supported by river zooplankton
F_s	Fish stocking weight supported by riverbed substrates materials
f_{cor}	The Coriolis parameter
$F_{i,t}$	Birth rate of for spawning fish at time t.
$f_{i,t}$	Basic birth rate of at time t for the stage of i.
g	Gravitational acceleration
h	Water depth
K_r	The ripple roughness
k	The fish preference for the specific fish food types
K_s	Strickler coefficient
K_s'	Grain roughness
n	Manning efficient.
$N_{i,t}$	Fish number at time t for stage i.
$N_{i,t+\Delta t}$	Fish number at time t+ Δt for stage i.
$NL_{i,t}, NL_{i,t+1}$	Fish numbers at time for t and t+ Δt for the i fish stage
p	The non-cohesive bed porosity
P/B	The ratio between total output and fish food density
P_h	The turbulent kinetic energy

$P_{kv}, P_{\varepsilon v}$	Production of k and ε respectively due to vertical velocity gradients particularly near the bottom.
$P_t^F, P_{t+\Delta t}^F$	Population numbers at time t and $t+\Delta t$
Q_b	Bed-load
R	Rouse number
r_h	Hydraulic radius
$s, \rho_s/\rho_0$	The relative density
$S_{i,t}$	Model survival rate at time t .
$S_{i,t}$	Basic survival rate at time t for the stage of i
S_t	Nikuradse bed roughness
S_t	Prandtl/Schmidt number
t	Time
T	The non-dimensional excess bed shear stress or called transport stage number
u^*	Bed shear velocity
U^*	The effective bed shear velocity related to grain roughness
U^*_{cr}	The critical bed shear velocity for sediment incipient motion
u, v	Depth average velocity components in x and y directions respectively
V	The river water volume
x, y	Horizontal space coordinates
Z_t	The bottom elevation

The following Greek symbols are used in this dissertation:

α, β	The empirical parameters in the logistic population model
$c_1, c_2, \sigma_k, \sigma_\varepsilon, \sigma_k$ and c_μ	Constant number
η	Water surface elevation
τ_{bx}, τ_{by}	Bed shear stresses
$\tau_{xx}, \tau_{xy}, \tau_{yx}, \tau_{yy}$	Depth-average Reynolds (turbulent) stresses
ρ_s	Sediment density
ρ_w	Water density
κ	Von Karman constant
ν_t	The eddy viscosity
ν_w	Water viscosity
ν_{tt}	Turbulence viscosity
e^*	The dimensionless diffusivity
θ'	Non-dimensional skin friction number/shields number
α	MPM parameter
ν	Viscosity of the water
u_*	Bed shear velocity
ε_t	Turbulence diffusivity scalar
μ	Bed form correction factor
w_s	Setting velocity

Abbreviations

The following abbreviations are used in this thesis

AVI	The volume percentage of sediment fraction j
B. D.	The river bed deformation
B-A	Brown trout adult life stage
B-F	Brown trout fry life stage
B-J	Brown trout juvenile life stage
B-S	Brown trout spawning life stage
C. F.	Caught fish number
CPUE	Mean catch per unit effort
D.	The downstream
E1, and E2	The scenario without consider hydromorphology model, and with consider hydromorphology model in Aare River
EAWAG	Swiss Federal Institute for Environmental Science and Technology
E. F. S.	The endemic fish species
F-A	Flannelmouth sucker adult life stage
F-F	Flannelmouth sucker fry life stage
F-J	Flannelmouth sucker juvenile life stage
F-S	Flannelmouth sucker spawning life stage
ISP, MSP, and LSP	The percentage of ideal, middle and unsuitable suitable habitat in the studied sites
M.	The middle stream
MPM	Meyer-Peter and Müller
N. L. P.	The national level protection
HSI	Habitat suitability index
O1, O2, O3, and O4	The computational option 1, 2, 3, and 4.
OSI	Overall suitability index
QN	Fish stocking number
P.D.	Fish population density
P.N.	Fish population number
R-A	Rainbow trout adult life stage
R-F	Rainbow trout fry life stage
R-J	Rainbow trout juvenile life stage
R-S	Rainbow trout spawning life stage
S. F.	Simulated fish number
S. L. P.	The states level protection
S. R.	Schizothorax (<i>Schizothorax</i>)
S. S.	Schizothorax (<i>Racoma</i>)
SI	Suitability index
U.	The upstream
USGS	U.S. Geological Survey
WUA	Weighted usable areas
S1, S2, S3, S3-2, and S3-3	Scenarios S1, S2, S3, S3-2, and S3-3 in Jiao-Mu River.
TW	The stocking fish weight

Appendix I:

The logistic population model:

$$\frac{dP}{dt} = rP\left(1 - \frac{P}{K}\right) \quad (\text{A-1})$$

Integrating the differential equation, first multiple K on both sides:

$$\frac{KdP}{dt} = rP(K - P) \quad (\text{A-2})$$

$$\frac{KdP}{P(K - P)} = rdt \quad (\text{A-3})$$

$$dP\left(\frac{1}{P} + \frac{1}{K - P}\right) = rdt \quad (\text{A-4})$$

$$\frac{dP}{P} + \frac{dP}{K - P} = rdt \quad (\text{A-5})$$

Do the integration on both side:

$$\int \frac{dP}{P} + \int \frac{dP}{K - P} = \int rdt \quad (\text{A-6})$$

Due to

$$\int \frac{dP}{P} = \text{Ln}P + C_1; \quad \int \frac{dP}{K - P} = -\text{Ln}(K - P) + C_2 \quad (\text{A-7})$$

The left side of equation (A-6) becomes:

$$\text{Ln}P - \text{Ln}(K - P) + C_3 = rt + C_4; \quad C_3 = C_1 + C_2 \quad (\text{A-8})$$

$$\text{Ln} \frac{P}{K - P} = rt + C_5; \quad C_5 = C_3 + C_4 \quad (\text{A-9})$$

$$e^{rt+C_5} = \frac{P}{K - P} \quad (\text{A-10})$$

$$P = Ke^{rt+C_5} - Pe^{rt+C_5} \quad (\text{A-11})$$

$$P = \frac{Ke^{rt+C_5}}{1 + e^{rt+C_5}} = \frac{K}{1 + Ce^{-rt}}; \quad C = e^{-C_5} \quad (\text{A-12})$$

Set $t=0$, $p=N_t$, then

$$C = \frac{K - N_t}{N_t} \quad (\text{A-13})$$

Introduce it into equation (A-12):

$$P = \frac{K}{1 + \left(\frac{K - N_t}{N_t}\right)e^{-rt}} = \frac{KN_t e^{rt}}{K + N_t(e^{rt} - 1)} \quad (\text{A-14})$$

In order to combine habitat model with population model, K is replaced by $\beta \times WUA$; rt is replaced by $\alpha \times (OSI_{t+\Delta t} - OSI_t)$, then the Equation (A-14) becomes:

$$P_{t+\Delta t} = \frac{\beta \times WUA_{t+\Delta t} \times P_t \times e^{\alpha \times (OSI_{t+\Delta t} - OSI_t)}}{\beta \times WUA_{t+\Delta t} + P_t \times \left(e^{\alpha \times (OSI_{t+\Delta t} - OSI_t)} - 1 \right)} \quad (\text{A-15})$$

In Equation (A-15), it should be noted that the α and β are the empirical parameters which are depended on the fish species and study areas. Further, if the Δt changed, the α and β are need update accordingly. In this dissertation, the α and β for different fish species models are listed in the following table:

Table I.1: The empirical parameters α and β for European grayling on two scenarios

Parameters	Without hydromorphology model				With hydromorphology model			
	E. G. 1	E. G. 2	E. G. 3	E. G. 4	E. G. 1	E. G. 2	E. G. 3	E. G. 4
α	7	7	2	3	8	8	7	7
β	6	2	4	1.6	7	3	15	15

Table I.2: The empirical parameters α and β for rainbow trout, brown trout, flannelmouth sucker, schizothorax (*Schizothorax*) and schizothorax (*Racoma*).

Parameters	R. T.	B. T.	F. S.	S. S.	S. R.
α	240	241	241	5	8
β	0.5	51	51	35	10

Where E. G. 1 is European grayling; R. T. is rainbow trout; B. T. is brown trout; F. S. is flannelmouth sucker; S. S. is schizothorax (*Schizothorax*); S. R. is schizothorax (*Racoma*).

Appendix II:

The comparison of ecohydraulic model and EAWAG report results

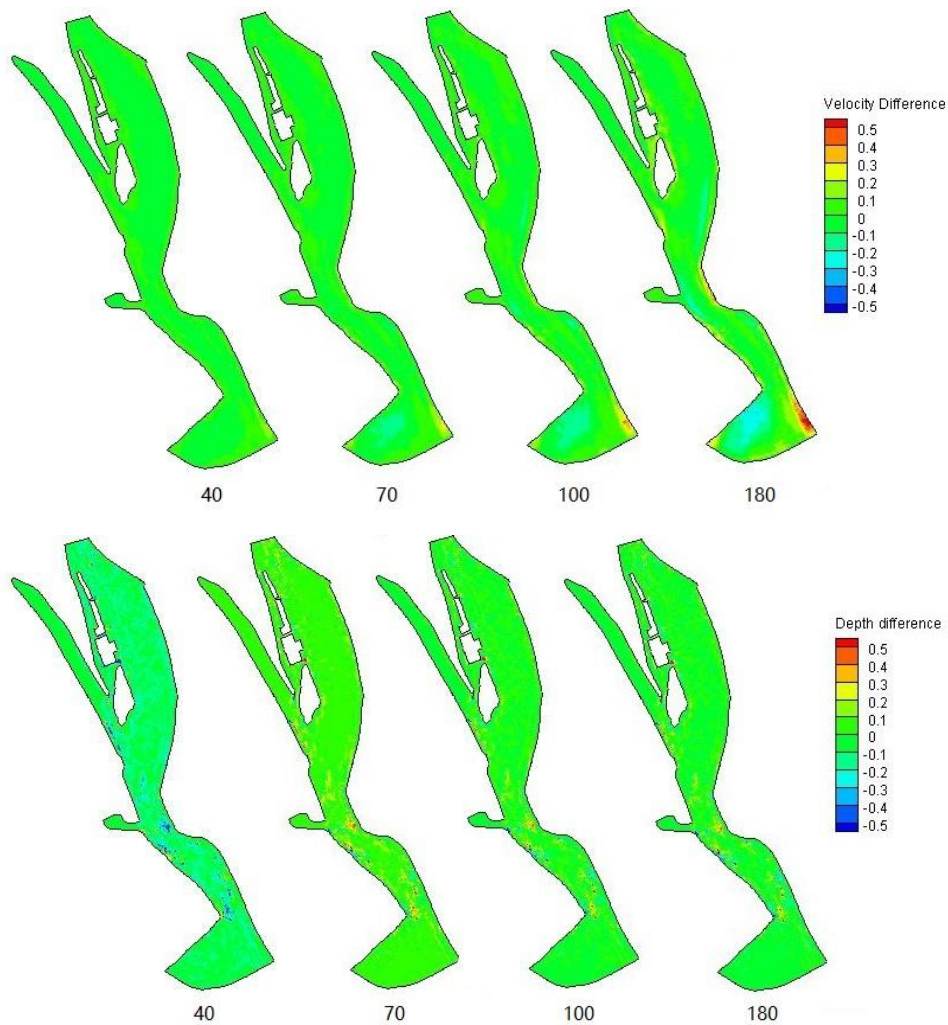


Figure II.1: Difference between the calculated hydraulic results and the data presented in the EAWAG report for different flow discharges (40 m³/s, 70 m³/s, 100 m³/s, and 180 m³/s).

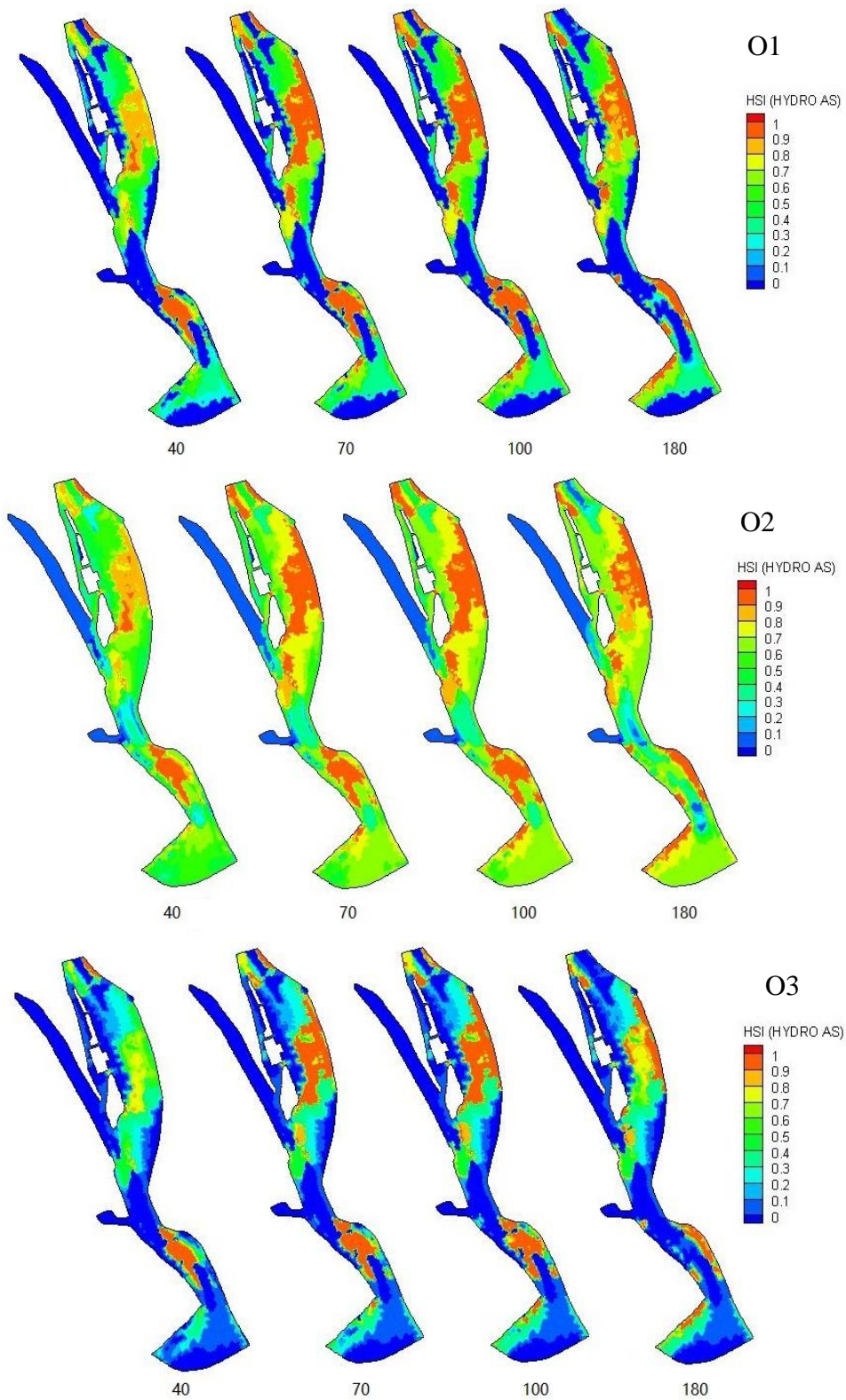


Figure II.2a: Habitat suitability index (HSI) based on HYDRO AS for 4 flow discharges (40 m³/s, 70 m³/s, 100 m³/s, 180 m³/s) using habitat computational options O1, O2, and O3.

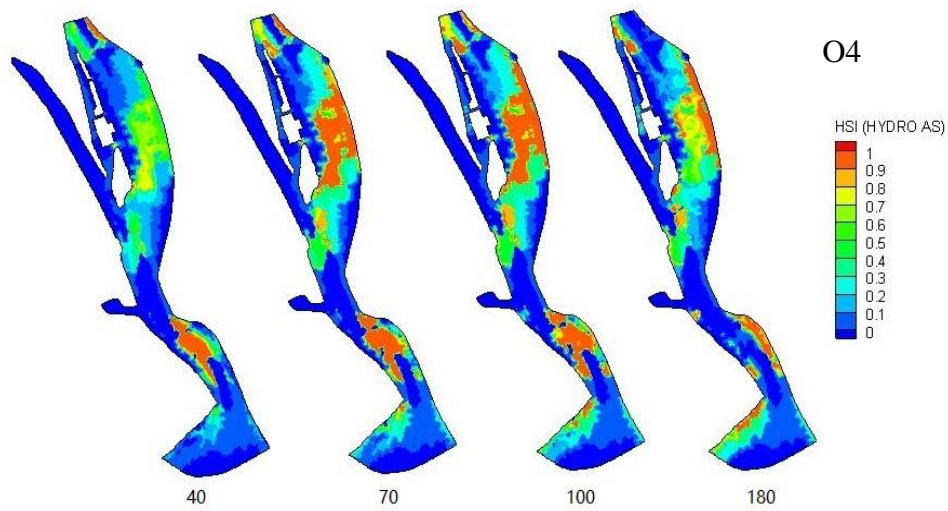


Figure II.2b: Habitat suitability index (HSI) based on HYDRO AS for 4 flow discharges ($40 \text{ m}^3/\text{s}$, $70 \text{ m}^3/\text{s}$, $100 \text{ m}^3/\text{s}$, $180 \text{ m}^3/\text{s}$) using habitat computational options O4.

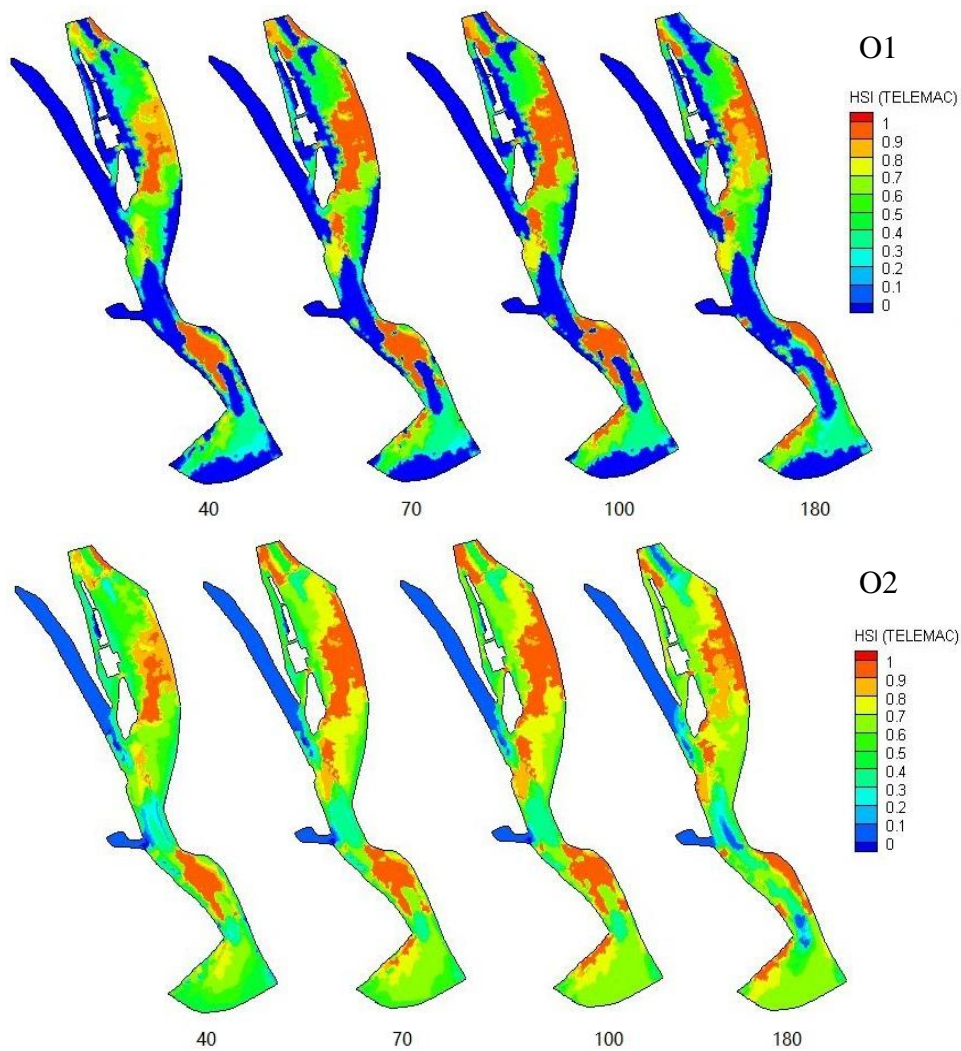


Figure II.3a: Habitat suitability index (HSI) based on TELEMAC for 4 flow discharges ($40 \text{ m}^3/\text{s}$, $70 \text{ m}^3/\text{s}$, $100 \text{ m}^3/\text{s}$, $180 \text{ m}^3/\text{s}$) using habitat computational options O1 and O2.

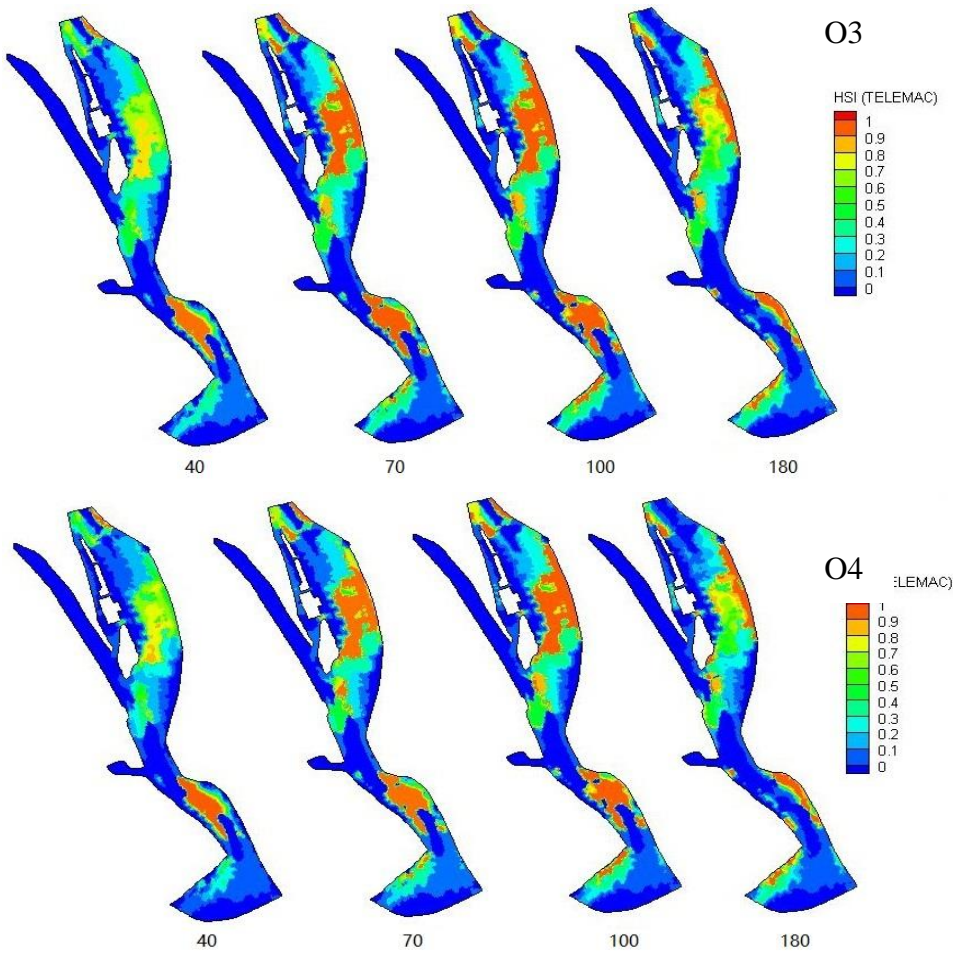


Figure II.3b: Habitat suitability index (HSI) based on TELEMAC for 4 flow discharges (40 m³/s, 70 m³/s, 100 m³/s, 180 m³/s) using habitat computational options O3 and O4.

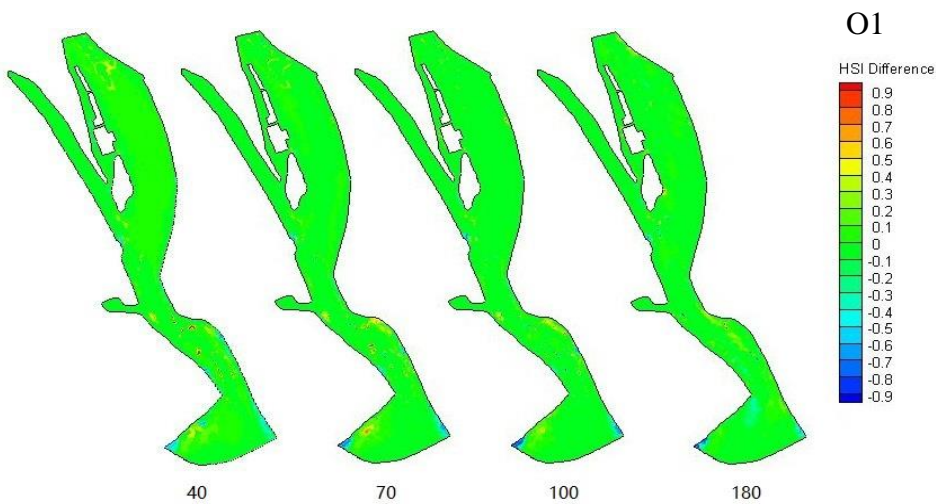


Figure II.4a: Habitat suitability index (HSI) difference for 4 flow discharges (40 m³/s, 70 m³/s, 100 m³/s, 180 m³/s) using habitat computational options O1.

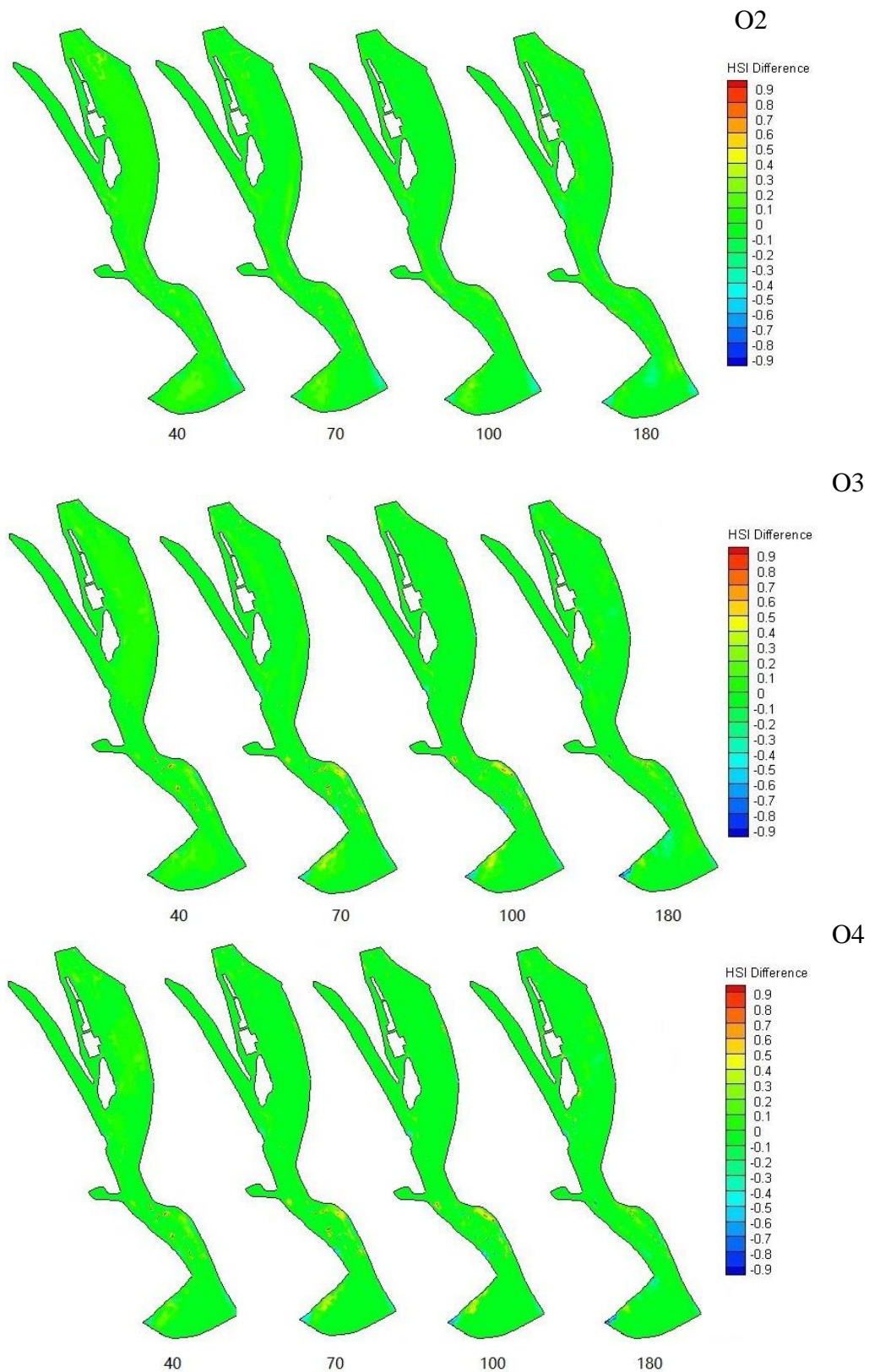


Figure II.4b: Habitat suitability index (HSI) difference for 4 flow discharges (40 m³/s, 70 m³/s, 100 m³/s, 180 m³/s) using habitat computational options O2, O3 and O4.

Appendix III:

The spawning European grayling HSI distribution and the European grayling population density distribution from 1970 to 2000 in four computational options O1, O2, O3, O4.

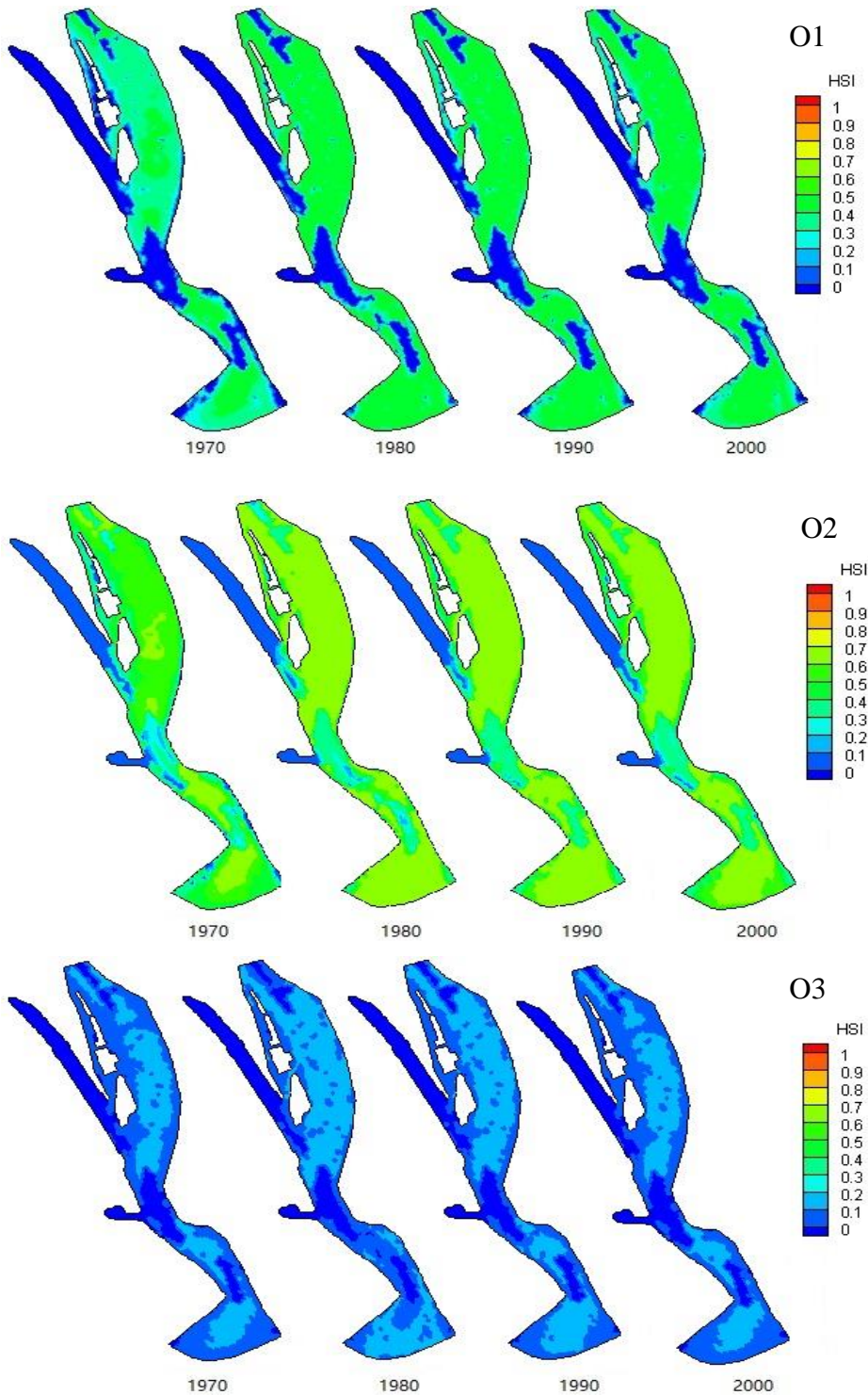


Figure III.1a: The HSI distribution at 1970, 1980, 1990 and 2000 under the scenario without considering hydromorphology (O1, O2, and O3 in scenario E1).

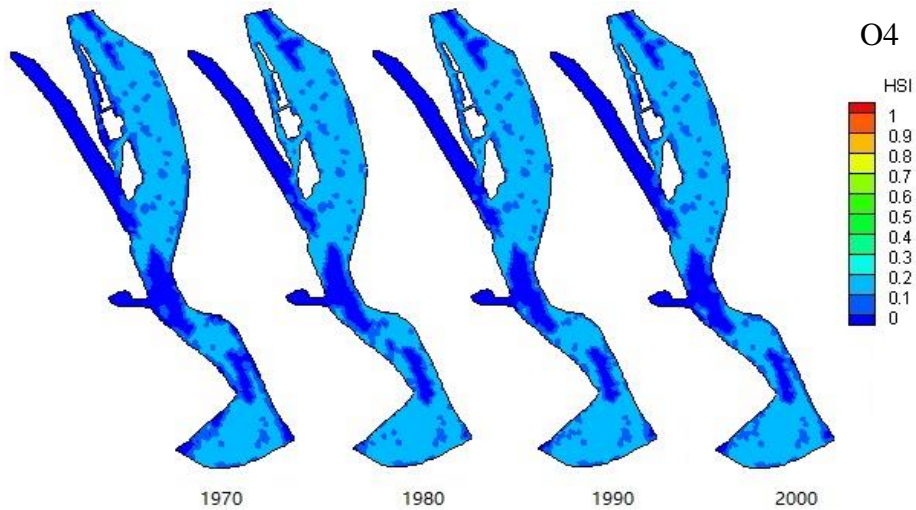


Figure III.1b: The HSI distribution at 1970, 1980, 1990 and 2000 under the scenario without considering hydromorphology (O4 in scenario E1).

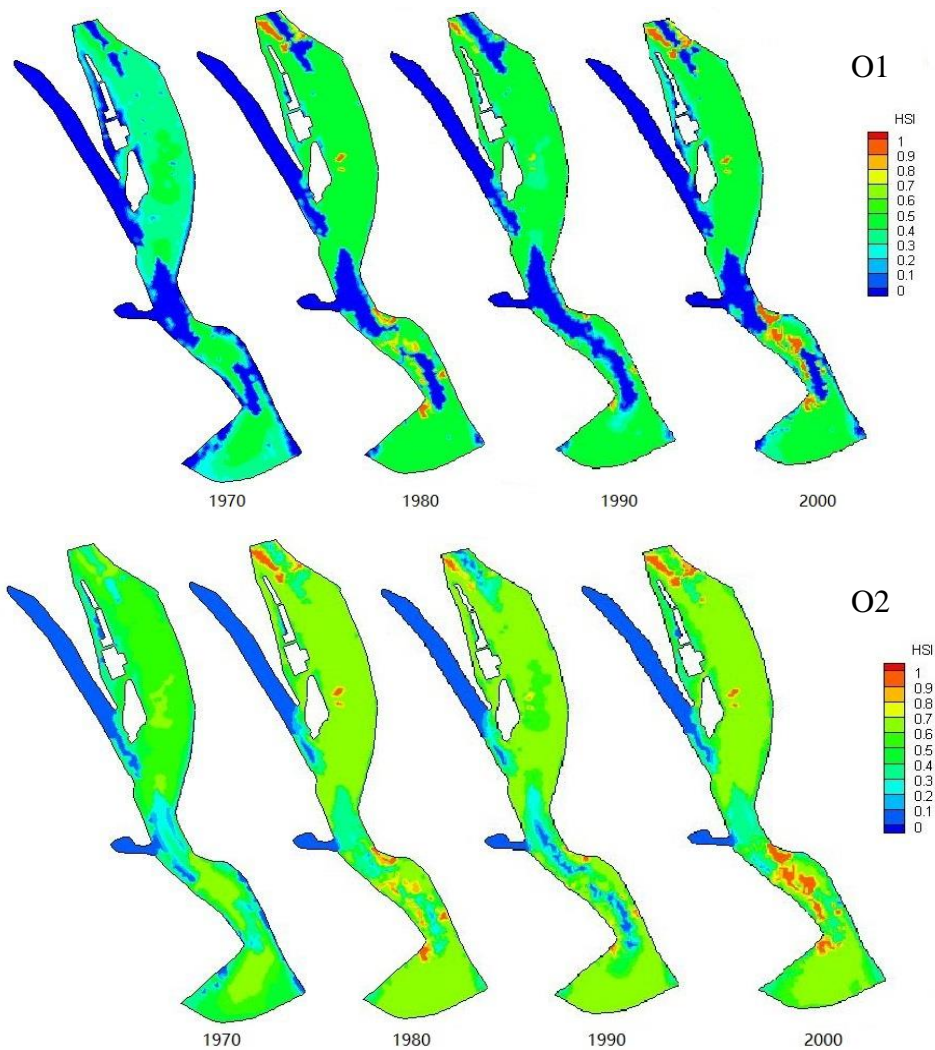


Figure III.2a: The HSI distribution at 1970, 1980, 1990 and 2000 under the scenario with considering hydromorphology (O1, and O2 in scenario E2).

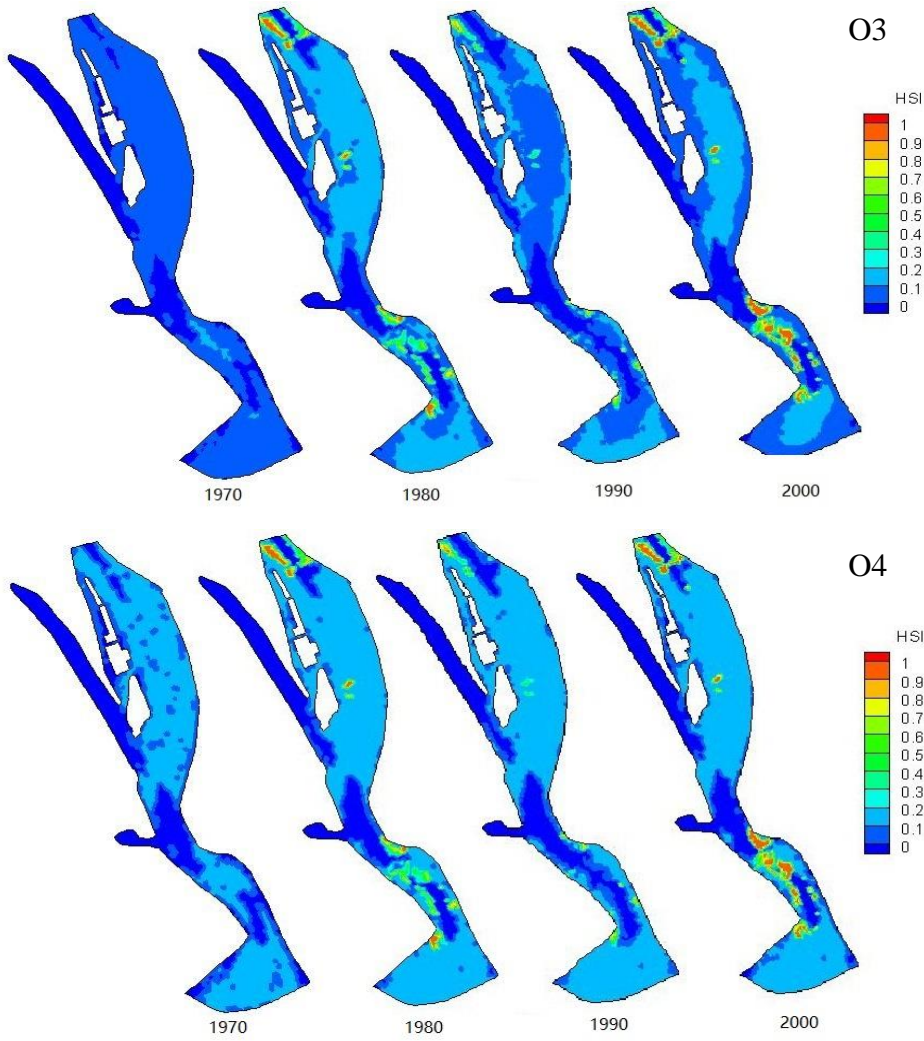


Figure III.2b: The HSI distribution at 1970, 1980, 1990 and 2000 under the scenario with considering hydromorphology (O3, and O4 in scenario E2).

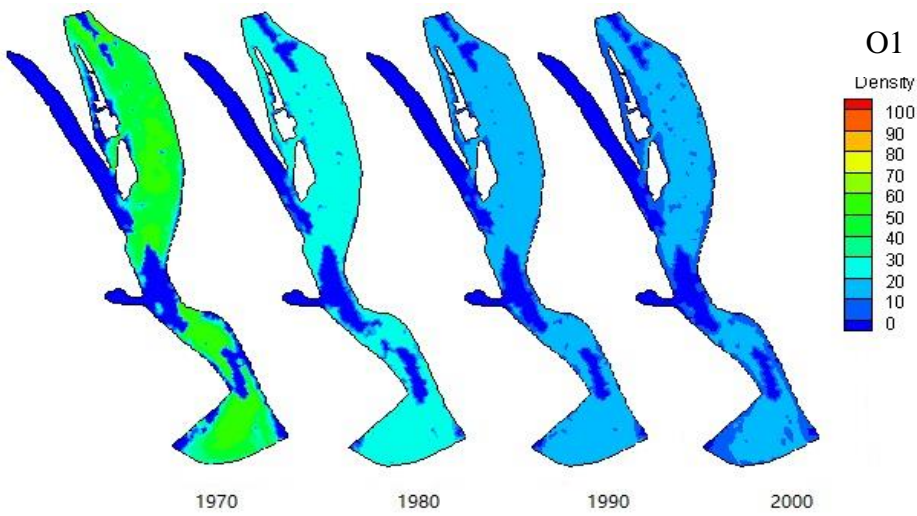


Figure III.3a: Logistic population density distribution for O1 in scenario without hydromorphology model (E1).

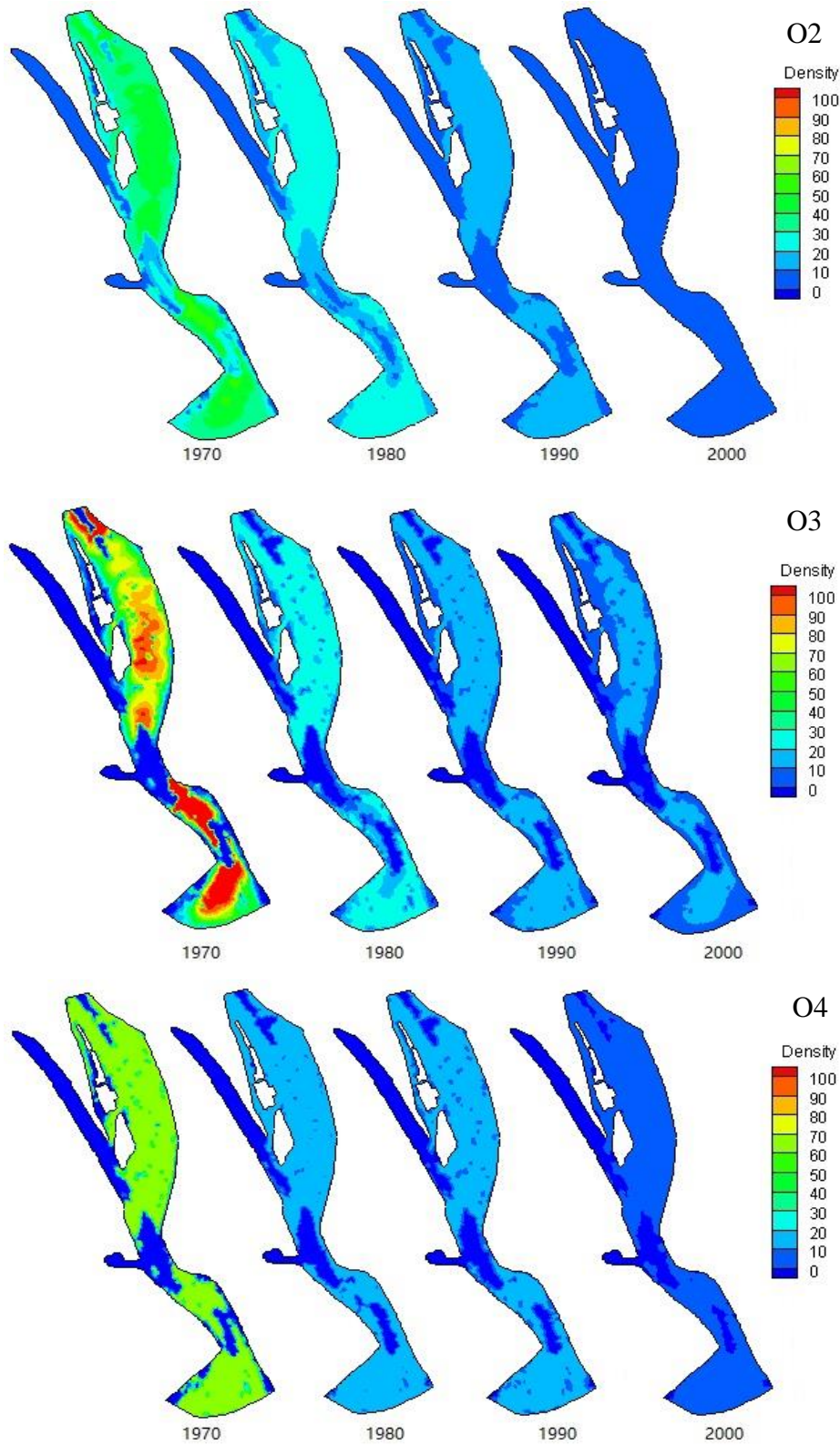


Figure III.3b: Logistic population density distribution for O2, O3 and O4 in scenario of without hydromorphology model (E1).

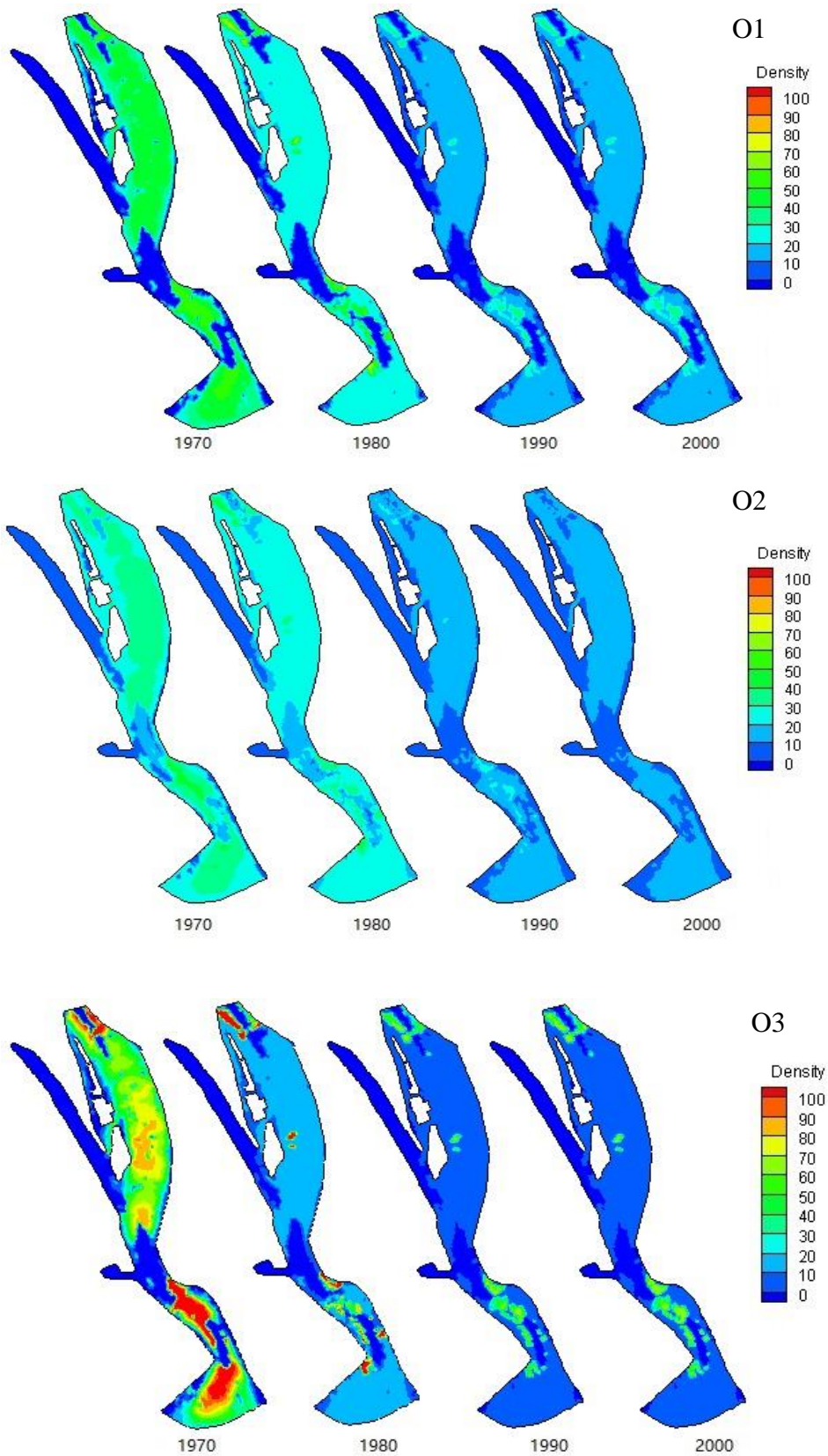


Figure III.4a: Logistic population density distribution for O1, O2, and O3 in scenario with hydromorphology model (E2).

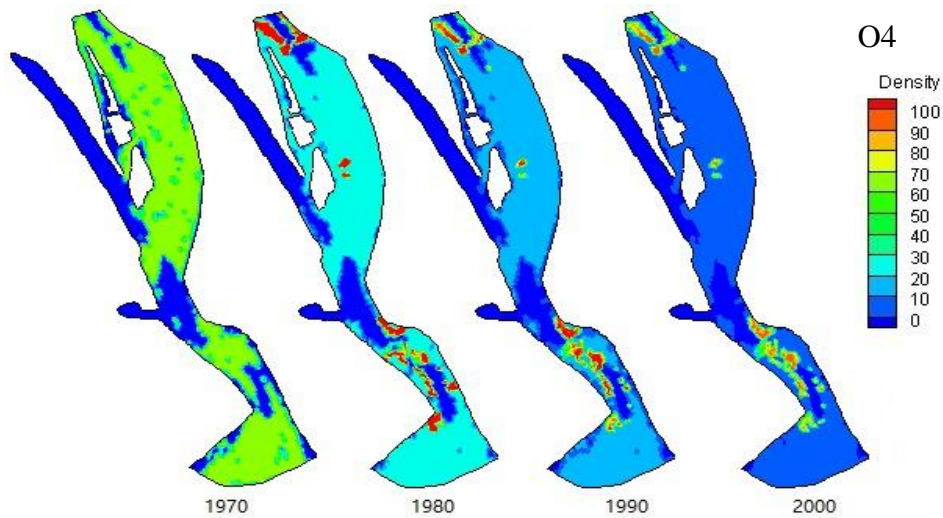


Figure III.4b: Logistic population density fluctuation for O4 in the scenario of with hydromorphology model (E2).

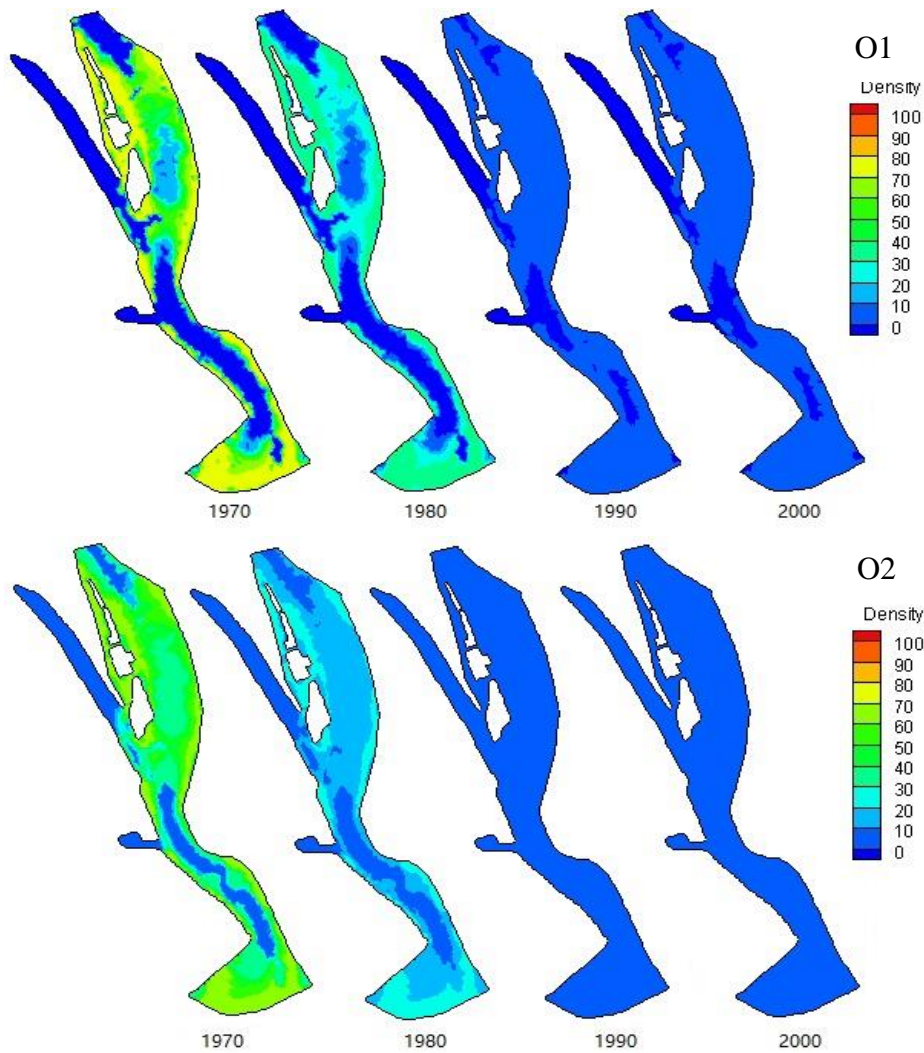


Figure III.5a: Population density distribution (O1 and O2) based on matrix population model without hydromorphology model (E1).

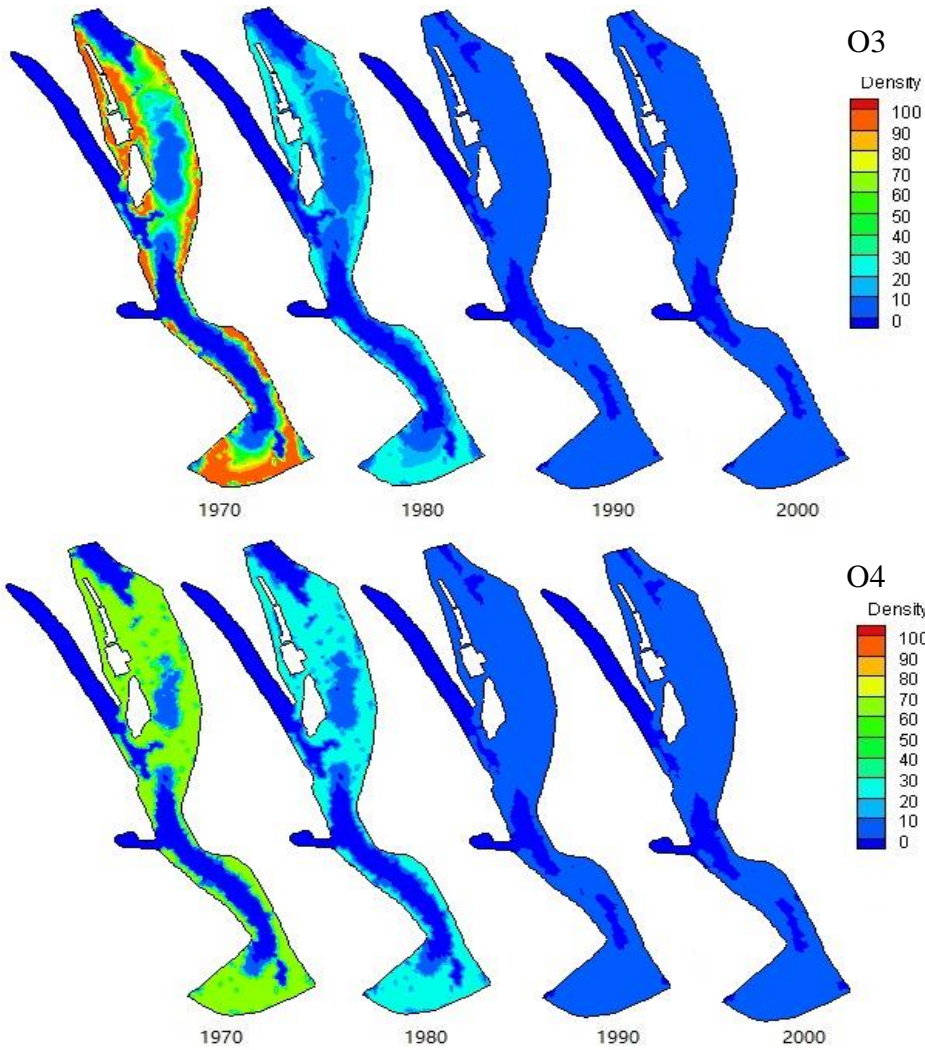


Figure III.5b: Population density distribution (O3 and O4) based on matrix population model without hydromorphology model (E1).

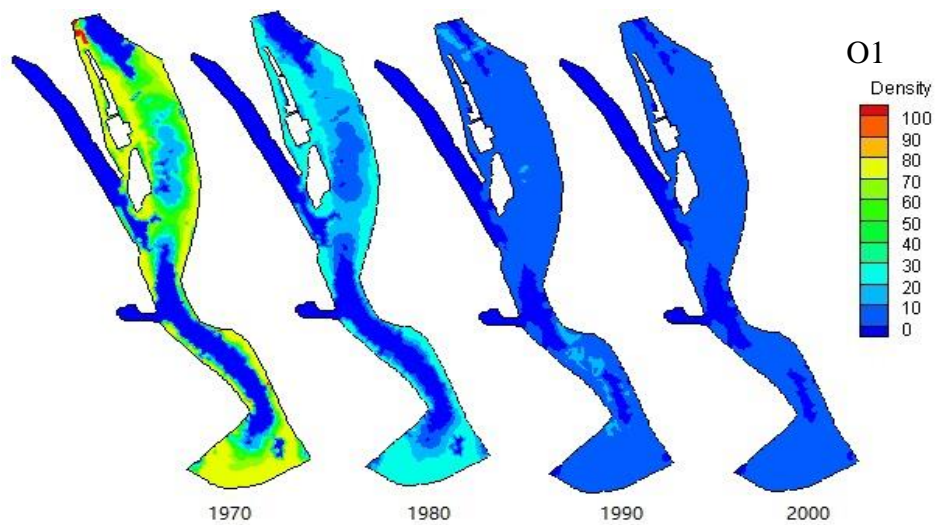


Figure III.6a: Population density distribution (O1) based on matrix population model with hydromorphology model (E2).

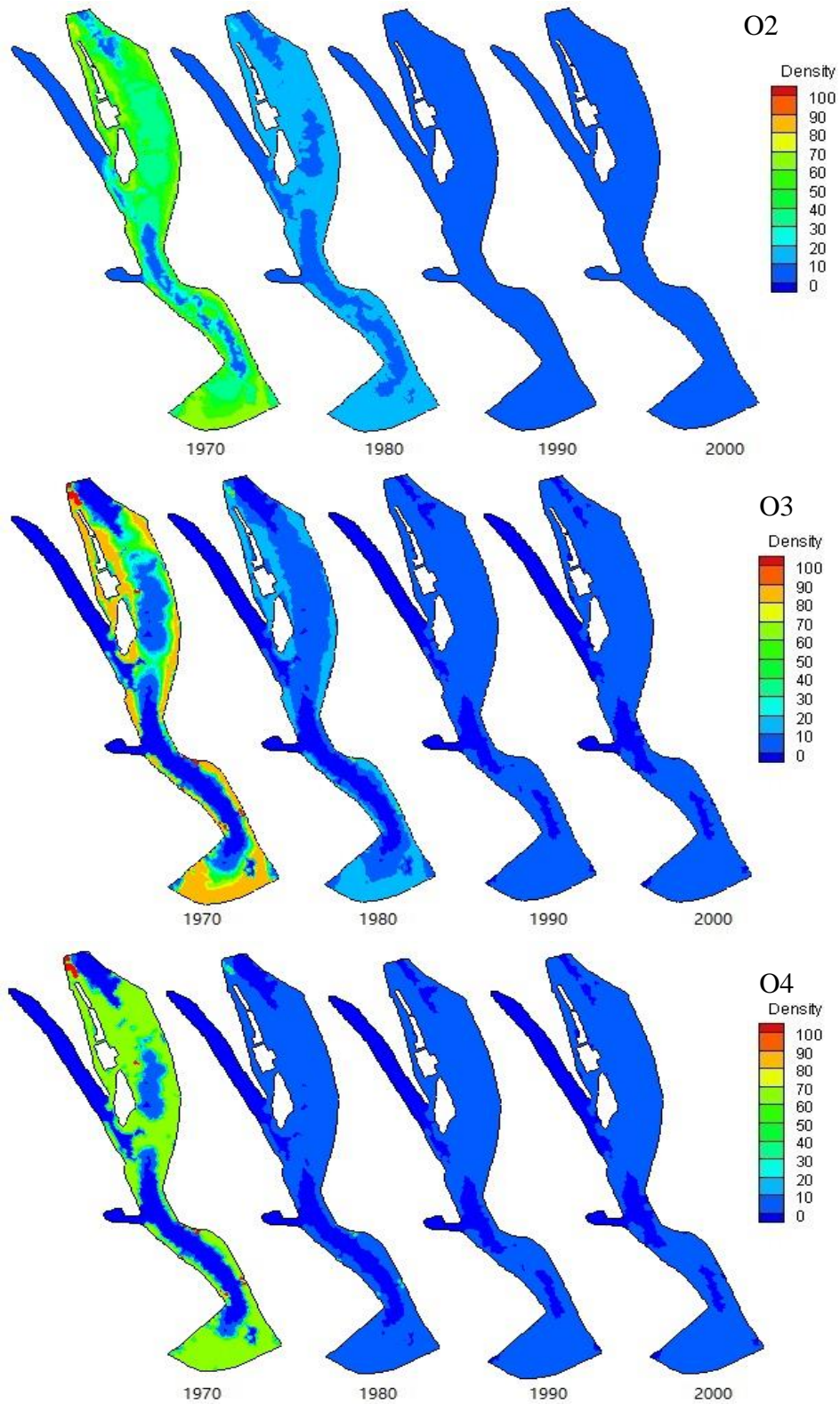


Figure III.6b: Population density distribution (O2, O3, and O4) based on matrix population model with hydromorphology model (E2).

Appendix IV:

Fish length distribution model for rainbow trout, brown trout, and flannelmouth sucker.

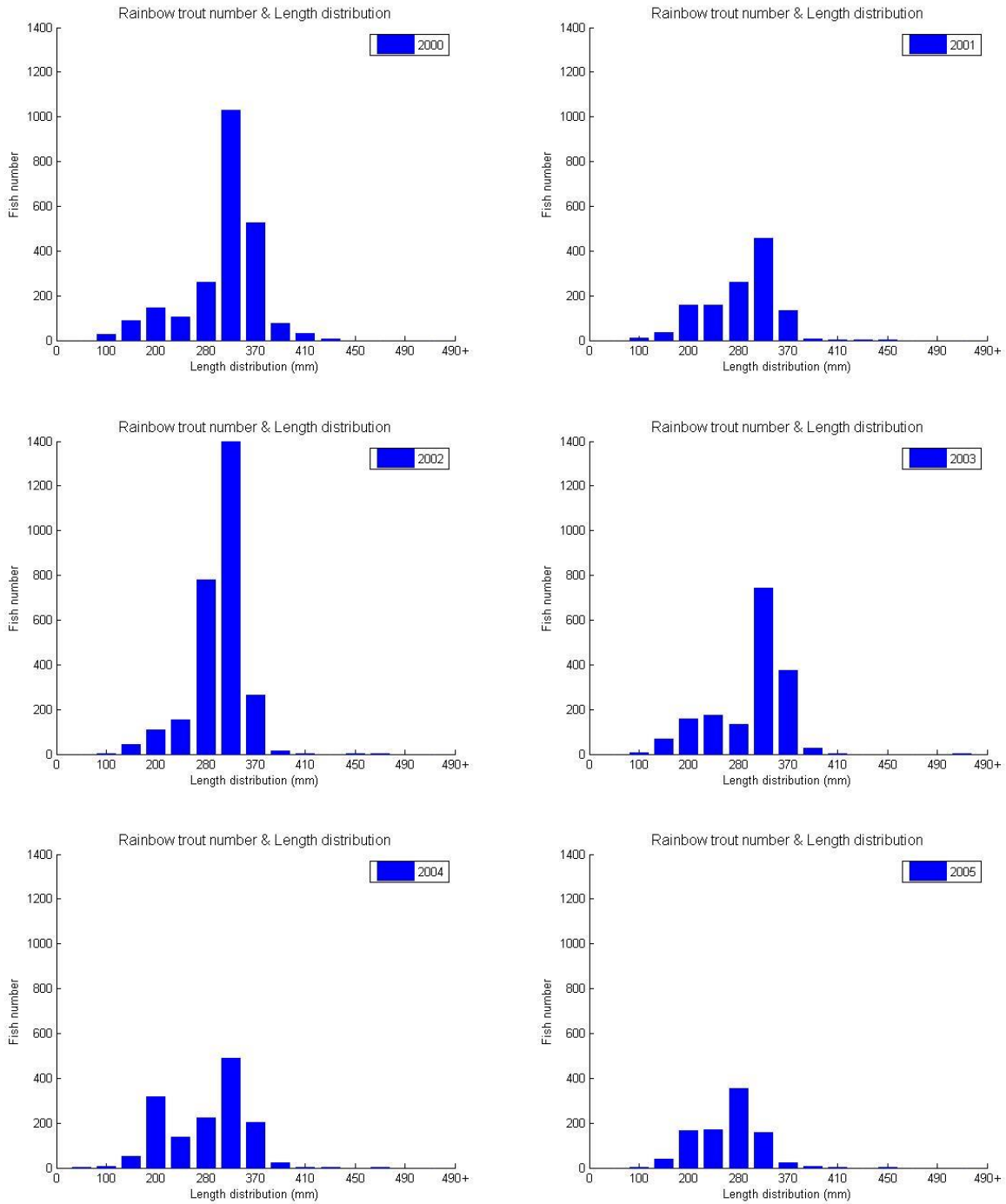


Figure IV.1a: Survey data for rainbow trout from 2000 to 2005.

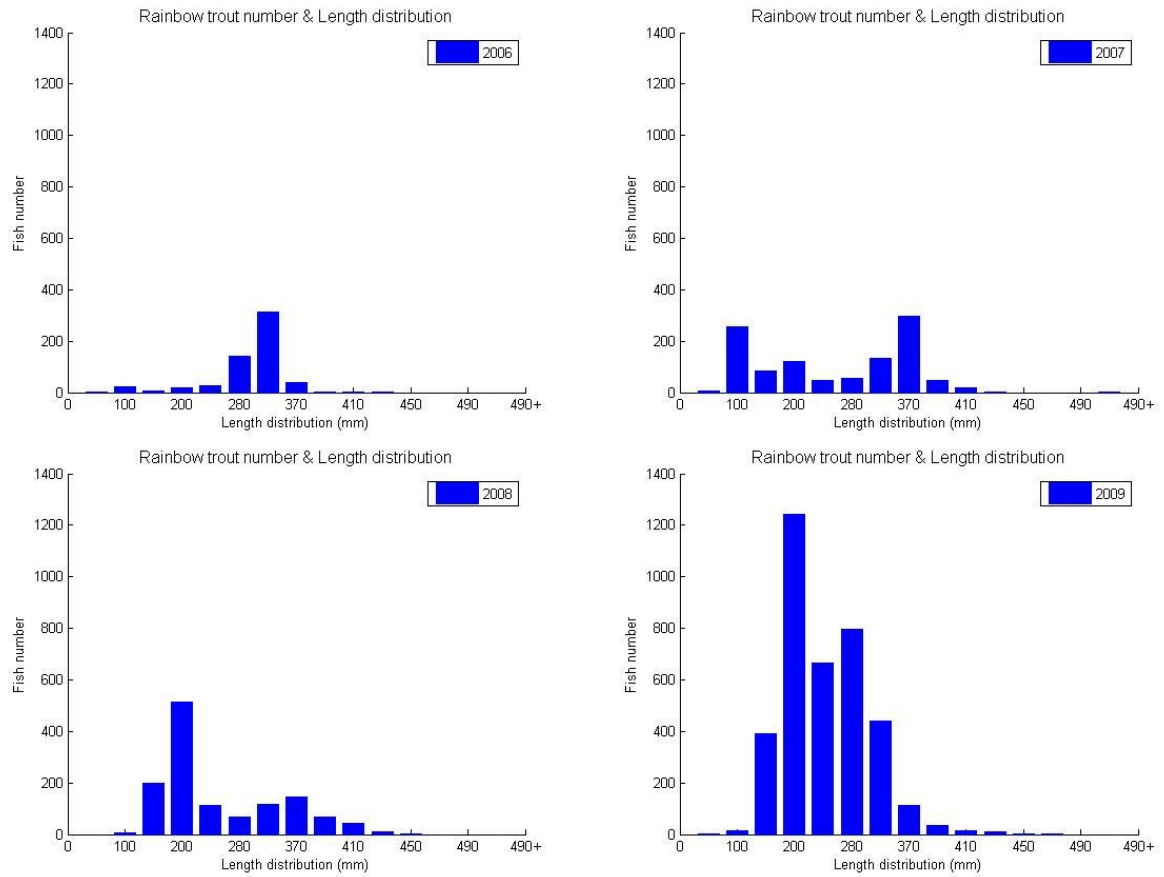


Figure IV.1b: Survey data for rainbow trout from 2006 to 2009.

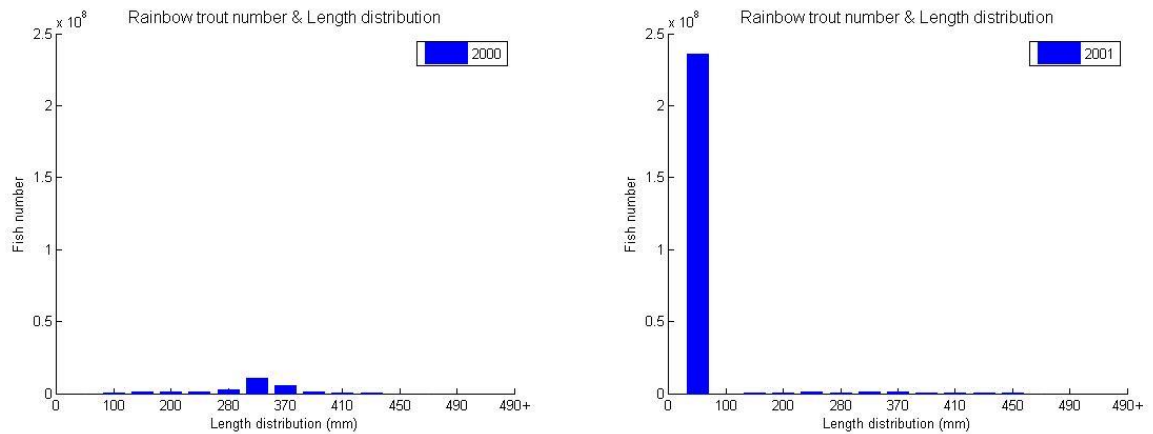


Figure IV.2a: Simulated rainbow trout distribution from 2000 to 2001.

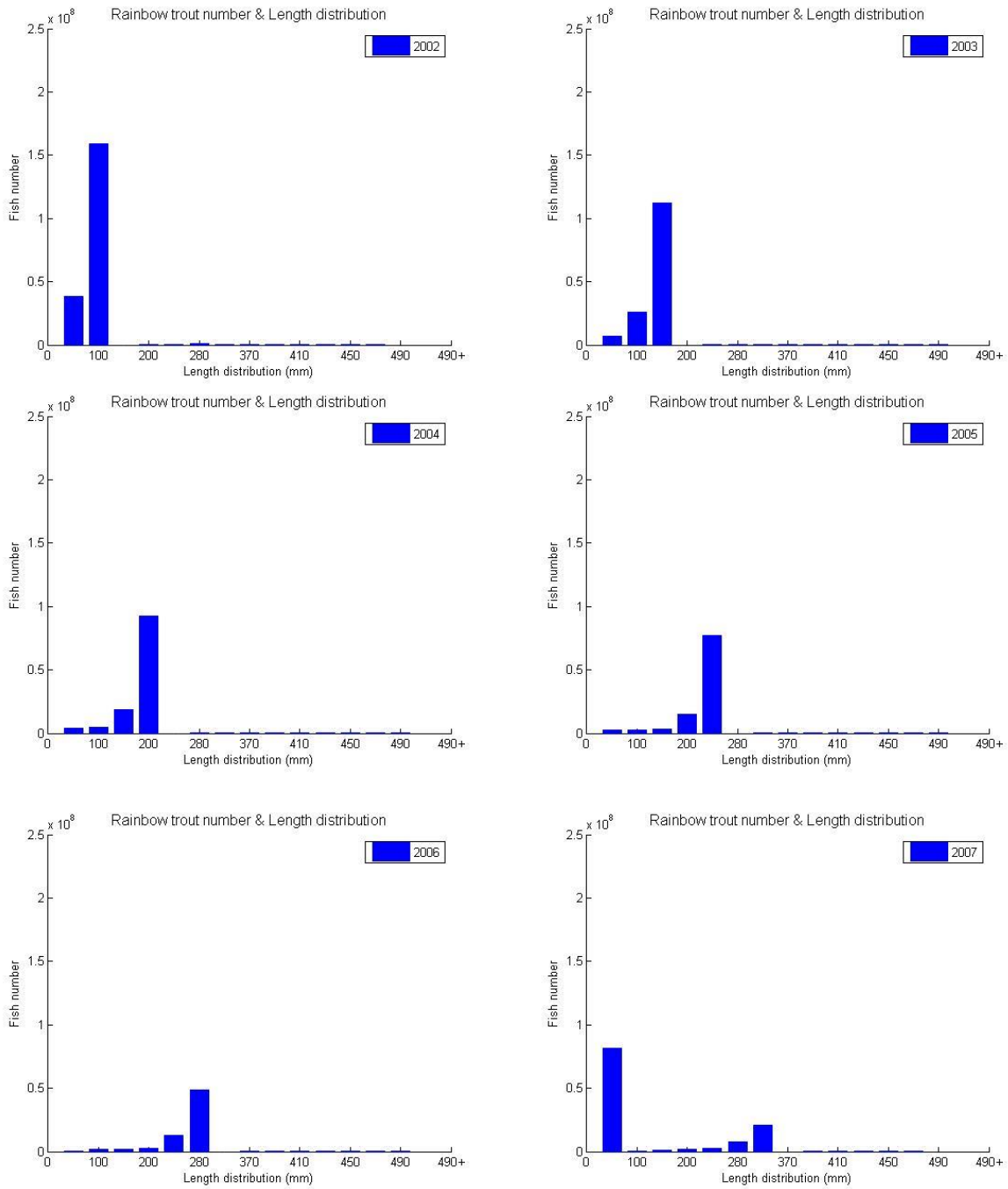


Figure IV.2b: Simulated rainbow trout distribution from 2002 to 2007.

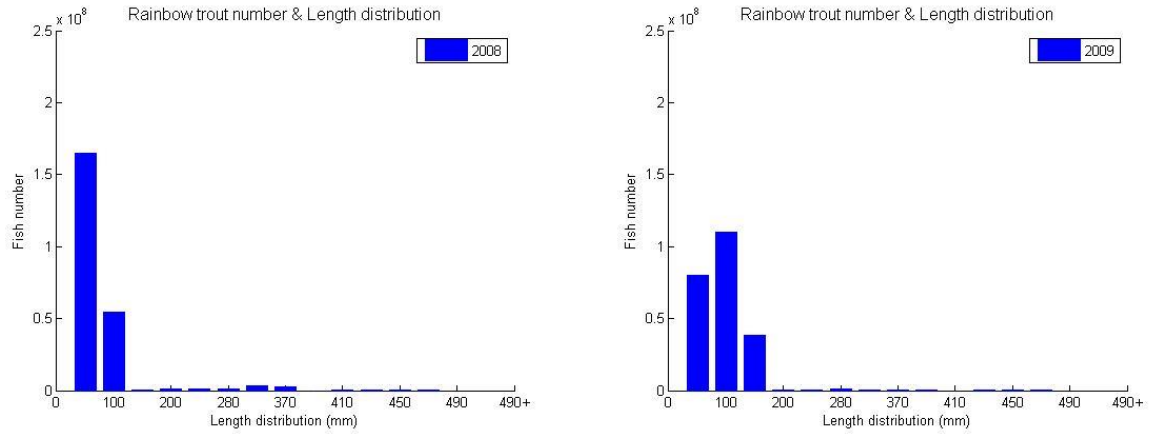


Figure IV.2c: Simulated rainbow trout distribution from 2008 to 2009.

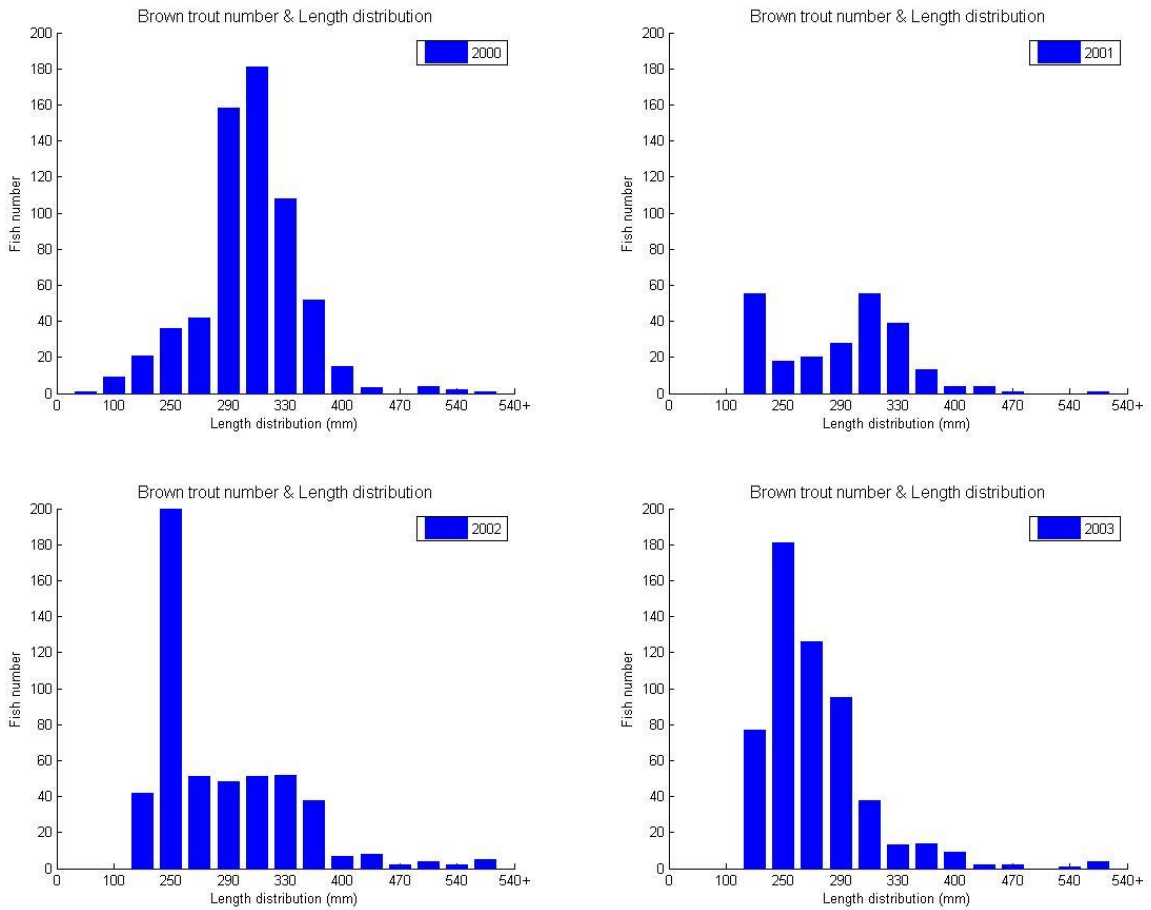


Figure IV.3a: Survey data for brown trout distribution from 2000 to 2003.

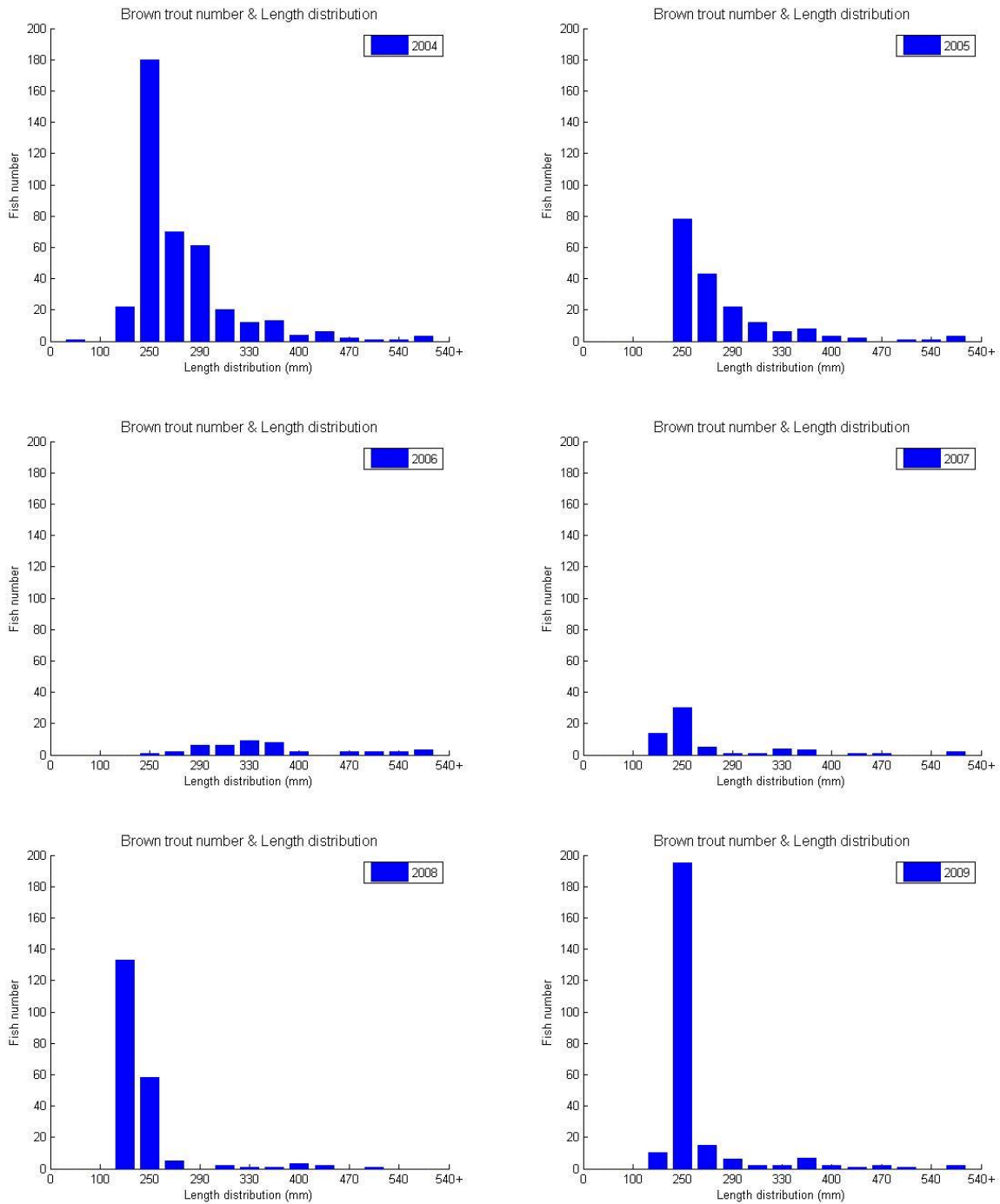


Figure IV.3b: Survey data for brown trout distribution from 2004 to 2009.

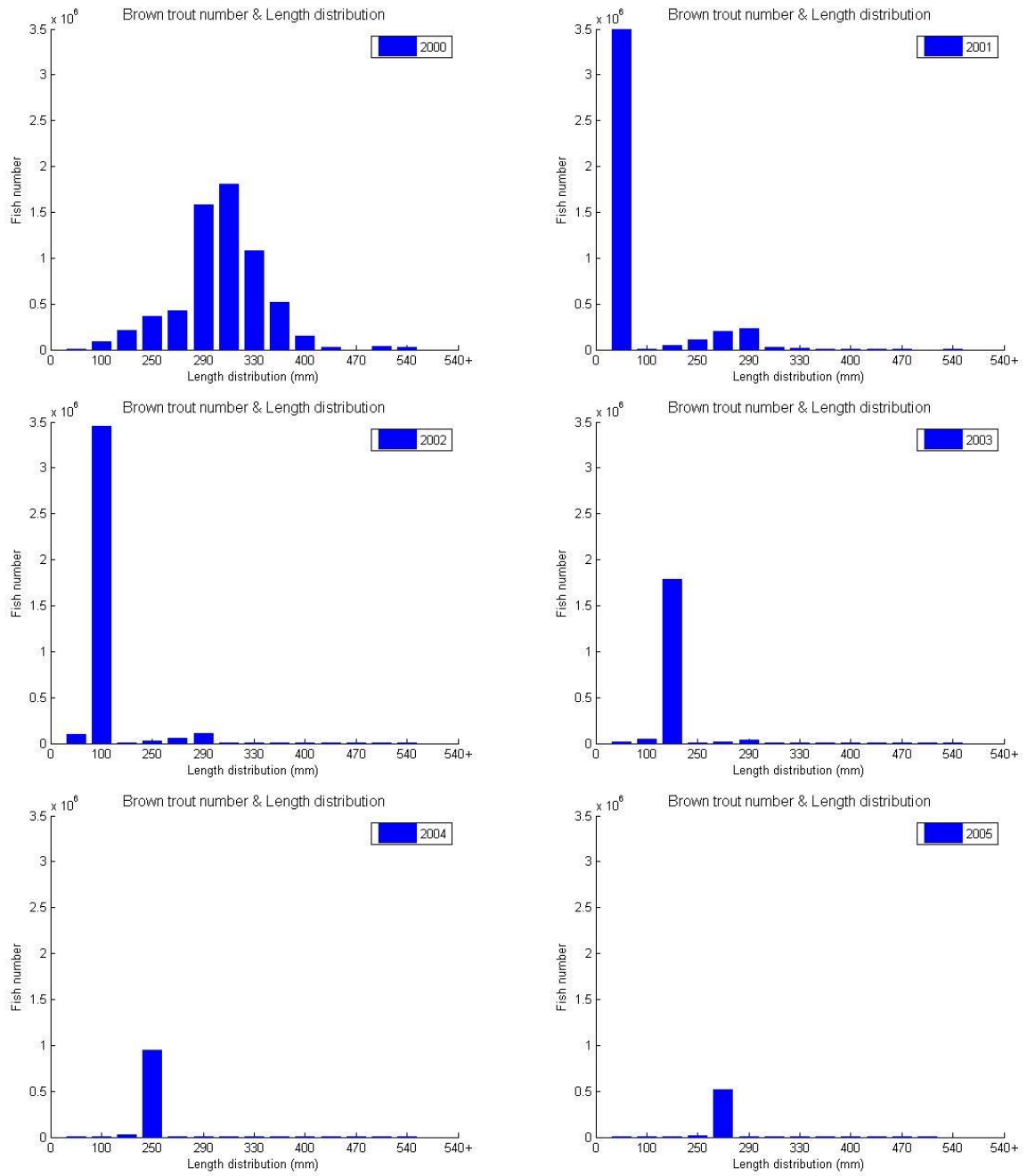


Figure IV.4a: Simulated brown trout distribution from 2000 to 2005.

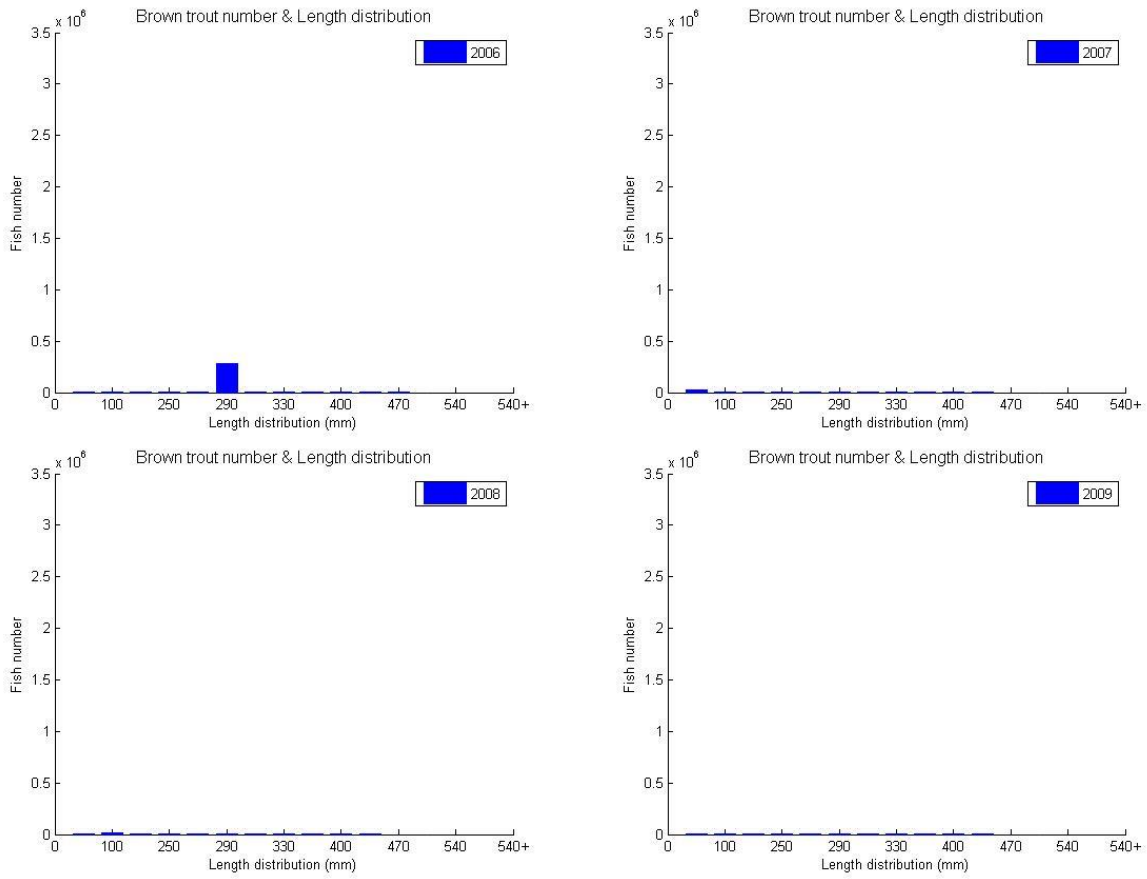


Figure IV.4b: Simulated brown trout distribution from 2006 to 2009.

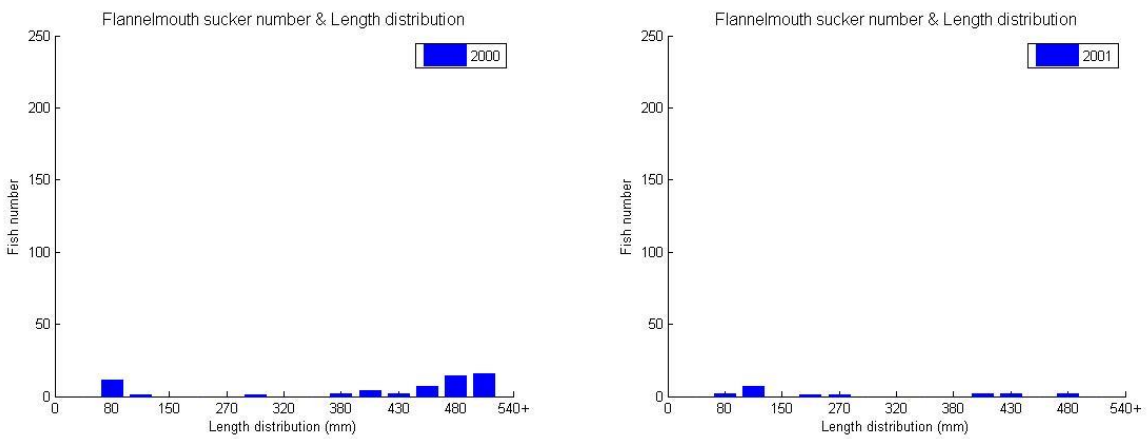


Figure IV.5a: Survey data for flannelmouth sucker from 2000 to 2001.

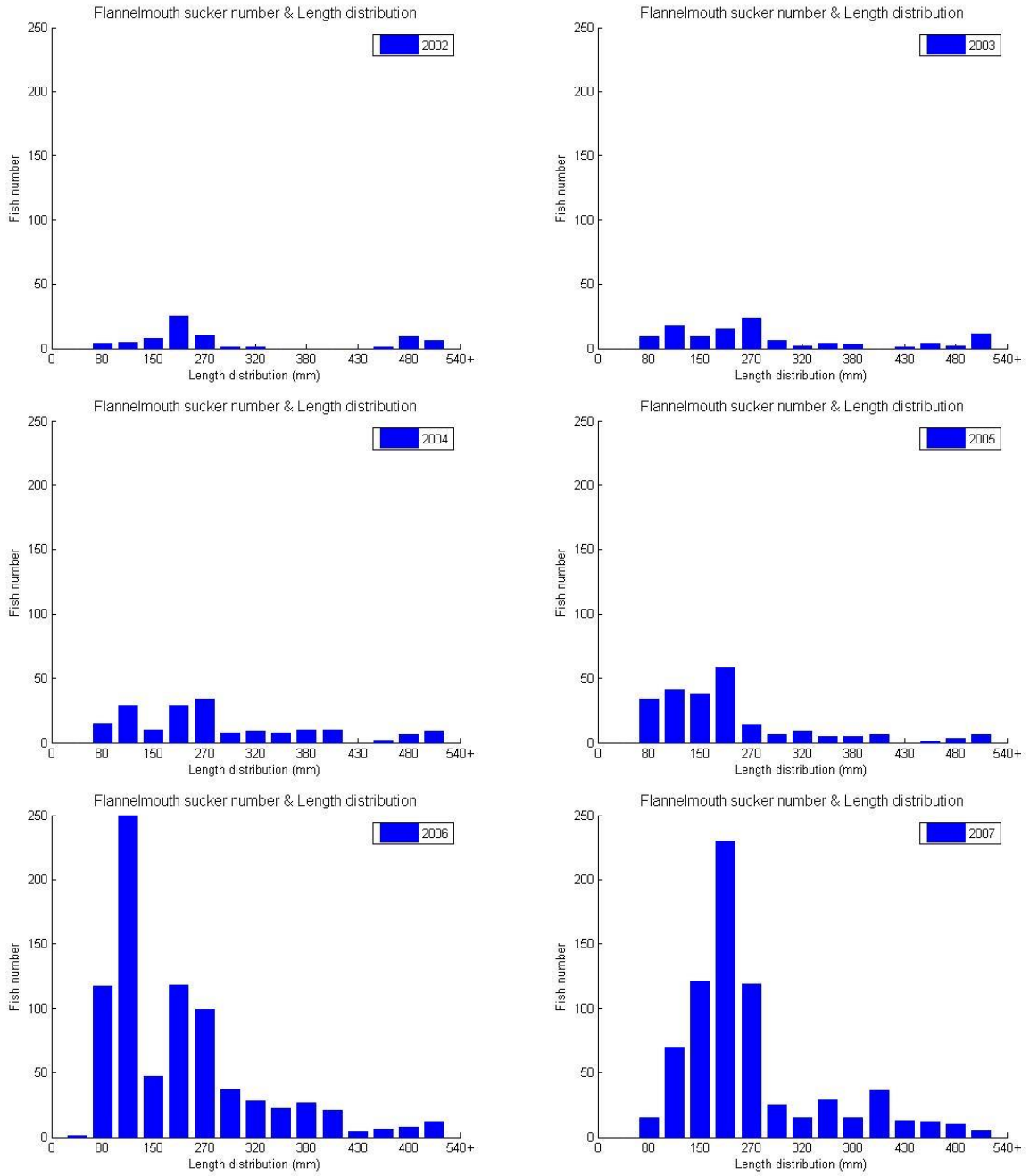


Figure IV.5b: Survey data for flannelmouth sucker from 2002 to 2007.

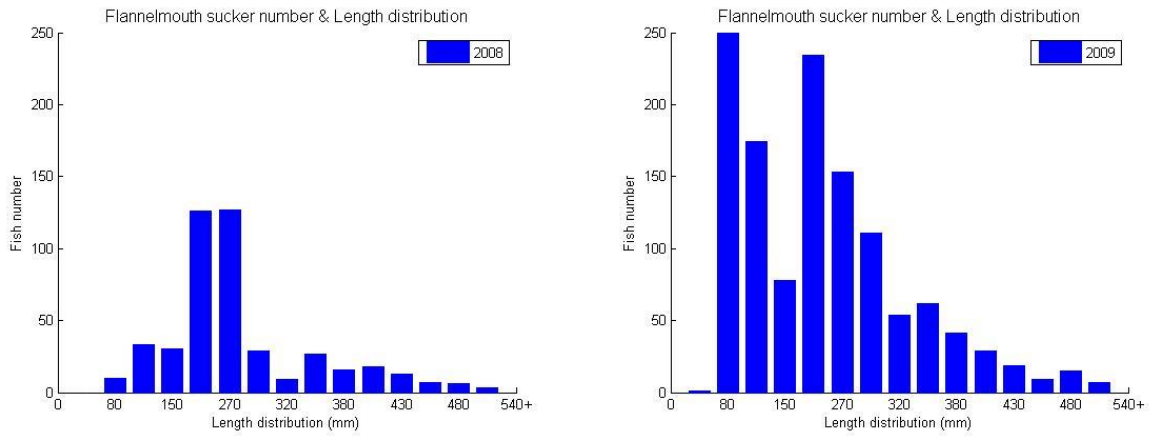


Figure IV.5c: Survey data for flannelmouth sucker from 2008 to 2009.

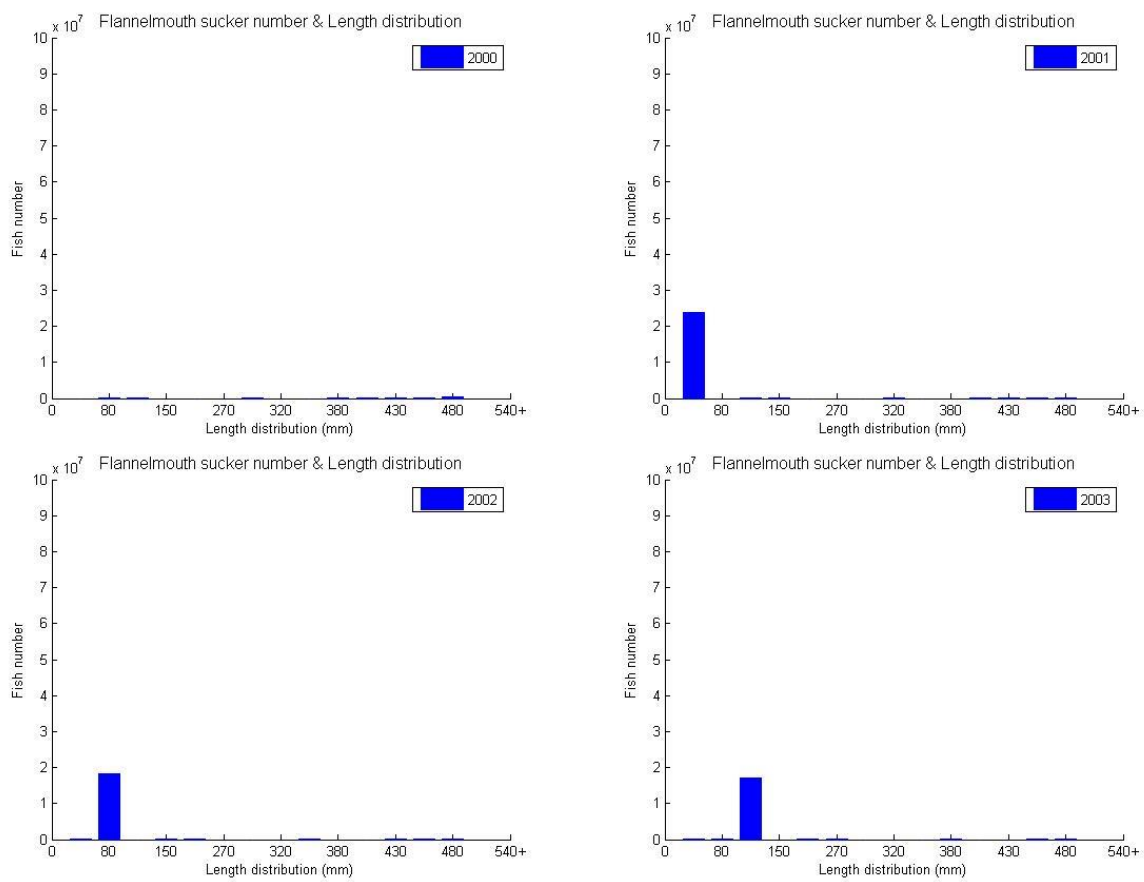


Figure IV.6a: Simulated flannelmouth sucker distribution from 2000 to 2003.

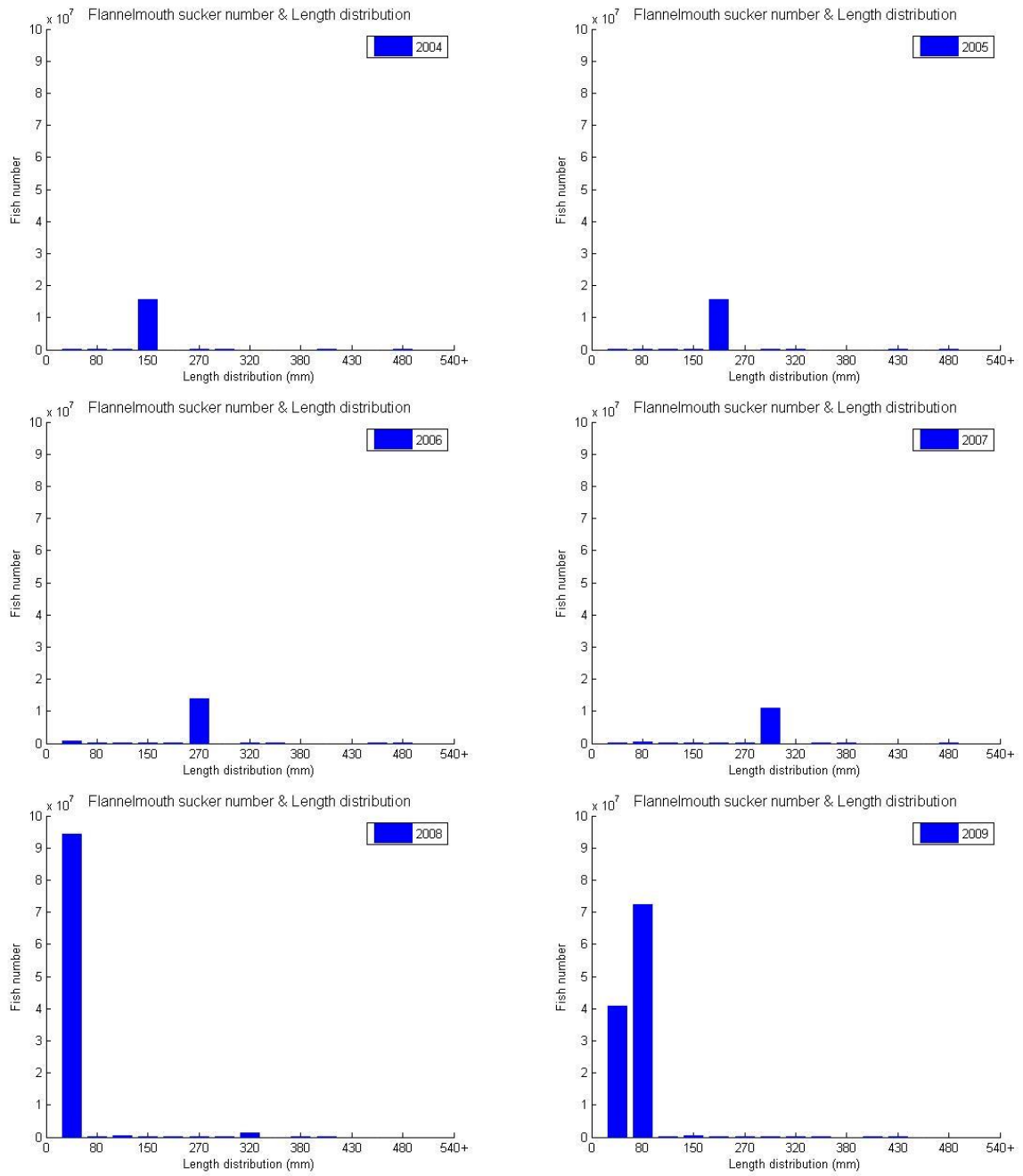


Figure IV.6b: Simulated flannelmouth sucker distribution from 2004 to 2009.

Appendix V:

Fish species living in Jiao-Mu River (Personal contact with Zhang). (U. is upstream; M. is middle stream; D. is downstream; N. L. P. is national level protection; S. L. P. is states level protection; E. F. S. is endemic fish species).

No.	Fish Latin name	U.	M.	D.	N. L. P.	S. L. P.	E. F. S.
1	<i>Hucho bleekeri</i> Kimura	+	—		○		●
2	<i>Anguilla japonica</i> Temminck et Schlegel		—	—			
3	<i>Myxocyprinus asiaticus</i> (Bleeker)			—	○		●
4	<i>Paracobitis variegatus</i> (Sauvage, Dabry et Thiersant)	+	+	+			
5	<i>Paracobitis potanini</i> (Günther)		+	+			●
6	<i>Oreias dabryi</i> Sauvage		+	+			●
7	<i>Triplophysa orientalis</i> (Herzenstein)	+					
8	<i>Triplophysa markehencensis</i>	+					
9	<i>Triplophysa angeli</i> (Fang)	+					
10	<i>Triplophysa brevicanda</i> (Herzenstein)	+					
11	<i>Triplophysa bleekeri</i> (Sauvage et Dabry)		+	+			
12	<i>Triplophysa stoliczkae</i> (Steindachner)	+	+				
13	<i>Botia superciliaris</i> Günther			+			
14	<i>Botia reevesae</i> Chang			+			●
15	<i>Leptobotia elongata</i> (Bleeker)		+	+			●
16	<i>Leptobotia microphthalmia</i> Fu et Ye		+	+		△	●
17	<i>Leptobotia rubrilabris</i> (Dabry et Thiersant)		+	+			●
18	<i>Misgurnus anguillicaudatus</i> (Cantor)	+	+	+			
19	<i>Zacco platypus</i> (Temminck et Schlegel)		+	+			
20	<i>Opsariichthys bidens</i> Günther		+	+			
21	<i>Gobiocypris rarus</i> Ye et Fu		+			△	●
22	<i>Luciobrama macrocephalus</i> (Lacépède)			—		△	
23	<i>Ctenopharyngodon idellus</i> (Cuvier et Valenciennes)		+	+			
24	<i>Squaliobarbus curriculus</i> (Richardson)			—			
25	<i>Elopichthys bambusa</i> (Richardson)			—		△	
26	<i>Xenocypris argentea</i> (Günther)			—			
27	<i>Xenocypris fangi</i> Tchang		—	—			●
28	<i>Distoechodon tumirostris</i> Peters			—			

No.	Fish Latin name	U.	M.	D.	N. L. P.	S. L. P.	E. F. S.
29	<i>Rhodeus sinensis</i> Günther		+	+			
30	<i>Acheilognathus omeiensis</i> (Shih et Tchang)		+	+			•
31	<i>Sinibrama changi</i> Chang		—	—			•
32	<i>Hemiculterella sauvagei</i> Warpachowsky			—			
33	<i>Hemiculter leucisculus</i> (Basilewsky)		+	+			
34	<i>Hemiculter tchangi</i> Fang		+	+			•
35	<i>Culter erythropterus</i> Basilewsky			—			
36	<i>Erythroculter ilishaeformis</i> (Bleeker)		—	—			
37	<i>Erythroculter mongolicus mongolicus</i> (Basilewsky)		—	—			
38	<i>Parabramis pekinensis</i> (Basilewsky)			—			
39	<i>Megalobrama pellegrini</i> (Tchang)			—			•
40	<i>Hemibarbus labeo</i> (Pallas)		+	+			
41	<i>Hemibarbus maculatus</i> Bleeker		+	+			
42	<i>Belligobio nummifer</i> (Boulenger)			—			
43	<i>Pseudorasbora parva</i> (Temminck et Schlegel)		+	+			
44	<i>Sarcocheilichthys sinensis sinensis</i> Bleeker			—			
45	<i>Sarcocheilichthys nigripinnis</i> (Günther)		—	—			
46	<i>Gnathopogon imberbis</i> (Sauvage et Dabry)		+	+			
47	<i>Squalidus argentatus</i> (Sauvage et Dabry)		+	+			
48	<i>Squalidus wolterstorffi</i> (Regan)			—			
49	<i>Coreius heterodon</i> (Bleeker)			—			
50	<i>Coreius guichenoti</i> (Sauvage et Dabry)			—			•
51	<i>Rhinogobio typus</i> Bleeker		—	—			
52	<i>Rhinogobio ventralis</i> Sauvage et Dabry			+			•
53	<i>Abbottina rivularis</i> (Basilewsky)		+	+			
54	<i>Abbottina obtusirostris</i> (Wu et Wang)		+	+			•
55	<i>Microphysogobio kiatingensis</i> (Wu)		+	+			
56	<i>Saurogobio dabryi</i> Bleeker		+	+			
57	<i>Gobiobotia filifer</i> (Garman)		—	—			
58	<i>Gobiobotia boulengeri</i> Tchang		+	+			•
59	<i>Spinibarbus sinensis</i> (Bleeker)		—	+			
60	<i>Percoypris pingi pingi</i> (Tchang)		—	+		Δ	•

No.	Fish Latin name	U.	M.	D.	N. L. P.	S. L. P.	E. F. S.
61	<i>Acrossocheilus yunnanensis</i> (Regan)		—	—			
62	<i>Onychostoma sima</i> (Sauvage et Dabry)		+	+			
63	<i>Onychostoma angustistomata</i> (Fang)		—	—			●
64	<i>Onychostoma daduensis</i> Ding,sp.nov.		—	—		Δ	●
65	<i>Tor (Folifer) brevifilis brevifilis</i> (Peters)		—	—			
66	<i>Sinilabeo rendahli rendahli</i> (Kimura)		—	—			
67	<i>Garra pingi pingi</i> (Tchang)		+	+			
68	<i>Semilabeo prochilus</i> (Sauvage et Dabry)		+	+			
69	<i>Schizothorax (Schizothorax) prenanti</i> (Tchang)	+	+				●
70	<i>Schizothorax (Racoma) davidi</i> (Sauvage)	+	+			Δ	●
71	<i>Schizothorax (Racoma) longbarbus</i> (Fang)	+	+				●
72	<i>Gynmoliptychus pachycheilus</i> Herzenstein	+					
73	<i>Schizopygopsis malacanthus</i> Herxenstein	+					
74	<i>Schizopygopsis malacanthus chengi</i> (Fang)	+	+				●
75	<i>Procypris rabaudi</i> (Tchang)		—	—		Δ	●
76	<i>Cyprinus (Cyprinus) carpio</i> Linnaeus	—	+	+			
77	<i>Carassius auratus</i> (Linnaeus)	—	+	+			
78	<i>Beaufortia Liui</i> Chang		+	—		Δ	●
79	<i>Beaufortia szechuanensis</i> (Fang)		+	+			●
80	<i>Lepturichthys fimbriata</i> (Günther)		+	+			
81	<i>Hemimyzon abbreviata</i> (Günther)		+	—			●
82	<i>Sinogastromyzon szechuanensis szechuanensis</i> Fang		—	—			●
83	<i>Sinogastromyzon sichangensis</i> Chang		+	+			●
84	<i>Metahomaloptera omeiensis</i> Chang		+	+			
85	<i>Silurus asotus</i> Linnaeus		—	—			
86	<i>Silurus meridionalis</i> Chen		+	+			
87	<i>Pelteobagrus vachelli</i> (Richardson)		+	+			
88	<i>Pelteobagrus vachelli</i> (Richardson)		—	—			
89	<i>Pseudobagrus truncatus</i> (Regan)		+	+			
90	<i>Pseudobagrus pratti</i> Günther			—			
91	<i>Pseudobagrus emarginatus</i> (Regan)		—	—			
92	<i>Mystus macropterus</i> (Bleeker)		—	—			

No.	Fish Latin name	U.	M.	D.	N. L. P.	S. L. P.	E. F. S.
93	<i>Liobagrus marginatus</i> (Günther)	—	+	+			
94	<i>Liobagrus nigricauda</i> Regan		+	+			
95	<i>Liobagrus marginatoides</i> (Wu)			—			●
96	<i>Glyptothorax fukiensis</i> (Rendahl)		+	+			
97	<i>Euchiloglanis davidi</i> (Sauvage)	+	+	+		Δ	●
98	<i>Euchiloglanis kishinouyei</i> Kimura	+	+	+			●
99	<i>Pareuchiloglanis sinensis</i> (Hora et Silas)	—	—				●
100	<i>Pareuchiloglanis robusta</i> Ding, Fu et Ye		+				●
101	<i>Pareuchiloglanis anteanalis</i> Fang ,Xu et Cui			—			●
102	<i>Oryzias latipes</i> (Temminck et Schlegel)		+	+			
103	<i>Monopterus albus</i> (Zuiew)		+	+			
104	<i>Siniperca chuatsi</i> (Basilewsky)		—	—			
105	<i>Siniperca kneri</i> Garman			—			
106	<i>Siniperca scherzeri</i> Steindachner			—			
107	<i>Hypseleotris swinhonis</i> (Günther)		+	+			
108	<i>Ctenogobius giurinus</i> (Rutter)		+	+			
109	<i>Ctenogobius chengtuensis</i> (Chang)		+	+		Δ	●
110	<i>Macropodus opercularis</i> (Linnaeus)		—	—			
111	<i>Channa argus</i> (Cantor)		+	+			